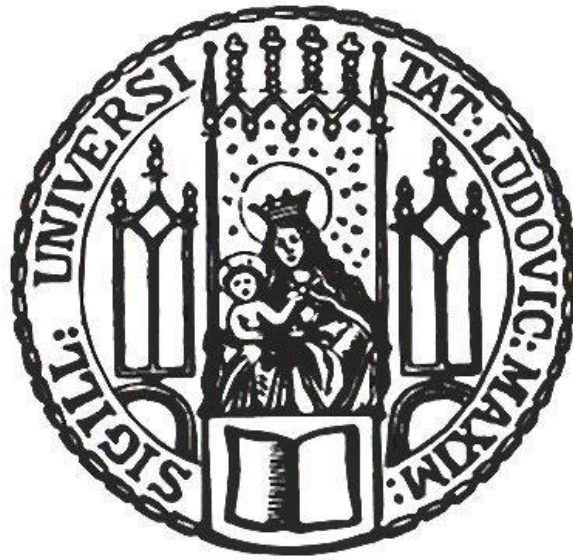


**Unraveling the cell type-specific effects and mechanisms of  
cross-disorder risk gene *CACNA1C***



**Dissertation**

zur Erlangung des Naturwissenschaftlichen  
Doktorgrades "Doctor rerum naturalium" (Dr. rer. nat.)  
an der Fakultät für Biologie der Ludwig-Maximilian-Universität München

**Srivaishnavi Loganathan**

June 2022

**Unraveling the cell type-specific effects and mechanisms of  
cross-disorder risk gene *CACNA1C***

Erstgutachter: PD Dr. Mathias Schmidt

Zweitgutachter: Prof. Dr. Laura Busse

Tag der Abgabe: 8 June 2022

Tag der mündlichen Prüfung: 19 December 2022

### **Eidesstattliche Erklärung**

Hiermit versichere ich an Eides statt, dass ich die vorliegende Arbeit selbstständig verfasst habe, keine als die angegebenen Quellen und Hilfsmittel benutzt wurden und alle Zitate kenntlich gemacht sind. Des Weiteren versichere ich, nicht anderweitig ohne Erfolg versucht zu haben, eine Dissertation einzureichen oder mich einer Doktorprüfung zu unterziehen. Die vorliegende Dissertation liegt außerdem keiner anderen Prüfungskommission vor.

I hereby confirm that I have written the accompanying thesis by myself, without contributions from any sources other than those cited in the text. This also applies to all graphics, drawings and images included in this thesis. Moreover, I declare that I have not submitted or defended a dissertation previously without success. This thesis has not been presented to any other examining board.

München, 08 June 2022

---

Srivaishnavi Loganathan

## Table of Contents

Abstract.....	I
Zusammenfassung.....	II
<b>1. Introduction.....</b>	<b>1</b>
1.1. What are psychiatric disorders?.....	1
1.2. Identification of candidate genes associated with psychiatric disorders.....	2
1.3. <i>CACNA1C</i> is a risk factor for psychiatric disorders.....	3
1.3.1. Risk variants of <i>CACNA1C</i> cause structural and functional changes in the human brain.....	4
1.4. <i>CACNA1C</i> codes for the $\alpha 1$ subunit of the L-type voltage-gated calcium channel $Ca_v1.2$ .....	7
1.5. Preclinical approaches to study psychiatric disorders.....	11
1.5.1. Sex as a biological variable in animal models.....	12
1.6. Role of environmental factors in the etiology of psychiatric disorders.....	13
1.7. Delving into the physiology of $Ca_v1.2$ channels.....	17
1.7.1. Studying $Ca_v1.2$ channel function <i>in vitro</i> .....	17
1.7.2. Pharmacological approaches: Calcium channel blockers.....	18
1.7.3. Genetically modified rodent models.....	19
<b>2. Objectives of the study.....</b>	<b>25</b>
Objective 1: How do the $Ca_v1.2$ channels interact with early life stress in mice?.....	25
Objective 2: Do female $Ca_v1.2$ -Nex conditional knockout mice exhibit behaviors previously reported in males?.....	25
Objective 3: How does $Ca_v1.2$ channel deletion in GABAergic neurons affect the behavioral phenotype of mice?.....	26
<b>3. Materials and methods.....</b>	<b>27</b>
3.1. Animals.....	27
3.2. Animal handling before and during behavioral testing.....	27
3.3. Transgenic mouse lines.....	27
3.4. Genotyping.....	28
3.5. Tamoxifen administration via food and intraperitoneal injection.....	29
3.6. Early life stress – limited bedding and nesting paradigm (ELS - LBN).....	30
3.7. Estrous cycle determination.....	31
3.8. Behavioral experiments.....	32
3.9. Golgi-cox staining.....	41
3.10. Image data acquisition and analysis in NeuroLucida.....	42
3.11. Protein extraction, Bradford assay and Western blot.....	43
3.12. Immunofluorescence staining for HA-tag.....	44

<b>3.13. Immunofluorescence staining for cFos quantification.....</b>	<b>45</b>
<b>3.14. Image acquisition and cFos cell quantification .....</b>	<b>45</b>
<b>3.15. minPROFILER assay .....</b>	<b>46</b>
<b>3.16. Statistical analyses .....</b>	<b>47</b>
<b>4. Results .....</b>	<b>48</b>
<b>4.1. Early life stress (ELS) – Limited bedding and nesting (LBN) paradigm.....</b>	<b>48</b>
4.1.1. LBN stressed animals exhibit reduced body weight at day 9 and at weaning .....	48
4.1.2. Assessment of locomotor activity and anxiety-related behavior in male and female mice following LBN stress .....	49
4.1.3. Consequences of early life stress on social interaction and cognitive performance .....	54
4.1.4. Assessment of stress coping and depression-related behavior following early life stress .....	58
<b>4.2. Controlling for potential effects of Cre expression on behavioral phenotypes.....</b>	<b>60</b>
<b>4.3. CKO animals show reduced dendritic arbor complexity but no differences in pCREB expression levels .....</b>	<b>66</b>
<b>4.4. Characterization of female Ca<sub>v</sub>1.2-Nex CKO mice.....</b>	<b>68</b>
4.4.1. Estrous cycle phenotyping of Ca <sub>v</sub> 1.2-Nex animals .....	69
4.4.2. Female CKO mice show hyperactivity and increased anxiety-related behavior.....	70
4.4.3. Female CKO mice show working and spatial memory deficits.....	73
4.4.4. Female CKO mice show enhanced active stress coping behavior .....	75
<b>4.5. Assessment of cellular and molecular alterations in female CKO mice.....</b>	<b>76</b>
<b>4.6. Addressing the role of Ca<sub>v</sub>1.2 in inhibitory GABAergic neurons.....</b>	<b>79</b>
4.6.1. Establishment of Ca <sub>v</sub> 1.2-GABA mouse lines .....	79
4.6.2. Ca <sub>v</sub> 1.2-PV CKO mice exhibit anxiogenic behavior.....	81
4.6.3. Ca <sub>v</sub> 1.2 deficiency in PV <sup>+</sup> GABAergic neurons does not alter social behavior .....	83
4.6.4. Assessment of cognitive performance in Ca <sub>v</sub> 1.2-PV mice .....	84
4.6.5. CKO-PV mice show enhanced passive stress coping behavior .....	86
<b>4.7. Ca<sub>v</sub>1.2 deficiency in excitatory and inhibitory neurons result in opposite effects on stress coping behavior .....</b>	<b>86</b>
<b>5. Discussion.....</b>	<b>90</b>
<b>5.1. Early life stress effects on the Ca<sub>v</sub>1.2-Nex mouse model .....</b>	<b>90</b>
<b>5.2. Ca<sub>v</sub>1.2-Nex female CKO mice exhibit behavioral alterations reminiscent of endophenotypes of psychiatric disorders .....</b>	<b>97</b>
5.2.1. Novelty induced hyperlocomotion in female Ca <sub>v</sub> 1.2-Nex CKO mice .....	97
5.2.2. Loss of Ca <sub>v</sub> 1.2 in excitatory neurons induces anxiety .....	99
5.2.3. Altered cognition, structural morphology, and basal activity in Ca <sub>v</sub> 1.2-Nex CKO mice .....	100

<b>5.3. Generation of a novel mouse model with Ca<sub>v</sub>1.2 deficiency in GABAergic neurons.....</b>	<b>103</b>
5.3.1. Ca <sub>v</sub> 1.2 deficiency in PV <sup>+</sup> GABAergic neurons induces anxiety.....	104
5.3.2. Ca <sub>v</sub> 1.2 deficiency in PV <sup>+</sup> GABAergic neurons results in cognitive impairment.....	104
5.3.3. Ca <sub>v</sub> 1.2 deficiency in PV <sup>+</sup> GABAergic neurons induces passive stress coping behavior .....	105
<b>5.4. Differential expression of cFos in CKO-Nex and CKO-PV mice .....</b>	<b>106</b>
<b>6. Conclusion and future directions.....</b>	<b>107</b>
<b>Bibliography .....</b>	<b>108</b>
<b>List of figures.....</b>	<b>134</b>
<b>List of tables.....</b>	<b>136</b>
<b>Abbreviations .....</b>	<b>137</b>
<b>Acknowledgements .....</b>	<b>141</b>

## Abstract

The cross-disorder risk gene *CACNA1C*, coding for the  $\alpha_1$  subunit of the L-type voltage gated calcium channel  $Ca_v1.2$ , has been repeatedly implicated in the etiology of psychiatric disorders. In humans, genetic variations in *CACNA1C* have a sex-dependent influence on the symptoms and age of onset of psychiatric disorders. In addition to genetic risk factors, environmental factors such as stress add considerably to the risk of development of psychiatric disorders. However, the underlying mechanisms which manifest the disease symptoms are not clearly understood. Rodent models of  $Ca_v1.2$  have revealed behavioral phenotypes reminiscent of core symptoms of psychiatric disorders but are largely biased toward male animals. In addition, role of  $Ca_v1.2$  channels in inhibitory neurons remains yet to be investigated. Thus, the aim of this study was to dissect  $Ca_v1.2$ -specific circuits and downstream signaling mechanisms to fundamentally increase our understanding of the role L-type calcium channels play in the pathogenesis of psychiatric disorders. To reach this goal, a series of behavioral, cellular, and molecular experiments were performed to investigate: 1) gene  $\times$  environment interactions in animals with a specific deletion of  $Ca_v1.2$  channels in excitatory neurons ( $Ca_v1.2$ -Nex) upon exposure to early life stress, 2) changes in disease-related endophenotypes and the effects of estrous cycle in female  $Ca_v1.2$ -Nex mice, 3) alterations in disease-related phenotypes caused by cell type-specific  $Ca_v1.2$  channel deletion in parvalbumin expressing inhibitory neurons and 4) alterations in  $Ca_v1.2$  downstream signaling pathways, structural plasticity, and their functional implications. The major findings of this study include: LBN stress induced only moderate effects on behavioral phenotypes of male and female  $Ca_v1.2$ -Nex mice and dendritic atrophy was observed in stressed mice. Female  $Ca_v1.2$ -Nex conditional knockout animals exhibited hyperactivity, anxiety-related behavior, cognitive deficits, active stress coping behavior, and structural impairments in the hippocampus. In addition, an enhanced baseline activity was observed in primary cortical neurons derived from  $Ca_v1.2$ -Nex knockout animals.  $Ca_v1.2$ -PV conditional knockout animals exhibited anxiety-related behavior, cognitive deficit, passive stress coping behavior and differential cFos expression in several brain regions.

## Zusammenfassung

Das krankheitsübergreifende Risikogen *CACNA1C*, das für die  $\alpha_1$ -Untereinheit des spannungsgesteuerten L-Typ-Kalziumkanals  $Ca_v1.2$  kodiert, wurde wiederholt mit der Ätiologie psychiatrischer Störungen in Verbindung gebracht. Beim Menschen haben genetische Variationen im *CACNA1C* einen geschlechtsabhängigen Einfluss auf die Symptome und den Zeitpunkt des Auftretens von psychiatrischen Störungen. Neben den genetischen Risikofaktoren tragen auch Umweltfaktoren wie Stress erheblich zum Risiko der Entwicklung psychiatrischer Störungen bei. Die zugrundeliegenden Mechanismen, die zur Manifestierung der Krankheitssymptome beitragen, sind jedoch nicht eindeutig geklärt. Nagetiermodelle für  $Ca_v1.2$  zeigen Verhaltensphänotypen, die an die Kernsymptome psychiatrischer Störungen erinnern. Allerdings wurden diese überwiegend bei männlichen Tieren untersucht. Darüber hinaus muss die Rolle der  $Ca_v1.2$ -Kanäle in hemmenden Neuronen noch untersucht werden. Ziel dieser Studie war es daher,  $Ca_v1.2$ -spezifische Schaltkreise und nachgeschaltete Signalmechanismen zu untersuchen, um unser Verständnis der Rolle von Kalziumkanälen des L-Typs in der Pathogenese psychiatrischer Störungen grundlegend zu verbessern. Um dieses Ziel zu erreichen, wurde eine Reihe von Verhaltens-, Zell- und Molekularexperimenten durchgeführt, um Folgendes zu untersuchen: 1) Gen-Umwelt-Interaktionen bei Tieren mit einer spezifischen Deletion von  $Ca_v1.2$  in exzitatorischen Neuronen ( $Ca_v1.2$ -Nex), wenn sie während frühkindlichem Stress ausgesetzt sind, 2) Veränderungen in krankheitsbezogenen Endophänotypen und die Auswirkungen des Östrogenzyklus bei weiblichen  $Ca_v1.2$ -Nex-Mäusen, 3) Veränderungen in krankheitsbezogenen Phänotypen, die durch zelltypspezifische  $Ca_v1.2$ -Deletion in Parvalbumin-exprimierenden inhibitorischen Neuronen verursacht werden, und 4) Veränderungen in den nachgeschalteten  $Ca_v1.2$ -Signalwegen, in der strukturellen Plastizität und ihre funktionellen Auswirkungen. Zu den wichtigsten Ergebnissen dieser Studie gehören: LBN-Stress induzierte nur mäßige Auswirkungen auf die Verhaltensphänotypen von männlichen und weiblichen  $Ca_v1.2$ -Nex-Mäusen, und bei gestressten Mäusen eine dendritische Atrophie beobachtet wurde. Weibliche  $Ca_v1.2$ -Nex bedingte Knockout-Tiere zeigten Hyperaktivität, verändertes angstbezogenes Verhalten, kognitive Defizite, aktives Stressbewältigungsverhalten und strukturelle Beeinträchtigungen im Hippocampus. Darüber hinaus wurde in primären kortikalen Neuronen, die von  $Ca_v1.2$ -Nex-Knockout-Tieren stammten, eine erhöhte Grundaktivität beobachtet.  $Ca_v1.2$ -PV bedingte Knockout-Tiere zeigten verändertes angstbezogenes Verhalten, kognitive Defizite, passives Stressbewältigungsverhalten und eine unterschiedliche cFos-Expression in verschiedenen Hirnregionen.

## 1. Introduction

### 1.1. What are psychiatric disorders?

Psychiatric disorders such as major depression (MD), bipolar disorder (BD), schizophrenia (SCZ), attention deficit hyperactivity disorder (ADHD) and autism spectrum disorder (ASD) are highly prevalent in the population worldwide and significantly contribute to the global disease burden. According to the World Health Organization (WHO), 1 in 4 people have encountered at least one episode of psychiatric disorder in their lifetime (**Figure 1**). Psychiatric disorders are complex and pleiotropic with shared genetic architecture and symptomatology across various disorders adding to their complexity (**Figure 2**) (Gandal et al. 2018; Egervari et al. 2019).

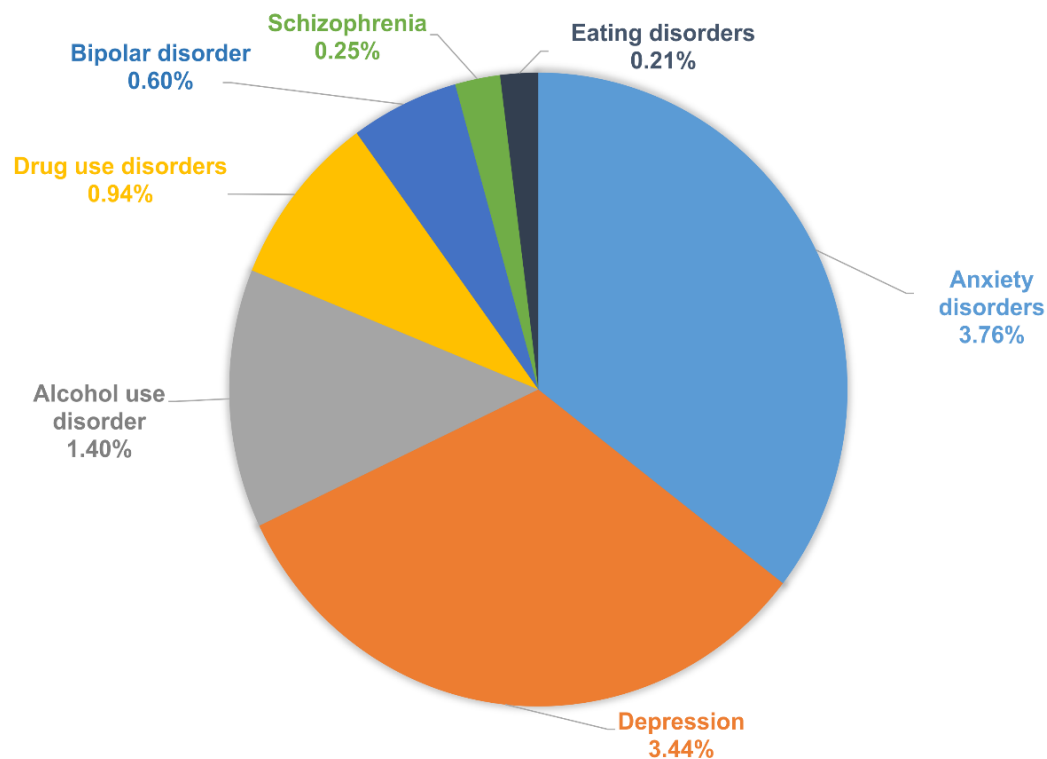


**Figure 1: Global prevalence of mental disorders.** Psychiatric disorders are highly prevalent across the world population with almost 10.7% of the population affected according to the latest data obtained in 2017. Data in this graph was obtained from <https://ourworldindata.org/mental-health#citation>.

In recent times, psychiatric disorders are diagnosed by a more established set of research diagnostic criteria identified in various classification systems such as the *International Classification of Diseases* (ICD) and the *Diagnostic and Statistical Manual* (DSM), but they are still largely based on clinical interviews with no biological markers available for diagnosis (Egervari et al. 2019;

Smoller et al. 2019). There are currently 21 distinct categories classified in ICD-11 (most recent version, published in 2022).

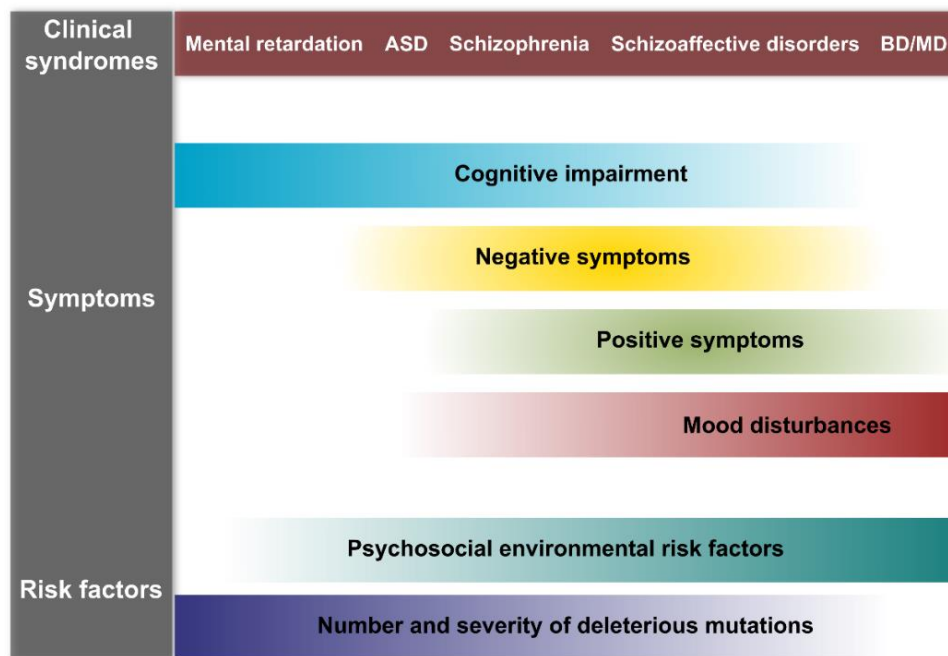


**Figure 2: Shared symptomology across various psychiatric disorders.** Psychiatric disorders are complex with shared symptomology due to their shared genetic etiology. In addition to genetic variations, environmental aspects are also risk factors for the development of psychiatric disorders. The image was adapted from Owen 2014 (Owen 2014).

Human genetic studies have identified several risk genes and variations within these genes that are associated with different psychiatric disorders (P. H. Lee et al. 2019; Yao et al. 2021). But ethical and practical difficulties of accessing and examining the living human brain limits our understanding of higher brain functions and further adds to the complexity of psychiatric disorders. Neurobiological studies in other model organisms add to a growing body of evidence deciphering molecular, cellular and circuit level mechanisms of psychopathology. However, despite the high global disease burden and decades of multiplying molecular evidence, our understanding of the causal psychopathological mechanisms and therapeutic breakthroughs are still rudimentary.

## 1.2. Identification of candidate genes associated with psychiatric disorders

Family, twin and adoption studies including molecular studies on post-mortem human brain largely contributed to early identification of genes that might be involved in the pathophysiology

of psychiatric disorders (Smoller et al. 2019). Due to practical difficulties of accessing the living human brain, other methods such as transcriptional profiling were especially necessary to probe into molecular signatures of psychiatric disorders (Egervari et al. 2019). More recent large-scale genome wide association studies (GWAS) and meta-analyses of GWAS have identified numerous overlapping variations in genes linked to psychiatric disorders that may explain their heterogeneous nature (Cichon et al. 2009). Genes from the calcium channel family, especially *CACNA1C*, are the most robustly replicated findings among others (Bhat et al. 2012). In a recent large-scale GWA study, *CACNA1C* was one of the two genes to be associated with all the five major psychiatric disorders (SCZ, BD, MD, ADHD and ASD) (Smoller et al. 2013).

### 1.3. *CACNA1C* is a risk factor for psychiatric disorders

Single nucleotide polymorphisms (SNPs) and variations in the *CACNA1C* gene are among the most robustly replicated findings associated with psychiatric disorders. The initial evidence for a relation of *CACNA1C* with psychiatric disorders however came from a rare autosomal-dominant disorder called Timothy syndrome. The disorder is caused by single *de novo* gain-of-function mutations in the coding region (exon 8) of *CACNA1C* (G406R, G402S) resulting in a severe neurodevelopmental disorder with multiorgan dysfunction. Timothy syndrome is characterized by cardiac arrhythmias, syndactyly, long QTs, congenital heart disease, dysmorphic facial features, cognitive abnormalities and autistic features (Splawski et al. 2004; 2005). These gain-of-function mutations within exon 8/8A of the *CACNA1C* gene reduce voltage-dependent channel inactivation and increase calcium influx during depolarization (Splawski et al. 2005; Marcantoni et al. 2020). In addition to reduced channel inactivation, increased basal transcription and dysregulated gene activity have also been observed in models carrying G406R mutants (Servili et al. 2020). Subsequently, GWAS and meta-analyses of GWAS first associated variations in *CACNA1C* with BD and then with other psychiatric disorders as well (Kempton et al. 2009; Green et al. 2010; Jogia et al. 2011; Smoller et al. 2013). In a 2013 study, SNPs in the *CACNA1C* gene were associated with all five major psychiatric disorders – BD, SCZ, MD, ASD and ADHD (Smoller et al. 2013). More recent meta- and multivariate- analyses of GWAS have replicated these findings with significant association of *CACNA1C* with BD and SCZ in larger samples (Xia et al. 2019; Jia et al. 2019; Stahl et al. 2019; Amare et al. 2020; H. J. Li et al. 2021).

### 1.3.1. Risk variants of *CACNA1C* cause structural and functional changes in the human brain

SNPs in the *CACNA1C* gene (chromosome 12, 12p13.33: 1969552..2697950) are mostly located in non-coding intronic regions of the gene, with majority of them localized in intron 3, which is the largest intron of the gene (Bhat et al. 2012). Because these SNPs are in the non-coding region, it is not fully understood whether they increase or decrease channel expression and function (Bigos et al. 2010; Yoshimizu et al. 2015; Gershon et al. 2014; Ramasamy et al. 2014; Cosgrove et al. 2017). Despite lack of mechanistic understanding of SNP functions, several case-control clinical studies associated SNPs in the *CACNA1C* gene with structural and functional changes in the brain. One of the most robustly replicated and well-studied SNP in the gene is rs1006737, which has been associated with BD, SCZ, MD and ASD across different populations (Green et al. 2010; Y. Liu et al. 2011; Zheng et al. 2014; J. Li et al. 2015). For example, risk allele carriers of rs1006737 exhibit altered amygdala microstructures and reduced or increased activity in different brain regions and altered grey and white matter volumes (Kempton et al. 2009; Bigos et al. 2010; Erk et al. 2010; Perrier et al. 2011; Krug et al. 2014; Woon et al. 2014; Mallas et al. 2017; Koch et al. 2019). Gene expression analysis from post-mortem brain tissues revealed that the risk allele of rs1006737 is linked to increased *CACNA1C* mRNA expression (Bigos et al. 2010) while rs2007044 was associated with reduced mRNA expression (see Table 1 for more details) (Cosgrove et al. 2017; Ramasamy et al. 2014).

Another SNP, rs1024582, associated with SCZ and BD, showed a clear sex dimorphism with females carrying the minor allele showing greater hostility and other negative schizotypic traits. Furthermore, risk allele carriers also showed a decreased activity in various brain regions at rest as well as during a working memory task (Takeuchi et al. 2018). A case-control study with SCZ patients and healthy subjects also revealed similar associations of the rs2007044 risk allele with reduced brain activity and poor working memory (Z. Zhang et al. 2018). A summary of reported *CACNA1C* SNPs and their effects on brain structure and function can be found in Table 1. Though imaging studies have identified several SNPs in the *CACNA1C* gene to be associated with alterations in brain function and activity, the underlying molecular mechanisms that cause these changes remain obscure to date.

**Table 1: Summary of reported single nucleotide polymorphisms (SNPs) of *CACNA1C* and the phenotypes (observed in healthy controls and patients) associated with them. (= indicates no effect, × indicates impaired, ↑ and ↓ means enhanced or reduced effects respectively)**

SNP	Disorders	Risk allele	SNP position	Phenotype	References
rs1006737	BD, MD, SCZ	A	Intron 3: 2236129	↑ <i>CACNA1C</i> mRNA levels, ↑ hippocampal and prefrontal cortex (PFC) activity, ↑ amygdala volume and activation	(Bigos et al. 2010; Jogia et al. 2011; Lancaster et al. 2016; Sumner et al. 2015; Tesli et al. 2013; Wessa et al. 2010; Wolf et al. 2014)
				↓ activation of hippocampus, anterior cingulate cortex, and prefrontal cortex	(Erk et al. 2010; Erk, Meyer-Lindenberg, Linden, et al. 2014; Erk, Meyer-Lindenberg, Schmierer, et al. 2014; Jogia et al. 2011; Krautheim et al. 2018; Krug et al. 2014; Paulus et al. 2014)
				↑ Grey matter volume and ↓ functional connectivity in corticolimbic regions, × white matter integrity, ↓ white matter	(Kempton et al. 2009; Perrier et al. 2011; F. Wang et al. 2011; Woon et al. 2014; Mallas et al. 2017)
				Moderates early life stress effects on cortisol awakening response	(Klaus et al. 2018)
				× cognitive performance, ↓ semantic verbal fluency	(Lancaster et al. 2014; M. G. Soeiro-de-Souza et al. 2013; Sykes et al. 2018; Thimm et al. 2011; Krug et al. 2010)
				↑ anxiety	(Pasparakis et al. 2015)

				↓ outflow of information from medial frontal gyrus to left putamen	(Radua et al. 2013)
				age-related cortical thinning, × facial emotion recognition	(Márcio Gerhardt Soeiro-de-Souza et al. 2012; M G Soeiro-de-Souza et al. 2017)
<b>rs2051992,</b> <b>rs2239050,</b> <b>rs7959938</b>	BD	G C A	Intron 3: 2332160 Intron 3: 2338248 Intron 3: 2341299	↑ Brainstem volume	(Franke et al. 2010)
<b>rs1051375</b>	BD	G	Intron 42: 2679713	Altered amygdala activation, early onset age of BD	(X. Zhang et al. 2013)
<b>rs2007044</b>	SCZ	G	Intron 3: 2235794	Altered reversal learning, ↓ cortical surface area (in dorsolateral prefrontal cortex and superior parietal cortex), ↓ activation of PFC	(Sykes et al. 2018; Z. Zhang et al. 2018; Zheng et al. 2016; 2014)
<b>rs882195</b> <b>rs1024582</b>	SCZ	G T	Intron 3: 2241235 Intron 3: 2293080	N/A	(Zheng et al. 2014)
<b>rs1006737</b> <b>rs4765905</b>	ASD	G G	Intron 3: 2236129 Intron 3: 2240418	N/A	(J. Li et al. 2015)
<b>rs4765914</b>	BD, MD, SCZ	T	Intron 3: 2311211	↓ amygdala volume	(Sumner et al. 2015)
<b>rs10774035</b>	SCZ	T	Intron 3: 2259508	Females - × recovery from SCZ episodes	(Heilbronner et al. 2015)

<b>rs10466907</b>	BD	G	3' UTR: 2695810	× Cognitive recovery (following treatment for	(Lin et al. 2017)
<b>rs58619945</b>		G	Intron 1: 2051659	major depressive episode)	
<b>rs10848683</b>	SCZ	C	Intron 42: 2681964	Behavioral disorders,	(S.-Y. Zhang et al. 2017)
<b>rs2238032</b>		G	Intron 1: 2113566	emotional and thinking disorders, perceptual	
<b>rs2299661</b>		C	Intron 1: 2115062	disorders	
<b>rs1024582</b>	SCZ, BD	A	Intron 3: 2293080	Female carriers - ↑ harm avoidance, frequency of paranoia, ↓ intrapersonal emotional intelligence, better sleep quality, ↓ brain activity during rest and during working memory in PFC, medial temporal, and medial parietal areas	(Takeuchi et al. 2018)
<b>rs73248708</b>	MD	A	Intron 3: 2442003	Interacts with adult trauma to predict	(Dedic et al. 2018)
<b>rs11662568</b>		T	Intron 1: 2006994	depressive symptoms	
<b>4</b>					

#### 1.4. CACNA1C codes for the $\alpha 1$ subunit of the L-type voltage-gated calcium channel $Ca_v1.2$

Voltage gated calcium channels (VGCCs) are vital moderators of cell signaling that regulate intracellular calcium concentration and contribute to calcium signaling in excitable cells, including neuronal cells. Calcium ions act as second messengers, initiating electrical signaling, synaptic transmission and gene expression upon depolarization (Obermair et al. 2004; Berger and Bartsch 2014). Depending on their electrophysiological properties, VGCCs can be broadly classified into high voltage activated (HVA) VGCCs and low voltage activated (LVA) VGCCs (Catterall et al. 1988; Berger and Bartsch 2014; Nanou and Catterall 2018). HVA calcium channels include L-type, N-type, P/Q-type, and R-type calcium channels while T-type calcium channels belong to the

LVA calcium channel family. All VGCCs are multi-subunit complexes comprising of a pore forming, channel property determining  $\alpha 1$  subunit, an intracellular  $\beta$  subunit, a transmembrane  $\gamma$  subunit and an extracellular  $\alpha 2\delta$  subunit (**Figure 3**). Different subtypes of VGCCs are localized in different neuronal subcellular compartments indicating specific roles for each subtype in various neuronal functions. P/Q- and N-type channels are localized to presynaptic terminals and play a role in neurotransmitter release (Nanou and Catterall 2018). Whereas L-type calcium channels (LTCC) are mostly expressed in the postsynaptic somatic and dendritic regions of the neuron and are important for excitation-transcription coupling and expression of calcium-dependent genes post excitation (Nanou and Catterall 2018; Berger and Bartsch 2014; Zeeba D. Kabir, Martínez-Rivera, and Rajadhyaksha 2017). There are 4 main subtypes of LTCCs:  $Ca_v1.1$  to  $Ca_v1.4$ .  $Ca_v1.2$  and  $Ca_v1.3$  channels have a broad expression pattern and are found in the heart, the smooth muscles, the pancreas, the adrenal glands, and the brain.  $Ca_v1.1$  expression is restricted to the skeletal muscles and  $Ca_v1.4$  to the retinal cells (Sven Moosmang et al. 2005).

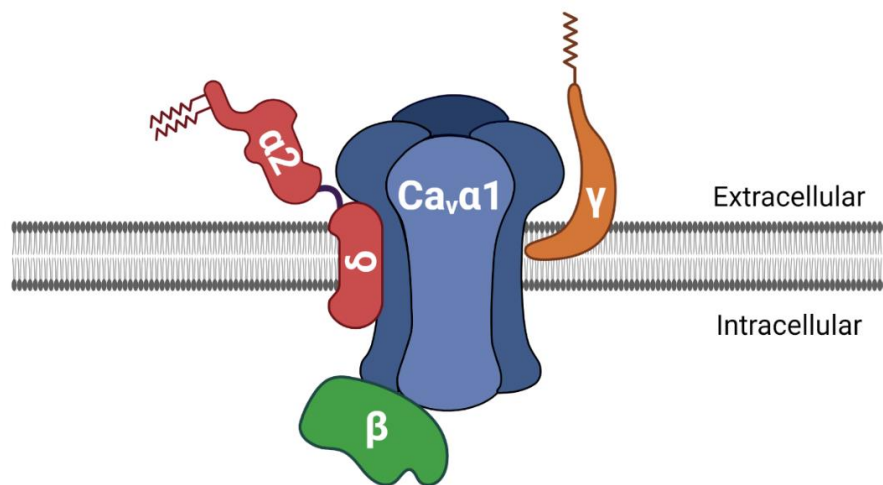


**Figure 3: Structure of a voltage gated calcium channel.** Voltage gated calcium channels are multi-subunit complexes consisting of a transmembrane pore-forming  $\alpha 1$  subunit, an intracellular  $\beta$  subunit that modulate current density by regulating channel open state probability, a transmembrane  $\gamma$  subunit that interacts with the voltage sensor on the  $\alpha 1$  subunit and an extracellular  $\alpha 2\delta$  subunit that regulates channel kinetics. (Image created with BioRender.com)

The *CACNA1C* gene, identified as a risk factor for psychiatric disorders, codes for the  $\alpha 1$  subunit of the  $Ca_v1.2$  calcium channel. As previously mentioned, the  $\alpha 1$  subunit is the pore-forming subunit that acts as a voltage sensor, selectivity filter, an ion conductivity pore and provides

binding sites for all calcium channel activators and blockers (Hofmann, Lacinová, and Klugbauer 1999).  $Ca_v1.2$  and  $Ca_v1.3$  are the predominant LTCCs in the brain with  $Ca_v1.2$  accounting for 89% of LTCCs and  $Ca_v1.3$  comprises of 11% (Berger and Bartsch 2014). Both channels have high levels of sequence and structural similarities and overlapping expression patterns. Due to the high degree of similarity between the two channels, they are indistinguishable by currently available agonists and antagonists.

Despite their overlapping expression patterns, recent studies have reported unique characteristics and contributions of the two channels in neuronal function and behavior (Zeeba D. Kabir, Martínez-Rivera, and Rajadhyaksha 2017). For example, analysis of expression patterns through development further revealed declining expression of  $Ca_v1.2$  mRNA in mouse cortex and hippocampus, with higher expression during embryonic and early postnatal stages (Schlick, Flucher, and Obermair 2010; Kramer et al. 2012).  $Ca_v1.3$  mRNA expression, on the other hand, was stable throughout development suggesting differential roles of the two channels through development and adulthood. To support this theory, a study by Dedic et. al., showed that embryonic deletion of  $Ca_v1.2$  channels in mouse forebrain glutamatergic neurons, resulted in impaired spatial memory and long term potentiation whereas deletion at adulthood resulted in improved memory in mice (Dedic et al. 2018).

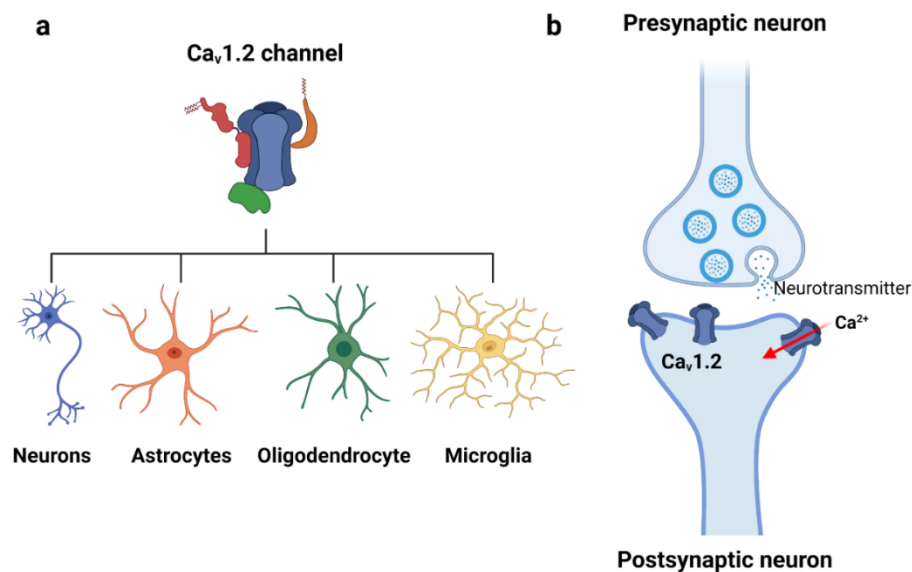


**Figure 4: Expression of Ca<sub>v</sub>1.2 calcium channels.** a) Ca<sub>v</sub>1.2 channels are expressed in different cell types of the brain - neurons, astrocytes, oligodendrocytes, and microglia. b) Ca<sub>v</sub>1.2 channels are mainly localized

in post synaptic neuronal dendritic spines and somato-dendritic regions (here expression is shown in a dendritic spine). (Image created with BioRender.com)

$Ca_v1.2$  LTCCs are expressed in neurons, oligodendrocytes, astrocytes and microglia (Cheli et al. 2016; 2018; Dedic et al. 2018; Nanou and Catterall 2018; Xinshuang Wang et al. 2019; Zamora et al. 2020; Pitman et al. 2020; Hopp 2021). They are mainly localized in postsynaptic dendritic spines and shafts and somatic regions of the neurons (**Figure 4**) (Leitch et al. 2009; Berger and Bartsch 2014; Zeeba D. Kabir, Martínez-Rivera, and Rajadhyaksha 2017). They are pivotal for experience-dependent plasticity in the brain and play key roles in processes involved in normal brain development and function.

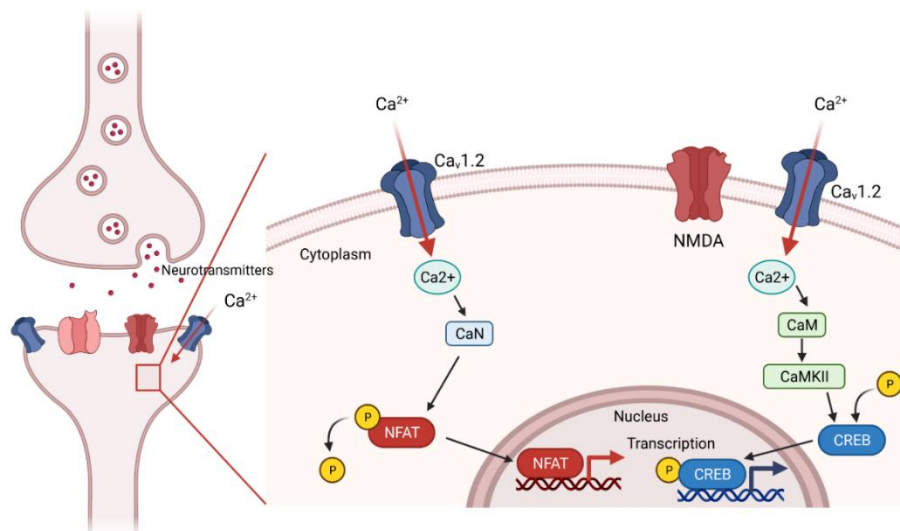


**Figure 5: Signaling cascades downstream of  $Ca_v1.2$  channels.** Entry of calcium ( $Ca^{2+}$ ) through  $Ca_v1.2$  channels after depolarization triggers a cascade of downstream signaling molecules that are required for activation and regulation of gene transcription. Abbreviations - CaN: calcineurin, NFAT: nuclear factor of activated T-cells, CamK:  $Ca^{2+}$ / calmodulin-dependent protein kinase, CREB: cAMP response element binding protein. (Image Created with BioRender.com)

*In vitro* and rodent studies have explored the functional role of  $Ca_v1.2$  channels in the brain.  $Ca_v1.2$  channels regulate activity dependent gene expression, also known as excitation-transcription (E-T) coupling (Wheeler et al. 2008; Marcantoni et al. 2020) and play a vital role in dendritic development (Morton et al. 2013; Krey et al. 2013), neuronal survival (Anni S. Lee et al. 2016; De Jesús-Cortés, Rajadhyaksha, and Pieper 2016), synaptic plasticity (Nanou and Catterall 2018),

memory formation, learning and behavior (Z. D. Kabir, Lee, and Rajadhyaksha 2016; Zeeba D. Kabir, Martínez-Rivera, and Rajadhyaksha 2017; Moon et al. 2018). Depolarization mediated calcium influx through  $Ca_v1.2$  channels along with other supporting proteins - like  $\beta$  subunit, AKAP (A-kinase anchoring protein) proteins and other kinases - triggers multiple signaling pathways such as the CAMKII ( $Ca^{2+}$ / calmodulin-dependent protein kinase II), MAPK/ERK (mitogen-activated protein kinase/ extracellular signal-regulated kinase) and Calcineurin/NFAT (nuclear factor of activated T-cells) pathways. This activates and translocates transcription factors like CREB (cAMP (cyclic adenosine monophosphate) response element binding protein) and NFAT to the nucleus, thereby triggering and regulating gene expression (**Figure 5**) (Berger and Bartsch 2014; Nanou and Catterall 2018).

### 1.5. Preclinical approaches to study psychiatric disorders

Practical limitations and challenges in accessing the living human brain to study higher order brain functions necessitate the need for animal models. These animal models help to improve our understanding of the neurobiological mechanisms involved in psychiatric disorders and to study pharmacological targets to treat the same (Nestler and Hyman 2010). Thus, animal models exhibiting endophenotypes of these complex psychiatric disorders serve as valuable preclinical tools. It is important here to distinguish between an animal model of psychiatric disorders and a behavioral test since the two terms are often ambiguously described. An animal model is analogous to the human pathological conditions, representing a complex range of cognitive and emotional symptoms and is used to understand the underlying biological processes in a disease condition. Whereas a behavioral test is essentially used for verifying the human symptomology in animals but is not specific to any disease (Teegarden 2012; Belovicova et al. 2017). Current advances in genetic engineering have provided the technology necessary for gene manipulations to generate animal models that can be used to study a particular disease. Rodent models are most popularly used in psychiatric disorders because of the ease with which genetic manipulations can be done and the many similarities in neuroanatomy, physiology and neurochemistry between human and rodent brains (Chadman, Yang, and Crawley 2009).

Transgenic rodent models are typically generated to target genes of interest that have previously been reported in human genetic and GWAS studies. With currently available genetic tools several modifications in rodents can be achieved - 1) addition of a new gene, 2) overexpression or

knockout of an existing gene including conditional tissue- and cell type-specific overexpression or knockouts, 3) knock-in of human disease-associated gene polymorphisms, 4) viral vector injections to generate knockdown or overexpression of genes in specific brain regions. But to be used as a disease model, rodent models need to fulfill the standard triad of requirements and the criteria for that include: construct validity, face validity and predictive validity (Jones, Watson, and Fone 2011; Chadman, Yang, and Crawley 2009).

Construct validity refers to the extent to which a method used to generate a particular animal model is relevant to the human disease etiology that is modeled. Face validity refers to the similarities of symptoms or characteristic features observed in the animal model to what is observed in the human disease. Predictive validity refers to the responses of the animal models to therapeutic treatments that are used in humans. However, due to the complex and heterogeneous nature of psychiatric disorders, generating rodent models that adhere to the standard triad of requirements can be challenging. For example, while some behavior aspects such as social withdrawal, anxiety, and working memory could be modeled with some approximation in rodents, other behavior traits such as hallucinations, delusions, sadness, or guilt which seem unique to humans are far more difficult or even impossible to model in animals. Thus, most studies employ a combination of genetic manipulations and behavioral assays that typically model individual components of disease symptoms to investigate and understand the neurobiological mechanisms depending on their hypotheses (Chadman, Yang, and Crawley 2009).

### **1.5.1. Sex as a biological variable in animal models**

Human clinical studies have repeatedly highlighted clear sex dimorphisms in psychiatric disorders. Women are twice as likely to develop anxiety, mood and other stress-related disorders as men (Bromet et al. 2011; Altemus, Sarvaiya, and Neill Epperson 2014). In SCZ, men are at a higher risk of early onset of disease and more negative symptoms compared to women (Aleman, Kahn, and Selten 2003; R. Li et al. 2016), whereas inconsistent gender roles have been reported in BD (Suwalska and Łojko 2014). Similarly, ADHD and ASD are reported more in men than in women (Werling and Geschwind 2013; Arnett et al. 2015).

Despite a clear distinction in diagnosis and manifestation of psychiatric disorders in clinical studies, preclinical research largely has a sex bias toward male animals. Analysis of published

articles in major biological fields showed a male bias in 8 out of the 10 fields analyzed, a strong bias seen especially in neuroscience (Shansky and Woolley 2016; Beery 2018). To curb this issue, a policy from the National Institute of Health (NIH) in 2014 urged scientists to consider sex as a biological variable (Arnegard et al. 2020). This mandate, however, has been met with equal amounts of support and criticism.

Bias toward use of male rodents arises mostly from certain presumptions: 1) females are more variable than males (this assumption is applied to both clinical and preclinical research), 2) female animals need to be tested across estrous cycle to account for variability arising from the impact of estrous cycle, 3) including both sexes in preclinical research increases variability and hence would require increased sample sizes. Multiple meta-analysis studies have however refuted these presumptions by showing that female rodents show an overall variability similar to male animals (Shansky and Woolley 2016; Becker, Prendergast, and Liang 2016; Beery 2018). A meta-analysis of gene expression in different tissues in mice and humans also showed no overall phenotypic variability between males and females (Itoh and Arnold 2015). Thus, inclusion of both sexes in preclinical research would provide valuable insights into the sex differences in the biological mechanisms that underlie disease manifestation.

### 1.6. Role of environmental factors in the etiology of psychiatric disorders

Family and twin heritability studies revealed the vital role of genetic factors in the etiology of psychiatric disorders. Heritability estimates from these twin studies range from around 80% for SCZ to 60-80% in BD and 41-49% in MD (Johansson et al. 2019; McGuffin et al. 2003; McMahon 2018; Corfield et al. 2017; Hilker et al. 2018; Cardno et al. 1999). A recent GWAS study reports considerably lower heritability estimates for the five major psychiatric disorders compared to family studies (between 17-28% for SCZ, BD, MD, ADHD and ASD) (S. H. Lee et al. 2013). Thus it could be hypothesized that in addition to genetic risk factors, other non-genetic factors such as environment also contribute to development of psychiatric disorders (Schmitt et al. 2014). Exposure to adverse experiences such as maternal separation, impoverished care, abuse or other traumatic events, especially during early life affects physiological and psychological development leading to an additive effect along with pre-existing genetics, thereby conferring risk to onset of psychiatric disorders (**Figure 6**) (Baram et al. 2012; Reinwald et al. 2018).

Maternal separation or inadequate maternal care is one of the major contributors of early life stress (ELS). In humans, adequate maternal care and attention are necessary to form secure attachments and this forms a basis for emotional regulation and social adeptness (Rincón-Cortés and Sullivan 2014). Cognitive and emotional deficits are associated with inadequate maternal care not only in humans, but also in non-human primates and rodents (Heim and Nemeroff 2001; Sánchez, Ladd, and Plotsky 2001). These studies attribute sensory signals from adequate maternal care to positively influence the developing brain and a lack thereof contribute to emotional and cognitive vulnerabilities in later life. Thus, there is a need to investigate the underlying mechanisms of environmental influences and their interaction with pre-existing genetic vulnerabilities in development of psychiatric disorders.

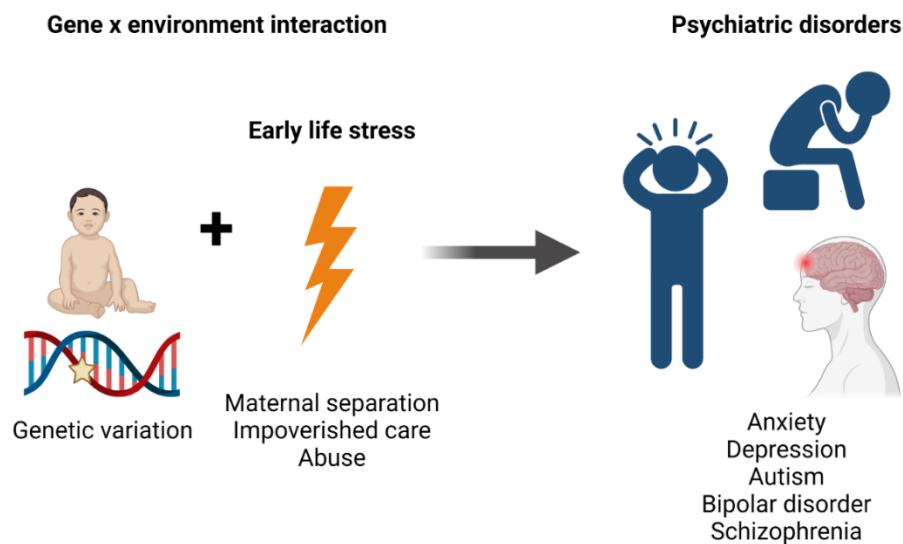


**Figure 6: Gene × environment interaction contributes to etiology of psychiatric disorders.** Genetic variations contribute to a small percentage of disease risk indicating that there are other risk factors involved in the development of psychiatric disorders. Early life adversity, which is one such example, can have an additive effect to pre-existing genetic variations, thereby leading to development of neuropsychiatric disorders in adulthood. (Image created with BioRender.com)

A number of clinical studies have attempted to explore such gene × environment interactions in relation to psychiatric disorders. In the context of *CACNA1C*, a study by Klaus et.al., showed that risk allele carriers of rs1006737 SNP had reduced cortisol awakening response (a biomarker of hypothalamic-pituitary-adrenal (HPA) axis regulation) which might be predictive of the susceptibility to ELS (Klaus et al. 2018). Although the exact mechanisms by which *CACNA1C*

interacts with the HPA axis is currently unknown, glucocorticoids are known to increase calcium channel expression and current (Karst et al. 2002; Chameau et al. 2007). Exposure to chronic stress and glucocorticoid release might increase calcium load and have deleterious long term effects on cell function (Joëls and Karst 2012). In another study, the *CACNA1C* risk allele in combination with childhood trauma suggested an increased vulnerability to schizotypal traits and increased or decreased ventral anterior cingulate cortex (vACC) activation depending on the minor/ major allele (Krautheim et al. 2018). Minor alleles of two other less studied SNPs, rs73248708 and rs116625684, were also shown to interact with adult trauma to increase the risk for depression (Dedic et al. 2018). Thus, to study the neurobiological mechanisms of gene  $\times$  environment interactions in the etiology of psychiatric disorders, stress paradigms specific for rodent models were designed.

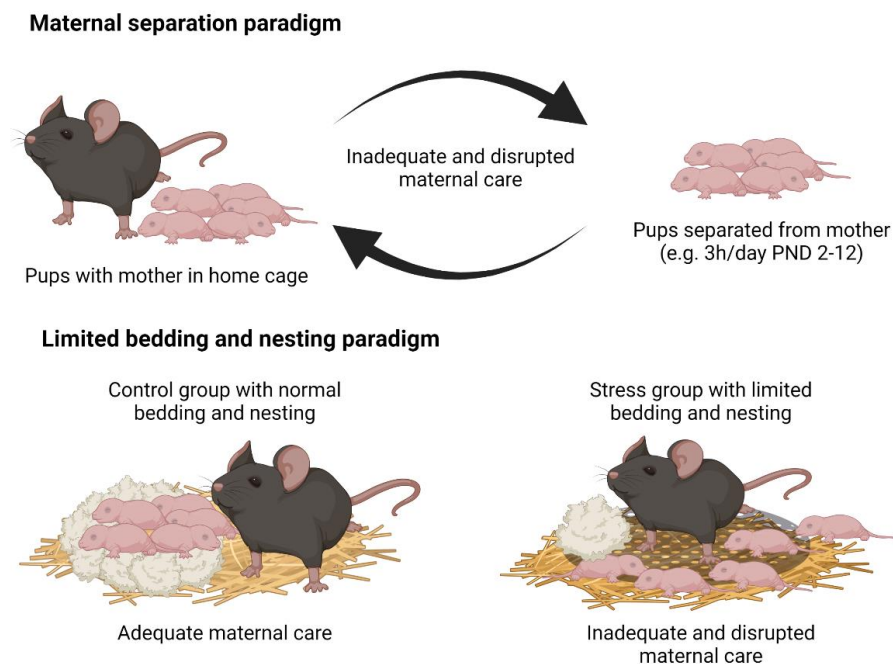


**Figure 7: Different types of early life stress paradigms used in rodents.** Maternal separation (top) is a commonly used well established early life stress paradigm where the pups are separated from the dams for extended periods of time over several days. It is also a clinically relevant model that targets aspects of childhood neglect. Limited bedding and nesting paradigm (bottom) is a more recently developed early life stress model that aims at inducing stress in pups by providing impoverished nesting environment for the dams. The impoverished environment affects the nursing behavior of the dams, thereby causing stressful situation for the pups. (Image created with BioRender.com)

Two commonly used methods to induce ELS in rodents are maternal separation (MS) and a more recently developed limited bedding and nesting (LBN) stress (**Figure 7**). MS is a well-established ELS model in rodents, where pups are separated from their mothers repeatedly for prolonged periods of time. This method is clinically relevant and illustrates aspects of childhood neglect. It is also associated with disrupted brain development and emotional and cognitive dysfunction in later life (Atrooz, Liu, and Salim 2019). Unlike human early life adversity, however, MS is highly predictable, might alter maternal behavior significantly and does not fully capture the poor parental care (Jenny Molet et al. 2014; Walker et al. 2017).

The LBN stress is a more recently developed model of impoverished environment during early life which leads to aberrant maternal care and thus stressful scenario for the rodents (Rice et al. 2008; Walker et al. 2017; Bolton et al. 2017). LBN stress is known to induce anxiety- and depression-related behaviors, deficits in social interaction and cognitive impairments, increased vulnerability to additional stress, along with structural changes such as reduced dendritic complexity and spine density and altered neurogenesis (Walker et al. 2017). Impaired memory performance, increased expression of the stress peptide corticotropin-releasing hormone (CRH), dendritic atrophy and LTP attenuation were observed in rats exposed to the LBN stress (Ivy et al. 2010). Similarly, reduced body weight, impaired spatial memory, disrupted long term potentiation (LTP) and reduced spine density were also seen in wildtype mice exposed to the LBN stress while genetic deletion of CRHR1 ameliorated these effects in LBN stressed mice (X. D. Wang et al. 2011; X.-D. Wang et al. 2012). Furthermore, LBN stress induced severe anhedonia in rodents along with altered pleasure/ reward and stress-network interactions and increased stress-related peptide CRH (Bolton, Molet, et al. 2018). Another study also showed a sex dependent effect of LBN stress, where stressed female mice but not males exhibited increased depression-related behavior (Goodwill et al. 2018). In addition, LBN stress has aggravating effects on models of neurodegeneration. When a mouse model of Alzheimer's disease was subjected to the LBN stress, it exacerbated A $\beta$  plaques, enhanced neuroinflammatory markers and reduced microglial complexity especially in the hippocampus (Hoeijmakers et al. 2017).

Other forms of stress, such as chronic unpredictable stress and chronic social defeat stress models have been vastly applied on mouse models of Ca<sub>v</sub>1.2. These studies report increased vulnerability associated with Ca<sub>v</sub>1.2 channels to develop stress-linked depression- and anxiety-related

phenotypes (Bavley et al. 2017; Chantelle E. Terrillion et al. 2017; Dedic et al. 2018). Effects of ELS on Ca<sub>v</sub>1.2 mouse models, however, are currently unexplored.

## 1.7. Delving into the physiology of Ca<sub>v</sub>1.2 channels

### 1.7.1. Studying Ca<sub>v</sub>1.2 channel function *in vitro*

Where access to the brain tissue proves to be a challenge and use of animal models is practically limited, *in vitro* studies proved resourceful in probing into the function and properties of LTCCs. From electrophysiological studies on brain slices to the use of induced pluripotent cells and other cells, *in vitro* studies have explored the diverse roles played by LTCCs.

Electrophysiological studies on aged rat hippocampal slices showed that LTCC facilitate long-term depression (LTD) during low synaptic activity whereas they impaired LTP upon high rates of synaptic activation (Norris, Halpain, and Foster 1998). This was probably one of the first studies to suggest an age-dependent role of Ca<sub>v</sub>1.2 channels in memory formation which has later been proven in rodent studies as well (Zanos et al. 2015; Dedic et al. 2018). Ca<sub>v</sub>1.2 channel deficiency at development and at adulthood had opposing effects on LTP and cognitive tasks. Mice with developmental deletion showed impaired LTP and cognitive flexibility, while mice with deletion of Ca<sub>v</sub>1.2 channels in adulthood showed enhanced LTP and better cognitive flexibility (Dedic et al. 2018).

Furthermore, another electrophysiological study identified two distinct types of LTP at thalamic circuits - LTCC-dependent and N-methyl-D-aspartate receptors (NMDAR)-dependent - an evidence supporting a role for LTCC in memory formation (Bauer, Schafe, and LeDoux 2002). In addition, studies *in vivo* revealed a differential role for the two LTP in fear memory formation where NMDAR-dependent LTP was required for both short-term and long-term memory, while VGCC-dependent LTP was required only for long-term memory formation. A similar differential role was also observed in a mouse model of Ca<sub>v</sub>1.2, where loss of Ca<sub>v</sub>1.2 channels resulted in a selective loss of NMDAR-independent late-phase LTP and spatial memory impairment (S. Moosmang 2005).

As mentioned previously, one of the main reasons for a male bias in rodent studies is related to possible effects of estrogen on behavior. Perhaps in support of this theory, an interesting study

revealed an interaction between estrogens and Ca<sub>v</sub>1.2 channels in hippocampal primary cultures and hippocampal slices (Sarkar et al. 2008). Low concentrations of estrogens reacted with Ca<sub>v</sub>1.2 channels to induce spinogenesis independent of the estrogen receptor. Although Ca<sub>v</sub>1.2 channels and estrogen interact *in vitro*, whether this interaction affects rodent behavior in Ca<sub>v</sub>1.2 models is yet to be investigated.

Other *in vitro* studies have mostly probed into the activation of downstream signaling cascades by Ca<sub>v</sub>1.2 channels. Introduction of Timothy syndrome mutations G406R and G402S into HEK 293 cells revealed that Ca<sub>v</sub>1.2 channels induce E-T coupling which requires the presence of auxiliary  $\beta$  subunit (Servili et al. 2018; 2020). Furthermore, depolarization-induced transcriptional activation was initiated by the Ras/ ERK/ CREB pathway. Timothy syndrome mutations caused slower channel inactivation due to reduced voltage- and calcium-dependent inactivation, which resulted in prolonged action potentials and calcium overload. Recording of spontaneous regenerative calcium transients (SRCaTs) in developing cortical neurons also revealed that Ca<sub>v</sub>1.2 channels are essential for neurite growth and radial migration of layer 2/3 cortical excitatory neurons (Kamijo et al. 2018). In summary, Ca<sub>v</sub>1.2 channels are a vital source of calcium that triggers a cascade of signaling pathways essential for development and maturation of the brain.

### 1.7.2. Pharmacological approaches: Calcium channel blockers

LTCC blockers such as verapamil and nifedipine are widely used to treat hypertension and angina. They might have some potential to be used as treatments for psychiatric disorders as well. LTCC blockers have been applied as experimental treatment for BD with no clear results but they induce other side effects like bradycardia, nausea, headaches, dizziness, weakness etc. (Dubovsky 2019). Pharmacological studies using LTCC activators and inhibitors imply a complex role for LTCCs in various brain functions including mood regulation and learning and memory. Dihydropyridine (DHP) drugs such as nifedipine are known to have anti-depressant properties in rodent models which were antagonized by the calcium channel agonist Bay K 8644 (Mogilnicka, Czyrak, and Maj 1988; Cohen, Perrault, and Sanger 1997). In contrast to DHP drugs, other LTCC blockers such as verapamil and diltiazem showed no such effects. This contrasting effect of different LTCC blockers has been attributed to different binding sites of DHP drugs and non-DHP drugs on the calcium channel (Cohen, Perrault, and Sanger 1997; Mogilnicka, Czyrak, and Maj 1988). Furthermore, LTCC blockers had ameliorating effects on age-related working memory deficits in

rodents and selectively impaired long term fear memory formation (Bauer, Schafe, and LeDoux 2002; Veng, Mesches, and Browning 2003). Studies with LTCC blockers also presented a role for LTCCs in drug dependence (Shibasaki, Kurokawa, and Ohkuma 2010). Pharmacological approaches using LTCC blockers in rodents provide some insights in the functioning of LTCCs but there are certain limitations. Firstly, systemic administration of high concentrations of LTCC blockers causes cardiovascular side effects, thereby increasing blood pressure and decreasing cardiac contractility. Thus, any phenotypes observed in *in vivo* studies, especially in experiments studying behavior, might be questionable and inconclusive at best. In addition, though LTCC blockers are specific for L-type calcium channels, distinction between subtypes  $Ca_v1.2$  and  $Ca_v1.3$  channels, both with overlapping expression patterns in the brain, is not possible, thus further limiting the use of this approach for *in vivo* studies (Sven Moosmang et al. 2005; Berger and Bartsch 2014).

### 1.7.3. Genetically modified rodent models

To overcome the limitations of lack of channel subtype discrimination by LTCC blockers, rodent models were generated using genetic approaches targeting specific channel properties and channel-specific genes. Studies with  $Ca_v1.2^{DHP-/-}$  mice with a selective elimination of DHP sensitivity of the  $Ca_v1.2$  channel revealed differential roles for  $Ca_v1.2$  and  $Ca_v1.3$  channels in activation of neuronal circuits as well as neurotransmitter release and a possible role of LTCC in mood disorders (Sinnegger-Brauns et al. 2004). One advantage of using this mouse model is that there are no compensatory effects from other calcium channels. However, this mouse model specifically targets  $Ca_v1.3$  channel activation and pharmacological interventions without insights into  $Ca_v1.2$  channel functions. Thus, a more targeted rodent model that is specific for the  $Ca_v1.2$  channels was required to investigate the role of  $Ca_v1.2$  channels in the brain.

One of the first genetic models designed to probe into  $Ca_v1.2$  channel functions used the Cre-lox recombination system to induce a cell type-specific deletion of  $Ca_v1.2$  channels in mouse forebrain glutamatergic neurons. This selective haploinsufficiency resulted in impaired spatial memory and loss of late-phase LTP (S. Moosmang 2005). Subsequently, many different models have been generated which either target the channel in a cell type-specific manner, focally in specific brain regions or pan-neuronal deletions of the channel in both mice and rats. Table 2 summarizes the different rodent models of  $Ca_v1.2$  targeting strategies and the phenotypes observed.

**Table 2: Summary of different animal models of Ca<sub>v</sub>1.2.** Genetic modifications used in different rodent models to study Ca<sub>v</sub>1.2 channel deletion effects on behavior and molecular phenotypes. (= indicates no effect, × indicates impaired, ↑ and ↓ means enhanced or reduced effects respectively)

Transgenic line	Targeting strategy	Rodent model	Phenotype	References
<b>Ca<sub>v</sub>1.2<sup>HCKO</sup> Inactivation in cerebral cortex and hippocampus</b>	Conditional Nex-Cre mediated inactivation	Mice	× spatial learning, × NMDAR-independent LTP, × CREB activation	(S. Moosmang 2005)
<b>Ca<sub>v</sub>1.2-Dev<sup>Glu-CKO</sup> Glutamatergic neuron-specific deletion</b>	Nex-Cre mediated	Mice	↑ anxiety, hyperlocomotion, × social interaction, ↑ active stress coping behavior, × cognitive flexibility	(Dedic et al. 2018)
<b>Ca<sub>v</sub>1.2<sup>CKO</sup> Forebrain deletion</b>	Conditional CamKII-Cre mediated inactivation	Mice	× remote (long-term) spatial memory	(White et al. 2008)
<b>Forebrain-cacna1c cKO (fbKO) Forebrain-specific inactivation (~70% elimination in hippocampus, prefrontal cortex, basolateral amygdala, striatum, and nucleus accumbens)</b>	CamKII-Cre mediated	Mice	↑ anxiety-like behaviors, × social behavior, × learning and memory, ↑ E/I ratio, ↓ protein synthesis, ↓ neuronal survival	(A S Lee et al. 2012; Anni S. Lee et al. 2016; Z. D. Kabir et al. 2017)
<b>Ca<sub>v</sub>1.2-Ad<sup>Glu-CKO</sup> Glutamatergic neuron-specific deletion in adults</b>	Camk2α-CreERT2 mediated inactivation induced by tamoxifen	Mice	= anxiety, social interaction, stress coping, partial hyperlocomotion, ↑ cognitive flexibility	(Dedic et al. 2018)

<b>cKO</b>	CamKII-Cre mediated	Mice	× dependence-induced alcohol seeking	(Uhrig et al. 2017)
<b>HET constitutive haploinsufficiency</b>	-	Mice	↓ exploratory behavior, ↓ response to amphetamine, antidepressant-like behavior, = working memory, prevented ageing-induced memory impairments in males, attenuates dopamine reuptake, altered locomotor response to dopamine-acting psychostimulants, ♀-specific <b>behaviors</b> - ↓ risk-taking behavior, ↑ attenuation of amphetamine-induced hyperlocomotion, ↓ learned helplessness and startle response	(Dao et al. 2010; Zanos et al. 2015; C E Terrillion et al. 2017)
<b>Ca<sub>v</sub>1.2<sup>ACC/Cre</sup> Inactivation in anterior cingulate cortex</b>	Cell permeable peptide based Cre-mediated inactivation	Mice	× observational fear learning, ↓ pain responses, = anxiety and innate fear	(Jeon et al. 2010)
<b>Ca<sub>v</sub>1.2<sup>NesCre</sup> Inactivation in whole CNS</b>	Conditional Nestin-Cre mediated inactivation	Mice	=pain perception, locomotor activity, motor balance, conditioned fear acquisition and brain morphology	(Langwieser et al. 2010)
<b>Ts2-neo Heterozygous G&gt;A point mutation in exon 8A</b>	Red/ET recombineering technology and homologous recombination	Mice	= physical characteristics, motor abilities and reflexes, = anxiety, locomotor, and diurnal rhythm, hypoactivity in novel environment, ↑ repetitive behavior, ↓ social preference, persistent fear memories, ↑ serotonin tissue content and	(Bader et al. 2011; Bett et al. 2012)

				axon innervation of dorsal striatum, ↑ active stress coping	
<b>Ca<sub>v</sub>1.2<sup>CKO</sup> Pan-neuronal deletion</b>	Conditional Syn1-Cre mediated inactivation	Mice		= anxiety, = contextual fear conditioning, × context discrimination and extinction of contextual fear, = spatial learning, × spatial learning when presented with limited cues in water maze, × neurogenesis and cell proliferation in dentate gyrus, shift in E/I balance	(Temme et al. 2016; Temme and Murphy 2017)
<b>Cacna1c conditional knockout Nucleus accumbens-specific deletion</b>	Viral based Cre mediated deletion (AAV-CMV-Cre-GFP)	Mice		↑ anxiety, ↑ susceptibility to social defeat stress	(Chantelle E. Terrillion et al. 2017)
<b>HET Specific deletion in prefrontal cortex</b>	Viral based Cre mediated deletion (AAV-CMV-Cre-GFP)	Mice		Antidepressant-like effect, ↓ REDD1 protein expression	(Zeeba D. Kabir et al. 2017)
<b>D1-cacna1c KO Specific deletion in dopamine receptor D1R expressing neurons</b>	Drd1-Cre mediated deletion	Mice		Attenuated extinction of conditional place preference, = CamKII and GluA1 phosphorylation levels in hippocampal post-synaptic density, persistent contextual fear, ↑ anxiety, × remote spatial memory, ↑ young hippocampal neuronal death	(Burgdorf et al. 2017; Bavley et al. 2020)
<b>Cacna1c<sup>-/-</sup> Specific deletion in 5-HT serotonergic neurons</b>	Tamoxifen induced Tph2iCre	Mice		= locomotor, ↑ anxiety, ↓ stress coping behavior, ↑ immobility, ↑ Fos expression in caudal	(Ehlinger and Commons 2019)

	mediated inactivation		dorsal raphe nucleus sub regions	
<b>Conditional deletion in oligodendrocyte progenitor cells (OPCs)</b>	NG2-CreER mediated Tamoxifen injection at P10 and P30	Mice	↓ myelin protein expression, OPC proliferation, myelinating oligodendrocytes, and migration	(Cheli et al. 2016)
<b>TgGlast-CreER/ <i>Cacna1c</i><sup>fl/fl</sup>/ RCE:loxP (Deletion in astrocyte-like stem cells)</b>	Inducible Glast-Cre mediated	Mice	↓ cell proliferation, ↓ neurons and ↑ astrocytes under differentiation conditions, ↓ neurogenesis	(Völkening et al. 2017)
<b>Inducible conditional KO in GFAP-positive cells</b>	GFAP-CreER <sup>T2</sup> mediated inactivation	Mice	↓ astrocyte and microglia activation, ↓ inflammation during demyelination, promotes remyelination in cuprizone model of myelin injury and repair	(Zamora et al. 2020)
<b>CreER: <i>Cacna1c</i><sup>fl/fl</sup></b>	Pdgfra-CreER mediated	Mice	↑ proliferation of OPCs, = oligodendrocyte numbers or myelination, ↓ OPC density in corpus callosum	(Pitman et al. 2020)
<b>HET <i>Cacna1c</i> heterozygous knockout</b>	Targeted inactivation of <i>Cacna1c</i> using Zinc-finger nuclease technology	Rat	= locomotion, anxiety, startle response, altered reversal learning, ↓ BDNF expression in prefrontal cortex, = spatial learning, reversal learning, reward sensitivity, cognitive flexibility, × socio-affective communication with sex-specific effects (hypermasculinization in female haploinsufficient rats)	(Sykes et al. 2018; Braun et al. 2018; Kisko et al. 2018; 2020)

The studies mentioned in Table 2 report mostly consistent phenotypes - increased anxiety, impaired social behavior, and cognitive deficits - with some exceptions. In addition, rodent studies have also indicated a role for Ca<sub>v</sub>1.2 channels in alcohol and drug dependency (Uhrig et al. 2017). Aside from specific deletions in neurons, mouse models harboring deletion in glial cells such as oligodendrocytes and astrocytes have provided us with further insights into the diverse roles played by Ca<sub>v</sub>1.2 channels. Not only do Ca<sub>v</sub>1.2 channels affect behavior, but they are also vital for neural cell fate decision, neuronal survival, and myelination and may even play a role in neuroinflammation. Thus, genetic models are useful tools to further explore the functional role of the Ca<sub>v</sub>1.2 channels in the etiology of psychiatric disorders and the underlying neurobiological mechanisms.

## 2. Objectives of the study

Association of SNPs in the *CACNA1C* gene with psychiatric disorders have been one of the most robustly replicated findings in GWA studies. A considerable number of studies have also reported an interaction of *CACNA1C* with stress in both clinical and preclinical reports. However, there are still several questions unanswered in terms of underlying mechanisms involved. This thesis aimed to address the following three questions.

### Objective 1: How do the $Ca_v1.2$ channels interact with early life stress in mice?

Clinical studies have shown that *CACNA1C* SNPs interact with early life adversity where the risk allele predicts vulnerability to stress (Klaus et al. 2018; Dedic et al. 2018). Preclinical  $Ca_v1.2$  mouse models exposed to chronic social defeat stress or chronic unpredictable stress also exhibited increased susceptibility to stress-associated depression- and anxiety-related phenotypes (Bavley et al. 2017; Chantelle E. Terrillion et al. 2017; Dedic et al. 2018). However, there are currently no studies that have explored the interaction of the  $Ca_v1.2$  channels with ELS in mice. We thus designed an experiment to expose  $Ca_v1.2$ -Nex mice (with a specific deletion of  $Ca_v1.2$  channels in glutamatergic neurons of the forebrain) to the LBN early life stress paradigm.  $Ca_v1.2$ -Nex animals are already known to show strong behavioral alterations compared to their control littermates (Dedic et al. 2018). Thus, I wanted to test if LBN stress in combination with the  $Ca_v1.2$  channel deletion would have an additional effect on those behavioral phenotypes. Furthermore, it is well known that chronic stress results in dendritic atrophy and  $Ca_v1.2$  channels are involved in structural plasticity including neurite elongation (Ivy et al. 2010; Morton et al. 2013; Walker et al. 2017; Kamijo et al. 2018). Thus, I wanted to explore the combined gene  $\times$  environment effects on cellular morphology and proteins downstream of  $Ca_v1.2$  signaling that are known to be involved in dendritic branching.

### Objective 2: Do female $Ca_v1.2$ -Nex conditional knockout mice exhibit behaviors previously reported in males?

Previous studies in  $Ca_v1.2$  mouse models have largely focused on male animals, including a study from our lab using the  $Ca_v1.2$ -Nex mice (Dedic et al. 2018). A major reason for such a bias is that the estrous cycle in female mice would introduce high variability in behavioral studies. In the context of  $Ca_v1.2$  channels, one *in vitro* study even revealed an interesting interaction between estrogen and  $Ca_v1.2$  channels. The study showed that low levels of estrogen could enhance  $Ca_v1.2$

signaling and result in spinogenesis in hippocampal cultures (Sarkar et al. 2008). Thus, I wanted to explore the phenotype of female  $Ca_v1.2$ -Nex animals in a behavioral test battery and whether the estrous cycle interacts with  $Ca_v1.2$  channels to affect the behavioral phenotype. Furthermore, I wanted to investigate the effect of  $Ca_v1.2$  channel deletion on dendritic morphology of hippocampal pyramidal neurons in female mice and further probe into the proteins involved in dendritogenesis.

### **Objective 3: How does $Ca_v1.2$ channel deletion in GABAergic neurons affect the behavioral phenotype of mice?**

One of the theories postulates that dysfunction of GABAergic neurons might contribute to the development of psychiatric disorders (Rossignol 2011; Marín 2012).  $Ca_v1.2$  channels are also known to play a role in maturation of parvalbumin positive interneurons (Jiang and Swann 2005). As summarized in Table 2, several conditional mouse models of  $Ca_v1.2$  exist. These models harbor modifications targeting  $Ca_v1.2$  channels either in all neurons or specifically in glutamatergic, serotonergic or dopaminergic neurons or in glial cells (S. Moosmang 2005; Cheli et al. 2016; Burgdorf et al. 2017; Ehlinger and Commons 2019; Zamora et al. 2020). To our knowledge no study has explored the role of  $Ca_v1.2$  channels specifically in GABAergic neurons. Thus, I designed experiments to generate and characterize mice harboring  $Ca_v1.2$  channel deletion in all GABAergic neurons and more specifically in parvalbumin positive GABAergic neurons using respective Cre driver mouse lines.

### 3. Materials and methods

#### 3.1. Animals

All animal experiments were conducted in accordance with and approved by the Guide of the Care and Use of Laboratory Animals of the Government of Bavaria, Germany. Mice were 4-6 months of age at the time of experimentation unless otherwise mentioned. Mice were group housed (unless mentioned otherwise) in standard IVC cages under standard laboratory conditions ( $22 \pm 1^\circ\text{C}$ ,  $55 \pm 5\%$  humidity) and were maintained on a 12-hour light-dark cycle (lights on between 6:00 am and 6:00 pm) with *ad libitum* food and water.

#### 3.2. Animal handling before and during behavioral testing

Mice were marked by ear-punching at weaning and a small tail-tip cut was taken for genotyping. Animals were transported to the experimental rooms at least a week prior to behavioral testing and weighed and handled by the experimenter whenever necessary prior to testing procedures. Mice were group housed or single housed whenever necessary depending on the experimental procedures. Animals were monitored for scars or wounds throughout the testing procedures and their weights recorded every four days or daily as required by the experiments.

#### 3.3. Transgenic mouse lines

$\text{Ca}_v1.2$ -Nex transgenic line with *Cacna1c* inactivation specifically in the forebrain glutamatergic neurons during development was generated by breeding heterozygous Nex-Cre mice with *Cacna1c*<sup>+/*lox*</sup> or *Cacna1c*<sup>*lox/lox*</sup> mice. Through this breeding control (Ctrl) animals (*Cacna1c*<sup>*lox/lox*</sup>) and conditional knockout (CKO) animals (*Cacna1c*<sup>*lox/lox*</sup>:*Nex-Cre*) were obtained.  $\text{Ca}_v1.2$ -GABA mouse line was generated by breeding mice with heterozygous inducible Cre-line *Gad2-CreER*<sup>T2</sup> mice with *Cacna1c*<sup>*lox/lox*</sup> mice to obtain *Cacna1c*<sup>*lox/lox*</sup> and *Cacna1c*<sup>*lox/lox*</sup>:*Gad2-CreER*<sup>T2</sup>. *Cacna1c* inactivation specifically in GABAergic inhibitory neurons was achieved upon tamoxifen administration via food or intraperitoneal injection.  $\text{Ca}_v1.2$ -PV transgenic mouse line was generated by breeding PV-Cre mice with *Cacna1c*<sup>*lox/lox*</sup> mice to obtain control (*Cacna1c*<sup>*lox/lox*</sup>) and PV-CKO (*Cacna1c*<sup>*lox/lox*</sup>:*PV-Cre*) mice with *Cacna1c* deletion specifically in parvalbumin expressing GABAergic neurons. All the transgenic lines included a modified allele of the ribosomal protein Rpl22, which upon Cre recombination activates a HA-tagged (Ribotag) variant of Rpl22. This feature was used as a Cre-dependent reporter for validation of the different lines by immunofluorescence staining.

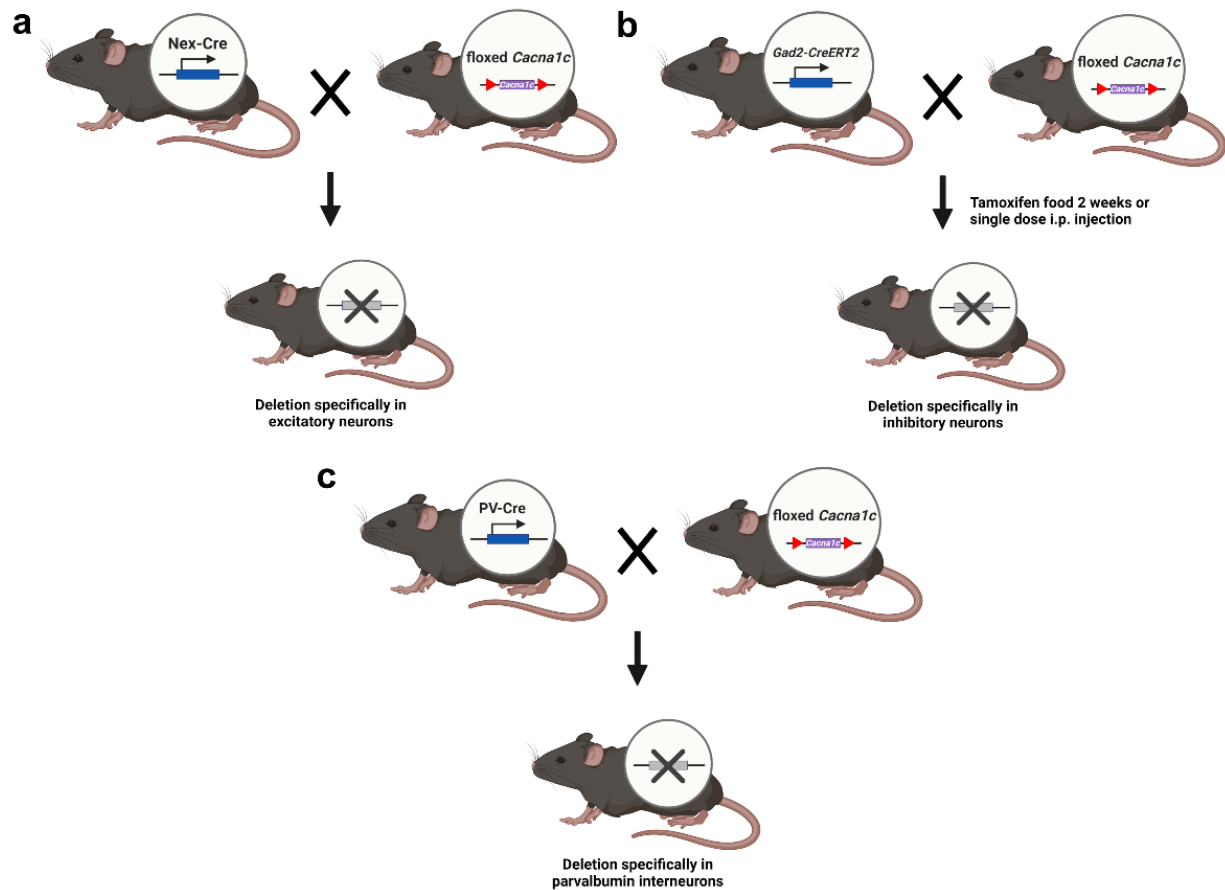


**Figure 8: Mouse models used in this study.** a)  $Ca_v1.2$ -Nex mouse line where floxed *Cacna1c* mice are crossed with Nex-Cre driver mice to obtain controls and CKO mice. b)  $Ca_v1.2$ -Gad2ERT2 mouse line where floxed *Cacna1c* mice are crossed with Gad2-CreERT2 Cre driver mice. Cre recombination is achieved by tamoxifen administration. c)  $Ca_v1.2$ -PV mouse line where floxed *Cacna1c* mice are crossed with PV-Cre driver mice to obtain controls and CKO-PV mice. (Image created with BioRender.com)

### 3.4. Genotyping

Tail biopsies were collected, digested and genomic DNA was isolated for genotyping. 2  $\mu$ l of DNA was amplified by PCR and the product separated by gel electrophoresis. The gels were imaged with a Quantum ST4 gel documentation system and software. The following primers were used for the PCR:

**Table 3: Primers used for genotyping the different transgenic mouse lines**

Gene	Primers	PCR product size
<b>Nex-Cre</b>	5'-AGAATGTGGAGTAGGGTGAC-3'	Wildtype: 770 bp
	5'-CCGCATAACCAGTGAAACAG-3'	Mutant: 525 bp
	5'-GAGTCCTGGAATCAGTCTTTTTC-3'	
<b>Cacna1c</b>	5'-TGGCCCCTAAGCAATGA-3'	WT + lox: 415 bp + 500 bp
	5'-AGGGGTGTTCAGAGCAA-3'	bp
	5'-CCCCAGCCAATAGAATGCCAA-3'	Mutant: 281 bp
<b>Ribotag</b>	5'-GGGACGCTTGCTGGATAT-3'	Wildtype: 243 bp
	5'-TTTCCAGACACAGGCTAAGTACAC-3'	Mutant: 290 bp
<b>Gad2-CreER<sup>T2</sup></b>	5'-ACGTTTCCTGTCCCTGTGTG-3'	Wildtype: 500 bp
	5'-CAGACGCTGCAGTCTTTCAG-3'	Mutant: 280 bp
	5'-AGGCAAATTTTGGTGTACGG-3'	
<b>PV-Cre</b>	5'-AAATGCTTCTGTCCGTTTGC-3'	Wildtype: 500 bp
	5'-ATGTTTAGCTGGCCCAAATG-3'	Mutant: 163 bp
	5'-CAGAGCAGGCATGGTACTA-3'	
	5'-AGTACCAAGCAGGCAGGAGA-3'	

### 3.5. Tamoxifen administration via food and intraperitoneal injection

For the validation of the Ca<sub>v</sub>1.2-GABA mouse line, Cre recombination was activated by tamoxifen administered either via food (400 mg/kg tamoxifen citrate) or intraperitoneal injection (**Figure 9**). One cohort of animals was administered tamoxifen-containing food for two weeks. After the administration and a 1-week washout period, the animals were sacrificed, and brain tissue harvested. For a second cohort, 100 mg/ml tamoxifen diluted in corn oil or vehicle was administered via a single intraperitoneal injection. One week after the injection, the brain tissues were harvested for immunofluorescence staining procedures.

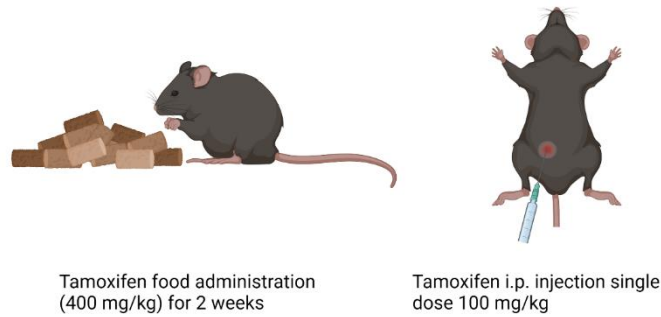


**Figure 9: Tamoxifen administration via food or intraperitoneal injection.** Cre recombination was activated by tamoxifen administration. One cohort of animals were provided with tamoxifen food (400 mg/kg) for two weeks and sacrificed after a 1-week washout period. Another cohort of animals were administered with a single dose of tamoxifen at 100 mg/kg concentration via intraperitoneal injection and sacrificed after a week. (Image created with BioRender.com)

### 3.6. Early life stress – limited bedding and nesting paradigm (ELS - LBN)

50 breeding pairs (Males - *Nex-Cre*<sup>+/*cre*</sup>: *Cacna1c*<sup>+/*lox*</sup>: *Ribotag*<sup>*tg*/*tg*</sup>; females - *Nex-Cre*<sup>+/*+*</sup>: *Cacna1c*<sup>+/*lox*</sup>: *Ribotag*<sup>*tg*/*tg*</sup>) were set up to acquire the required genotypes and to perform the early life stress paradigm. The LBN stress was performed as previously described (**Figure 10**) (Rice et al. 2008).

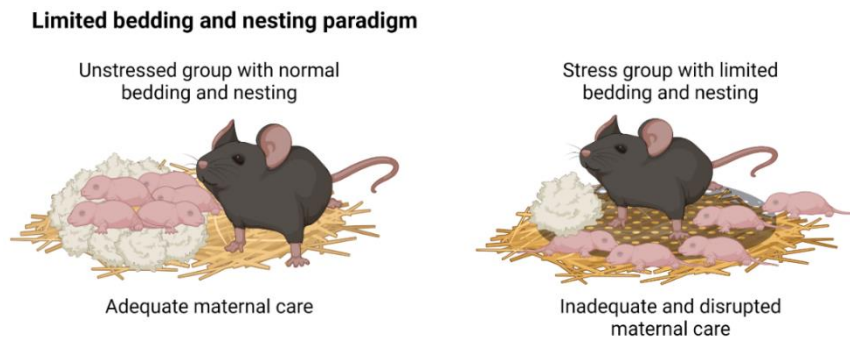


**Figure 10: Limited bedding and nesting stress.** Animals in the unstressed group are provided with normal amount of bedding and nesting materials. Thus, dams provide sufficient maternal care to the pups. Stressed group animals are provided with reduced bedding and nesting material thereby disrupting maternal interaction with pups and creating a stressful early life environment. (Image created with BioRender.com)

Briefly, the males were separated from the females after 14 days and females were checked daily for offspring. The birth of the pups was considered day 0. At day 2, the female mice and their pups were assigned to unstressed or ELS groups randomly. The unstressed group was housed in a

normal cage with normal amount of bedding and 1 complete nestlet. The ELS group was housed in a cage with a metal grid on the floor of the cage, reduced bedding and half a nestlet. The litter sizes were maintained to up to 10 animals per litter with a balanced sex ratio. The LBN stress was conducted for 7 days (day 2 to day 9) after which all the animals were returned to normal housing conditions. The pups were weaned at day 24-26 and their ears were marked for identification. The pups were weighed on day 9 (immediately after LBN stress) and at weaning. Behavior tests were conducted at 4 - 6 months of age. For the behavioral testing following the LBN stress, male animals were single housed and female animals were kept in group house conditions due to space constraints. Brain tissues were processed for either molecular or cellular studies after behavior testing.

### 3.7. Estrous cycle determination

For estrous cycle determination, vaginal lavages were collected (**Figure 11**). Sample collection was carried out in the afternoon between 03:00 pm and 05:00 pm.

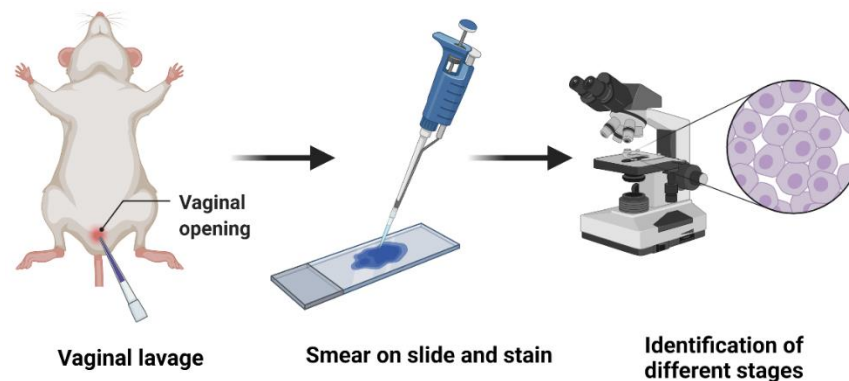


**Figure 11: Estrous cycle determination.** Vaginal lavages are collected and smeared on slides. The smears are stained, and the different estrous cycle stages are determined based on the different cell types observed. (Image created with BioRender.com)

The mice were placed on the food grid with the rear end elevated for easy sample collection. 40  $\mu$ l of 1 $\times$  PBS was aspirated on the vaginal canal using a pipette taking care not to penetrate the opening. PBS was aspirated 4-5 times or until the solution became cloudy. The fluid was then spread on a glass slide. After sample collection, the smears were allowed to dry at 37°C for 30 minutes. Once dry, the slides stained with Wright-Giemsa (Sigma, #WG16-500ML) stain for 30 seconds and then placed in water for 3 minutes. The slides were then rinsed off with water to

remove the excess stain and allowed to dry. Once dry, the samples were observed under a bright field microscope to determine the various stages of the cycle using the following criteria:

**Table 4: Various stages of the estrous cycles and their characteristic features**

<b>Cycle stage</b>	<b>Description</b>
<b>Proestrous</b>	Presence of small and large nucleated epithelial cells, round in shape, found in clusters. The sample appears blue/ light blue to violet in color.
<b>Estrous</b>	Presence of cornified squamous epithelial cells, densely packed clusters and anucleated or with ghost nucleus. Sample appears blue/ light blue in color.
<b>Metestrous</b>	Presence of small leukocytes and cornified squamous epithelial cells. Sample appears dark purple/ blue purple.
<b>Diestrous</b>	Abundant presence of leukocytes along with some nucleated epithelial cells and very few cornified squamous epithelial cells. Sample appears dark purple.

### 3.8. Behavioral experiments

All behavioral experiments were conducted between 09:00 am and 05:00 pm. The animals were group housed or single housed depending on the experiments. The video recording and analysis were conducted using ANY-Maze software (Version 4.3, Stoelting Co., Wood Dale, Illinois), unless mentioned otherwise.

#### Home cage activity

Activity in the home cage was monitored using an automated infrared tracking system (Mouse-E-motion 2.3.6, Infra-E-Motion, Hagendeel, Germany). Animals were single housed for the home cage activity measurements and the animals were left undisturbed for 7 days after the monitor was set up. The activity data was taken after a day of habituation (day 2) for 96 hours to obtain an accurate measure of activity during both light and dark cycles.

#### Open field test (OFT)

Locomotor activity and anxiety-related behavior was assessed using the open field test apparatus (**Figure 12**). The apparatus (50 × 50 × 40 cm) was virtually divided into an outer zone and an inner zone (30 × 30 cm) and evenly illuminated (10-20 Lux). The mice were placed in a corner at the

beginning of the test and allowed to freely explore the apparatus for 30 minutes. Total distance travelled, time spent in the inner zone and number of inner zone entries were assessed.

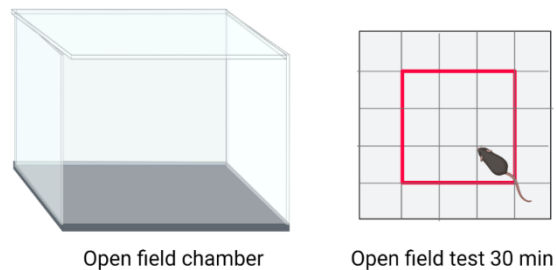


**Figure 12: Open field apparatus.** Open field test was performed for 30 mins. Total distance travelled, time spent in the inner zone (marked by red square) and number of inner zone entries were calculated. (Image created with BioRender.com)

### Elevated plus maze test (EPM)

The elevated plus maze test was used to assess anxiety-related behavior in mice. A plus shaped elevated maze (30 cm) with two opposite open arms (5 × 30 cm), two closed arms (30 × 5 × 15 cm) and a central zone (5 × 5 cm) was used (**Figure 13**). The illumination in the open arms was 30 lux and <10 lux in the closed arms. The animals were placed in the central zone facing one of the closed arms and were allowed to freely explore the maze for 10 minutes. Total distance travelled, time spent in the open arms and number of open arm entries were assessed.

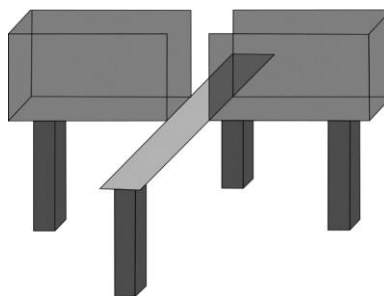


**Figure 13: Elevated plus maze apparatus.** EPM test was performed for 10 minutes. The apparatus is plus shaped with two closed arms, two open arms and a center zone. Total distance travelled, time spent in open arms and number of open arm entries were assessed using ANY-Maze. (Image created with Inkscape)

### Light/ Dark box test (LDB)

The light/ dark box test is another test that assesses anxiety-related behavior in mice. The apparatus consisted of a smaller dark chamber (15 × 25 × 21 cm) and a brightly illuminated chamber (30 ×

25 × 21 cm) that were connected by a small tunnel (5 × 7 cm) (**Figure 14**). The illumination in the bright chamber was maintained at 700 lux to create a highly aversive environment. The mice were placed in the dark chamber and allowed to freely explore for 10 minutes. The parameters assessed included latency to enter the lit zone, number of entries into and time spent in the lit zone.



Light/ dark box test 10 min

**Figure 14: Light/ dark box apparatus.** LDB test was performed for 10 mins. The apparatus consists of a smaller dark chamber and a larger brightly lit chamber (700 lux). Latency to enter brightly lit zone, number of entries into and time spent in the lit zone were calculated. (Image created with BioRender.com)

### Three-chambered social interaction test (3CT)

The three-chambered social interaction test assesses sociability and social novelty preference in mice (**Figure 15**). The testing apparatus (50 × 25 × 40 cm) consists of three chambers: two larger outer chambers (19 × 25 × 40 cm) and a center chamber (12 × 25 × 40 cm). Two small openings connect the three chambers. The illumination in the apparatus was maintained at 30 lux. The conspecific mice used as social mice in the test were 8-12 weeks old in the ELS experiments and 4 months old otherwise and were pre-habituated to the holding cups for two days prior to testing. The paradigm consists of three stages with no inter-stage intervals. For each mouse, all three stages were performed before moving to the next animal. The scoring was done manually, and the parameters assessed were time spent in each chamber, time spent sniffing the empty holding cups and time spent sniffing the social mice during stages 2 and 3.

First stage:

The first stage is the habituation stage. The wire holding cups were placed in the top corners of the outer chambers. The test animals are placed in the center chamber and allowed to explore the apparatus freely for 10 minutes. At the end of 10 minutes, the test animal was removed from the apparatus and placed in the home cage.

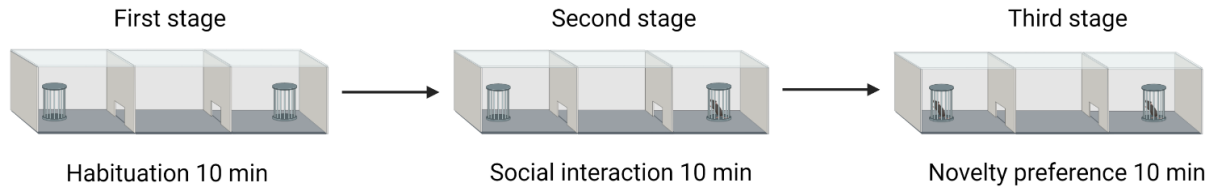


**Figure 15: Three-chambered social interaction test.** 3CT test consists of three stages: habituation, sociability, and novelty preference stages each lasting for 10 mins without inter-stage intervals. For each test mouse all stages were performed before moving to the next mouse. Time sniffing the empty cups or social mouse was manually calculated. (Image Created with BioRender.com)

Second stage:

In the second stage, an adult conspecific mouse (social mouse 1) was placed in one of the holding cups randomly and the other one was left empty. The test animal was placed in the center chamber and allowed to freely explore the apparatus for 10 minutes. After the testing time, the test animal was returned to its home cage. The time spent sniffing the social mouse or the empty cup and the time spent in the left or right chambers were scored and sociability was calculated according to the formula:

$$\text{Sociability} = \frac{\text{Interaction time with social mouse 1}}{\text{Total interaction time with both holding cups}} \times 100$$

Third stage:

In the third stage, a novel conspecific mouse (social mouse 2) was placed in the other empty holding cup. The test animal was again placed in the center chamber and allowed to explore the apparatus freely for 10 minutes. After completion of the test, the test animals and the conspecifics were returned to their respective home cages. The time spent sniffing the novel mouse versus the familiar mouse and the time spent in the chambers was scored and the novelty preference and discrimination index were calculated accordingly:

$$\text{Novelty preference} = \frac{\text{Interaction time with social mouse 2}}{\text{Total interaction time with both social mice}} \times 100$$

$$\text{Discrimination index} = \frac{\text{Interaction time with (social mouse 2 – social mouse 1)}}{\text{interaction time with both social mice}}$$

### Novel object recognition (in open field apparatus) (NOR)

The novel object recognition (NOR) test is an effective way of testing different phases of learning and memory. Here it was used to assess short term recognition memory. The open field apparatus (50 × 50 × 40 cm) was used for the testing paradigm and illumination was maintained at 30 lux (**Figure 16**).

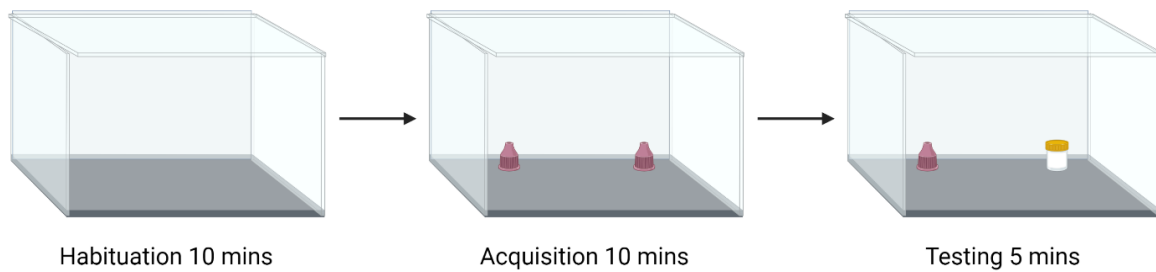


**Figure 16: Novel object recognition task.** NOR test was performed in three stages: habituation, acquisition, and testing. Animals were habituated to the open field chamber during the habituation stage. During the acquisition stage, animals were allowed to interact with two familiar objects. During testing stage, one object is replaced with a novel object and the time spent interacting with the novel object is calculated. (Image created with BioRender.com)

Objects of different shapes and patterns (two similar and one novel) were used in the test. The test consisted of three stages: Habituation, acquisition, and testing stage. The test animals were first habituated to the open field apparatus for 15 minutes. Then during the acquisition stage, two similar objects were placed equidistant to one another and close to the top part of the arena. The animals were allowed to explore the objects for 10 minutes. At the end of the acquisition stage, the test animals were returned to their home cage for a 20-minute inter-trial interval (ITI). After the interval, one of the objects was replaced with a novel object and the test animals were returned to the arena to explore for 5 minutes. The time spent interacting with the familiar objects during acquisition stage and the time spent interacting with the novel object during the testing stage were scored manually. The object bias, total interaction times, novelty preference and discrimination index were calculated accordingly.

$$\%Object\ bias = \frac{Interaction\ time\ with\ object\ 1}{Total\ interaction\ time\ with\ both\ objects} \times 100$$

$$\%Total\ interaction\ time = \frac{Total\ interaction\ time\ with\ both\ objects}{Total\ time\ of\ the\ experiment} \times 100$$

$$\%Novelty\ preference = \frac{Interaction\ time\ with\ novel\ object\ or\ novel\ location}{Total\ interaction\ time\ with\ both\ objects} \times 100$$

$$Discrimination\ index = \frac{Interaction\ time\ (novel\ object - familiar\ object)}{Total\ interaction\ time\ with\ both\ objects}$$

### Y maze test

Y maze spontaneous alternation test was used to measure spatial working memory. The apparatus consisted of three opaque arms at 120° angle from each other (30 × 10 × 15 cm) (**Figure 17**). Illumination in the testing apparatus was maintained at 30 lux. The arms were virtually labeled clockwise as A, B and C starting with the left arm. The test animal was introduced in the arm C facing the wall and was allowed to freely explore the maze for 10 minutes.

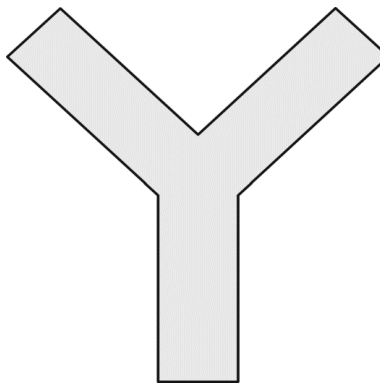


**Figure 17: Y maze apparatus.** Y maze spontaneous alternation task was performed for 10 mins. The animals were allowed to explore the apparatus and number of spontaneous alternations were calculated manually. (Image created with Inkscape)

The number of triads (for example: ABC, BCA, CAB...) and the total number of arm entries were scored manually while the total distance travelled in the maze was measured using the ANY-Maze video tracking system. The percentage of spontaneous alternations was calculated using the following formula:

$$\%spontaneous\ alternation = \frac{Number\ of\ triads}{Total\ number\ of\ arm\ entries - 2} \times 100$$

### Novel object and Spatial object recognition in the Y maze apparatus (NOR and SOR)

The NOR and SOR tests were performed in the Y maze apparatus for Ca<sub>v</sub>1.2-Nex female mice and Ca<sub>v</sub>1.2-PV mice (**Figure 18**).

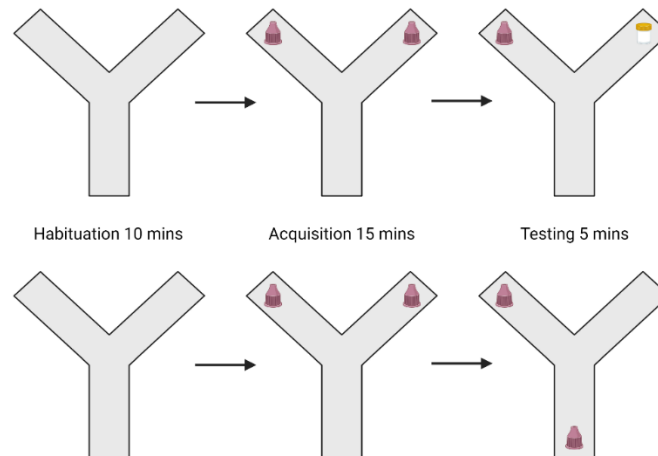


**Figure 18: Novel (top) and spatial (bottom) object recognition in Y maze apparatus.** Animals were habituated to the Y maze and then NOR and SOR acquisition and testing stages were performed as described above. Object interaction times were calculated manually and the novelty preference, object bias and discrimination index were calculated according to the formula given above. (Image created with BioRender.com and Inkscape)

Here lego blocks assembled in different shapes (two similar and one novel) were used as objects in the test. The tests consisted of three stages: habituation (10 minutes), acquisition (15 minutes) and test (5 minutes) with an ITI of 20 minutes between the acquisition and test stages. The objects were placed at the end of arms A and B during the acquisition stage for both NOR and SOR tests and cues of different shapes were used for SOR tests to help the animals orient themselves. During the testing stage of the NOR, the familiar object was replaced with a novel object in either arm A or arm B randomly. Similarly, during the testing stage of the SOR, the object from either arm A or arm B was moved to arm C randomly. The object interaction times were scored manually and novelty preference, object bias and discrimination index were calculated accordingly.

$$\%Object\ bias = \frac{Interaction\ time\ with\ object\ 1}{Total\ interaction\ time\ with\ both\ objects} \times 100$$

$$\%Total\ interaction\ time = \frac{Total\ interaction\ time\ with\ both\ objects}{Total\ time\ of\ the\ experiment} \times 100$$

$$\%Novelty\ preference = \frac{Interaction\ time\ with\ novel\ object\ or\ novel\ location}{Total\ interaction\ time\ with\ both\ objects} \times 100$$

$$Discrimination\ index = \frac{Interaction\ time\ (novel\ object - familiar\ object)}{Total\ interaction\ time\ with\ both\ objects}$$

### Morris water maze (MWM)

The Morris water maze test is another cognitive test used to study spatial learning and memory. The apparatus was a large cylindrical tank with a diameter of 150 cm and height of 40 cm filled with water up to 35 cm high (**Figure 19**). The tank was virtually divided into four quadrants: northeast, northwest, southeast and southwest. A circular platform (10 cm × 30 cm) was submerged just below the water at the center of southwest quadrant. Large cues of different shapes were placed on the four walls of the testing room to help mice orient themselves while swimming and to find the platform. The test consisted of three stages: training, probe test and long-term probe test.

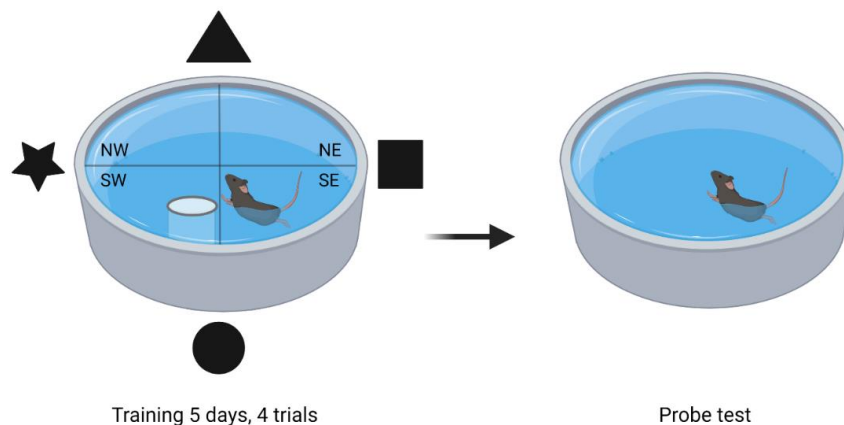


**Figure 19: Morris water maze.** MWM was performed in two stages: training and probe test. Training was performed for five days, four trials per day where the animals were trained to find the platform. The platform was placed in the southwest (SW) quadrant (left) (NW - northwest, NE - northeast, SE - southeast, SW -

southwest). During probe test, the platform is removed, and animals are allowed to swim freely (right). Time spent in each quadrant was calculated. (Image created with BioRender.com)

The training stage consisted of five training days with four trials per day. Each mouse was released from a different direction in each trial and trial sessions lasted for about 90 seconds with an inter-trial interval of 20 minutes. If the mouse reached the platform before the session was over, it was allowed to sit on the platform for 10 seconds before drying them and returning them to the home cage. If a mouse did not reach the platform within the 90 seconds, it was guided to the platform and allowed to sit there for 20 seconds. The latency to reach the platform in every trial was measured and average latencies per training day were calculated.

The probe test was conducted on day 6, 24 hours after the last training session. The platform was removed, and the animals were released from the northeast quadrant. The animals were allowed to swim freely for 1 minute and the time spent in each quadrant was measured. The long-term probe test was performed 7 days after the last training day and lasted for 1 minute per mouse. The platform was removed from the southwest quadrant and the animals were released from the northeast quadrant. They were allowed to swim freely, and the time spent in each quadrant was measured.

### Sucrose preference test

The sucrose preference test was used to study hedonic behavior after the stress paradigm. The animals were single housed, and the test was conducted for 10 days (**Figure 20**).

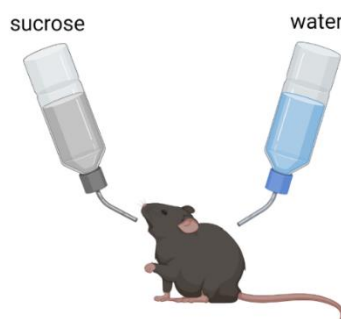


**Figure 20: Sucrose preference test.** Animals were single housed and sucrose preference test was performed in their home cages for 10 days. Amount of sucrose consumed was calculated and plotted. (Image created with BioRender.com)

The metal food grids contained two slots for bottles - one bottle was filled with water while the other was filled with 1% sucrose solution. The bottles were weighed before the start of the test to measure the starting volume. After that, the weight of the bottles was measured every day to obtain the amount of water or sucrose consumed by the animal. An average percentage of sucrose solution consumed was calculated at the end of the test period.

### **Forced swim test (FST)**

The forced swim test was used to assess the animal's stress coping behavior in an aversive environment. A two-liter glass beaker (radius: 11 cm, height: 23.5 cm) filled with water up to 1.5 liters was used as the apparatus (**Figure 21**). The water was maintained at room temperature (25°C). Each animal was placed in the water and allowed to swim for 6 minutes. Time spent struggling, swimming, and floating was scored manually.

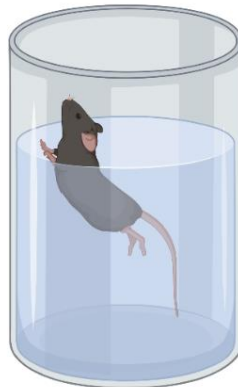


**Figure 21: Forced swim test.** The forced swim test was performed for 6 mins. Time spent struggling, swimming, and floating was scored manually. (Image created with BioRender.com)

A mouse was considered to be struggling if they were vigorously swimming, with all four paws involved and reaching behavior to find an escape, with front paws breaking the surface of water, usually at the walls of the beaker. A mouse was considered to be swimming if the movement involved only two limbs in a goal directed manner. A mouse was considered to be floating, if it stopped all movements except for those necessary to keep its head above water.

### **3.9. Golgi-cox staining**

One week after the behavioral test procedures, the animals were sacrificed, and fresh brain tissues were collected. Golgi-cox staining was done to study the cellular morphology of neurons at basal

levels. Golgi-cox staining was performed as directed in the superGolgi Kit from Bioenno (Catalogue number 003010, Bioenno Tech). The freshly harvested brain tissues were directly placed in 10 ml of solution A (impregnation solution) from the kit in brown glass bottles. The solution was replaced with new solution after 2 days. The brains were stored in solution A at room temperature and in a dark area for a total of 14 days. After 14 days, the brains were transferred to post-impregnation buffer (solution B - 30% sucrose diluted in distilled water). Solution B was refreshed after one day and the brains were stored in solution B until they could be processed. The brain tissues were cut at 150  $\mu\text{m}$  thickness using a vibratome. 6% sucrose in distilled water was used as a cutting solution. The brain sections were collected in a 24-well plate containing 30% sucrose solution. The brain sections were stored in the 24-well plates until further processing. Gelatin-coated slides were prepared by dipping superfrost plus glass slides (Thermoscientific, product number 11950657) in 3% gelatin dissolved in water at 55°C and drying them for at least 2 days prior to use. The brain sections were carefully mounted on the slides (8 sections per slide) using a wide brush. The remaining sucrose solution on the slide was removed by pressing a soft tissue gently on the slide to ensure attachment of sections to the slide. A small amount of sucrose solution was placed on the sections to avoid fragmented sections due to long exposure to air. The slides were then stored overnight, and the post-staining procedures were performed on the next day. The slides were washed in 0.01 M PBS-Triton X-100 for 30 minutes and placed in a diluted solution C from the kit (3:5 dilution with H<sub>2</sub>O) for 20 minutes in a closed staining jar stored in a dark area. Following that, the slides were moved to post-staining buffer solution D for 20 minutes, also placed in a dark area. The slides were washed in 0.01 M PBS-Triton for 30 minutes. The sections were then dehydrated in 100% ethanol for 40 minutes and cleared in xylol (xylene substitute) for 30 minutes. Coverslips were placed on the slides using the DPX mounting medium, and the slides were allowed to air dry overnight. The slides were stored in a dark area at room temperature until imaging.

### **3.10. Image data acquisition and analysis in NeuroLucida**

Images from Golgi-cox staining were obtained using a bright field microscope (Zeiss Axio Imager M2) and the NeuroLucida software (v.2017, MicroBrightField, USA). Briefly, neurons from CA1 region of dorsal hippocampus were selected. A total of 20 neurons were traced per animal and 4 - 5 animals were used per group (Ctrl vs CKO). Neurons with at least three completely stained dendritic trees were selected for tracings. The tracings were done live with 40 $\times$  lens using the

NeuroLucida software and the required data such as sholl analysis and branched structure analysis were obtained with the NeuroLucida explorer. The data was further processed for plotting of graphs. Spines on secondary and tertiary branches were also traced live with 100× oil lens for spine density analysis. Total number of spines and total length of the dendritic segments were obtained from branch segment analysis on NeuroLucida explorer, and the spine density was calculated as follows:

$$\text{Spine density}/\mu\text{m} = \frac{\text{Total number of spines}}{\text{Total length of dendritic segment}}$$

### 3.11. Protein extraction, Bradford assay and Western blot

Hippocampus and prefrontal cortex (PFC) were dissected from fresh brain tissues and homogenized in 500  $\mu\text{l}$  1× RIPA buffer (50 mM Tris, pH 8.0, 150 mM NaCl, 0.1% SDS, 1% Triton X-100 and 0.5% Na deoxycholate). For the Bradford protein assay, serial dilutions of bovine serum albumin (BSA) were prepared from a stock concentration of 1 mg/ml as standards for the standard curve and the protein samples were diluted accordingly. A 96-well plate was used for the Bradford assay. 100  $\mu\text{l}$  of the standards and samples were pipetted into the wells in triplicates. 5× Bradford protein assay reagent (BioRad, #500-0006) was diluted 1:1 with water. 50  $\mu\text{l}$  of the diluted Bradford reagent was added to each well and incubated for 5 minutes at room temperature. The optical density (O.D.) of the samples was measured at 595 nm using the microplate reader (Cytation 3 cell imaging multi-mode reader, BioTek instruments Inc.). The unknown protein concentrations were calculated from the standard curve. For Western blotting experiments, 20 - 40  $\mu\text{g}$  of protein samples were loaded and separated in 10% SDS-PAGE and then transferred to 0.45  $\mu\text{m}$  PVDF membranes (Millipore). The membranes were blocked in 5% milk-PBST (1× PBS + 1 ml tween 20) for one hour at room temperature and then incubated in primary antibodies at 1:1000 dilutions in 5% milk-PBST overnight. Primary antibodies used include pCREB (Millipore, #06-519), and  $\beta$ -actin (Cell signaling, #4967S) (Table 5). The membranes were washed with PBST and incubated in 1:5000 dilutions of secondary anti-rabbit IgG HRP-conjugated antibody (Cell signaling, #7074S). Chemiluminescence signals were visualized and captured in a ChemiDoc station (BioRad) and analyzed using ImageJ (Fiji).

### 3.12. Immunofluorescence staining for HA-tag

Mice were euthanized and fresh brains were harvested for HA-tag immunofluorescence staining. Freshly harvested brains were snap frozen on dry ice and stored in  $-80^{\circ}\text{C}$  until further processing. The brains were sectioned at  $20\ \mu\text{m}$  thickness using a cryostat, collected on slides, and stored in  $-20^{\circ}\text{C}$  until further use. For immunofluorescence staining procedures, the sections were fixed in ice cold 4% paraformaldehyde (PFA) in  $1\times$  PBS for 15 minutes at room temperature. The slides were then rinsed in  $1\times$  PBS three times for 5 min each and placed in a blocking buffer ( $1\times$  PBS, 5% normal goat serum (NGS), 0.3% triton X-100) for 60 minutes. A barrier was drawn on the edges of the slides using a hydrophobic marker (Immedge hydrophobic barrier PAP pen, Vector laboratories, #H-4000) and placed horizontally in a slide box. Wet tissues were placed beneath the slides to create a humidifying chamber to avoid drying of solutions.

**Table 5: List of primary and secondary antibodies used for western blot and immunofluorescence experiments**

Antibody	Concentration	Company
HA-Tag	1:1000	Cell Signaling #C29F4
cFos	1:1000	Abcam # ab190289
Alexa Fluor 594	1:1000	Life technology #A11037
Alexa Fluor 568	1:500	Invitrogen #A11036
pCREB	1:1000	Millipore, #06-519
$\beta$ -actin	1:1000	Cell signaling, #4967S
Anti-rabbit IgG HRP-conjugated	1:5000	Cell signaling, #7074S

Primary antibodies (the antibodies used, and their concentrations are given in table 5 below) were diluted in required concentrations in an antibody buffer ( $1\times$  PBS, 1% BSA, 0.3% Triton X-100) and about  $500\ \mu\text{l}$  of the antibody solution were pipetted on the slides. The sections were incubated in primary antibody overnight at  $4^{\circ}\text{C}$ . The slides were then rinsed in  $1\times$  PBS three times for 5 min each. A fluorochrome-conjugated secondary antibody (Table 5) diluted in antibody buffer was placed on the slides and incubated for 2 hours at room temperature. The slides were again rinsed in  $1\times$  PBS three times for 5 minute each. Coverslips were placed on the slides with Fluoromount-G mounting medium with DAPI (Southern Biotech, #0100-20) and the slides were left to dry at

room temperature overnight. Images were acquired using Olympus SlideScanner VS120S6 and processed using ImageJ (Fiji).

### 3.13. Immunofluorescence staining for cFos quantification

For cFos quantification, mice were anaesthetized with isoflurane and transcardially perfused with 4% PFA 90 minutes after forced swim test. Brains were extracted and post-fixed in 4% PFA overnight at 4°C. Brains were then moved to 30% sucrose and stored at 4°C until further processing. Brains were sectioned at 50 µm thickness (series of 6), collected in 24-well plates containing antifreeze solution (Glycerol: Ethylene glycol: 1× PBS – 1:1:2 ratio) and stored at -20°C until further processing. For immunofluorescence staining, brain sections were first washed in 1× PBS three times for 5 minutes each, then blocked in blocking solution (1.5% NGS, 0.3% Triton X-100 and 1× PBS) for 60 minutes at room temperature. Brain sections were incubated in cFos antibody diluted at 1:1000 concentration (Table 5) in antibody solution (1.5% NGS, 0.3% Triton X-100 and 1× PBS) at 4°C for 48 hours. After 48 hours, brain sections were washed three times in 1× PBS for 5 mins each and incubated in secondary antibody Alexa Fluor 568 (Table 5) in antibody solution for 2 hours at room temperature. Brain sections were again washed three times in 1× PBS and mounted on slides. Coverslips were placed on the slides with Fluoromount-G mounting medium with DAPI (Southern Biotech, #0100-20) and the slides were left to dry at room temperature overnight.

### 3.14. Image acquisition and cFos cell quantification

20 brain regions potentially activated during the FST according to previously reported studies, were selected based on the Paxinos and Franklin's mouse brain atlas (Franklin and Paxinos 1997) (**Figure 22**). Images were acquired using Olympus SlideScanner VS120S6. An overview of each slide was obtained to identify each brain region. 200 µm × 200 µm square regions of interest were drawn across the different brain regions and Z stack images of these areas were taken at 20× magnification with a Z distance of 20 µm and Z spacing of 1 µm. Images were taken from two consecutive sections and image processing and analysis was done using ImageJ. For pre-processing of images, bioformats plugin (<https://www.openmicroscopy.org/bio-formats/downloads/>) was downloaded to open .vsi files from the slide scanner. Max intensity images were obtained in ImageJ and type adjusted to 8-bit images. The threshold was set between 70-255 for an 8-bit image and if some cells were overlapping, watershed function was used to

separate them. For automatic quantification of cFos positive cells, “analyze particles” function in ImageJ was used. The cell size criteria were set at  $16 \mu\text{m}^2$  - infinity and circularity at 0.00 - 1.00. Outlines of cells and summary results were obtained. In cases of high background which fell within threshold range, the cells were counted manually.

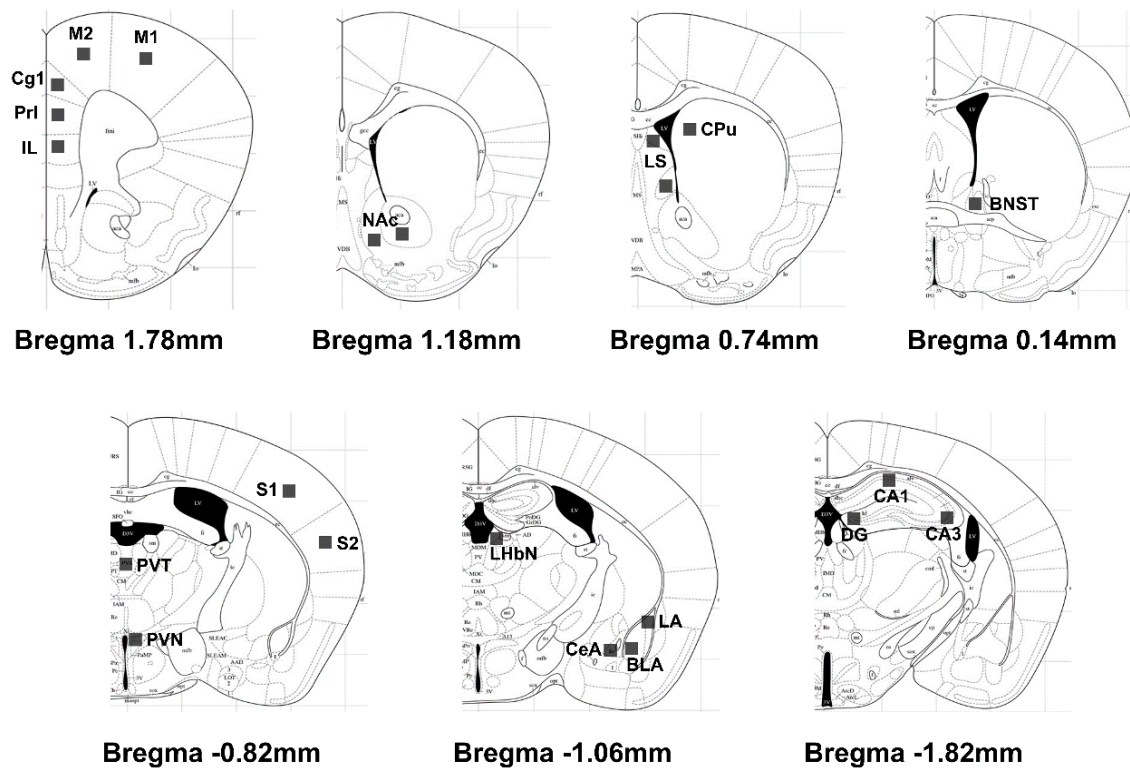


**Figure 22: 20 selected brain regions for cFos positive cell quantification.** The brain regions include: M1 - primary motor cortex, M2 - secondary motor cortex, Cg1 - cingulate cortex, PrL - prelimbic cortex, IL - infralimbic cortex, NAc - nucleus Accumbens, CPu - caudate putamen, LS - lateral septum, BNST - bed nucleus of stria terminalis, S1 - primary somatosensory cortex, S2 - secondary somatosensory cortex, PVT - paraventricular thalamic nucleus, PVH - paraventricular hypothalamic nucleus, LHbN - lateral habenular nucleus, LA - lateral amygdala, BLA - basolateral amygdala, CeA - central amygdala, DG - dentate gyrus.

### 3.15. minPROFILER assay

minPROFILER assay was performed in collaboration with Prof. Dr. Moritz Rossner, Department of Psychiatry and Psychotherapy, LMU Klinikum, Munich, Germany as per their set protocols (Herholt et al. 2018). Briefly, primary neurons from cortices of embryonic day E15.5  $\text{Ca}_v1.2$ -Nex mice were isolated and cultured. 21 genetically encoded pathway sensors (consisting of cis-regulatory elements) linked to EXT barcodes and luciferase were packed into adeno-associated

viruses (AAVs). DIV12 (days *in vitro*) primary neurons were infected with these minPROFILER-containing AAVs and stimulated with different concentrations (0.1 M, 1 M, 10 M, and 100 M) of bicuculline (BIC),  $\alpha$ -Amino-3-hydroxy-5-methyl-4-isoxazolepropionic acid (AMPA), N-methyl-D-aspartic acid (NMDA), brain-derived neurotrophic factor (BDNF), Forskolin and phorbol 12-myristate 13-acetate (PMA). RNA was isolated after 4 hours; 24 hours and 48 hours of stimulation and deep sequencing of the barcodes was performed to obtain expression levels of pathway sensors post-stimulation.

### 3.16. Statistical analyses

All statistical analyses were conducted using GraphPad Prism version 8.0. For early life stress experiments, effects of genotype and stress on all phenotypes were measured using two-way ANOVA. Genotype differences in all other experiments were measured using Student's t-test (two tailed). In places where more than two groups were compared, One-way ANOVA was used. Time-dependent measures were calculated using repeated measures analysis of variance (RM-ANOVA). Bonferroni post-hoc tests were performed whenever necessary. Data were considered as statistically significant if  $p < 0.05$ . All data are represented as mean  $\pm$  S.E.M.

## 4. Results

### 4.1. Early life stress (ELS) – Limited bedding and nesting (LBN) paradigm

Stress is a known environmental factor that contributes to the development of psychiatric disorders in addition to genetic risk factors. To understand gene  $\times$  environment interaction and its impact on the behavioral phenotype of mice, I subjected the  $Ca_v1.2$ -Nex mouse line to the LBN stress paradigm. Out of 50 breeding pairs, 33 pairs gave birth to pups. The genotypes of animals used in the behavioral testing are listed in Table 6.

**Table 6: Genotypes of the animals that were used for behavioral testing following the LBN stress.**

Cre	lox	HA-tag
+/+ or +/-cre	+/+	tg/tg
+/-cre	lox/lox	tg/tg

#### 4.1.1. LBN stressed animals exhibit reduced body weight at day 9 and at weaning

As a first step to confirm stress effects, I weighed the pups at two time points - day 9 when the stress paradigm ended and day 26 at weaning and monitored the loss of pups and litter sizes. Both groups had similar litter sizes at weaning despite loss of pups (Student's t-test,  $t_{31} = 0.4931$ ,  $p = 0.6254$ ) (**Figure 23b**). The stressed (ELS) litters showed a slightly higher number of lost pups compared to unstressed (US) litters (Student's t-test,  $t_{31} = 1.874$ ,  $p = 0.0703$ ) (**Figure 23c**). ELS male and female animals showed a significant reduction in their body weights at day 9 compared to the US group (Student's t-test, male:  $t_{70} = 3.338$ ,  $p = 0.0014$ ; female:  $t_{107} = 4.13$ ,  $p < 0.0001$ ) (**Figure 23d, f**). In ELS males, the reduced body weight persisted until weaning compared to US males, whereas ELS females only showed a trend toward decreased body weight compared to the US group (Student's t-test, male:  $t_{70} = 2.52$ ,  $p = 0.014$ ; female:  $t_{83} = 1.963$ ,  $p = 0.053$ ) (**Figure 23e, g**). Taken together, these results suggest effects of the LBN stress on physiological parameters but not on general survival. Thus, the pups of the required genotype were selected, and further behavioral testing was carried out at 4-6 months of age. A scheme of the behavioral tests conducted are depicted in **Figure 23a**.

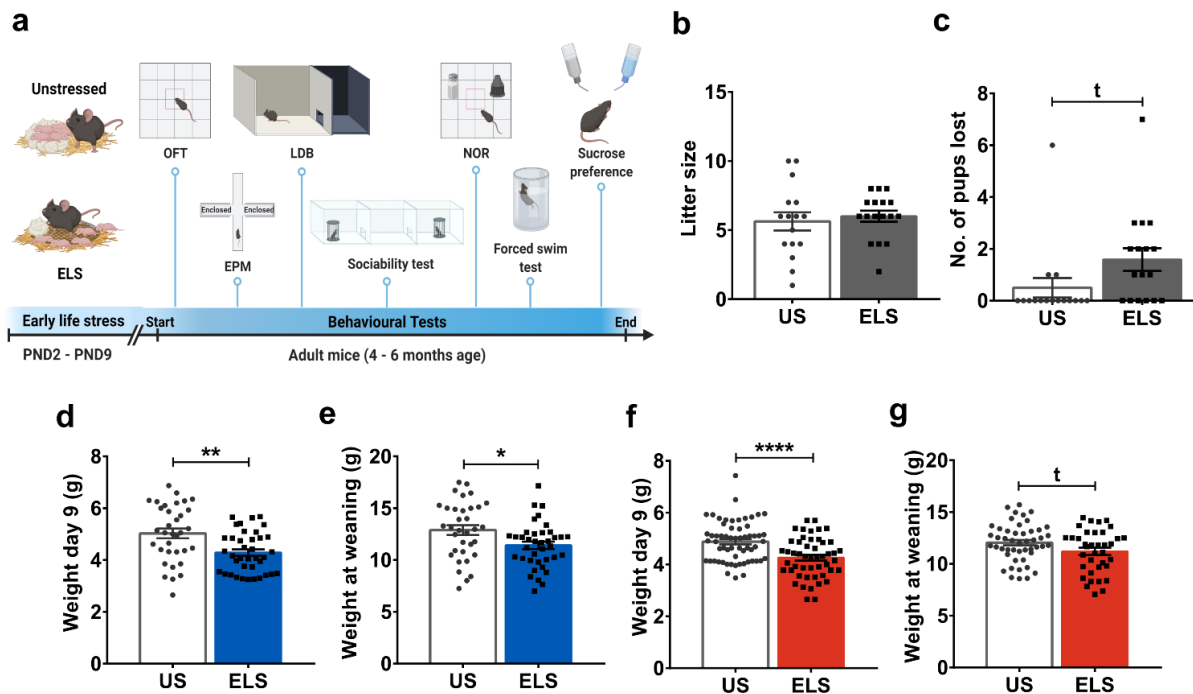


**Figure 23: Limited bedding and nesting paradigm (LBN).** a) Schematic of LBN paradigm and behavioral tests performed. b) Litter size of US and ELS groups at day 0 (birth of pups). c) Number of pups lost after the completion of LBN stress (on day 9) (Student's t-test,  $t = \text{trend}$ ,  $p = 0.0703$ ). d, e) Body weights of male  $Ca_v1.2-Nex$  mice on day 9 (at the end of LBN paradigm) and at weaning (Student's t-test,  $p < 0.05$ ). f, g) Body weights of female  $Ca_v1.2-Nex$  mice on day 9 and at weaning (Student's t-test,  $p < 0.05$ ,  $t = \text{trend}$ ,  $p = 0.053$ ). Abbreviations: ELS - early life stress, PND - postnatal day, US - unstressed, OFT - open field test, EPM - elevated plus maze test, LDB - light/ dark box test, NOR - novel object recognition test.

#### 4.1.2. Assessment of locomotor activity and anxiety-related behavior in male and female mice following LBN stress

Previous studies have reported hyperactivity and anxiogenic behavior in conditional  $Ca_v1.2-Nex$  knockout mice (CKO) compared to control littermates (Ctrl) (Dedic et al. 2018). Furthermore, the LBN stress has also been shown to affect anxiety-related behavior in mice (X.-D. Wang et al. 2012; Jaric et al. 2019). Thus, to investigate the effects of stress on locomotor activity and anxiety-related behavior,  $Ca_v1.2-Nex$  mice were assessed in the OFT, EPM and LDB tasks.

In the OFT, US CKO male and female mice showed hyperlocomotion compared to their control littermates (**Figure 24a, b, e, f**). A similar genotype effect on hyperlocomotion was also observed in ELS male and female groups (Two-way ANOVA repeated measures, male - interaction,  $F_{(15, 90)} = 1.47$ ,  $p = 0.13$ ; time,  $F_{(5, 90)} = 3.784$ ,  $p = 0.0037$ ; genotype,  $F_{(3, 18)} = 12.37$ ,  $p = 0.0001$ ; female -

interaction,  $F_{(15, 165)} = 0.87$ ,  $p = 0.5956$ ; time,  $F_{(5, 165)} = 3.31$ ,  $p = 0.0071$ ; genotype,  $F_{(3, 33)} = 20.19$ ,  $p < 0.0001$ ). Interestingly, while hyperlocomotion was independent of stress in male CKO mice, ELS induced an increased hyperlocomotion in female CKO mice compared to US CKO mice (**Figure 24b, f**) (Total distance: two-way ANOVA, male - interaction,  $F_{(1, 18)} = 2.42$ ,  $p = 0.1373$ ; genotype,  $F_{(1, 18)} = 26.38$ ,  $p < 0.0001$ ; condition,  $F_{(1, 18)} = 2.67$ ,  $p = 0.1199$ ; female - interaction,  $F_{(1, 33)} = 5.87$ ,  $p = 0.0210$ ; genotype,  $F_{(1, 33)} = 51.32$ ,  $p < 0.0001$ ; condition,  $F_{(1, 33)} = 1.98$ ,  $p = 0.1686$ ).

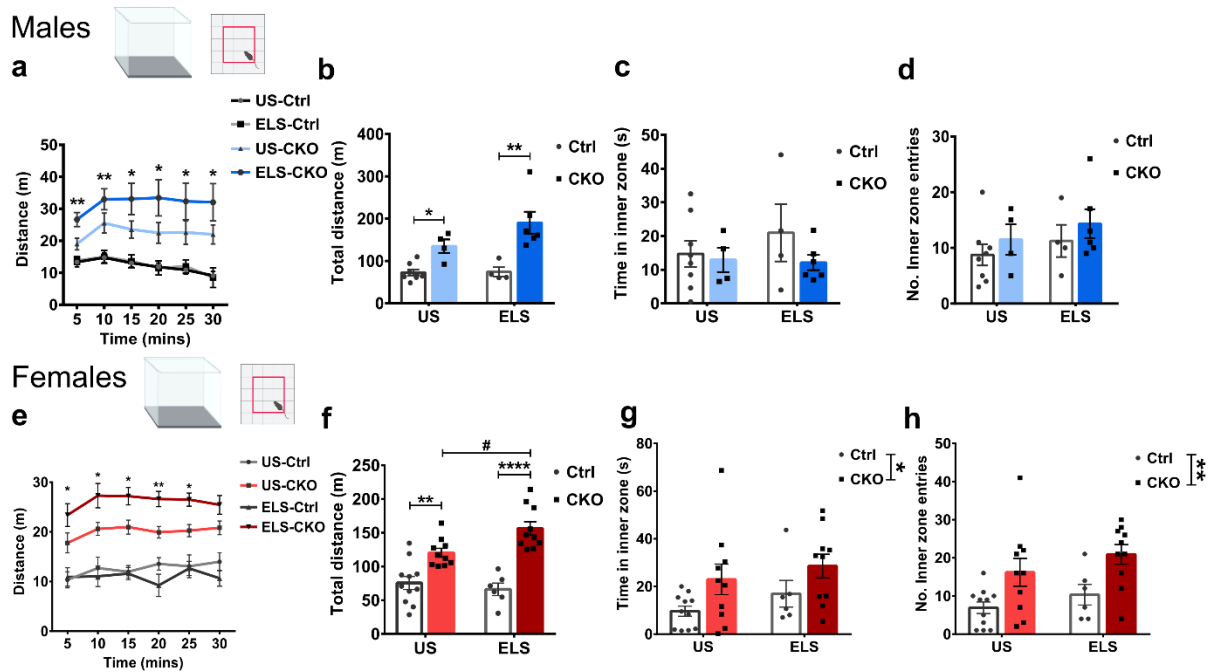


**Figure 24: Assessment of locomotor activity and anxiety-related behavior after the LBN stress in male and female  $Ca_v1.2-Nex$  animals.** a, e) Distance covered in 5-min time bins through the 30-min test duration. b, f) Total distance covered during the total duration of OFT. c, g) Time spent in inner zone of open field. d, h) Number of entries into the inner zone of open field. (Two-way ANOVA + Bonferroni post hoc,  $p < 0.05$ , \* represents comparison with Ctrl of the same condition, # represents comparison with unstressed group of the same genotype).

In contrast to previous reports, no significant alterations in anxiety-related behavior were observed in the first 5 mins of the OFT in US male CKO mice compared to their Ctrl littermates. This is indicated by the lack of significant difference among groups in the time spent in the inner zone of the open field (**Figure 24c**). Furthermore, CKO male mice exhibited similar number of entries to the center zone as compared to their control littermates, which was independent of the stress condition (**Figure 24d**) (two-way ANOVA: interaction,  $F_{(1, 18)} = 0.0042$ ,  $p = 0.9489$ ; genotype,  $F_{(1,$

$_{18}) = 1.29, p = 0.2705$ ; condition,  $F_{(1, 18)} = 1.08, p = 0.3124$ ). Whereas female US and ELS CKO mice spent more time in the inner zone and showed increased number of entries to the inner zone compared to their Ctrl littermates (**Figure 24g, h**). ELS did not alter the time spent in the inner zone by male Ctrl and CKO mice (two-way ANOVA: interaction,  $F_{(1, 18)} = 0.56, p = 0.4624$ ; genotype,  $F_{(1, 18)} = 1.27, p = 0.2744$ ; condition,  $F_{(1, 18)} = 0.34, p = 0.5694$ ). Similarly in females, the differences were genotype specific with no effects of the LBN stress (two-way ANOVA: inner zone time - interaction,  $F_{(1, 33)} = 0.03, p = 0.8658$ ; genotype,  $F_{(1, 33)} = 6.16, p = 0.0184$ ; condition,  $F_{(1, 33)} = 1.64, p = 0.2093$ / inner zone entry - interaction,  $F_{(1, 33)} = 0.052, p = 0.8216$ ; genotype,  $F_{(1, 33)} = 12.51, p = 0.0012$ ; condition,  $F_{(1, 33)} = 2.094, p = 0.1573$ ).

In the LDB, male and female US Ctrl and CKO mice exhibited similar latencies to enter the lit zone and spent similar amounts of time in the lit zone (**Figure 25a, b, d, e**). Male US CKO mice, however, showed increased entry to the lit zone compared to their Ctrl littermates irrespective of the stress condition (**Figure 25c**). Female US CKO mice showed similar number of entries compared to their Ctrl littermates (**Figure 25f**). ELS male and female Ctrl and CKO mice also showed similar latencies to enter the lit zone (Two-way ANOVA: male - interaction,  $F_{(1, 19)} = 0.1287, p = 0.7237$ ; genotype,  $F_{(1, 19)} = 0.6664, p = 0.4244$ ; condition,  $F_{(1, 19)} = 0.3892, p = 0.5401$ ; female - interaction,  $F_{(1, 33)} = 0.06335, p = 0.8028$ ; genotype,  $F_{(1, 33)} = 0.2674, p = 0.6085$ ; condition,  $F_{(1, 33)} = 1.21, p = 0.2792$ ) (**Figure 25a, d**). Interestingly, male ELS CKO mice spent significantly lesser time in the lit zone compared to their Ctrl littermates (Two-way ANOVA: interaction,  $F_{(1, 19)} = 3.993, p = 0.0602$ ; genotype,  $F_{(1, 19)} = 8.024, p = 0.0106$ ; condition,  $F_{(1, 19)} = 0.3992, p = 0.5350$ ) (**Figure 25b**). No such stress effect was observed in female Ctrl or CKO mice (Two-way ANOVA: interaction,  $F_{(1, 33)} = 1.465, p = 0.2348$ ; genotype,  $F_{(1, 33)} = 3.474, p = 0.0713$ ; condition,  $F_{(1, 33)} = 0.04016, P=0.8424$ ) (**Figure 25e**). ELS male and female CKO mice exhibited an increased number of entries into the lit zone compared to their Ctrl littermates (Two-way ANOVA: male - interaction,  $F_{(1, 19)} = 0.09589, p = 0.7602$ ; genotype,  $F_{(1, 19)} = 5.425, p = 0.0310$ ; condition,  $F_{(1, 19)} = 0.03063, p = 0.8629$ ; female - interaction,  $F_{(1, 33)} = 6.734, p = 0.0140$ ; genotype,  $F_{(1, 33)} = 5.482, p = 0.0254$ ; condition,  $F_{(1, 33)} = 2.035, p = 0.1631$ ) (**Figure 25c, f**). While this phenotype was independent of stress in male mice, there was a more pronounced effect of stress in female CKO mice. In fact, female ELS CKO mice showed increased number of entries into the lit zone compared to their Ctrl littermates and to the US CKO mice.

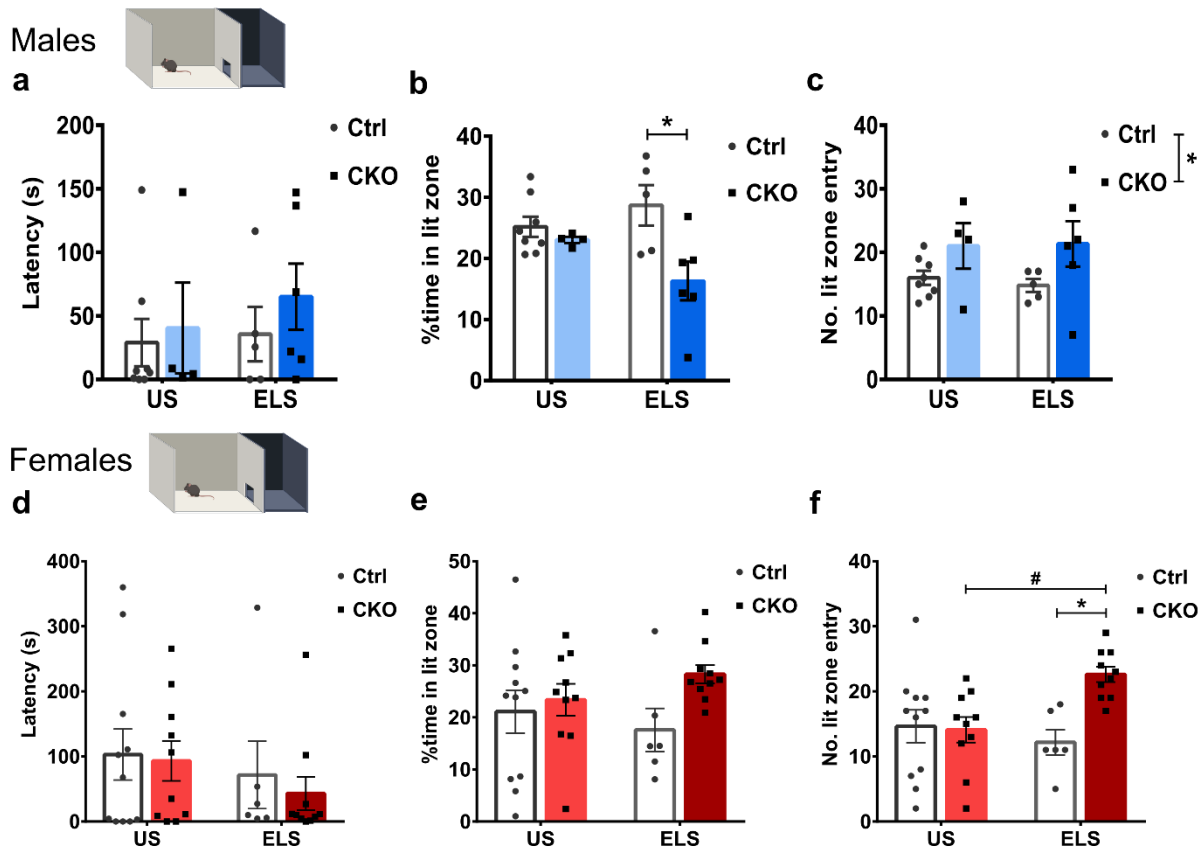


**Figure 25: Assessment of anxiety-related behavior in  $Ca_v1.2$ -Nex mice following the LBN stress in LDB test.** a, d) Latency to enter into the lit zone. b, e) Percentage time spent in the lit zone. c, f) Number of entries into the lit zone. (Two-way ANOVA + Bonferroni post hoc,  $p < 0.05$ , \* represents comparison to control group of the same condition, # represents comparison to unstressed group of the same genotype).

In the EPM test, no significant alterations were found in the time spent in open arms or number of entries into the open arms in male and female US Ctrl and CKO mice (**Figure 26b, c, e, f**). Hyperlocomotion was persistent in female US CKO mice compared to their Ctrl littermates (**Figure 26d**), whereas male US CKO mice showed locomotor activity similar to Ctrl littermates (**Figure 26a**). Stress however had a pronounced effect on locomotion in male and female mice. Male ELS CKO mice showed hyperlocomotion compared to their Ctrl littermates (Two-way ANOVA: interaction,  $F_{(1, 19)} = 1.399$ ,  $p = 0.2515$ ; genotype,  $F_{(1, 19)} = 17.01$ ,  $p = 0.0006$ ; condition,  $F_{(1, 19)} = 0.7501$ ,  $p = 0.3972$ ) (**Figure 26a**), whereas hyperlocomotion was further enhanced in female ELS CKO mice compared to their Ctrl littermates and to the US CKO mice (Two-way ANOVA: interaction,  $F_{(1, 33)} = 1.693$ ,  $p = 0.2022$ ; genotype,  $F_{(1, 33)} = 29.2$ ,  $p < 0.0001$ ; condition,  $F_{(1, 33)} = 6.344$ ,  $p = 0.0168$ ) (**Figure 26d**). LBN stress effects on the time spent in open arms and number of entries into the open arms were absent in male Ctrl and CKO mice whereas female ELS

mice showed enhanced time in the open arm and increased number of entries into the open arm independent of the genotype (Two-way ANOVA: open arm time, male - interaction,  $F_{(1, 19)} = 0.008546$ ,  $p = 0.9273$ ; genotype,  $F_{(1, 19)} = 0.0005523$ ,  $p = 0.9815$ ; condition,  $F_{(1, 19)} = 0.122$ ,  $p = 0.7307$ ; female - interaction,  $F_{(1, 33)} = 0.3365$ ,  $p = 0.5658$ ; genotype,  $F_{(1, 33)} = 0.2308$ ,  $p = 0.6341$ ; condition,  $F_{(1, 33)} = 7.142$ ,  $p = 0.0116$ / open arm entry, male - interaction,  $F_{(1, 19)} = 0.005809$ ,  $p = 0.9400$ ; genotype,  $F_{(1, 19)} = 0.004067$ ,  $p = 0.9498$ ; condition,  $F_{(1, 19)} = 0.002035$ ,  $p = 0.9645$ ; female - interaction,  $F_{(1, 33)} = 0.4002$ ,  $p = 0.5314$ ; genotype,  $F_{(1, 33)} = 2.288$ ,  $p = 0.1399$ ; condition,  $F_{(1, 33)} = 5.256$ ,  $p = 0.0284$ ) (Figure 26b, c, e, f).

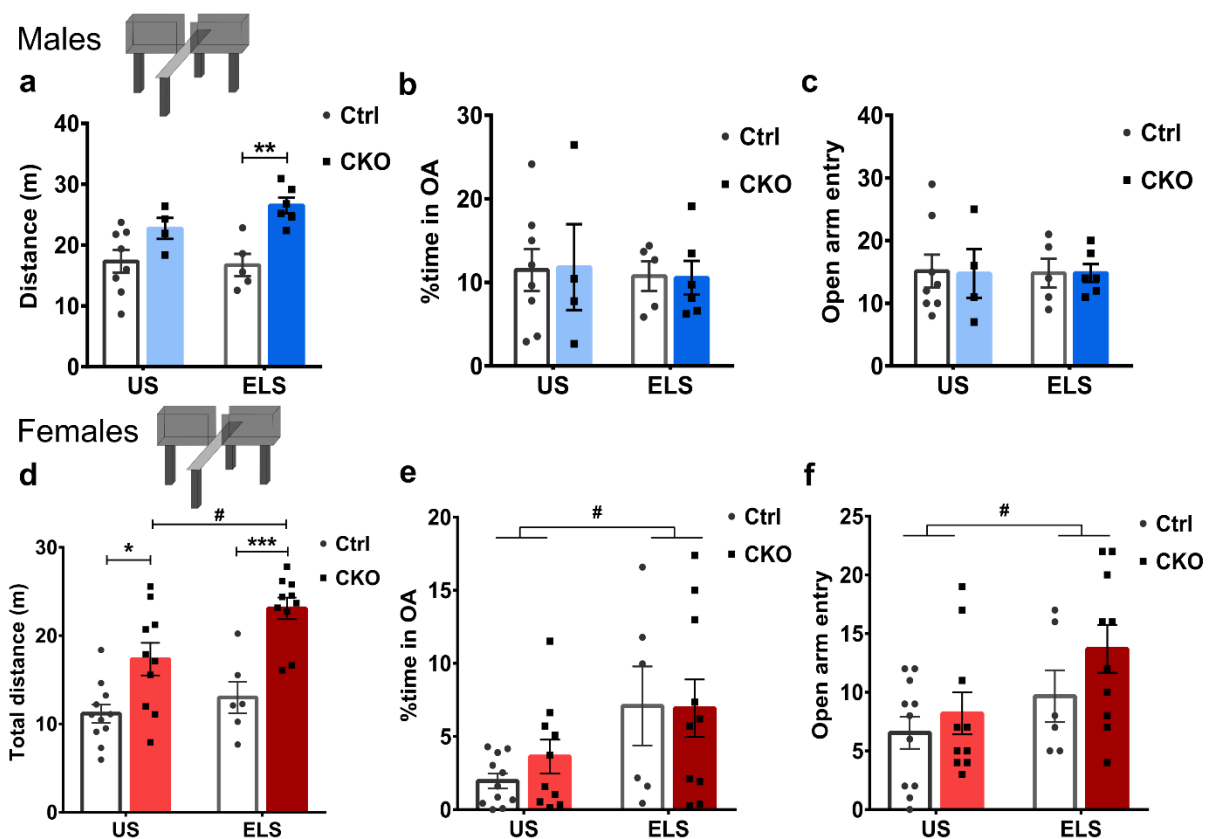


**Figure 26: Assessment of anxiety-related behavior in  $Ca_v1.2$ -Nex mice after the LBN stress in the EPM test.** a, d) Total distance travelled in the apparatus. b, e) Percentage time spent in open arms. c, f) Number of entries into open arms. (Two-way ANOVA + Bonferroni post hoc,  $p < 0.05$ , \* represents comparison to control group of the same condition, # represents comparison to unstressed group of the same genotype)

Taken together these results suggest a partial task-specific stress effect on anxiety-related behavior. However, in contrast to the previously reported anxiogenic phenotype observed in conditional

Ca<sub>v</sub>1.2-Nex knockout animals, no anxiogenic phenotype was observed in US CKO animals in the ELS experiments which could be due to low sample numbers. More pronounced effects of the LBN stress were seen especially in female mice where a genotype-specific hyperlocomotion was further enhanced by the LBN stress in female CKO mice. In addition, LBN stress enhanced the number of entries into, and time spent in the open arms independent of the genotypes of animals.

#### 4.1.3. Consequences of early life stress on social interaction and cognitive performance

Stress, specifically LBN stress has previously been shown to affect social behavior and cognitive performance in mice (Ivy et al. 2010; Naninck et al. 2015; J. Molet et al. 2016). Hence, to further investigate the effects of LBN stress on social interaction and cognition of Ca<sub>v</sub>1.2-Nex mice, we used the 3CT and NOR tests.

Male and female US Ctrl and CKO mice exhibited comparable sociability which was indicated by the increased interaction time with social conspecific mice compared to the empty cage (**Figure 27a, f**). A closer look at the percentage of interaction time with the social mouse revealed similar levels of interaction in male and female US-CKO compared to their Ctrl littermates (**Figure 27c, h**). ELS Ctrl and CKO male and female mice also showed comparable sociability indicated by the increased interaction with the social mouse compared to the empty cage (**Figure 27a, f**) (Two-way ANOVA: male - interaction,  $F_{(3, 38)} = 6.36$ ,  $p = 0.0013$ ; genotype,  $F_{(3, 38)} = 2.961$ ,  $p = 0.0443$ ; social mouse,  $F_{(1, 38)} = 119.2$ ,  $p < 0.0001$ ; female - interaction,  $F_{(3, 62)} = 0.6362$ ,  $p = 0.5945$ ; genotype,  $F_{(3, 62)} = 0.4368$ ,  $p = 0.7274$ ; social mouse,  $F_{(1, 62)} = 53.47$ ,  $p < 0.0001$ ). Interestingly, male ELS CKO mice showed reduced percentage of interaction time with social mouse compared to their Ctrl littermates and to the US CKO (**Figure 27c**) (Two-way ANOVA: interaction,  $F_{(1, 19)} = 7.019$ ,  $p = 0.0158$ , genotype,  $F_{(1, 19)} = 3.685$ ,  $p = 0.0700$ ; condition,  $F_{(1, 19)} = 18.67$ ,  $p = 0.0004$ ). In contrast, female ELS Ctrl and CKO mice spent similar amounts of time interacting with social conspecific (**Figure 27h**) (Two-way ANOVA: interaction,  $F_{(1, 31)} = 0.3347$ ,  $p = 0.5671$ ; genotype,  $F_{(1, 31)} = 0.468$ ,  $p = 0.4990$ ; condition,  $F_{(1, 31)} = 0.08628$ ,  $p = 0.7709$ ).

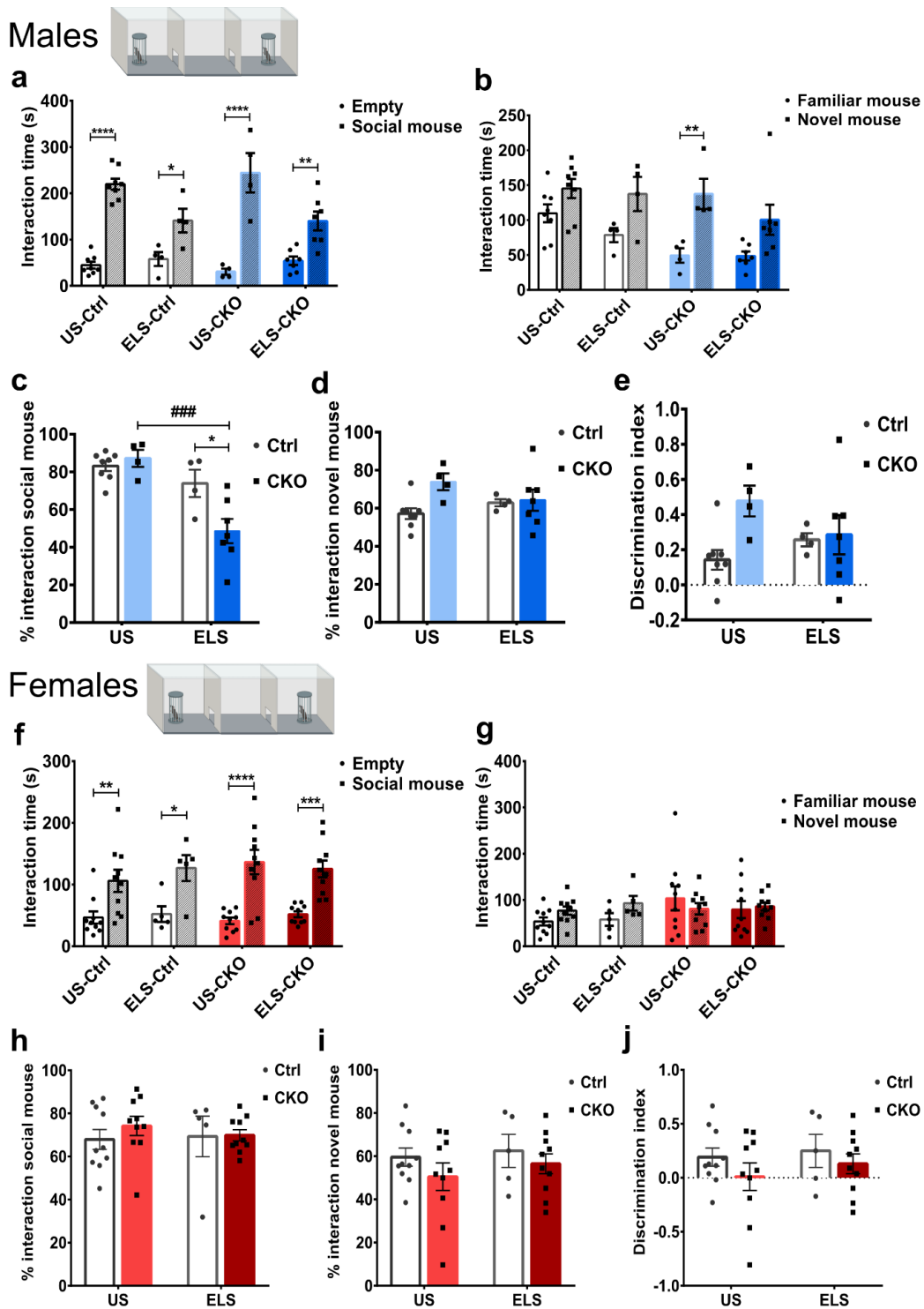


**Figure 27: Effect of LBN on social interaction in  $Ca_v1.2$ -Nex mice.** a, f) Interaction time with empty cage vs social mouse. b, g) Interaction time with familiar mouse vs novel mouse. c, h) Percentage of interaction time with social mouse. d, i) Percentage of interaction time with novel mouse. e, j) Discrimination index of novel mouse from familiar mouse. (Two-way ANOVA + Bonferroni post hoc,  $p <$

0.05, \* represents comparison to Ctrl mice of the same condition, # represents comparison to unstressed mice of the same genotype)

In social novelty preference, however, only male US CKO mice showed significantly higher interaction with novel social mouse compared to familiar mouse while no differences were seen in female US mice or other groups (**Figure 27b, g**) (Two-way ANOVA: male - interaction,  $F_{(3, 38)} = 0.8464$ ,  $p = 0.4771$ ; genotype,  $F_{(3, 38)} = 4.911$ ,  $p = 0.0056$ ; novel mouse,  $F_{(1, 38)} = 24.14$ ,  $p < 0.0001$ ; female - interaction,  $F_{(3, 62)} = 1.196$ ,  $p = 0.3187$ ; genotype,  $F_{(3, 62)} = 1.194$ ,  $p = 0.3195$ ; condition,  $F_{(1, 62)} = 0.8444$ ,  $p = 0.3617$ ). No significant alterations were observed in percentage interaction with novel mouse or discrimination index in male and female US Ctrl and CKO (**Figure 27d, e, i, j**).

Furthermore, stress effects on interaction times and discrimination index were also absent in male and female Ctrl and CKO mice (**Figure 27d, e, i, j**) (Two-way ANOVA: novel mouse interaction time, male - interaction,  $F_{(1, 19)} = 2.861$ ,  $p = 0.1071$ ; genotype,  $F_{(1, 19)} = 4.013$ ,  $p = 0.0596$ ; condition,  $F_{(1, 19)} = 0.1864$ ,  $p = 0.6708$ ; female - interaction,  $F_{(1, 31)} = 0.06967$ ,  $p = 0.7936$ ; genotype,  $F_{(1, 31)} = 1.7$ ,  $p = 0.2019$ ; condition,  $F_{(1, 31)} = 0.5946$ ,  $p = 0.4465$ / discrimination index, male - interaction,  $F_{(1, 19)} = 2.861$ ,  $p = 0.1071$ ; genotype,  $F_{(1, 19)} = 4.013$ ,  $p = 0.0596$ ; condition,  $F_{(1, 19)} = 0.1864$ ,  $p = 0.6708$ ; female - interaction,  $F_{(1, 31)} = 0.06967$ ,  $p = 0.7936$ ; genotype,  $F_{(1, 31)} = 1.7$ ,  $p = 0.2019$ ; condition,  $F_{(1, 31)} = 0.5946$ ,  $p = 0.4465$ ).

In the acquisition session of the NOR, male US Ctrl and CKO mice showed similar interaction times with the objects, while female US CKO mice showed enhanced interaction with objects compared to their Ctrl littermates (**Figure 28a, d**). Similarly, while male ELS Ctrl and CKO mice showed similar interaction times with the objects, female ELS CKO mice spent more time interacting with the objects (**Figure 28a, d**). Increased object interaction time in female mice were independent of stress (Two-way ANOVA: male - interaction,  $F_{(1, 20)} = 1.301$ ,  $p = 0.2674$ , genotype,  $F_{(1, 20)} = 6.549$ ,  $p = 0.0187$ ; condition,  $F_{(1, 20)} = 4.269$ ,  $p = 0.0520$ ; female - interaction,  $F_{(1, 33)} = 0.003071$ ,  $p = 0.9561$ ; genotype,  $F_{(1, 33)} = 31.69$ ,  $p < 0.0001$ ; condition,  $F_{(1, 33)} = 2.856$ ,  $p = 0.1004$ ).

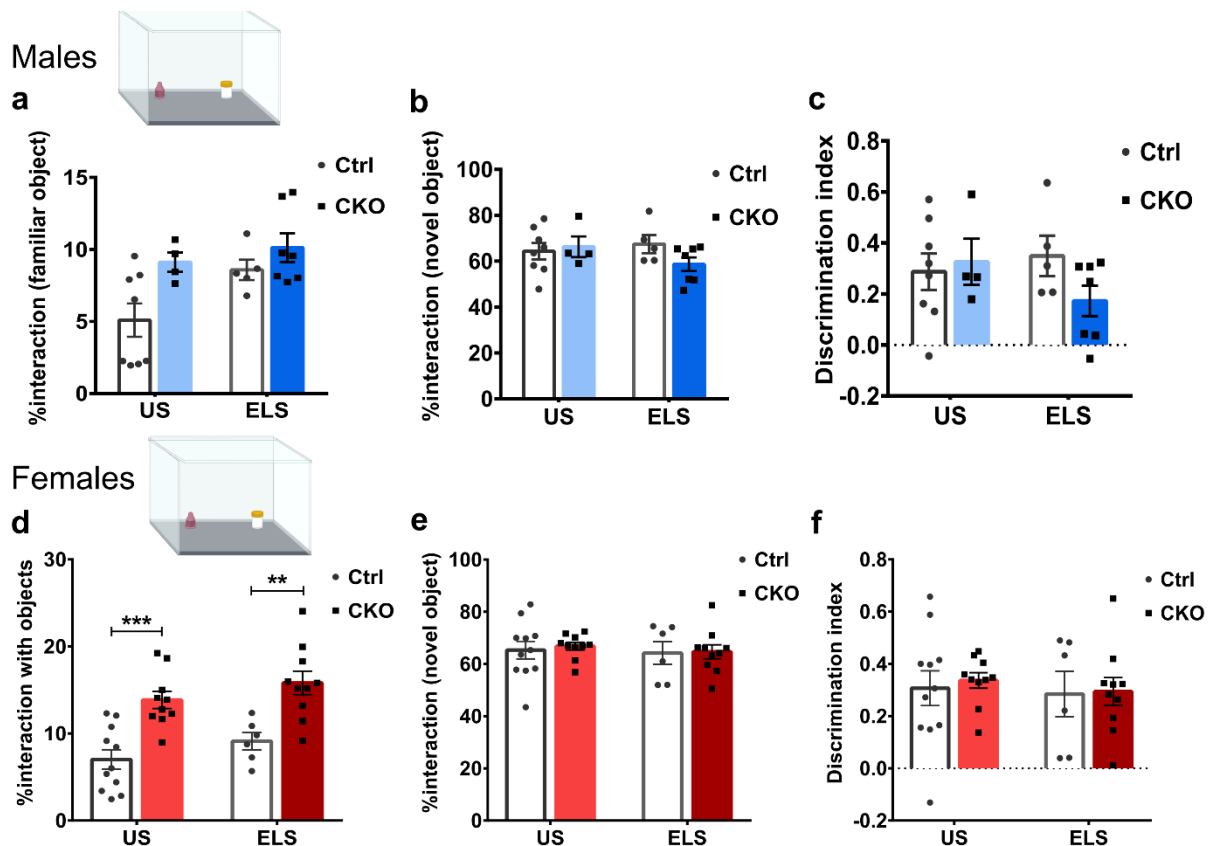


**Figure 28: Effects of LBN stress on object recognition in  $Ca_v1.2$ -Nex mice.** a, d) Percentage interaction time with familiar objects. b, e) Percentage interaction time with novel object. c, f) Discrimination index of novel object vs familiar object. (Two-way ANOVA + Bonferroni post hoc,  $p < 0.05$ , \* represents comparison to the Ctrl group of the same condition)

All groups (male and female US and ELS Ctrl and CKO mice) spent more than 50% of the time interacting with the novel object during the testing session with no significant effects of genotype or stress condition (**Figure 28b, e**) (Two-way ANOVA: male - interaction,  $F_{(1, 20)} = 1.955$ ,  $p = 0.1774$ ; genotype,  $F_{(1, 20)} = 0.7959$ ,  $p = 0.3829$ ; condition,  $F_{(1, 20)} = 0.3475$ ,  $p = 0.5621$ ; female - interaction,  $F_{(1, 33)} = 0.02837$ ,  $p = 0.8673$ ; genotype,  $F_{(1, 33)} = 0.106$ ,  $p = 0.7468$ ; condition,  $F_{(1, 33)} = 0.2937$ ,  $p = 0.5915$ ). Furthermore, no significant alterations were found in the discrimination index in male and female US Ctrl and CKO mice or ELS Ctrl and CKO mice (**Figure 28c, f**) (Two-way ANOVA: male - interaction,  $F_{(1, 20)} = 1.955$ ,  $p = 0.1774$ ; genotype,  $F_{(1, 20)} = 0.7959$ ,  $p = 0.3829$ ; condition,  $F_{(1, 20)} = 0.3475$ ,  $p = 0.5621$ ; female - interaction,  $F_{(1, 33)} = 0.02836$ ,  $p = 0.8673$ ; genotype,  $F_{(1, 33)} = 0.106$ ,  $p = 0.7468$ ; condition,  $F_{(1, 33)} = 0.2937$ ,  $p = 0.5915$ ).

To summarize, LBN stress impaired social interaction only in male CKO mice but not in female mice. A genotype-specific increased object interaction time was observed in female mice with no obvious stress effects. However, since mice in all groups spent less than 20% of the time interacting with the objects during the acquisition session, data from the NOR has to be interpreted with caution.

#### 4.1.4. Assessment of stress coping and depression-related behavior following early life stress

The LBN stress has previously been shown to induce depression-related anhedonia behavior in wildtype mice (Bolton, Molet, et al. 2018). Thus, to investigate how stress affects depression-related behavior in  $Ca_v1.2$ -Nex mice, FST and SPT were performed.

Mice in all groups (male and female US/ ELS Ctrl and CKO mice) spent comparable amounts of time struggling (**Figure 29a, e**) (Two-way ANOVA: male - interaction,  $F_{(1, 19)} = 0.08855$ ,  $p = 0.7693$ ; genotype,  $F_{(1, 19)} = 0.7407$ ,  $p = 0.4002$ ; condition,  $F_{(1, 19)} = 3.419$ ,  $p = 0.0801$ ; female - interaction,  $F_{(1, 29)} = 0.4848$ ,  $p = 0.4918$ ; genotype,  $F_{(1, 29)} = 3.745$ ,  $p = 0.0628$ ; condition,  $F_{(1, 29)} = 0.1114$ ,  $p = 0.7410$ ). Male US CKO mice showed increased swimming and decreased immobility time in the FST indicating enhanced active stress coping behavior (**Figure 29b, c**). Female CKO mice showed enhanced swimming and reduced immobility time compared to their Ctrl littermates independent of stress conditions (**Figure 29f, g**). No significant differences in swim time or immobility were observed in ELS male Ctrl and CKO mice (**Figure 29b, c**) (Two-way ANOVA: swim time, male - interaction,  $F_{(1, 19)} = 0.8514$ ,  $p = 0.3677$ ; genotype,  $F_{(1, 19)} = 20.15$ ,  $p = 0.0003$ ; condition,  $F_{(1, 19)} = 0.09192$ ,  $p = 0.7650$ ; female - interaction,  $F_{(1, 29)} = 0.07199$ ,  $p = 0.7904$ ; genotype,  $F_{(1, 29)} = 8.976$ ,  $p = 0.0056$ ; condition,  $F_{(1, 29)} = 0.2891$ ,  $p = 0.5949$ / immobility time, male - interaction,  $F_{(1, 19)} = 0.7366$ ,  $p = 0.4014$ ; genotype,  $F_{(1, 19)} = 18.73$ ,  $p = 0.0004$ ; condition,  $F_{(1, 19)} = 0.3028$ ,  $p = 0.5886$ ; female - interaction,  $F_{(1, 29)} = 0.0002233$ ,  $p = 0.9882$ ; genotype,  $F_{(1, 29)} = 12.97$ ,  $p = 0.0012$ ; condition,  $F_{(1, 29)} = 0.6118$ ,  $p = 0.4405$ ).

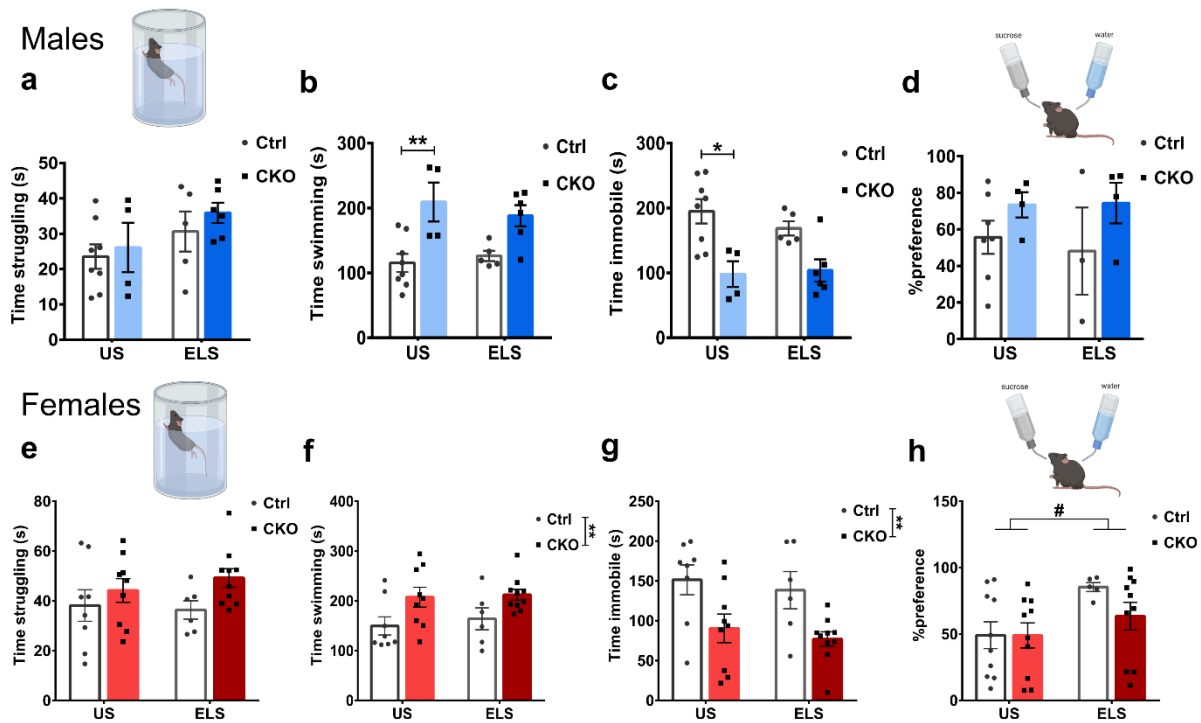


**Figure 29: Effects of LBN stress on depression-related behavior in  $Ca_v1.2$ -Nex mice.** a, e) Time spent struggling. b, f) Time spent swimming. c, g) Time spent immobile. d, h) Percentage preference for sucrose (Two-way ANOVA + Bonferonni post hoc,  $p < 0.05$ , \* represents comparison to Ctrl mice of the same condition, # represents comparison to unstressed mice of same genotype)

Furthermore, male, and female US Ctrl and CKO mice showed similar preference for sucrose suggesting similar hedonic behavior (**Figure 29d, h**). Male ELS Ctrl and CKO mice also showed similar preference for sucrose with no effects of the LBN stress (**Figure 29d**) (Two-way ANOVA: interaction,  $F_{(1, 14)} = 0.1164$ ,  $p = 0.7380$ ; genotype,  $F_{(1, 14)} = 3.115$ ,  $p = 0.0994$ ; condition,  $F_{(1, 14)} = 0.06964$ ,  $p = 0.7957$ ). Interestingly, while female ELS Ctrl and CKO mice had similar preference for sucrose, stressed mice showed an overall higher preference for sucrose compared to unstressed mice irrespective of the genotype (**Figure 29h**) (Two-way ANOVA: interaction,  $F_{(1, 31)} = 1.076$ ,  $p = 0.3075$ ; genotype,  $F_{(1, 31)} = 1.11$ ,  $p = 0.3003$ ; condition,  $F_{(1, 31)} = 5.868$ ,  $p = 0.0215$ ).

Taken together, these results show that the differences arising in stress coping behavior largely stem from genotype effects rather than stress effects. Also, while stress did not affect hedonic behavior in males, in contrary to previous reports LBN stress seemingly enhances preference for sucrose in females.

#### 4.2. Controlling for potential effects of Cre expression on behavioral phenotypes

Since  $Ca_v1.2$ -Nex CKO animals showed hyperlocomotion in a novel environment, I wanted to investigate if this could be a result of the insertion of Cre recombinase into the Nex/ Neurod6 locus as this leads to a disruption of the targeted allele. Since such effects are rarely controlled for or reported, I ran control experiments using the Nex-Cre driver mouse line to confirm that the behavioral phenotype seen in  $Ca_v1.2$ -Nex mice is related to the  $Ca_v1.2$  inactivation rather than to unspecific effects connected to expression of the Cre recombinase. Tests for locomotor activity, anxiety-related behavior, cognition, and stress coping behavior were conducted in heterozygous Nex-Cre mice ( $Neurod6^{+/Cre}$ , represented as Cre) in comparison to their control littermates ( $Neurod6^{+/+}$ , represented as Ctrl).

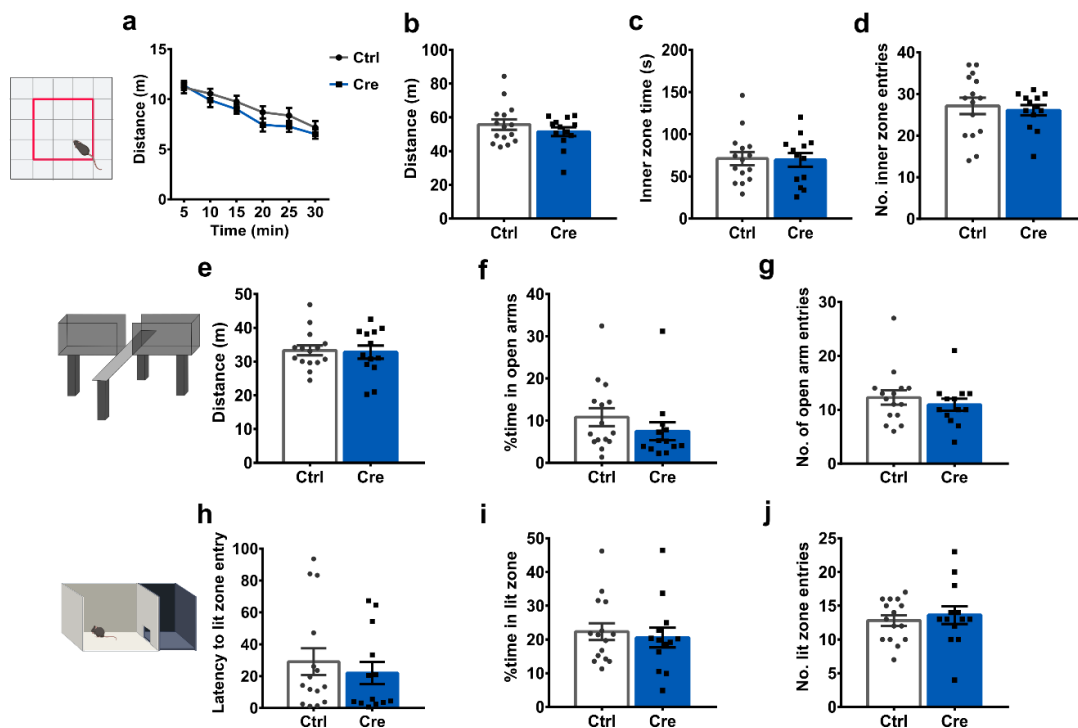


**Figure 30: Characterization of anxiety-related behavior of Nex-Cre males.** a, b) Distance travelled in the open field (Two-way ANOVA-repeated measures, Locomotor: interaction,  $F_{(5, 130)} = 0.8719$ ,  $p = 0.5020$ ; genotype,  $F_{(1, 26)} = 1.044$ ,  $p = 0.3164$ ; time,  $F_{(5, 130)} = 36.94$ ,  $p < 0.0001$ ; Student's t-test, Total distance:  $t_{26} = 1.022$ ,  $p = 0.3164$ ). c, d) Time spent in and number of entries to the inner zone. (Student's t-test, Inner zone time:  $t_{26} = 0.144$ ,  $p = 0.8866$ ; Inner zone entry:  $t_{26} = 0.4365$ ,  $p = 0.6661$ ). e) Distance travelled in the elevated plus maze (Student's t-test,  $t_{26} = 0.218$ ,  $p = 0.8291$ ). f, g) Percentage time in and number of entries to the open arms (Student's t-test, Open arm time:  $t_{26} = 1.109$ ,  $p = 0.2775$ ; Open arm entry:  $t_{26} = 0.7614$ ,  $p$

= 0.4533). h) Latency to entry into the lit zone (Student's t-test,  $t_{26} = 0.6492$ ,  $p = 0.5219$ ). i, j) Time spent in and number of entries to the lit zone. (Student's t-test, Lit time:  $t_{26} = 0.4555$ ,  $p = 0.6525$ ; Lit entry:  $t_{26} = 0.5462$ ,  $p = 0.5896$ ).

Male and female Nex-Cre mice were evaluated in the OFT, LDB and EPM tests. In all three tests, male and female Cre positive animals were indistinguishable from their Ctrl littermates (**Figures 30 and 31**). They showed comparable locomotor activity and anxiety-related behaviors.

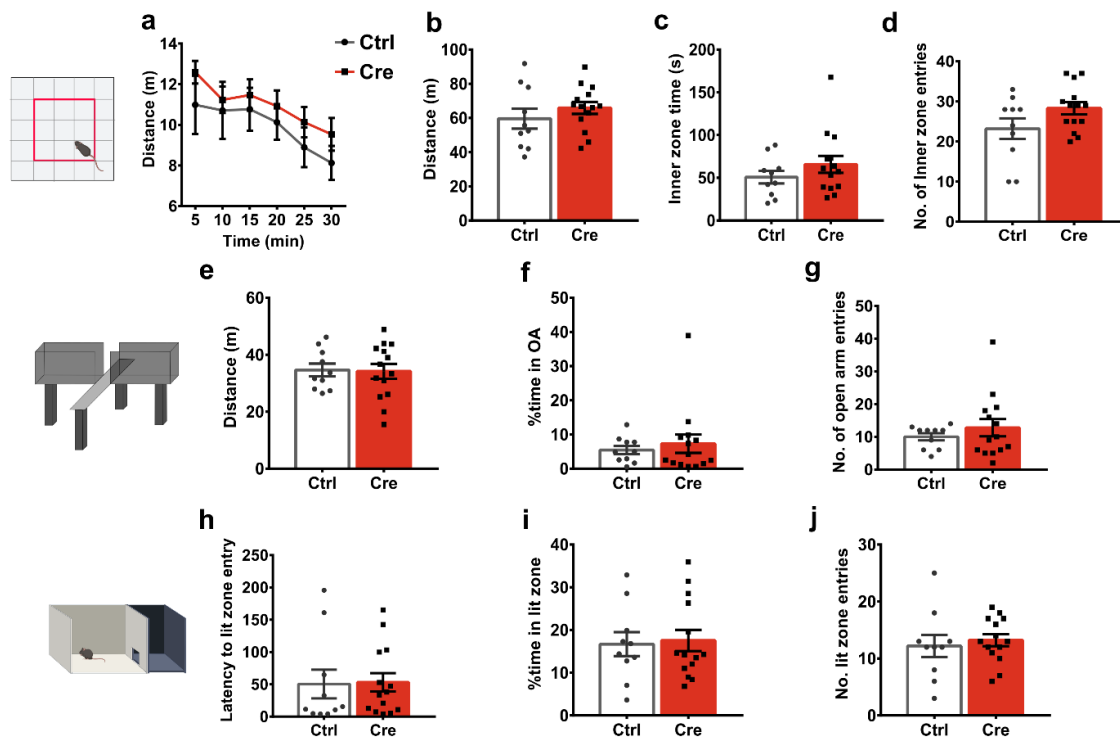


**Figure 31: Characterization of anxiety-related behavior of Nex-Cre females.** a, b) Distance travelled in the open field (Two-way ANOVA-repeated measures, Locomotor: interaction,  $F_{(5, 110)} = 0.3286$ ,  $p = 0.8947$ ; genotype,  $F_{(1, 22)} = 0.9508$ ,  $p = 0.3401$ ; time,  $F_{(5, 110)} = 8.399$ ,  $p < 0.0001$ ; Student's t-test, Total distance:  $t_{22} = 0.9751$ ,  $p = 0.3401$ ). c, d) Time spent in and number of entries to the inner zone (Student's t-test, Inner zone time:  $t_{22} = 1.121$ ,  $p = 0.2743$ ; Inner zone entry:  $t_{22} = 1.804$ ,  $p = 0.085$ ). e) Distance travelled in the elevated plus maze (Student's t-test,  $t_{22} = 0.1273$ ,  $p = 0.8998$ ). f, g) Percentage time in and number of entries to the open arms (Student's t-test, Open arm time:  $t_{22} = 0.5497$ ,  $p = 0.588$ ; Open arm entry:  $t_{22} = 0.8544$ ,  $p = 0.4021$ ). h) Latency to entry into the lit zone (Student's t-test,  $t_{22} = 0.1047$ ,  $p = 0.9176$ ). i, j) Time spent in and number of entries to the lit zone (Student's t-test, Lit time:  $t_{22} = 0.2262$ ,  $p = 0.8231$ ; Lit entry:  $t_{22} = 0.4936$ ,  $p = 0.6265$ ).

Further investigation of cognitive behavior revealed no significant differences between Ctrl and Cre positive male and female mice in any of the cognitive tests (**Figures 32 and 33**). Male and female Ctrl and Cre animals were indistinguishable with similar spontaneous alternations and arm entries in the Y-maze, similar object bias, object interaction times, novelty preference and discrimination index in the NOR and SOR tests.

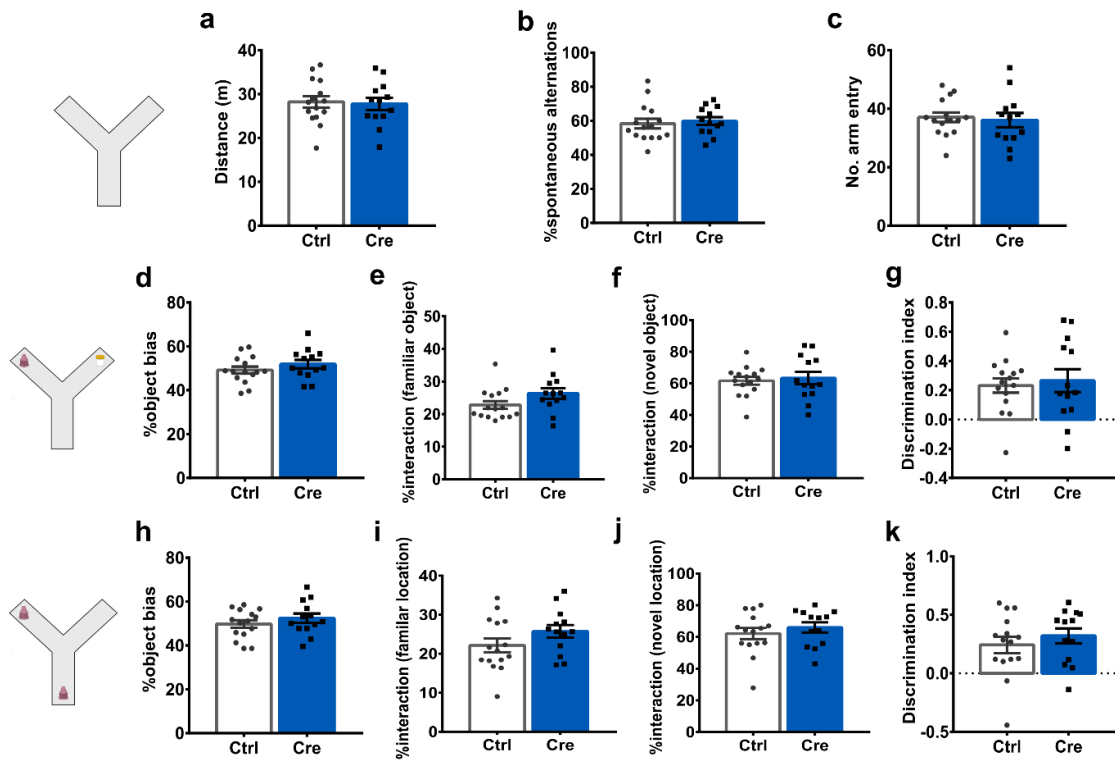


**Figure 32: Characterization of cognitive performance of Nex-Cre males.** a) Distance traveled in Y-maze (Student's t-test,  $t_{26} = 0.234$ ,  $p = 0.8168$ ). b, c) Percentage spontaneous alternations and number of arm entries (Student's t-test, Spontaneous alternations:  $t_{26} = 0.4062$ ,  $p = 0.6879$ ; Arm entries:  $t_{26} = 0.345$ ,  $p = 0.7328$ ). d) Percentage object bias in NOR (Student's t-test,  $t_{26} = 1.106$ ,  $p = 0.2787$ ). e) Percentage interaction time with objects (Student's t-test,  $t_{26} = 1.773$ ,  $p = 0.0879$ ). f) Percentage interaction time with novel object in NOR (Student's t-test,  $t_{26} = 0.3789$ ,  $p = 0.7078$ ). g) Discrimination index (Student's t-test,  $t_{26} = 0.3789$ ,  $p = 0.7078$ ). h) Percentage object bias in SOR (Student's t-test,  $t_{26} = 0.9846$ ,  $p = 0.3339$ ). i) Percentage interaction time with objects in SOR (Student's t-test,  $t_{26} = 1.498$ ,  $p = 0.1463$ ). j) Percentage interaction time with novel location in SOR (Student's t-test,  $t_{26} = 0.8066$ ,  $p = 0.4272$ ). k) Discrimination index in SOR (Student's t-test,  $t_{26} = 0.8066$ ,  $p = 0.4272$ ).

In the sociability stage of the 3CT social cognition task, male and female Ctrl and Cre positive mice showed higher preference for social mouse rather than the empty cage with similar interaction

with the social mouse indicating comparable sociability (**Figure 34b, d, h, j**). In the social novelty preference, male Ctrl mice showed higher preference to novel mouse over a familiar conspecific. Cre positive mice showed a tendency toward increased interaction with novel mouse, though it did not reach statistical significance (**Figure 34c**). Ctrl and Cre mice had similar levels of interaction with the novel mouse with no differences observed in their discrimination index (**Figure 34e, f**). In contrast, female Ctrl and Cre mice did not show a higher preference for the novel mouse (**Figure 34i**). Instead, they exhibited similar levels of interaction with familiar and novel mouse with no obvious difference in the discrimination index (**Figure 34k, l**).

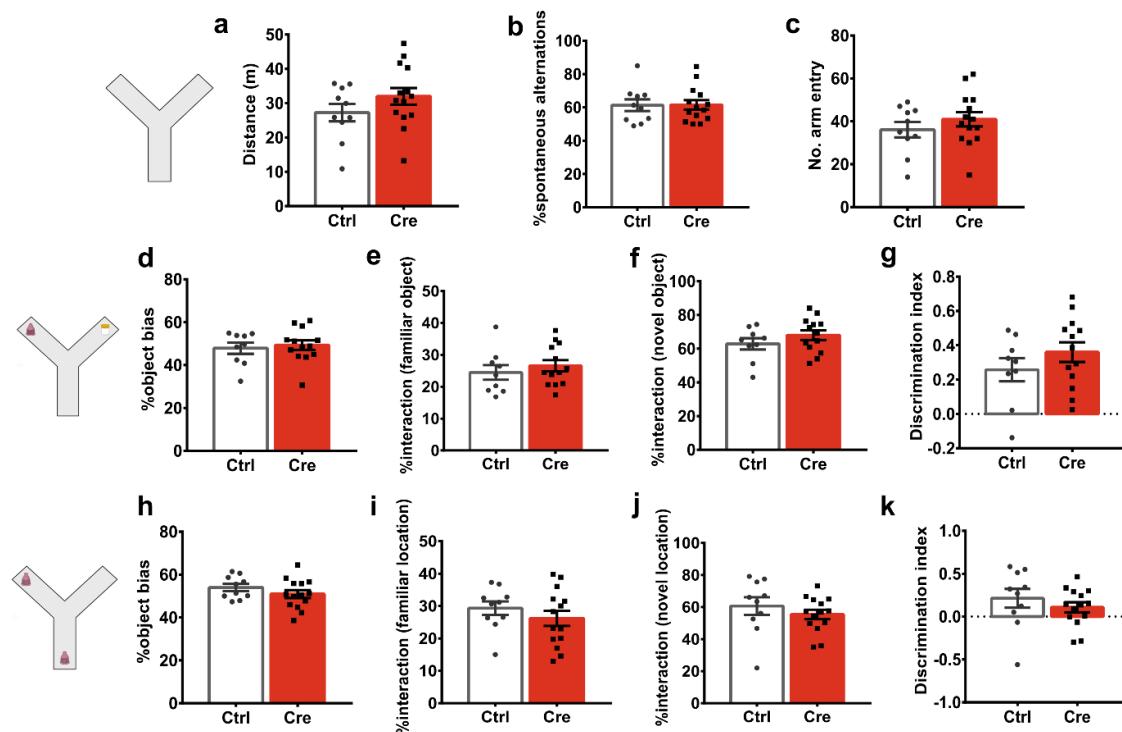


**Figure 33: Characterization of cognitive performance of Nex-Cre females.** a) Distance traveled in Y-maze (Student's t-test,  $t_{22} = 1.33$ ,  $p = 0.197$ ). b, c) Percentage spontaneous alternations and number of arm entries (Student's t-test, Spontaneous alternations:  $t_{22} = 0.05155$ ,  $p = 0.9594$ ; Arm entries:  $t_{22} = 0.9759$ ,  $p = 0.3397$ ). d) Percentage object bias in NOR (Student's t-test,  $t_{20} = 0.4136$ ,  $p = 0.6835$ ). e) Percentage interaction time with objects (Student's t-test,  $t_{20} = 0.7428$ ,  $p = 0.4663$ ). f) Percentage interaction time with novel object in NOR (Student's t-test,  $t_{20} = 1.157$ ,  $p = 0.2611$ ). g) Discrimination index (Student's t-test,  $t_{20} = 1.157$ ,  $p = 0.2611$ ). h) Percentage object bias in SOR (Student's t-test,  $t_{22} = 1.167$ ,  $p = 0.2556$ ). i) Percentage interaction time with objects in SOR (Student's t-test,  $t_{22} = 0.9396$ ,  $p = 0.3576$ ). j) Percentage interaction time with novel location in SOR (Student's t-test,  $t_{22} = 0.9042$ ,  $p = 0.3757$ ). k) Discrimination index in SOR (Student's t-test,  $t_{22} = 0.9042$ ,  $p = 0.3757$ ).

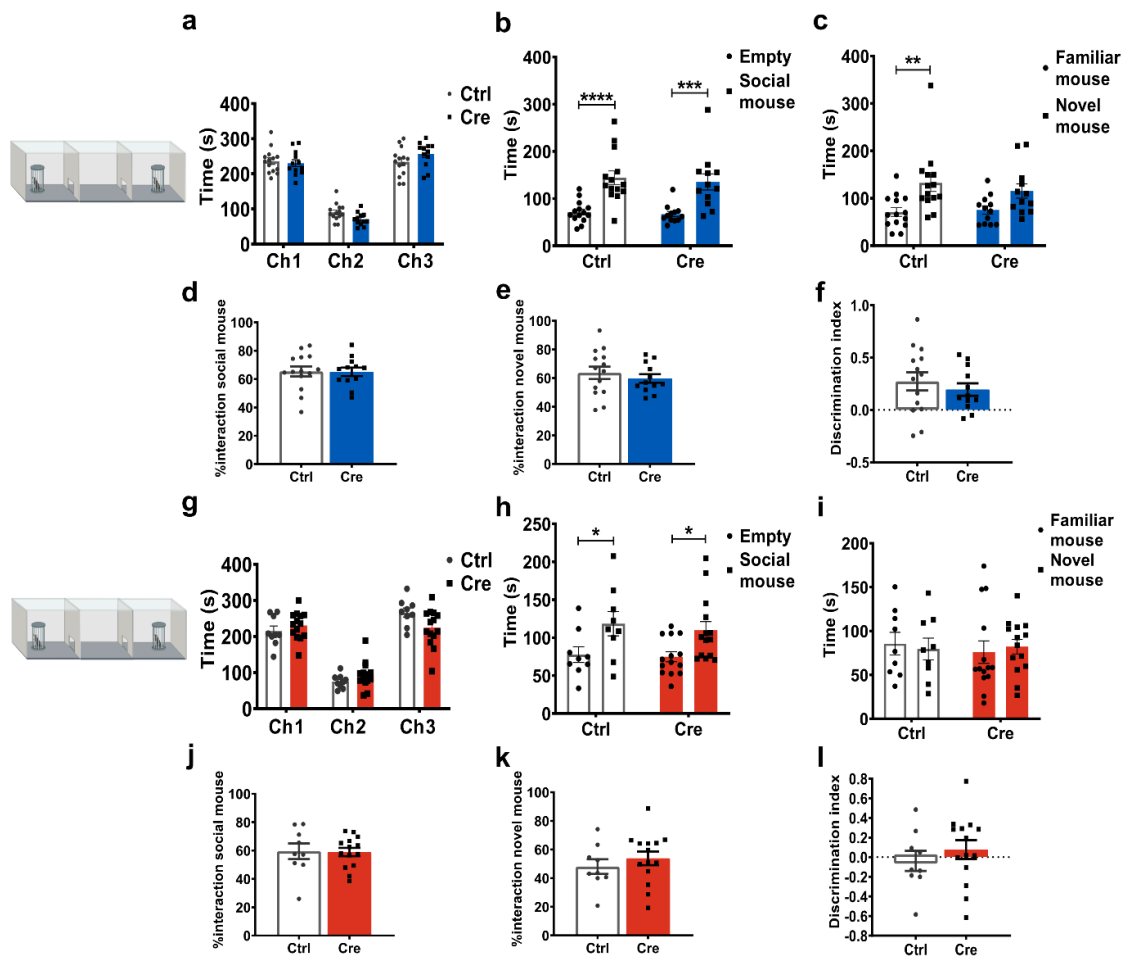


**Figure 34: Characterization of social behavior of Nex-Cre male and female mice.** a, g) Time spent in each of the three chambers during habituation by male (top) and female (bottom) Nex-Cre mice. b, h) Time spent interacting with empty cage vs social mouse by male (top) (Two-way ANOVA: interaction,  $F_{(1, 48)} = 0.03053$ ,  $p = 0.8620$ ; genotype,  $F_{(1, 48)} = 0.3225$ ,  $p = 0.5728$ ; social mouse,  $F_{(1, 48)} = 34.77$ ,  $p < 0.0001$ ) and female (bottom) (Two-way ANOVA: interaction,  $F_{(1, 42)} = 0.06566$ ,  $p = 0.7990$ ; genotype,  $F_{(1, 42)} = 0.2601$ ,  $p = 0.6127$ ; social mouse,  $F_{(1, 42)} = 11.66$ ,  $p = 0.0014$ ) Nex-Cre mice. c, i) Time spent interacting with familiar mouse vs. novel mouse by male (top) (Two-way ANOVA: interaction,  $F_{(1, 48)} = 0.6303$ ,  $p = 0.4312$ ; genotype,  $F_{(1, 48)} = 0.2303$ ,  $p = 0.6335$ ; novel mouse,  $F_{(1, 48)} = 13.91$ ,  $p = 0.0005$ ) and female (bottom) (Two-way ANOVA: interaction,  $F_{(1, 42)} = 0.2661$ ,  $p = 0.6087$ ; genotype,  $F_{(1, 42)} = 0.08603$ ,  $p = 0.7707$ ; novel mouse,  $F_{(1, 42)} = 0.0001352$ ,  $p = 0.9908$ ) Nex-Cre mice. d, j) Percentage interaction time with social mouse in male (top) (Student's t-test,  $t_{24} = 0.06377$ ,  $p = 0.9497$ ) and female (bottom) (Student's t-test,  $t_{21} = 0.09832$ ,  $p = 0.9226$ ) mice. e, k) Percentage interaction time with novel mouse - male (top) (Student's t-test,  $t_{24} = 0.7196$ ,  $p = 0.4787$ ) and female (bottom) (Student's t-test,  $t_{21} = 0.7958$ ,  $p = 0.435$ ) mice. f, l) Discrimination index - male (top) (Student's t-test,  $t_{24} = 0.7196$ ,  $p = 0.4787$ ) and female (bottom) (Student's t-test,  $t_{21} = 0.7958$ ,  $p = 0.435$ ) mice.

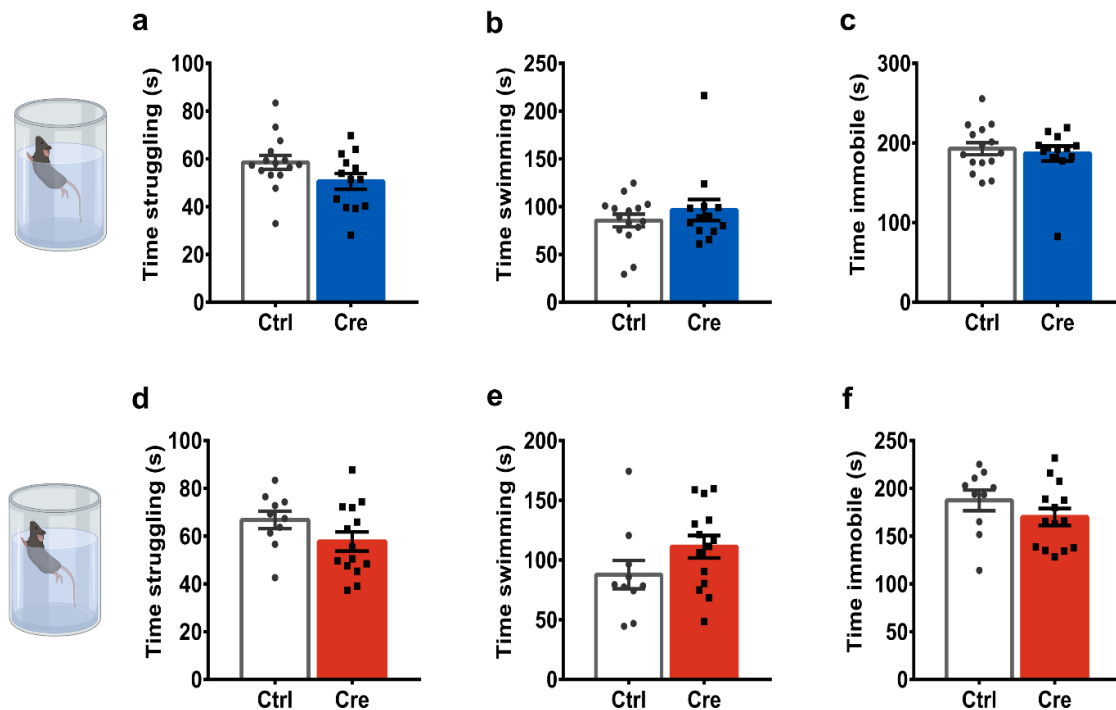


**Figure 35: Characterization of Nex-Cre mice in the forced swim test.** a, d) Time spent struggling in male (top) (Student's t-test,  $t_{26} = 1.813$ ,  $p = 0.0814$ ) and female mice (bottom) (Student's t-test,  $t_{22} = 1.599$ ,  $p = 0.1241$ ). b, e) Time spent swimming in male (top) (Student's t-test,  $t_{26} = 0.8811$ ,  $p = 0.3863$ ) and female (bottom) (Student's t-test,  $t_{22} = 1.564$ ,  $p = 0.132$ ) mice. c, f) Immobility time in male (top) (Student's t-test,  $t_{26} = 0.5037$ ,  $p = 0.6187$ ) and female (bottom) (Student's t-test,  $t_{22} = 1.248$ ,  $p = 0.2253$ ) mice.

Characterizing Nex-Cre mice with respect to stress coping behavior in the FST revealed similar stress coping in male and female Ctrl and Cre mice (**Figure 35**). Male and female Ctrl and Cre mice were indistinguishable in the time they spent struggling, swimming and immobile during the task.

Taken together, these results suggest that the phenotypes observed in the  $Ca_v1.2$ -Nex CKO mice are due to inactivation of  $Ca_v1.2$  and not a result of the transgene insertion into the *Neurod6* locus or Cre activity.

### 4.3. CKO animals show reduced dendritic arbor complexity but no differences in pCREB expression levels

To study the effects of Ca<sub>v</sub>1.2 inactivation in glutamatergic forebrain neurons and stress on the cellular morphology, Golgi-cox staining was performed to visualize the dendritic branches of pyramidal neurons in female animals. Brain tissues from male animals were used for protein analysis because of limited availability of samples.

Stress effects on dendritic complexity were evaluated by Sholl analysis of traced CA1 neurons of the dorsal and dorso-ventral hippocampus. US CKO animals showed decreased dendritic complexity and dendritic length compared to their Ctrl littermates. In addition, ELS Ctrl animals also showed reduced dendritic complexity compared to US Ctrl mice (**Figure 36b, c, f - i**) (#intersections: three-way ANOVA, distance × stress × genotype,  $F_{(53, 11236)} = 1.473$ ,  $p = 0.0144$ ; dendritic length: three-way ANOVA, distance × stress × genotype,  $F_{(53, 11236)} = 1.929$ ,  $p < 0.0001$ ; #interactions: one-way ANOVA,  $F_{(3, 212)} = 10.72$ ,  $p < 0.0001$ ; total dendritic length: one-way ANOVA,  $F_{(3, 212)} = 8.920$ ,  $p < 0.0001$ ). ELS Ctrl animals also showed reduced number of branches and branch points per cell compared to US Ctrl mice (**Figure 36d, e**) (#branches/cell: one-way ANOVA,  $F_{(3, 204)} = 11.25$ ,  $p < 0.0001$ ; #branch points/cell: one-way ANOVA,  $F_{(3, 204)} = 9.611$ ,  $p < 0.0001$ ). Taken together, although no strong genotype effects could be observed, LBN stress indeed induced dendritic atrophy which was clear in Ctrl animals but not in the CKO mice.

Phospho-CREB or pCREB is a known downstream target of Ca<sub>v</sub>1.2 signaling pathway and it also plays a role in dendritic branching (Rajadhyaksha et al. 1999; Wheeler et al. 2008; Finsterwald et al. 2010). To investigate whether Ca<sub>v</sub>1.2 in combination with early life stress affects pCREB expression, I checked pCREB protein expression at basal levels in the PFC and hippocampus of Ca<sub>v</sub>1.2-Nex mice. In male mice, no significant genotype or condition effects were observed in the basal expression of pCREB (**Figure 37a, c, d**) (One-way ANOVA, hippocampus:  $F_{(3, 19)} = 1.537$ ,  $p = 0.2374$ ; PFC:  $F_{(3, 19)} = 1.522$ ,  $p = 0.2412$ ). Similarly, female mice in all groups showed similar levels of pCREB expression at basal levels (**Figure 37b, e, f**) (One-way ANOVA, hippocampus:  $F_{(3, 22)} = 2.331$ ,  $p = 0.1021$ ; PFC:  $F_{(3, 21)} = 0.08394$ ,  $p = 0.9680$ ).

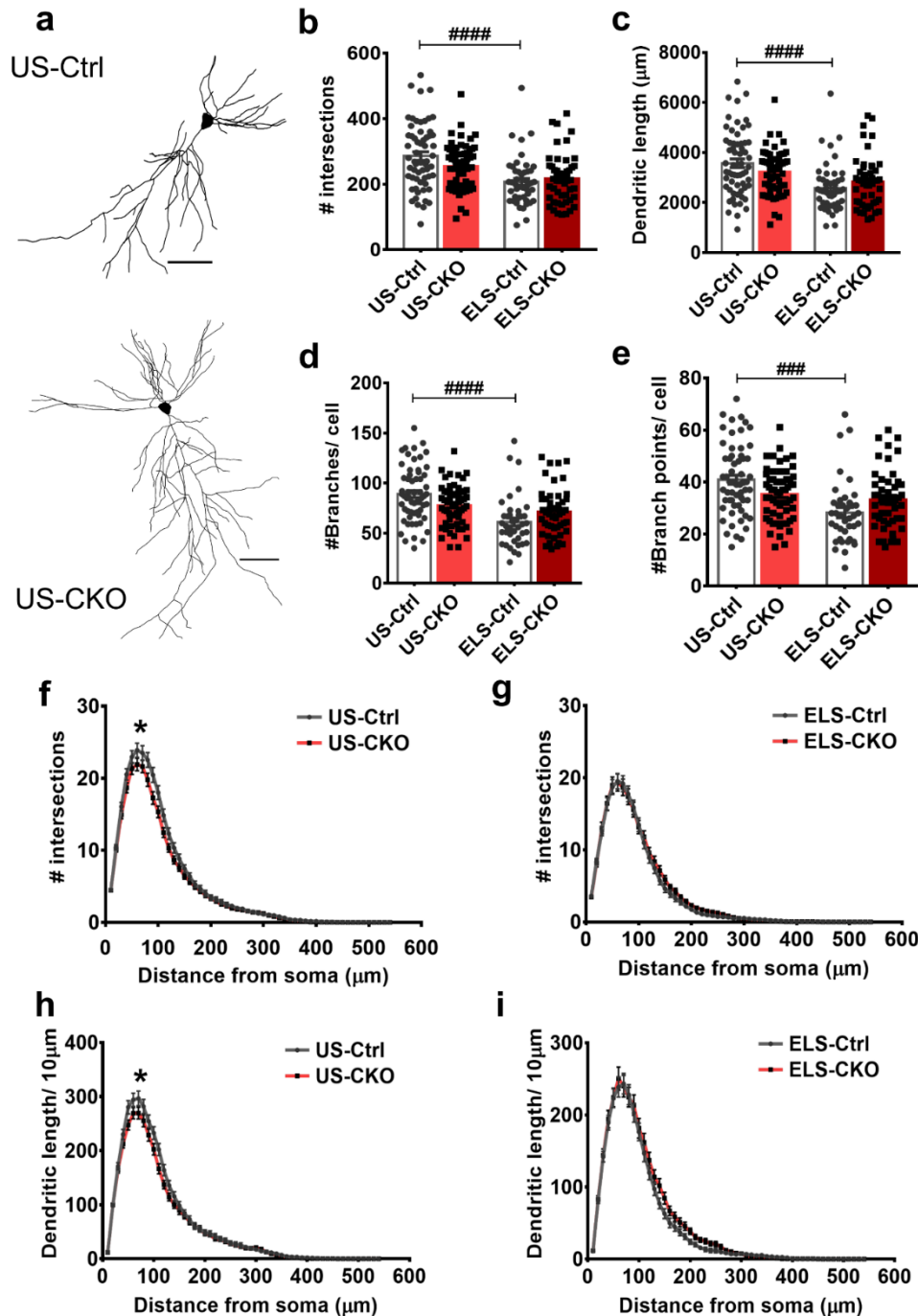


**Figure 36: Evaluation of dendritic complexity in unstressed and stressed female  $\text{Ca}_v1.2\text{-Nex}$  mice.** a) Representative tracings of neurons (top panel: US-Ctrl, bottom panel: US-CKO), b) Total number of intersections. c) Total dendritic length. d, e) Total number of branches and branch points per neuron. f, g) Sholl curve for number of intersections in unstressed and stressed mice. h, i) Sholl curve for dendritic length in unstressed and stressed mice. (One-way ANOVA + Bonferroni post hoc, Two-way ANOVA-repeated measures + Bonferroni post hoc,  $p < 0.05$ , \* represents comparison to Ctrl mice of the same condition, # represents comparison to unstressed mice of the same genotype)

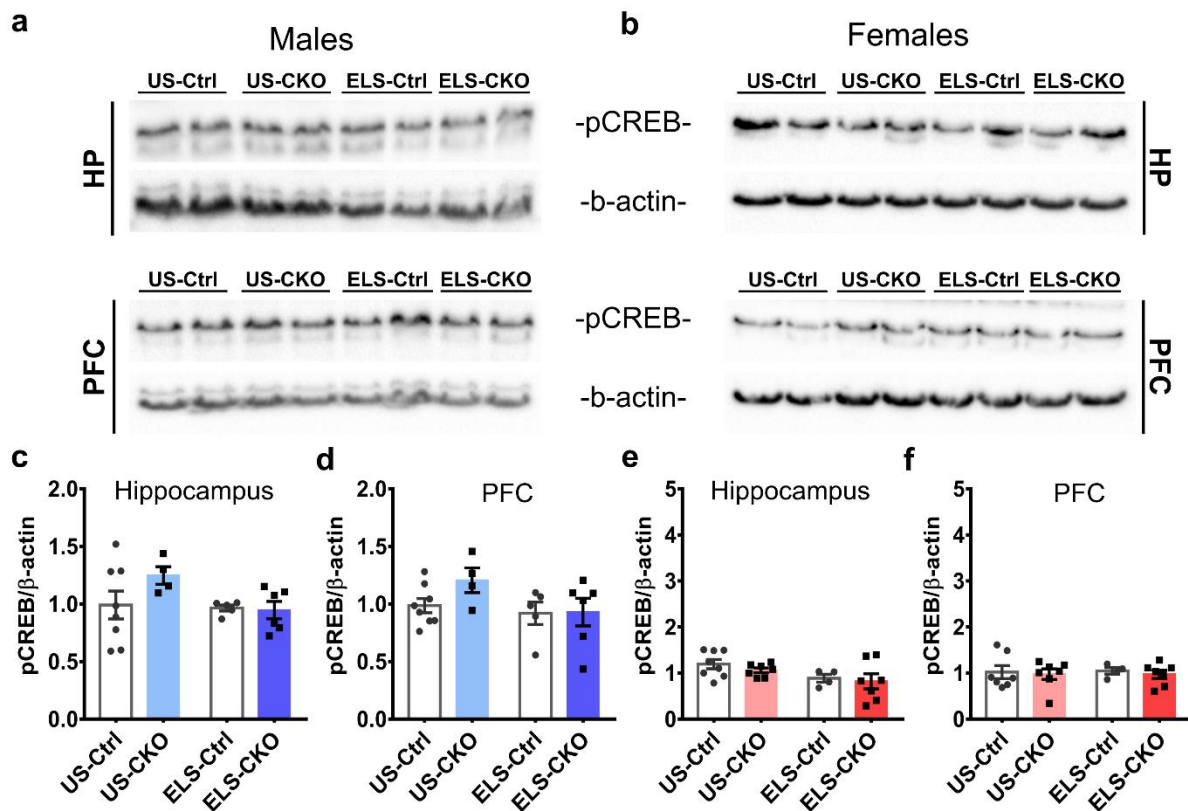


**Figure 37: Western blot analysis of pCREB expression in hippocampal and PFC tissues in male and female mice.** a, b) pCREB expression in hippocampus (HP) and prefrontal cortex (PFC) in male and female mice. Relative intensity of pCREB normalized to  $\beta$ -actin in male c) hippocampal tissue, d) PFC tissue and female e) hippocampal tissue, f) PFC tissue. (One-way ANOVA + Bonferroni post hoc) (Brain tissues from all male  $Ca_v1.2$ -Nex animals used in behavior tests were used for protein analysis due to small sample numbers. Brain tissues from female mice were distributed randomly for Golgi-cox staining and protein analysis).

#### 4.4. Characterization of female $Ca_v1.2$ -Nex CKO mice

Previous studies have reported robust phenotypes in different mouse models with  $Ca_v1.2$  inactivation, including the  $Ca_v1.2$ -Nex mouse line. However, most of these studies were conducted in male animals. Thus, to investigate the effects of  $Ca_v1.2$  inactivation in forebrain glutamatergic neurons in female animals and to check if estrous cycle played a role in these phenotypes, I evaluated them in a series of behavioral tests.

#### 4.4.1. Estrous cycle phenotyping of $Ca_v1.2$ -Nex animals

To investigate if the stage of the estrous cycle in female mice influenced behavioral phenotyping and if conditional inactivation of  $Ca_v1.2$  affected the estrous cycle, I monitored the estrous cycle of female animals for a period of 14 days prior to the behavioral testing. Different stages of estrous cycle were identified depending on the presence of different types of cells in each stage as summarized in Table 4 (see Methods section). Ctrl and CKO animals had similar durations of different stages of the estrous cycle and normal cycling during the period of investigation (**Figure 38**).

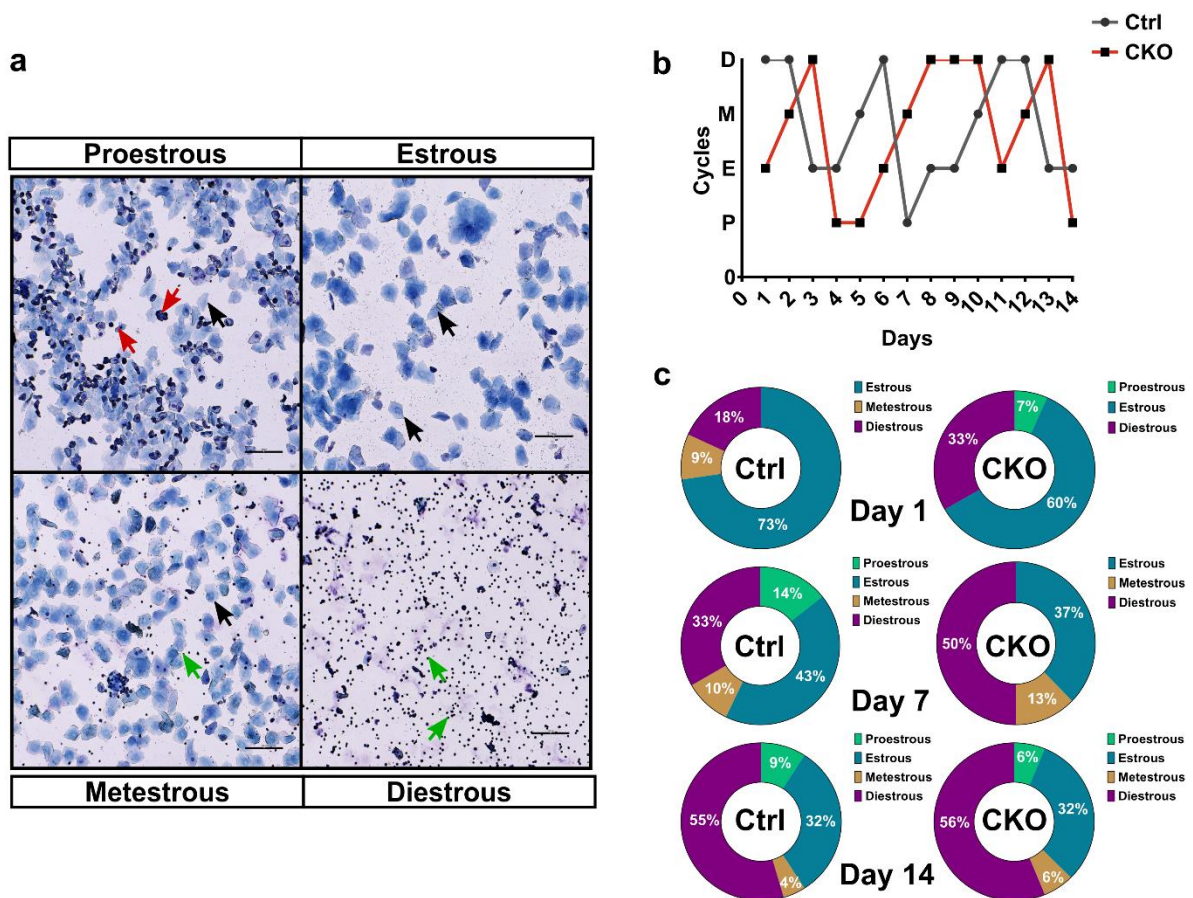


**Figure 38: Example of different stages of estrous cycle in Ctrl and CKO mice.** a) Different stages of estrous cycle distinguished by characteristic cell types (Red arrow: nucleated epithelial cells, Black arrow: anucleated cornified epithelial cells, green arrow: leukocytes). b) Sample graph representing the stages of estrous cycle through the 14-day period in Ctrl and CKO groups. (Abbreviations: P - proestrous, E - estrous, M - Metestrous, D - Diestrous). c) Percentage of animals in different stages of the cycle on days 1, 7 and 14.

#### 4.4.2. Female CKO mice show hyperactivity and increased anxiety-related behavior

Previous studies reported hyperlocomotion and altered anxiety-related behavior in male  $Ca_v1.2$ -Nex mice (Dedic et al. 2018). Thus  $Ca_v1.2$ -Nex CKO females and their Ctrl littermates were assessed for their locomotor activity and anxiety-related behavior in OFT, EPM and LDB. In the OFT, female CKO mice were hyperactive compared to the Ctrl animals (**Figure 39a, b**) (Locomotor activity: two-way ANOVA, interaction,  $F_{(5, 165)} = 3.077$ ,  $p = 0.0111$ ; genotype,  $F_{(1, 33)} = 25.99$ ,  $p < 0.0001$ ; time,  $F_{(5, 165)} = 3.004$ ,  $p = 0.0127$ ; total distance: Student's t-test,  $t_{33}=5.098$ ,  $p < 0.0001$ ). Furthermore, CKO mice spent lesser time in the inner zone in the first five minutes of the test compared to the Ctrl littermates with no difference in the inner zone entries (**Figure 39c, d**) (Student's t-test, inner zone time:  $t_{33} = 2.931$ ,  $p = 0.0061$ ; inner zone entries:  $t_{33} = 1.546$ ,  $p = 0.1317$ ).

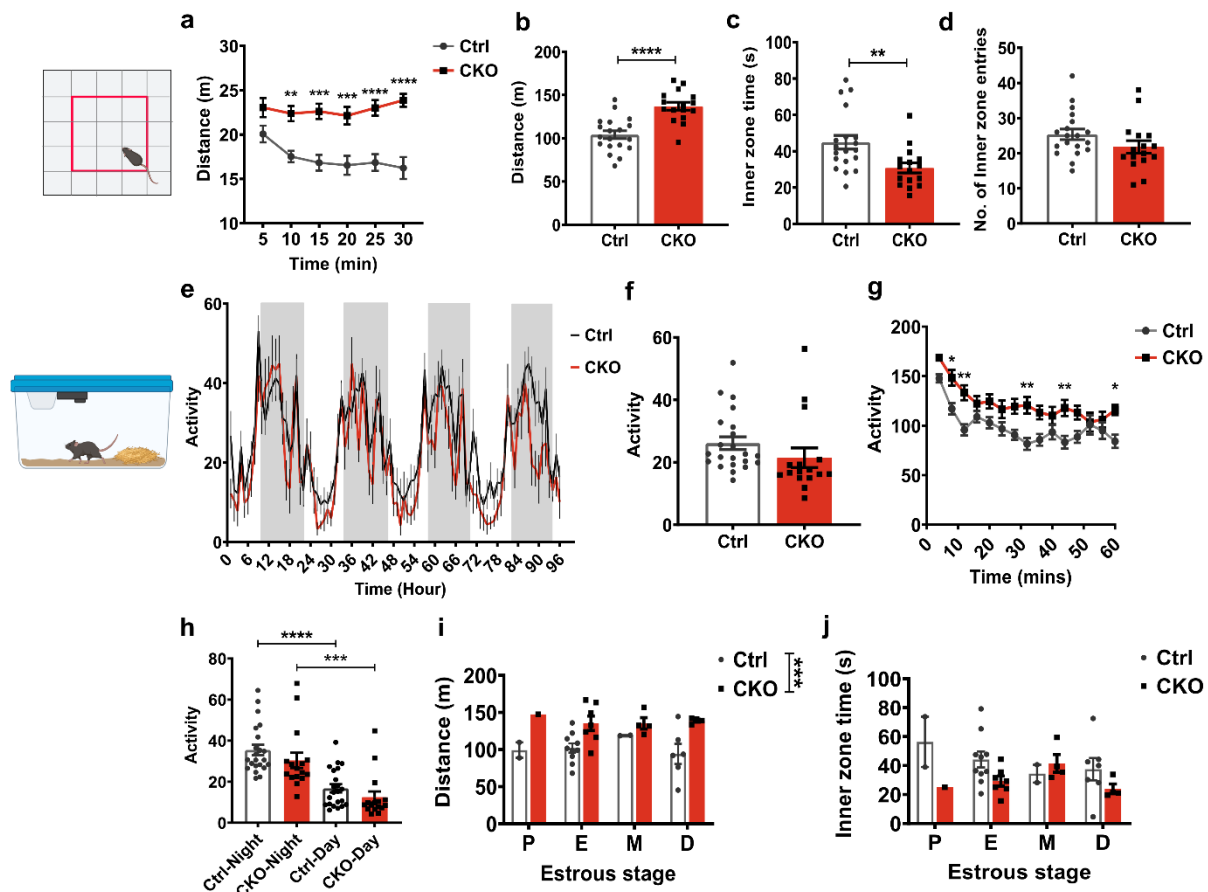


**Figure 39: Female  $Ca_v1.2$ -Nex CKO mice show hyperlocomotion and increased anxiety-related behavior in the OFT but normal basal activity.** a) Distance covered in 5-min time segments. b) Total distance traveled during open field exploration. c) Time spent in the inner zone during first 5 minutes of the OFT. d) Number of inner zone entries during the first 5 minutes of the test. e) Home cage activity across

96 hours (gray regions indicate dark phase and white regions indicate light phase). f) Average activity across 4 days. g) Activity during the first hour after introduction to a novel home cage. h) Activity during day and night in the home cage. i, j) Comparison of animals in different stages of the estrous cycle during the OFT (Abbreviations: P - Proestrous, E - Estrous, M - Metestrous, D - Diestrous) (Two-way ANOVA repeated measures + Bonferroni post hoc, Student's t-test, one-way and two-way ANOVA + Bonferroni post hoc, \* represents  $p < 0.05$ )

Since female CKO animals showed hyperlocomotion in a novel environment, home cage activity was assessed to evaluate if they were hyperactive even at basal housing conditions. After acclimatization to the novel home cage, the CKO animals showed activity similar to their Ctrl littermates (**Figure 39e, f**) (home cage locomotion: two-way ANOVA; interaction,  $F_{(95, 3420)} = 1.144$ ,  $p = 0.1633$ ; genotype,  $F_{(1, 36)} = 1.697$ ,  $p = 0.2010$ ; time,  $F_{(95, 3420)} = 15.28$ ,  $p < 0.0001$ ; average activity: Student's t-test,  $t_{36} = 1.302$ ,  $p = 0.201$ ). CKO animals showed hyperactivity during the first 60 minutes after being introduced into a novel cage suggesting that CKO female mice show hyperactivity in a novel environment (**Figure 39g**) (Two-way ANOVA; interaction,  $F_{(14, 504)} = 1.562$ ,  $p = 0.0857$ ; genotype,  $F_{(1, 36)} = 15.75$ ,  $p = 0.0003$ ; time,  $F_{(14, 504)} = 15.09$ ,  $p < 0.0001$ ). As expected for nocturnal animals, Ctrl and CKO animals were more active during the dark phase compared to the light phase (**Figure 39h**) (one-way ANOVA,  $F_{(3, 72)} = 16.66$ ,  $p < 0.0001$ ).

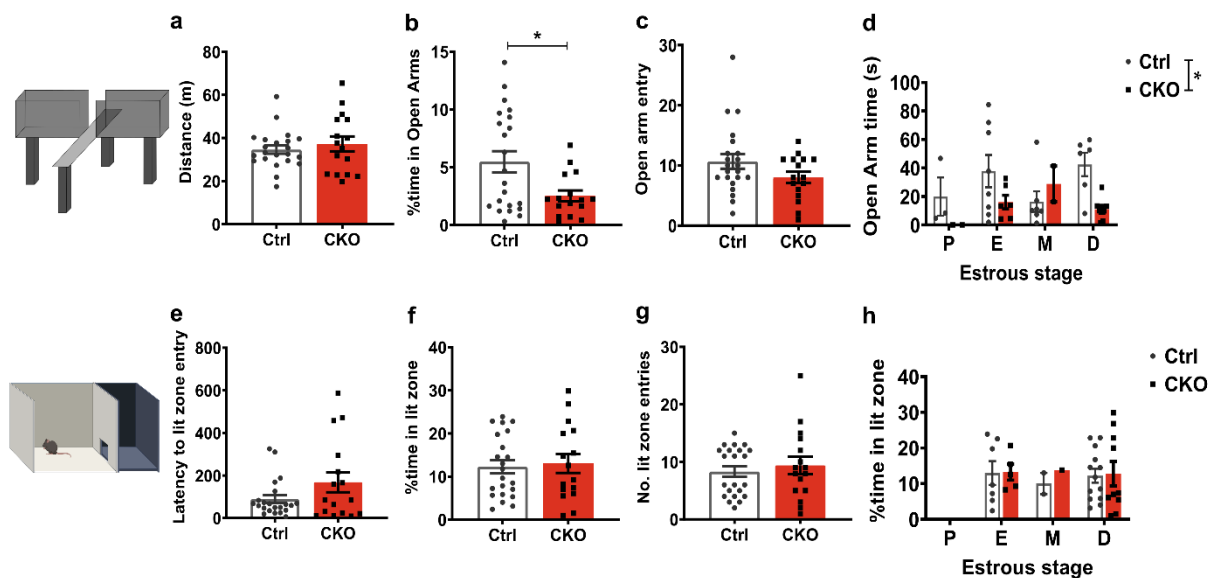


**Figure 40: Female  $Ca_v1.2$ -Nex CKO mice show increased anxiety-related behavior in EPM but not LDB.** a) Distance travelled in EPM. b) Percentage time spent in open arms. c) Number of open arm entries. e) Latency to enter the lit zone in LDB. f) Percentage time spent in the lit zone. g) Number of entries into

the lit zone. d, h) Animals in different stages of the estrous cycle and the time spent in open arm and lit zone. (Student's t-test, two-way ANOVA + Bonferroni post hoc, \* represents  $p < 0.05$ ).

CKO mice spent significantly lesser time in the open arms of the EPM compared to their Ctrl littermates with no difference in the number of open arm entries, suggesting an anxiogenic phenotype (Student's t-test, open arm time:  $t_{36} = 2.564$ ,  $p = 0.0147$ ; open arm entries:  $t_{36} = 1.63$ ,  $p = 0.1118$ ) (**Figure 40b, c**). In addition, Ctrl and CKO were indistinguishable in the total distance they travelled during the EPM task suggesting that hyperactivity did not influence the number of open arm entries or time spent in the open arms (Student's t-test,  $t_{36} = 0.7345$ ,  $p = 0.4674$ ) (**Figure 40a**).

However, in the LDB test, which is another test for anxiety-related behavior, no significant differences were observed between the two groups in the time spent in the lit zone, number of entries to the lit zone or the latency to enter the lit zone (**Figure 40e - g**) (Student's t-test, Latency to lit zone:  $t_{36} = 1.756$ ,  $p = 0.0875$ ; lit zone time:  $t_{36} = 0.3038$ ,  $p = 0.763$ ; lit zone entry:  $t_{36} = 0.6253$ ,  $p = 0.5357$ ).

The estrous cycle of the animals was evaluated after each behavioral test to check if it influenced the phenotype of the animals. The different cycle stages did not have a significant impact on the total distance travelled in the OFT (Two-way ANOVA: interaction,  $F_{(3, 28)} = 0.544$ ,  $p = 0.6562$ ; genotype,  $F_{(1, 28)} = 13.84$ ,  $p = 0.0009$ ; estrous stage,  $F_{(3, 28)} = 0.2932$ ,  $p = 0.8300$ ) (**Figure 39i**), time spent in the inner zone of the OFT (Two-way ANOVA: interaction,  $F_{(3, 29)} = 1.069$ ,  $p = 0.3776$ ; genotype,  $F_{(1, 29)} = 3.979$ ,  $p = 0.0555$ ; estrous stage,  $F_{(3, 29)} = 0.4981$ ,  $p = 0.6865$ ) (**Figure 39j**), time spent in the EPM open arms (Two-way ANOVA: interaction,  $F_{(3, 34)} = 1.71$ ,  $p = 0.1834$ ; genotype,  $F_{(1, 34)} = 4.39$ ,  $p = 0.0437$ ; estrous stage,  $F_{(3, 34)} = 0.9592$ ,  $p = 0.4231$ ) (**Figure 40d**) or time spent in the LDB lit zone (Two-way ANOVA: interaction,  $F_{(2, 32)} = 0.04903$ ,  $p = 0.9522$ ; genotype,  $F_{(1, 32)} = 0.1495$ ,  $p = 0.7015$ ; estrous stage,  $F_{(2, 32)} = 0.03077$ ,  $p = 0.9697$ ) (**Figure 40h**). Taken together, these results confirm that female  $Ca_v1.2$ -Nex CKO animals show hyperactivity in a novel environment and increased anxiety-related behavior which are reminiscent of endophenotypes of psychiatric disorders. These phenotypes are independent of the estrous cycle.

#### 4.4.3. Female CKO mice show working and spatial memory deficits

Since it is well established that  $Ca_v1.2$  channels play an important role in memory formation (White et al. 2008; Zanos et al. 2015; Temme et al. 2016; Dedic et al. 2018), different cognitive tasks were used to assess how deletion of  $Ca_v1.2$  in glutamatergic neurons of the forebrain affects the cognitive performance in female mice. The cognitive tests included Y-maze test for working memory, NOR, SOR and MWM.

Female CKO mice showed a significant deficit in the working memory as indicated by the reduced number of spontaneous alternations compared to Ctrl mice in the Y-maze task (**Figure 41b**) (Student's t-test,  $t_{36} = 2.3$ ,  $p = 0.0273$ ). Ctrl and CKO mice did not differ in the number of entries they made into each arm and hyperlocomotion was absent in the CKO mice (**Figure 41a, c**) (Student's t-test, arm entries:  $t_{36} = 1.933$ ,  $p = 0.0611$ ; distance:  $t_{36} = 1.795$ ,  $p = 0.0811$ ). Analysis of the estrous cycle after the behavioral test did not reveal any significant differences suggesting that the spontaneous alternations were independent of the stages of the estrous cycle (**Figure 41d**) (Two-way ANOVA: interaction,  $F_{(3,30)} = 0.5489$ ,  $p = 0.6528$ ; genotype,  $F_{(1,30)} = 3.582$ ,  $p = 0.0681$ ; estrous stage,  $F_{(3,30)} = 0.3836$ ,  $p = 0.7655$ ).

To further investigate the impact of  $Ca_v1.2$  inactivation on learning and memory, I assessed the animals also in the NOR and SOR tasks which were carried out in the Y-maze apparatus. In both tasks, neither group showed a bias toward a particular object or location (**Figure 41e, i**) (Student's t-test, Object bias, NOR:  $t_{36} = 0.5657$ ,  $p = 0.5751$ ; SOR:  $t_{36} = 1.32$ ,  $p = 0.1951$ ). In addition, Ctrl and CKO animals spent more than 20% of the time interacting with the objects, with no genotype differences (**Figure 41f, j**) (Student's t-test, Object interaction time (NOR):  $t_{36} = 1.14$ ,  $p = 0.262$ ; object interaction time (SOR):  $t_{36} = 1.198$ ,  $p = 0.2386$ ).

Furthermore, Ctrl and CKO mice did not differ in their novelty preference for a novel object or location (**Figure 41g, k**) (Student's t-test, novelty preference, NOR:  $t_{36} = 0.6007$ ,  $p = 0.5518$ ; SOR:  $t_{36} = 0.3378$ ,  $p = 0.7374$ ) nor in their discrimination index for the novel object (**Figure 41h**) or novel location (**Figure 41l**) (Student's t-test, discrimination index, NOR:  $t_{36} = 0.6007$ ,  $p = 0.5518$ ; SOR:  $t_{36} = 0.3378$ ,  $p = 0.7374$ ). Moreover, estrous cycle did not have any effect on the assessed parameters (**Figure 41m, n**) (Two-way ANOVA, NOR discrimination index: interaction,  $F_{(3,30)} = 0.3234$ ,  $p = 0.8084$ ; genotype,  $F_{(1,30)} = 0.0003104$ ,  $p = 0.9861$ ; estrous stage,  $F_{(3,30)} = 0.5528$ ,  $p =$

0.6502; SOR discrimination index: interaction,  $F_{(3, 30)} = 0.3838$ ,  $p = 0.7654$ ; genotype,  $F_{(1, 30)} = 0.4403$ ,  $p = 0.5120$ ; estrous stage,  $F_{(3, 30)} = 1.711$ ,  $p = 0.1858$ ).

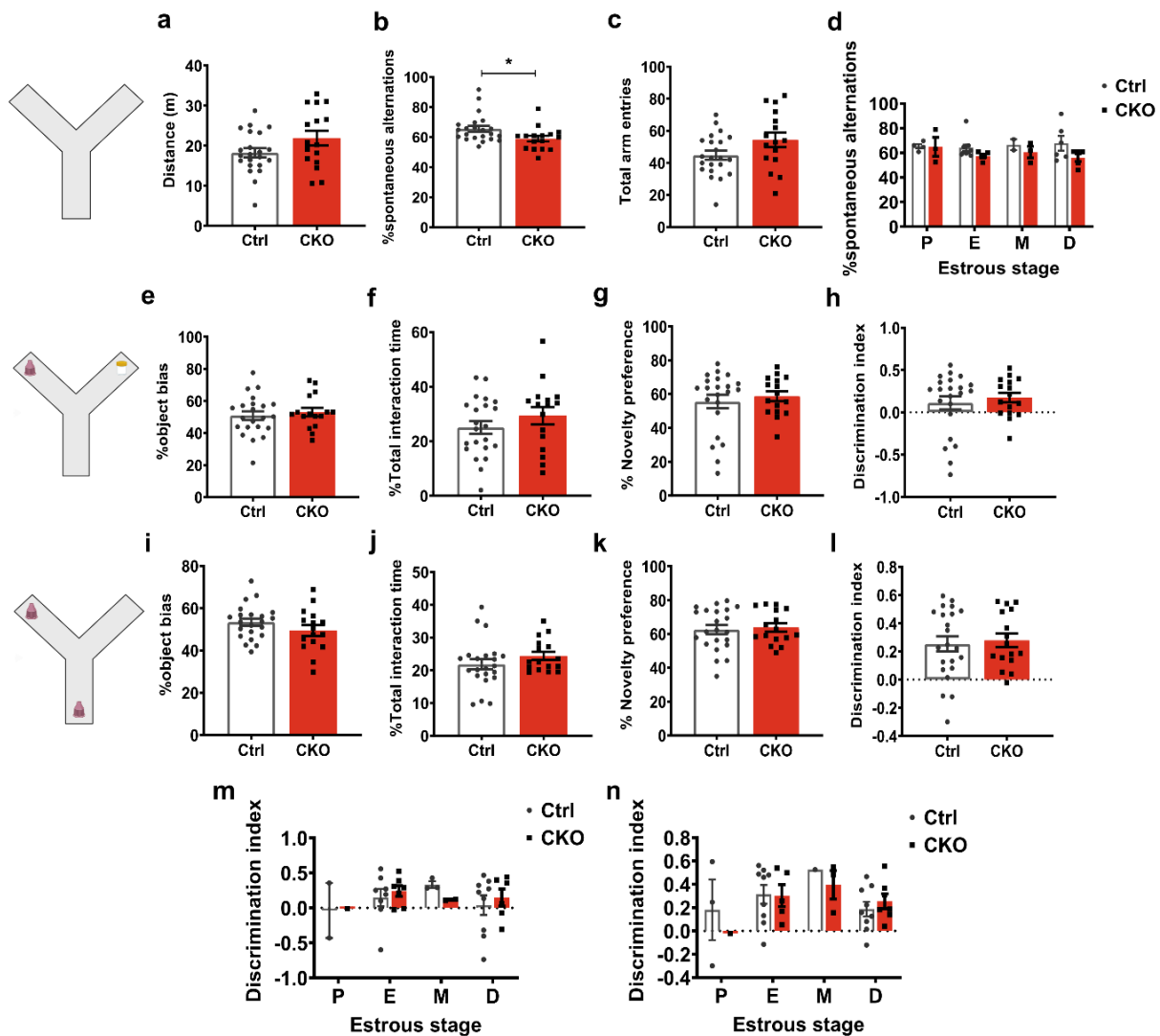


**Figure 41: Characterization of cognitive performance of female  $Ca_v1.2$ -Nex mice.** a) Distance travelled in the Y-maze apparatus. b) Percentage spontaneous alternations. c) Total number of arm entries. d) Comparison of spontaneous alternations for animals in different stages of estrous cycle. e, i) Percentage object bias in NOR (e) and SOR (i). f, j) Percentage interaction time with objects in NOR (f) and SOR (j). g, k) Novelty preference for object in NOR (g) and novel location in SOR (k). h, l) Discrimination index in NOR (h) and SOR (l). m, n) Comparison of discrimination index of animals in different stages of estrous cycle in NOR (m) and SOR (n). (Student's t-test, two-way ANOVA + Bonferroni post hoc, \* represents  $p < 0.05$ ).

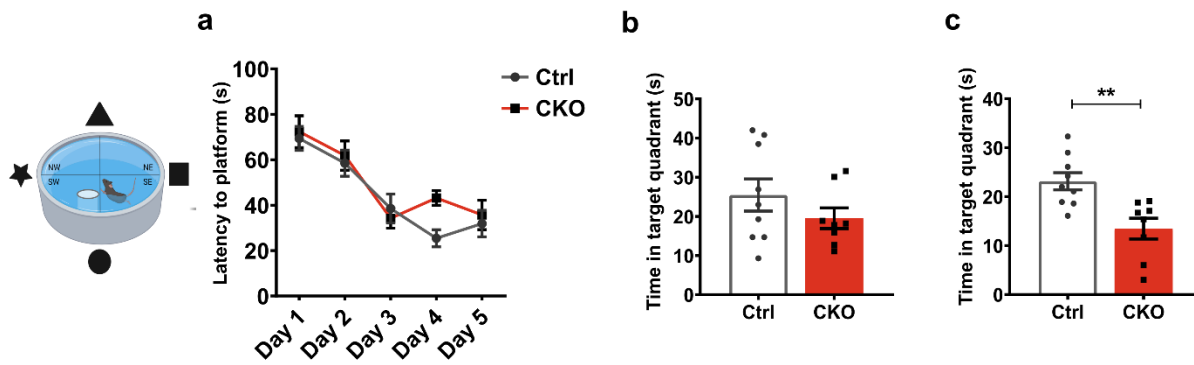


**Figure 42:  $Ca_v1.2$ -Nex CKO mice exhibit spatial memory deficits.** a) Latency to finding the platform during training days. b) Time spent in the target quadrant during probe test 24 hours after the last training day. c) Time spent in target quadrant in probe trial after 7 days. (Two-way ANOVA repeated measures + Bonferroni post hoc, Student's t-test, \* represents  $p < 0.05$ ).

Previous studies have reported deficits in spatial memory in  $Ca_v1.2$  CKO mice, particularly in the Morris water maze task (White et al. 2008; Dedic et al. 2018). To verify whether female CKO mice also showed similar deficits in spatial learning, a different cohort of animals was tested in the Morris water maze task. Ctrl and CKO animals showed similar latency to finding the hidden platform during the training days (**Figure 42a**) (Two-way ANOVA-repeated measures: interaction,  $F_{(4, 60)} = 0.903$ ,  $p = 0.4680$ ; genotype,  $F_{(1, 15)} = 3.428$ ,  $p = 0.0839$ ; time,  $F_{(4, 60)} = 16.87$ ,  $p < 0.0001$ ). Ctrl and CKO mice also spent similar times in the target quadrant during the probe trial (**Figure 42b**) (Student's t-test,  $t_{15} = 1.177$ ,  $p = 0.2574$ ). Interestingly, CKO mice spent significantly less time in the target quadrant compared to their Ctrl littermates indicating impaired remote spatial memory (**Figure 42c**) (Student's t-test,  $t_{15} = 3.526$ ,  $p = 0.0031$ ).

Taken together, these results suggest that  $Ca_v1.2$ -Nex CKO animals show working, and remote spatial memory deficits as indicated in the Y maze and MWM tests.

#### 4.4.4. Female CKO mice show enhanced active stress coping behavior

Since an earlier study reported an enhanced active stress coping behavior following  $Ca_v1.2$  inactivation in male mice, I assessed the  $Ca_v1.2$ -Nex female animals in the FST. Female CKO animals showed significantly enhanced swimming and reduced immobility compared to their Ctrl littermates indicating an enhanced active stress coping behavior, similar to earlier reports in male animals (**Figure 43b, c**) (Student's t-test, time swimming:  $t_{36} = 5.971$ ,  $p < 0.0001$ ; time immobile:  $t_{36} = 6.744$ ,  $p < 0.0001$ ). Ctrl and CKO mice were indistinguishable in the time spent struggling

(**Figure 43a**) (Student's t-test,  $t_{36} = 1.602$ ,  $p = 0.1179$ ). In addition, immobility in the FST was independent of the different stages of the estrous cycle (**Figure 43d**) (Two-way ANOVA: interaction,  $F_{(3, 30)} = 0.06948$ ,  $p = 0.9758$ ; genotype,  $F_{(1, 30)} = 30.23$ ,  $p < 0.0001$ ; estrous stage,  $F_{(3, 30)} = 0.6581$ ,  $p = 0.5842$ ).

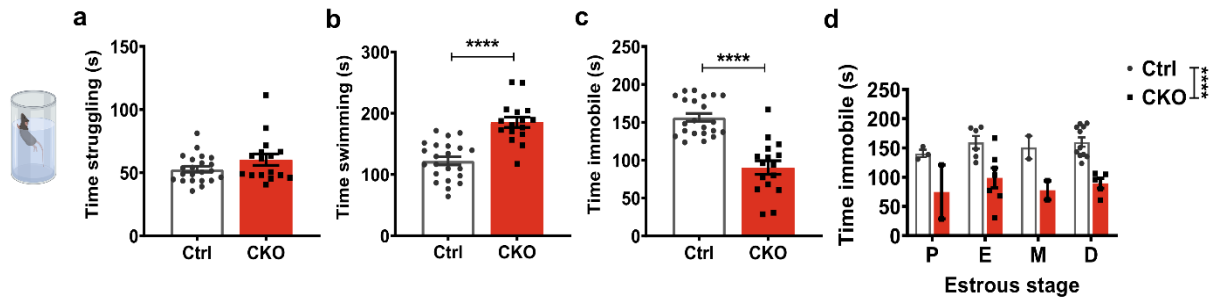


**Figure 43:  $Ca_v1.2$ -Nex female CKO mice showed enhanced active stress coping behavior.** a) Time spent struggling. b) Time spent swimming. c) Time spent immobile. d) Comparison of immobility time in animals in different estrous stages. (Student's t-test, two-way ANOVA + Bonferroni post hoc, \* represents  $p < 0.05$ ).

#### 4.5. Assessment of cellular and molecular alterations in female CKO mice

Since preliminary data from early life stress experiments revealed reduced dendritic complexity in the CKO mice, I wanted to further investigate the effects of selective  $Ca_v1.2$  inactivation in glutamatergic neurons on the morphology of hippocampal pyramidal neurons in female  $Ca_v1.2$ -Nex animals. I performed Golgi-cox staining on brain tissues to visualize the dendritic branches of pyramidal neurons in the CA1 region of dorsal and dorso-ventral hippocampus.

CKO mice showed reduced number of intersections (**Figure 44c**) (Student's t-test,  $t_{170} = 4.541$ ,  $p < 0.0001$ ), total dendritic length (**Figure 44d**) (Student's t-test,  $t_{170} = 5.145$ ,  $p < 0.0001$ ), number of branches per cell (**Figure 44e**) (Student's t-test,  $t_{171} = 2.684$ ,  $p = 0.0080$ ) and number of branch points per cell (**Figure 44f**) (Student's t-test,  $t_{171} = 2.988$ ,  $p = 0.0032$ ) compared to the Ctrl mice, all indicating reduced dendritic complexity. Furthermore, Sholl analysis revealed reduced dendritic complexity, especially between the radius of 50-150  $\mu\text{m}$  distance from the soma (**Figure 44g, h**) (Two-way ANOVA-repeated measure; #intersections: interaction,  $F_{(49, 8330)} = 11.72$ ,  $p < 0.0001$ ; distance,  $F_{(49, 8330)} = 856.2$ ,  $p < 0.0001$ ; genotype,  $F_{(1, 170)} = 20.62$ ,  $p < 0.0001$ ; dendritic length: interaction,  $F_{(49, 8330)} = 10.46$ ,  $p < 0.0001$ ; distance,  $F_{(49, 8330)} = 837.5$ ,  $p < 0.0001$ ; genotype,  $F_{(1, 170)} = 26.47$ ,  $p < 0.0001$ ). In addition to decreased dendritic complexity, CKO mice also

exhibited significantly reduced spine density compared to the Ctrl mice (**Figure 44i**) (Student's *t*-test,  $t_{128} = 2.105$ ,  $p = 0.0372$ ). From these results, it can be concluded that  $Ca_v1.2$  plays a role in dendritic branching and deletion of  $Ca_v1.2$  specifically in glutamatergic neurons during development affects dendritic branching and development.

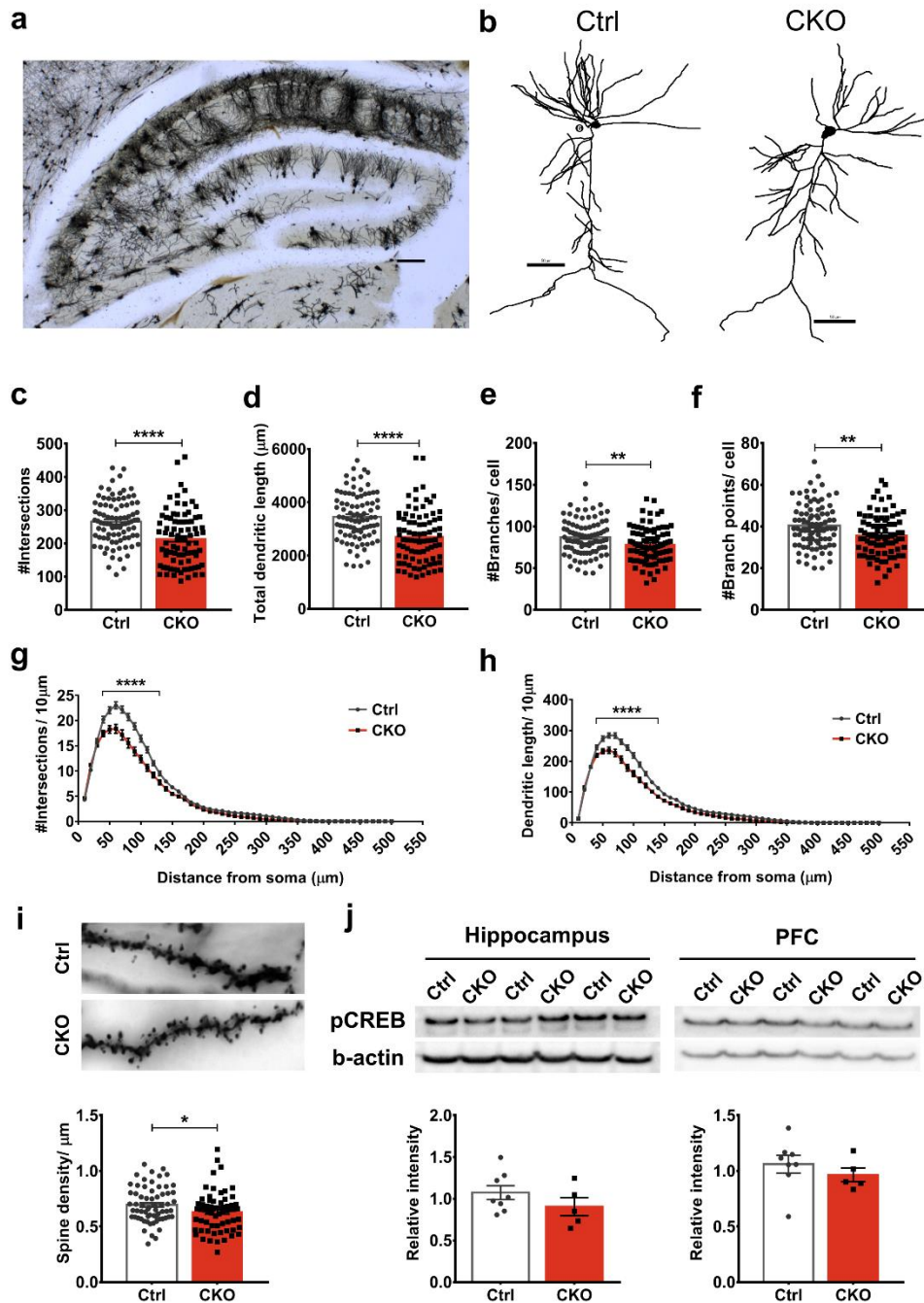


**Figure 44: Dendritic branching complexity, spine density and pCREB expression in  $Ca_v1.2$ -Nex female mice.** a) Representative image of hippocampal neurons (5× magnification) from Golgi-cox staining

procedure. b) Representative neuronal tracings of hippocampal CA1 pyramidal neurons. c) Total number of intersections. d) Total dendritic length. e) Number of branches per cell. f) Number of branch points per cell, g, h) Sholl analysis data for number of intersections and dendritic length, i) Spine density/ $\mu\text{m}$ . j) pCREB expression in the hippocampus and PFC (Ctrl:  $n = 5$ , CKO:  $n = 5$  for Golgi staining procedures, Ctrl:  $n = 8$ , CKO:  $n = 5$  for western blot, Student's t-test,  $p < 0.05$ ; Two-way ANOVA-repeated measures + Bonferroni post hoc,  $p < 0.05$ ).

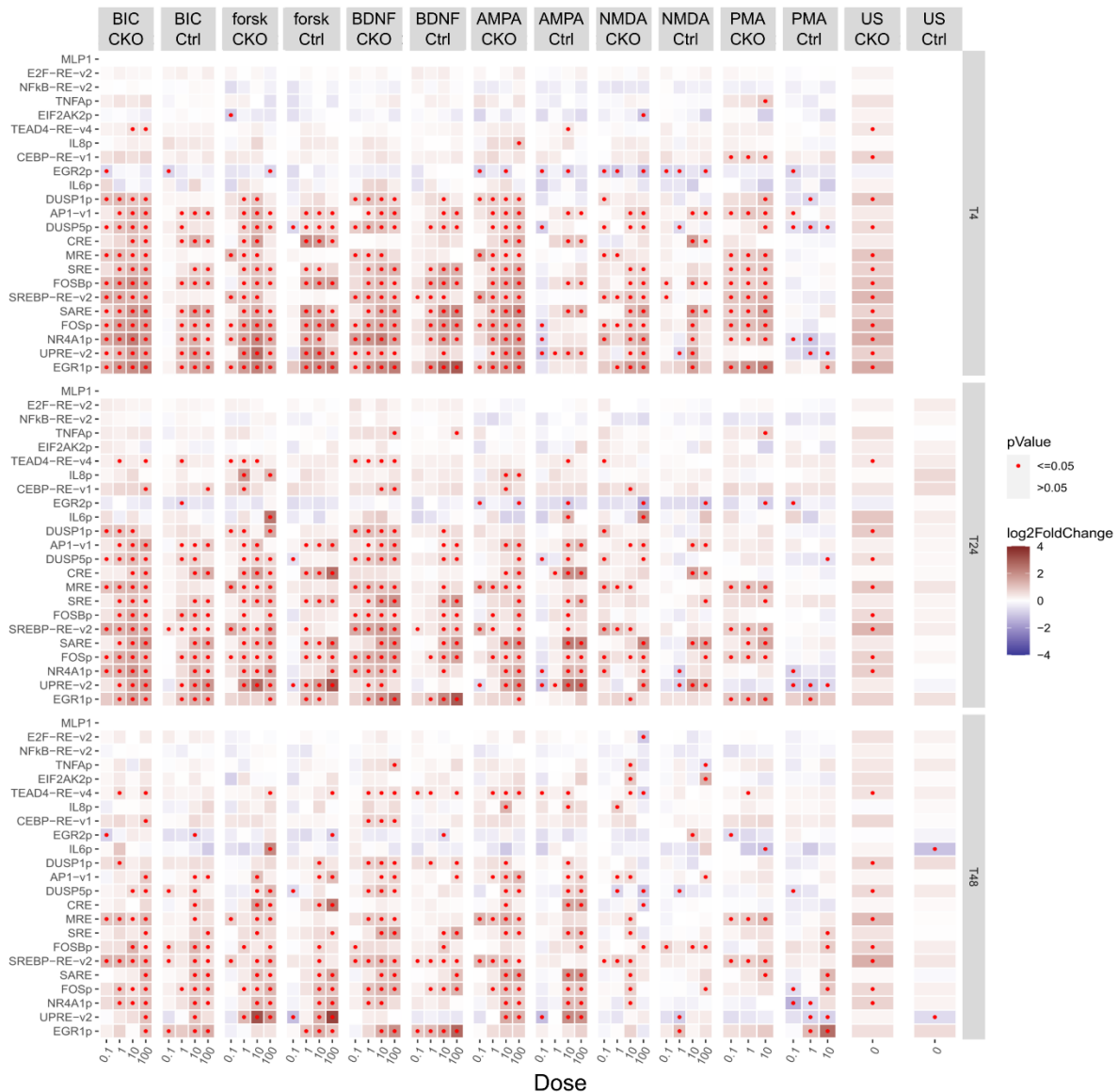


**Figure 45: minPROFILER assay.** The heatmap shows expression of 23 barcoded sensors (left y-axis) at different time points (right y-axis) after stimulation with different doses of 6 stimulants (top and bottom x-axis). CKO neurons showed higher basal level activity compared to Ctrl neurons. (Red dot indicates significant values).

Since pCREB is a well-known downstream target of Ca<sub>v</sub>1.2 signaling and plays a role in dendritic branching (White et al. 2008; Rajadhyaksha et al. 1999; Finsterwald et al. 2010), pCREB protein expression was analyzed in the Ca<sub>v</sub>1.2-Nex female mice. Probing of basal expression levels of pCREB in the hippocampus and PFC regions revealed no significant alterations between Ctrl and CKO mice (**Figure 44j**) (Student's t-test, hippocampus:  $t_{11} = 1.239$ ,  $p = 0.2413$ ; prefrontal cortex:  $t_{11} = 0.8511$ ,  $p = 0.4128$ ).

The minPROFILER assay is a multiplexed cell-based assay targeting individual cellular signaling events based on EXTassay technology (Herholt et al. 2018). The assay was performed by our collaborators at the Department of Psychiatry and Psychotherapy, LMU Klinikum, Munich, Germany. Differential expression of 23 barcoded sensors representing seven signaling pathways in primary cortical neurons were analyzed upon stimulation with different concentrations of 6 stimulants (**Figure 45**). Each stimulant yielded differential expressions of several genes in CKO samples compared to the Ctrl samples. Interestingly, unstimulated CKO samples already showed a higher basal activity compared to the Ctrl neurons. To validate these results and assess whether this high basal activity in CKO neurons is an artifact, further validation is required.

#### 4.6. Addressing the role of Ca<sub>v</sub>1.2 in inhibitory GABAergic neurons

Recently, a growing body of evidence suggests an involvement of inhibitory GABAergic neurons in the etiology of psychiatric disorders (Rossignol 2011; Marín 2012; Yang and Tsai 2017; van Bokhoven, Selten, and Nadif Kasri 2018; Xu and Wong 2018; Fogaça and Duman 2019). Several other studies suggested a cell type-specific role for Ca<sub>v</sub>1.2, thus I wanted to specifically address the effects of Ca<sub>v</sub>1.2 deletion in GABAergic neurons.

##### 4.6.1. Establishment of Ca<sub>v</sub>1.2-GABA mouse lines

To target all GABAergic neurons, first a conditional mouse line was generated using the tamoxifen-inducible GAD2-CreER<sup>T2</sup> driver line to allow temporally controlled inactivation at two different time points - development or early postnatal days versus adulthood. To validate this mouse line (Ca<sub>v</sub>1.2-Gad2-CreER<sup>T2</sup>), Cre recombination was induced using tamoxifen-containing chow provided to adult animals. Activation of a Cre-dependent HA-tagged reporter was visualized by immunofluorescence staining. However, only a sparse labeling of HA-tag positive cells was observed. Hence, to check if this was due to insufficient recombination, two new cohorts of mice

were treated with tamoxifen - either by tamoxifen-containing chow or by intraperitoneal injection of tamoxifen. Normal chow/ saline was administered to the respective control animals. However, similar to the first batch, this approach also yielded no or very few HA-tag positive cells even in regions that are known to be abundant in GABAergic neurons (**Figure 46**).

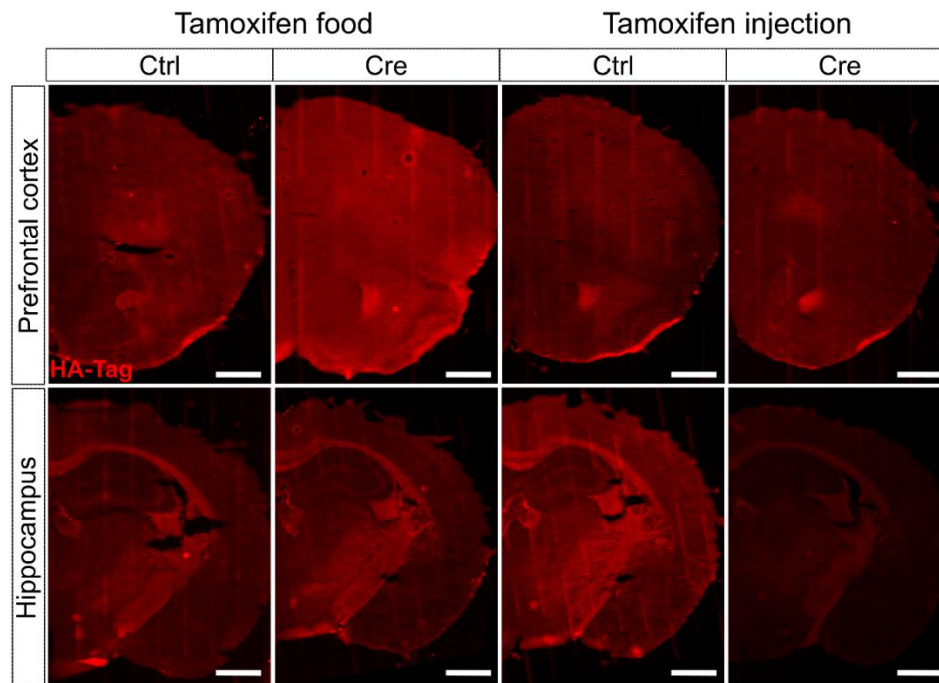


**Figure 46: Validation of  $Ca_v1.2$ -Gad2-CreER<sup>T2</sup> animals following tamoxifen administration.** Representative images of prefrontal cortical and hippocampal sections from Ctrl and Cre positive animals after: left - administration of tamoxifen-containing chow for two weeks and sacrifice after one-week washout period, right: single dose of tamoxifen intraperitoneal injection and sacrifice after one-week washout period. Scalebar: 1 mm.

Since the  $Ca_v1.2$ -Gad2-CreER<sup>T2</sup> mouse line showed only limited signs of Cre recombinase activity, another mouse line with  $Ca_v1.2$  inactivation specifically in parvalbumin-expressing (PV<sup>+</sup>) GABAergic neurons was generated by breeding floxed *Cacna1c* mice with the PV-Cre driver line ( $Ca_v1.2$ -PV). Immunofluorescence staining for the Cre-dependent HA-tagged reporter was used to confirm Cre-mediated recombination and to demonstrate the functionality of the mouse line.  $Ca_v1.2$ -PV mice showed a good percentage of HA-tag positive cells in the cortex, thalamus, amygdala, hippocampus, reticular thalamic nucleus, globus pallidus and caudate putamen regions reflecting the expected distribution pattern of PV<sup>+</sup> neurons (**Figure 47**). Thus, the  $Ca_v1.2$ -PV

mouse line was used for further behavioral phenotyping and analysis. The control and conditional knockout animals are referred to as Ctrl and CKO-PV henceforth.

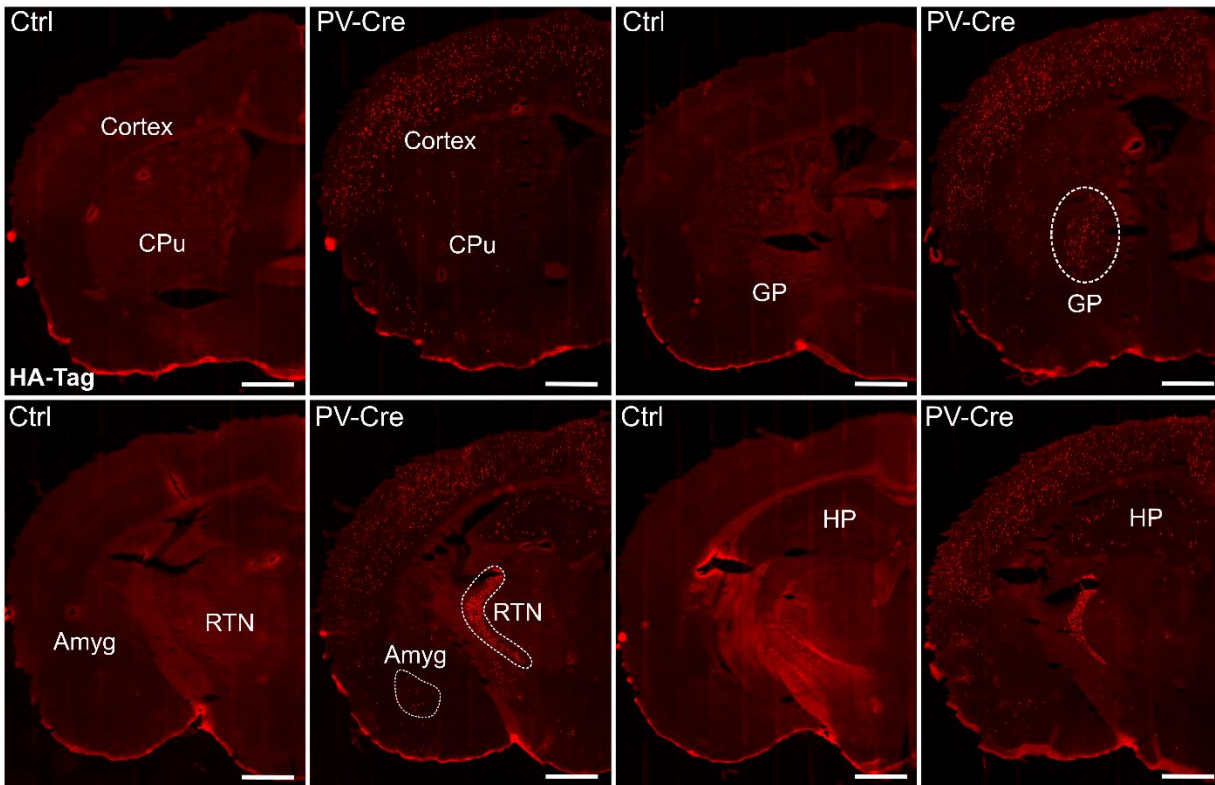


**Figure 47: Validation of the  $Ca_v1.2$ -PV mouse line.** Representative images showing expression of Cre-dependent HA-tagged reporter was seen in cortex, globus pallidus (GP), reticular thalamic nucleus (RTN), amygdala (Amyg), hippocampus (HP) and a sparse expression in caudate putamen (CPu). Scalebar: 1 mm.

#### 4.6.2. $Ca_v1.2$ -PV CKO mice exhibit anxiogenic behavior

To investigate the effects of  $Ca_v1.2$  deletion in  $PV^+$  GABAergic neurons on locomotor activity and anxiety-related behaviors,  $Ca_v1.2$ -PV mice were evaluated in the OFT, EPM and LDB tests. CKO-PV mice and their Ctrl littermates showed similar exploratory behavior in the OFT (**Figure 48a, b**) (Locomotor activity: two-way ANOVA-repeated measures; interaction,  $F_{(5, 165)} = 0.1605$ ,  $p = 0.9765$ ; genotype,  $F_{(1, 33)} = 1.617$ ,  $p = 0.2124$ , time,  $F_{(5, 165)} = 26.99$ ,  $p < 0.0001$ ; total distance: student's t-test,  $t_{33} = 1.272$ ,  $p = 0.2124$ ). CKO-PV mice showed increased anxiety-related behavior during the first five minutes of the test as indicated by reduced time spent in the center zone. The number of entries to the center zone was comparable between Ctrl and CKO-PV animals (**Figure 48c, d**) (Student's t-test, inner zone time:  $t_{32} = 2.202$ ,  $p = 0.035$ ; inner zone entry:  $t_{33} = 0.4041$ ,  $p = 0.6887$ ).

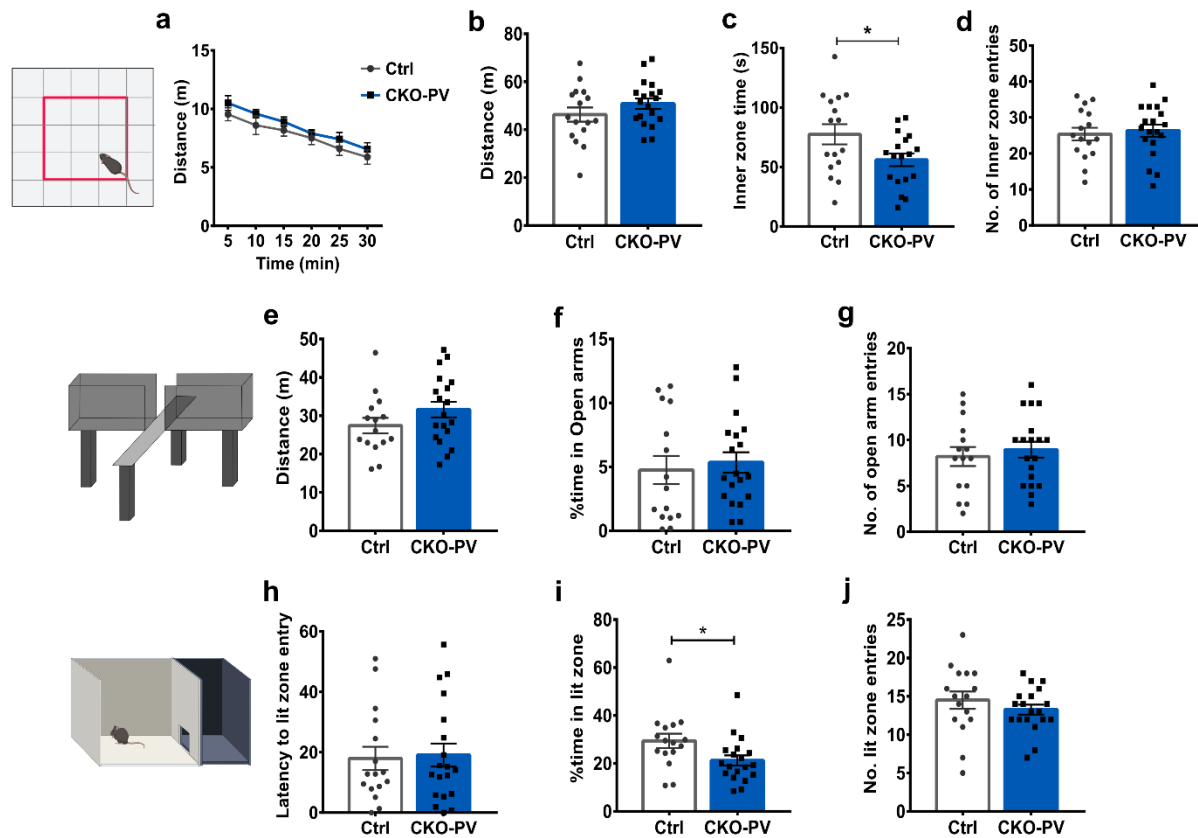


**Figure 48:  $Ca_v1.2$ -PV CKO mice show normal exploratory but anxiogenic behavior.** a) Distance travelled in 5-min time segments. b) Total distance traveled during exploration of open field. c) Time spent in the inner zone. d) Number of entries to the inner zone. e) Distance travelled in EPM. f) Time spent in open arms. g) Number of entries into the open arms. h) Latency to enter the lit zone. i) Time spent in the lit zone. j) Number of entries into the lit zone. (Two-way ANOVA repeated measures + Bonferroni post hoc, Student's t-test, \* represents  $p < 0.05$ )

Ctrl and CKO-PV mice were indistinguishable in the EPM test with comparable exploration and absence of alterations in the anxiety-related behavior (**Figure 48e**) (Student's t-test,  $t_{32} = 1.443$ ,  $p = 0.1588$ ). Accordingly, Ctrl and CKO-PV animals spent similar amount of time in the open arms of the apparatus (**Figure 48f**) (Student's t-test,  $t_{32} = 0.445$ ,  $p = 0.6593$ ). The number of entries into the open arm was also not significantly different between the Ctrl and CKO-PV animals (**Figure 48g**) (Student's t-test,  $t_{32} = 0.5556$ ,  $p = 0.5823$ ). Interestingly, CKO-PV showed altered anxiety-related behavior in the LDB test. CKO-PV animals spent significantly less time in the lit zone compared to their Ctrl littermates (**Figure 48i**) (Student's t-test,  $t_{33} = 2.274$ ,  $p = 0.0296$ ) while both groups had similar latencies to enter the lit zone (**Figure 48h**) (Student's t-test,  $t_{33} = 0.2051$ ,  $p =$

0.8387). There was no difference in the number of entries made to the lit zone between the two groups (**Figure 48j**) (Student's t-test,  $t_{33} = 0.9831$ ,  $p = 0.3327$ ). Taken together, these results suggest that  $Ca_v1.2$ -PV CKO animals exhibit a normal locomotor activity with signs of anxiogenic behavior.

#### 4.6.3. $Ca_v1.2$ deficiency in PV<sup>+</sup> GABAergic neurons does not alter social behavior

Investigation of social behavior in  $Ca_v1.2$ -PV mice revealed that CKO-PV animals showed social behavior similar to their control littermates. Both groups spent similar times in the different chambers (**Figure 49a**). In stage 2, both Ctrl and CKO-PV animals spent more time interacting with the social mouse than with the empty cage (**Figure 49b**) (Two-way ANOVA: interaction,  $F_{(1, 58)} = 0.1511$ ,  $p = 0.6989$ ; genotype,  $F_{(1, 58)} = 0.6155$ ,  $p = 0.4359$ ; social mouse,  $F_{(1, 58)} = 94.06$ ,  $p < 0.0001$ ). However, no genotype differences were observed i.e., both groups spent similar time interacting with the social mouse (**Figure 49d**) (Student's t-test,  $t_{29} = 0.1449$ ,  $p = 0.8858$ ).

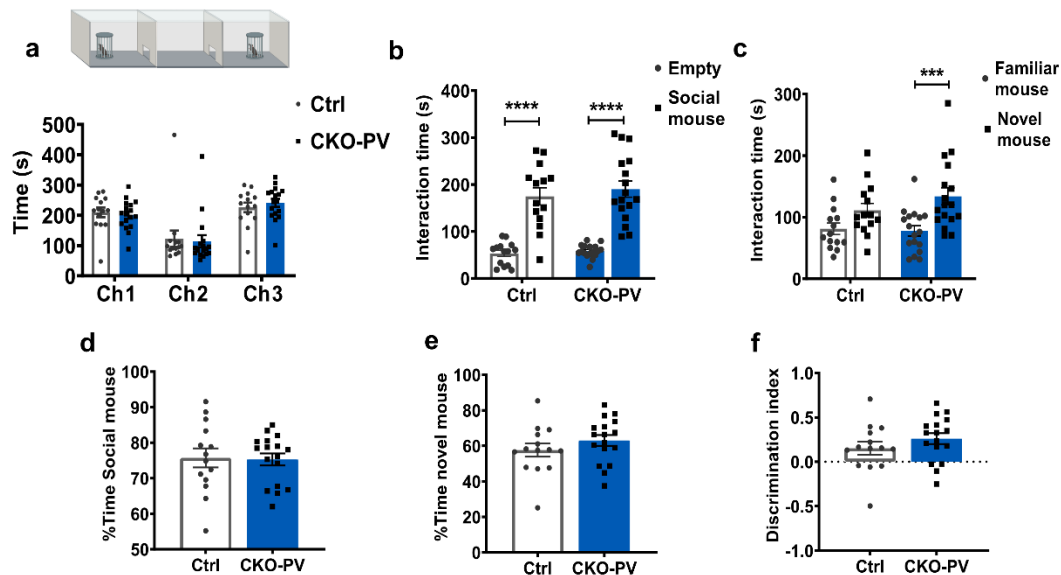


**Figure 49: Assessment of social behavior in  $Ca_v1.2$ -PV mice.** a) Time spent in the three chambers of the 3CT apparatus. b) Interaction time with empty cage vs social mouse. c) Interaction time with familiar mouse vs novel mouse. d) Percentage interaction time with social mouse. e) Percentage interaction time with novel mouse. f) Discrimination index. (Two-way ANOVA + Bonferroni post hoc,  $p < 0.05$ , Student's t-test).

In stage 3, when a novel social mouse was introduced, CKO-PV mice interacted with the novel social mouse more than the familiar mouse while control animals showed only a trend toward increased interaction with novel mouse (**Figure 49c**) (Two-way ANOVA: interaction,  $F_{(1, 58)} =$

1.36,  $p = 0.2484$ ; genotype,  $F_{(1, 58)} = 0.7449$ ,  $p = 0.3916$ ; novel mouse,  $F_{(1, 58)} = 14.92$ ,  $p = 0.0003$ ). No differences between the genotypes were observed in time spent interacting with the novel mouse or discrimination between novel and familiar social mice (**Figure 49e, f**) (Student's t-test, percentage interaction time:  $t_{29} = 1.141$ ,  $p = 0.2632$ ; discrimination index:  $t_{29} = 1.141$ ,  $p = 0.2632$ ). These results suggest that  $Ca_v1.2$  deficiency in  $PV^+$  GABAergic neurons does not alter social behavior.

#### 4.6.4. Assessment of cognitive performance in $Ca_v1.2$ -PV mice

Cognitive performance was further investigated in learning and memory tasks (Y maze, NOR, SOR and MWM). In the Y-maze, Ctrl and CKO-PV animals showed comparable locomotor activity, and working memory as indicated by the similar spontaneous alternations and total number of arm entries (**Figure 50a, b, c**) (Student's t-test, distance:  $t_{33} = 1.863$ ,  $p = 0.0715$ ; spontaneous alternations:  $t_{33} = 0.2116$ ,  $p = 0.8337$ ; arm entry:  $t_{33} = 1.831$ ,  $p = 0.0761$ ).

In the NOR task, both groups spent similar time interacting with the objects during the training stage and there was no object bias (**Figure 50d, e**) (Student's t-test, interaction time:  $t_{31} = 0.4956$ ,  $p = 0.6237$ ; object bias:  $t_{31} = 0.2329$ ,  $p = 0.8174$ ). Interestingly, CKO-PV mice spent lesser time interacting with the novel object in the testing phase compared to the Ctrl group (**Figure 50f**) (Student's t-test,  $t_{31} = 2.135$ ,  $p = 0.0407$ ). CKO-PV animals were also unable to discriminate the novel object from the familiar one as indicated by the discrimination index (**Figure 50g**) (Student's t-test,  $t_{31} = 2.135$ ,  $p = 0.0407$ ). In the SOR task, both groups spent similar time interacting with the objects in the training stage with no object bias (**Figure 50h, i**) (Student's t-test, interaction time:  $t_{30} = 0.2032$ ,  $p = 0.8403$ ; object bias:  $t_{25} = 0.3939$ ,  $p = 0.697$ ). Ctrl and CKO-PV mice were indistinguishable with regards to the time spent interacting with the object in a novel location or the discrimination index (**Figure 50j, k**) (Student's t-test, interaction time:  $t_{30} = 0.8982$ ,  $p = 0.3762$ ; discrimination index:  $t_{30} = 0.8982$ ,  $p = 0.3762$ ).

To further investigate spatial memory in a different task,  $Ca_v1.2$ -PV animals were subjected to the Morris water maze task. In the water maze, Ctrl and CKO-PV animals showed similar latencies to find the platform during the training trials indicating that both groups learnt the task similarly (**Figure 50l**) (Two-way ANOVA-repeated measure: interaction,  $F_{(4, 128)} = 0.5211$ ,  $p = 0.7204$ ; genotype,  $F_{(1, 32)} = 0.007799$ ,  $p = 0.9302$ ; time,  $F_{(4, 128)} = 37.93$ ,  $p < 0.0001$ ). Furthermore, both

groups spent more time in the target quadrant (which had the platform) in the probe trial (**Figure 50m**) (One-way ANOVA:  $F_{(7, 128)} = 3.5$ ,  $p = 0.0018$ ). However, there was no significant difference in the time Ctrl and CKO-PV mice spent in the target quadrant (**Figure 50n**) (Student's t-test,  $t_{32} = 0.5544$ ,  $p = 0.5831$ ). Taken together these results suggest that  $Ca_v1.2$  deficiency in  $PV^+$  GABAergic neurons results in cognitive deficits only in the NOR task.

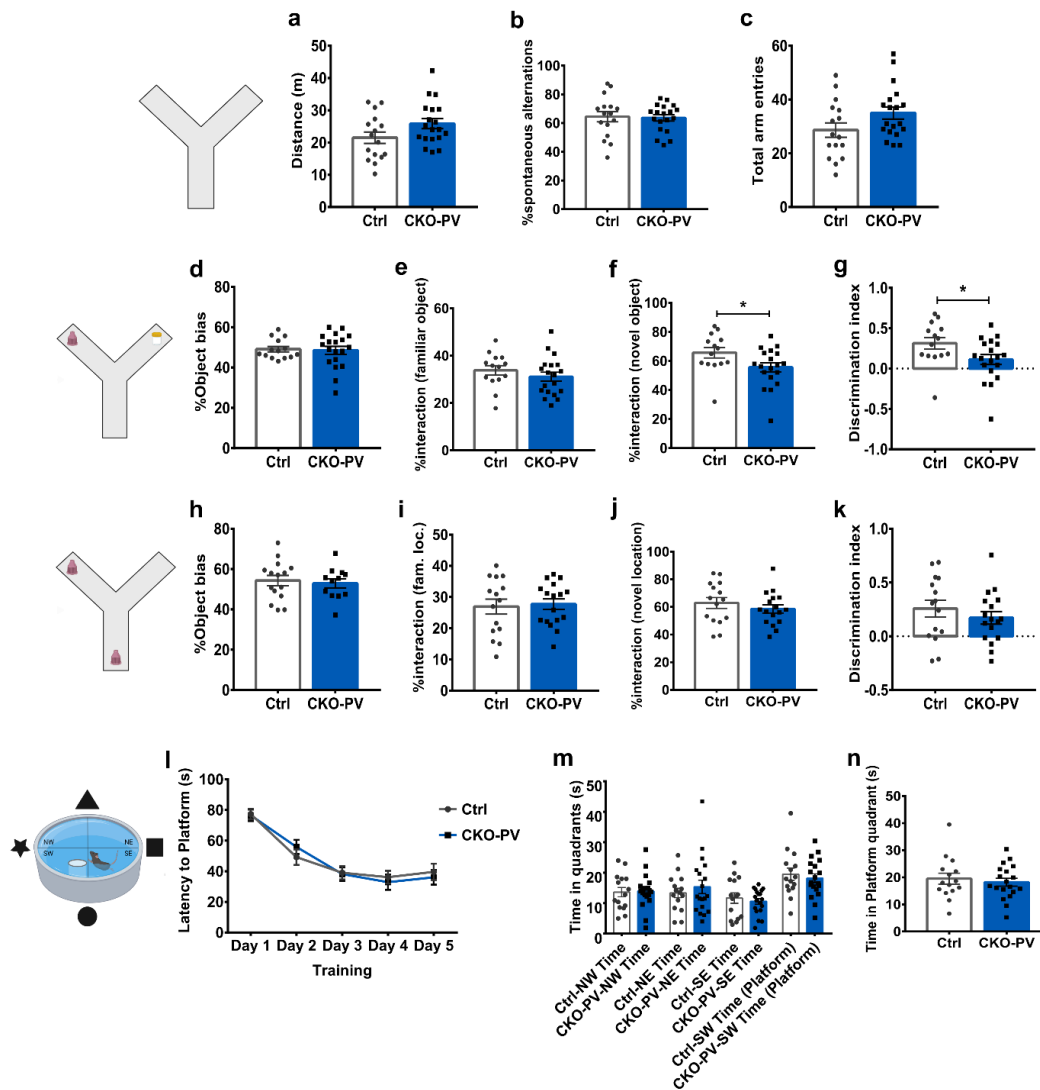


**Figure 50: Assessment of cognitive performance of  $Ca_v1.2$ -PV mice.** a) Distance travelled in Y-maze. b) Percentage spontaneous alternations. c) Number of arm entries. d) Percentage object bias in NOR. e) Percentage interaction time with objects in NOR. f) Percentage interaction with novel object in NOR. g) Discrimination index in NOR. h) Percentage object bias in SOR. i) Percentage interaction time with objects in SOR. j) Percentage interaction time with object in novel location in SOR. k) Discrimination index in SOR. l) Latency to platform during training in water maze. m) Time spent in different quadrants during

probe trial. n) Time spent in the target (platform) quadrant during probe trial. (Student's t-test, two-way ANOVA-repeated measures, \* represents  $p < 0.05$ ).

#### 4.6.5. CKO-PV mice show enhanced passive stress coping behavior

Experiments with  $Ca_v1.2$ -Nex mice showed an enhanced active stress coping behavior. Thus, I wanted to investigate the effects of  $Ca_v1.2$  inactivation in  $PV^+$  GABAergic neurons on stress coping behavior. In the FST, Ctrl and CKO-PV animals spent similar times struggling at the beginning of the test (**Figure 51a**) (Student's t-test,  $t_{33} = 0.2074$ ,  $p = 0.837$ ). Interestingly, CKO-PV mice showed a passive stress coping strategy. CKO-PV mice spent lesser time swimming and more time floating or immobile compared to their Ctrl littermates (**Figure 51b, c**) (Student's t-test, time swimming:  $t_{33} = 4.013$ ,  $p = 0.0003$ ; time immobile:  $t_{33} = 4.362$ ,  $p = 0.0001$ ).

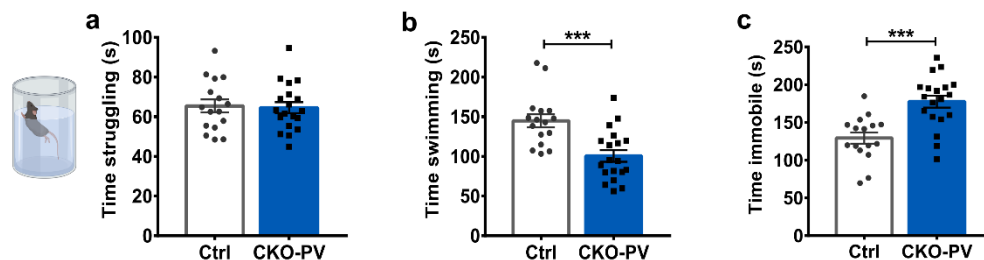


**Figure 51:  $Ca_v1.2$ -PV CKO mice showed passive stress coping behavior.** a) Time spent struggling. b) Time spent swimming. c) Time spent immobile. (Student's t-test, \* represents  $p < 0.05$ ).

#### 4.7. $Ca_v1.2$ deficiency in excitatory and inhibitory neurons result in opposite effects on stress coping behavior

Since  $Ca_v1.2$ -Nex CKO mice showed increased active stress coping behavior whereas  $Ca_v1.2$ -PV CKO mice showed more pronounced passive stress coping behavior, I wanted to further dissect the brain circuitries responsible for this opposite effect by quantifying cells expressing the immediate early gene cFos in different brain regions after the FST. For this I performed the FST simultaneously on  $Ca_v1.2$ -Nex and  $Ca_v1.2$ -PV mouse lines to confirm this opposite pattern in stress coping behavior.

Indeed,  $Ca_v1.2$ -Nex CKO mice showed enhanced active stress coping behavior while  $Ca_v1.2$ -PV CKO mice showed increased passive stress coping behavior compared to their respective Ctrl littermates while no differences were found in the time that each group spent struggling (**Figure**

**52a - c)** (One-way ANOVA, time struggling:  $F_{(3, 21)} = 0.3506$ ,  $p = 0.7891$ ; time swimming:  $F_{(3, 21)} = 7.305$ ,  $p = 0.0015$ ; time immobile:  $F_{(3, 21)} = 9.163$ ,  $p = 0.0004$ ).

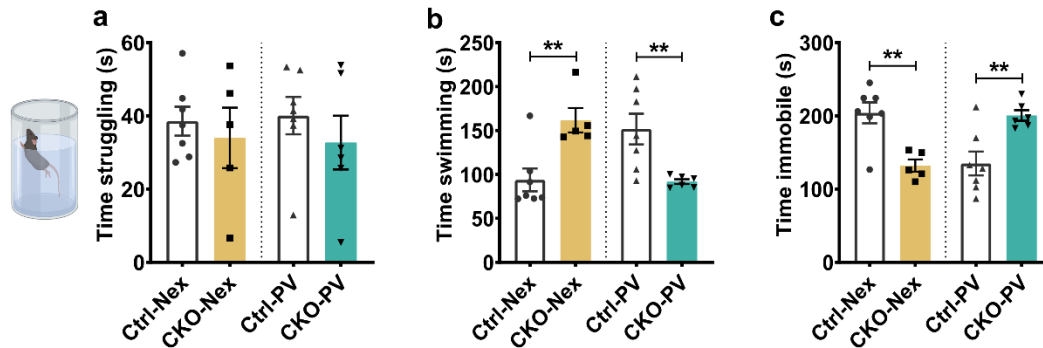


**Figure 52: Stress coping strategies in  $Ca_v1.2$ -Nex and  $Ca_v1.2$ -PV mice.** a) Time spent struggling. b) Time spent swimming. c) Time spent immobile. (One-way ANOVA + Bonferroni post hoc; \* represents  $p < 0.05$ ).

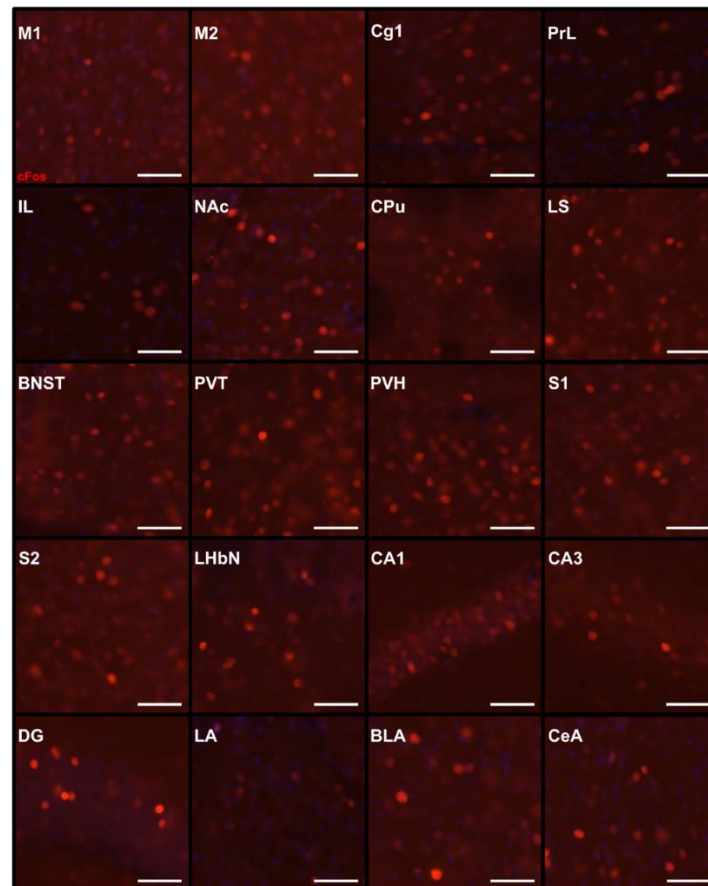


**Figure 53: Representative images of cFos expression in different brain regions.** Abbreviations - M1: Primary motor cortex, M2: secondary motor cortex, Cg1: cingulate cortex, PrL: prelimbic cortex, IL: infralimbic cortex, NAc: nucleus accumbens, CPu: caudate putamen, LS: lateral septum, BNST: bed nucleus of stria terminalis, PVT: paraventricular thalamic nucleus, PVH: paraventricular hypothalamic

nucleus, S1: primary somatosensory cortex, S2: secondary somatosensory cortex, LHbN: lateral habenular nucleus, DG: dentate gyrus, LA: lateral amygdala, BLA: basolateral amygdala, CeA: central amygdala. Scalebar: 50  $\mu$ m.

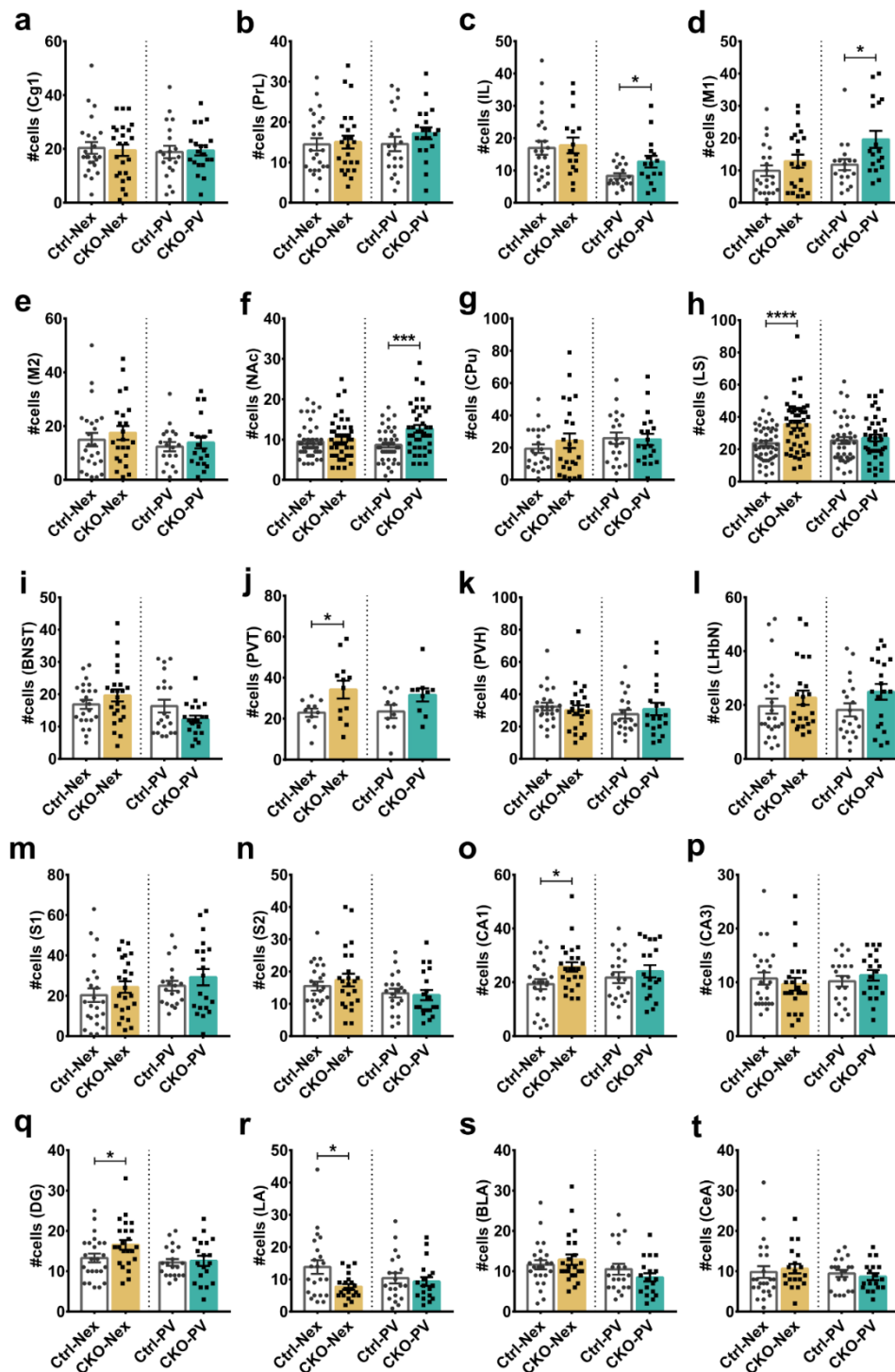


**Figure 54: Quantification of cFos positive cells in different brain regions.** Graphs represent number of cells quantified in a 200  $\mu$ m  $\times$  200  $\mu$ m square region of interest in each brain regions bilaterally. (Student's

t-test, \* represents  $p < 0.05$ ). Abbreviations - Cg1: cingulate cortex, PrL: prelimbic cortex, IL: infralimbic cortex, M1: primary motor cortex, M2: secondary motor cortex, NAc: nucleus accumbens, CPu: caudate putamen, LS: lateral septum, BNST: bed nucleus of stria terminalis, PVT: paraventricular thalamic nucleus, PVH: paraventricular hypothalamic nucleus, LHbN: lateral habenular nucleus, S1: primary somatosensory cortex, S2: secondary somatosensory cortex, DG: dentate gyrus, LA: lateral amygdala, BLA: basolateral amygdala, CeA: central amygdala.

Interestingly, quantification of cFos positive cells in the  $Ca_v1.2$ -Nex mice revealed an enhanced cFos expression in CKO-Nex mice compared to their Ctrl littermates in LS (**Figure 54h**) (Student's t-test;  $t_{94} = 4.223$ ,  $p < 0.0001$ ), PVT (**Figure 54j**) (Student's t-test;  $t_{21} = 2.278$ ,  $p = 0.0333$ ), CA1 (**Figure 54o**) (Student's t-test;  $t_{46} = 2.465$ ,  $p = 0.0175$ ) and DG (**Figure 54q**) (Student's t-test;  $t_{46} = 2.021$ ,  $p = 0.0491$ ) and a reduced expression in the lateral amygdala (LA) (**Figure 54r**) (Student's t-test;  $t_{41} = 2.653$ ,  $p = 0.0113$ ). Whereas in  $Ca_v1.2$ -PV animals, CKO-PV mice showed enhanced cFos expression in IL (**Figure 54c**) (Student's t-test;  $t_{33} = 2.339$ ,  $p = 0.0256$ ), M1 (**Figure 54d**) (Student's t-test;  $t_{34} = 2.483$ ,  $p = 0.0181$ ) and NAc (**Figure 54f**) (Student's t-test;  $t_{78} = 3.544$ ,  $p = 0.0007$ ) regions compared to their Ctrl littermates.

In summary, the FST resulted in differential cFos expression in several brain regions in  $Ca_v1.2$ -Nex and  $Ca_v1.2$ -PV mice. Furthermore, the data also revealed that the response to the FST is mediated by specific brain circuitries that possibly are contributing to the opposite stress coping effects seen in the two lines.

## 5. Discussion

In this thesis, I explored the interaction of  $Ca_v1.2$  with stress during early life using a mouse model with a specific deletion of *Cacna1c* in forebrain glutamatergic neurons ( $Ca_v1.2$ -Nex). The LBN stress had moderate effects as indicated by hyperlocomotion of female CKO mice, higher sucrose preference of ELS female mice, task specific alterations in anxiety and impaired social behavior of male CKO mice. Besides, no significant consequences of LBN stress were observed on other behavioral readouts. At the cellular level, LBN stress induced dendritic atrophy as indicated by reduced dendritic complexity.

I further evaluated the behavioral phenotype of female  $Ca_v1.2$ -Nex mice to investigate whether they exhibit behavioral deficits that have previously been observed in male  $Ca_v1.2$ -Nex mice. In line with previous studies, I observed increased anxiety and hyperlocomotion in CKO mice, working memory and remote spatial memory impairment and an enhanced active stress coping behavior. Furthermore, I also found reduced dendritic complexity and spine density in CKO mice compared to Ctrl mice with no changes in pCREB protein expression. Additionally, through a minPROFILER assay, we found signs of increased baseline activity in CKO primary neurons when compared to their unstimulated control neurons.

Moreover, I also generated a novel mouse model with a specific deletion of *Cacna1c* in inhibitory  $PV^+$  neurons. Behavioral characterization of these mice revealed increased anxiety, normal social behavior, deficits in novel object recognition and a more passive stress coping strategy in the FST of CKO-PV mice compared to Ctrl littermates. Further comparison of  $Ca_v1.2$ -PV with  $Ca_v1.2$ -Nex mice to understand their opposite stress coping behavior revealed differential expression of cFos in different brain regions that might contribute to the opposing behavior observed in the FST.

### 5.1. Early life stress effects on the $Ca_v1.2$ -Nex mouse model

Early life adversity in combination with genetic predisposition is a well-known risk factor aiding in the development of psychiatric disorders. In support of this, clinical studies have reported increased vulnerability of *CACNA1C* risk allele carriers to early life stress and increased risk for development of psychiatric disorders (Krautheim et al. 2018; Klaus et al. 2018; Dedic et al. 2018). These studies necessitate the need to further explore the mechanisms underlying gene  $\times$  environment interactions. The LBN stress, a recently developed ELS model for rodents, is known

to capture naturalistic early life adversity seen in humans through disrupted maternal care provided to pups in the first two weeks of life due to an impoverished environment. The LBN stress induces a diverse set of phenotypes including altered anxiety- and depression-related behavior, cognitive deficits and structural impairments such as reduced dendritic complexity and spine density (Ivy et al. 2010; X. D. Wang et al. 2011; Walker et al. 2017). In this study I investigated the gene  $\times$  environment interactions by subjecting  $Ca_v1.2$ -Nex mice, which harbors a specific deletion of *Cacna1c* in forebrain glutamatergic neurons, to the LBN stress. Male and female animals were used for this experiment to also account for well-known sexual dimorphisms in stress effects (Kundakovic et al. 2013; Hill et al. 2014; Farrell et al. 2016; Goodwill et al. 2018; Takahashi 2021). Examination of physiological parameters revealed significant differences in the body weight of pups. In line with previous studies, ELS animals showed reduced body weight compared to their unstressed counterparts with a trend toward increased loss of pups in the ELS group. In addition to weights and litter sizes, other physiological parameters such as adrenal weight and corticosterone levels are often monitored during the first weeks immediately after the LBN stress and after the behavioral phenotyping. In this study, however, these measures were not monitored, and behavioral studies were directly carried out in adult animals (4-6 months old) which is one of the limitations of this study. Upon behavioral phenotyping at adulthood, only moderate stress effects were observed, which suggests the possibility that the LBN stress was too mild a stressor with stress effects that might not persist into adulthood.

Consistent with previous reports on  $Ca_v1.2$ -Nex mice, male and female CKO animals showed hyperactivity in a novel environment which was independent of stress in male mice. Stress however further enhanced hyperlocomotion in female CKO animals without an effect on the ELS-Ctrl group which is of note here. Other reports on ELS models such as maternal separation have reported a stress induced hyperactivity in a novel environment which results from the activation of various brain circuits (Bock et al. 2017; Deal et al. 2021; E. Fitzgerald et al. 2021). Considering that ELS enhanced the hyperactivity already seen in female CKO mice,  $Ca_v1.2$  deficient mice are perhaps more vulnerable to ELS compared to their unstressed counterparts. In addition, since the effects of ELS seem to be specific to females, this could also suggest a sexually dimorphic effect of stress. However, care should be taken while interpreting these results, since compared to the female group, the male group had relatively lower sample numbers which might affect the interpretation of data.

Increased anxiety-related behavior in rodents exposed to the LBN stress has been reported previously (X.-D. Wang et al. 2012; Prusator and Greenwood-Van Meerveld 2015). In the present study, I did not observe any genotype or stress induced effects on anxiety in male and female mice in the OFT. In the EPM, however, genotype or stress effects on the parameters measured were absent in male mice, but in female mice the LBN stress seemingly induced an anxiolytic effect compared to the unstressed group without a genotype effect. One possible explanation is that ELS-induced hyperlocomotion, which is more pronounced in ELS-CKO female mice but not in ELS-Ctrl mice, results in an increased open arm time and number of entries. Other studies have also reported hyperlocomotion induced by ELS (Bock et al. 2017; E. Fitzgerald et al. 2021; Deal et al. 2021). Thus, the anxiolytic effect in the EPM is possibly the result of ELS-induced hyperlocomotion in both ELS-Ctrl and ELS-CKO female mice. However, why this hyperlocomotion is not reflected in the total distance covered by ELS-Ctrl mice in the EPM apparatus is currently unclear. In the LDB test, ELS CKO male mice showed increased anxiety compared to ELS-Ctrl mice with an absence of genotype effect in the unstressed group. This would suggest an increased vulnerability of  $Ca_v1.2$  deficient mice in a task-specific manner, since the LDB with its higher illumination intensity might be considered as a more stressful task compared to OFT and EPM performed in low light conditions. Several studies have reported contrary effects of the LBN stress on anxiety-related phenotypes including unaltered anxiety behavior (Naninck et al. 2015; J. Molet et al. 2016). A possible explanation for a lack of strong stress effects could be that a single hit of LBN stress is not sufficient to produce behavioral effects persisting into adulthood. In support of this theory, studies with two-hit models of stress (early life stress in combination with another stressor during adolescence) have reported increased anxiety induced by this two-hit model rather than in the single hit model (Jaric et al. 2019; Shi et al. 2021; Eiland and McEwen 2012). Thus, introducing another stressor as a second hit might provide the required strength to introduce long-lasting behavioral changes in adulthood. Of note here is the lack of genotype effects in the unstressed groups. Increased anxiety is a robust phenotype observed in  $Ca_v1.2$  mouse models (Dao et al. 2010; A. S. Lee et al. 2012; Z. D. Kabir et al. 2017; Dedic et al. 2018). Here, however, I did not see an anxiogenic behavior in US-CKO mice in any of the anxiety tests which could be due to the low number of animals in each group and the high variability introduced by several external factors. In summary, lack of sufficient samples, clear genotype or stress effects limit the interpretation of the data considerably. A further exploration with sufficient

sample numbers per group and perhaps the use of two-hit stress models might give better insights into the gene  $\times$  environment interactions.

Cognitive and social interaction deficits are another well-known consequence of early life adversity in humans and often robustly replicated in animal models as well (Ivy et al. 2010; X. D. Wang et al. 2011; Walker et al. 2017; Hedges and Woon 2011; Krugers et al. 2017). In both rats and mice, the LBN stress induces significant cognitive and social deficits when tested at different timepoints in adulthood (Rice et al. 2008; X. D. Wang et al. 2011; Ivy et al. 2010; Kohl et al. 2015; Raineke et al. 2012). In our study, however, I did not observe cognitive impairments arising from either genotype- or stress-effects in male and female animals. In social approach tasks, male and female animals of both genotypes showed higher preference for the social conspecific rather than the empty chamber. Whereas in social novelty preference, all groups were equally impaired in distinction between the familiar and novel social mice with the exception of male US-CKO mice which raises the question of whether the mice are no longer interested in the task. Data from the social approach trial however suggested a preference for social interaction in all groups which was not influenced by genotype or stress factors. Notably, upon further dissection of individual percentages of time spent interacting with the social conspecific mice in each trial, I found that ELS-CKO male mice spent almost half as much time interacting with a social conspecific compared to the ELS-Ctrl and US-CKO. This effect is lost in the social novelty preference trial. Whether the loss of effect is due to loss of overall interest in the task or due to other reasons is currently unclear. In females, effects of ELS on social approach behavior or on social novelty preference are lacking. One plausible explanation for a loss of overall interest in the novelty preference trial could be that the social conspecific mice were not age matched to the experimental animals (animals used as social mice were 8-10 weeks old while experimental animals were 4-6 months of age). Although, this might introduce a dominant behavior in the experimental animals, there is no evidence for such behavior in the current study. Nevertheless, use of younger animals as social conspecific is a limitation of this study. Another factor that might contribute to these differences observed in males and females might be their housing conditions. During experimentation, while male animals were single housed throughout the duration of the experiment (long-term single housing), female animals were group housed due to their large numbers and a lack of space. Since long durations of social isolation is known to have deleterious effects on social cognition, it is possible that single housing might have had an additive effect leading to more

pronounced effects of ELS on social approach task in males (Reinwald et al. 2018; N. Liu et al. 2020).

The LBN stress introduces quite significant deficits also in the NOR task (Rice et al. 2008; Ivy et al. 2010). In the present study, performance in the NOR task was especially low with mice in all groups exhibiting exceptionally low object interaction times. Male and female mice, irrespective of their genotype or stress conditions, spent less than 20% of the total testing time interacting with the objects during the acquisition phase. Increased interaction time of female CKO animals during the acquisition phase is probably the result of their hyperactivity in the open field as the NOR task was performed in the open field apparatus. However, differences related to the genotype or stress effects in the novelty preference and discrimination index were absent in male and female groups. Since object interaction times were lesser than the threshold in the acquisition stage, it would not be possible to discriminate genotype- or stress- effects on cognition in this task. A reduced interaction with the objects could arise because of several reasons. For example, the handling of mice and habituation to the apparatus and to the objects might not be sufficient. This might introduce anxiety leading to reduced exploration times. Another reason could be that the mice are simply not interested in the objects which would lead to reduced exploration times (Antunes and Biala 2012; Lueptow 2017). In either case, reduced exploration times in the acquisition phase partly explains the lack of any effects on the novelty preference or discrimination index.

Another robust effect of the LBN stress is anhedonia in the sucrose preference test especially in rats (J. Molet et al. 2016; Bolton, Molet, et al. 2018; Bolton, Ruiz, et al. 2018). In contrast to these reports, however, male unstressed and ELS groups were similar in their preference for sucrose over water with no genotype differences. Since hedonic behavior is an unexplored area in  $Ca_v1.2$ -Nex animals, further investigation to understand how  $Ca_v1.2$  deficiency might affect reward seeking behavior is required. There are some studies exploring reward sensitivity and responsiveness in humans as well as  $Ca_v1.2$  models which report mixed results (Wessa et al. 2010; Lancaster et al. 2014; Braun et al. 2018). Interestingly, in females, stress had an opposite effect on sucrose preference. Irrespective of genotype, stressed mice had a higher preference for sucrose compared to the unstressed group. Since sucrose preference in unstressed animals was exactly at chance levels, whether the unstressed animals have a lower preference for sucrose or the stressed animals indeed have higher preference for sucrose was incomprehensible.

Stress coping behavior is a less explored phenotype in the field of LBN stress. Depression-related behavior in FST is seen after the LBN stress in rats but to our knowledge such phenotype has not been reported for mice (Raineke et al. 2012; Cui et al. 2006). Active stress coping behavior is an established phenotype in  $Ca_v1.2$ -Nex CKO mice (Dao et al. 2010; Zeeba D. Kabir et al. 2017; Dedic et al. 2018). Not surprisingly, I saw clear genotype effects in the FST independent of the stress factor. Male and female CKO animals exhibited enhanced active stress coping behavior compared to their Ctrl littermates. Since CKO animals exhibited hyperactivity in a novel environment, it is highly likely that this influences the phenotype observed in the FST. In humans, ADHD is often in high comorbidity with other psychiatric disorders such as BD, anxiety disorders and even MD. Furthermore, hyperactivity is a shared symptom across several psychiatric disorders (Sobanski 2006; Kunwar, Dewan, and Faraone 2007; Miró et al. 2012). Rodent studies have previously evaluated the hyperactive phenotype; however, underlying mechanisms still remain elusive (Yen et al. 2013). Hyperactivity in response to a novel environment or to an acute stressor such as the FST may be due to hyperarousal or a manifestation of a manic-like behavior in response to novelty or stress. Whether the enhanced active stress coping behavior is due to hyperactivity observed in CKO mice or a hyperarousal response to an acute stressor are indistinguishable in the current study and remains to be investigated.

In addition to anxiety-, depression-related phenotypes, social and cognitive impairments, the LBN stress induces strong structural changes in the brain. Reduced dendritic complexity and spine densities in the hippocampus are often reported in stressed animals which have an impact on cognitive performance (Ivy et al. 2010; X. D. Wang et al. 2011; Walker et al. 2017). Early postnatal stages, with their heightened plasticity, are periods of enhanced vulnerability to external inputs. Thus, any sensory input including early life stressors during this critical period can significantly affect the development of dendritic branches and thus would also affect behavioral phenotypes (Chen and Baram 2016; Lo, Sng, and Augustine 2017; Macharadze et al. 2019; Wong-Riley 2021). Although in the current study I observed very moderate stress effects on behavior, preliminary data from neuronal reconstruction and analysis suggested an influence of the LBN stress on dendritic branching with dendritic atrophy in ELS-Ctrl animals compared to unstressed Ctrl mice. Although genotype- or stress-effects are imperceptible in the current data due to limited availability of samples, the data are in line with previous reports. Furthermore, the reconstruction data were obtained only from female mice, Thus, further studies exploring effects of the LBN

stress on male and female mice might provide us with interesting insights on whether sexual dimorphisms can also be seen at a structural level. *In vitro* studies have reported a vital role for Ca<sub>v</sub>1.2 in neurite elongation (Obermair et al. 2004; Krey et al. 2013; Kamijo et al. 2018). However, to my knowledge, there is no *in vivo* evidence of an involvement of Ca<sub>v</sub>1.2 in dendritic branching so far. In support of our hypothesis, preliminary neuronal reconstructions revealed subtle genotype differences in dendritic branching with US-CKO exhibiting reduced dendritic complexity. Since sample numbers were limited (n=2-3 per group), further tracings of more samples could possibly enhance this subtle genotype difference, providing us with *in vivo* evidence for the involvement of Ca<sub>v</sub>1.2 in dendritic branching. pCREB is a well-known downstream target of Ca<sub>v</sub>1.2 signaling and plays a vital role in dendritic branching (Rajadhyaksha et al. 1999; Wheeler et al. 2008; Finsterwald et al. 2010). A previous study by Moosmang et.al., revealed reduced pCREB expression at baseline conditions in Ca<sub>v</sub>1.2-Nex CKO mice. In contrast, differences in baseline expression of pCREB were absent in male and female US-CKO mice compared to their Ctrl littermates in the current study. In addition, LBN stress also had no effect on pCREB expression. It is possible that any subtle differences due to genotype or stress effects might be diluted in the total protein samples and a more localized sample collection, for example from synaptosomes might shed better light on the subtle differences in pCREB expression levels.

Overall, moderate effects of the LBN stress on behavioral phenotypes were observed even though stress caused dendritic atrophy. However, the current study had several limitations. Firstly, sample numbers per group were relatively low to achieve any strong genotype- or stress- effects on behavioral level, especially in males. Although 50 breeding pairs were set up to account for stress condition and genotype, only 33 pairs gave birth to pups and the final sample numbers of pups for each genotype were limited. This resulted in high variability leading to a lack of robust genotype differences previously reported and hence limited the interpretation of data. Moreover, handling of a large number of animals simultaneously and different housing conditions (single housing of male animals and group housing of female animals) might have introduced higher variability in the behavior. Testing another cohort of animals controlling for all factors would provide clearer interpretation of the stress as well as genotype effects. Further, though two-hit stress models produce mixed results, it would provide better understanding of whether the LBN stress confers susceptibility or resilience to additional stress in addition to genetic predisposition.

## 5.2. $Ca_v1.2$ -Nex female CKO mice exhibit behavioral alterations reminiscent of endophenotypes of psychiatric disorders

In humans, sexual differences can be seen across the spectrum of psychiatric disorders. While women are twice as likely to be affected by depression and mood disorders than males, there is a higher incidence of ASD in males (Pinares-Garcia et al. 2018; Altemus, Sarvaiya, and Neill Epperson 2014; Tannenbaum and Boksa 2019). Gender differences are also found in the response to treatments for psychiatric disorders, although these differences are subtle and not often consistent (Khan et al. 2005; Viguera, Tondo, and Baldessarini 2000; Goldstein et al. 2002). In preclinical research however, there is a strong bias toward usage of male animals for studying behaviors related to endophenotypes of psychiatric disorders owing to the presumption that estrous cycle in female animals would introduce higher variability in behaviors (Beery 2018). Previous studies with  $Ca_v1.2$  models have also largely focused on male animals with few using both sexes for experimentation. Thus, in this study I investigated the impact of  $Ca_v1.2$  deficiency on behaviors related to psychiatric disorders in female mice and whether estrous cycle influenced these behaviors. Monitoring the estrous cycle of  $Ca_v1.2$ -Nex females for 2 weeks revealed similar cycling and lengths of each stage of the cycle in Ctrl and CKO animals. With the lack of any variations in the estrous cycle, I moved forward with behavioral phenotyping of these mice that included tests spread across the entire spectrum of endophenotypes including anxiety, cognition, and stress coping. The current study revealed behavioral phenotypes in female  $Ca_v1.2$ -Nex CKO mice that were consistent with phenotypes previously reported in male animals and are reminiscent of endophenotypes of psychiatric disorders.

### 5.2.1. Novelty induced hyperlocomotion in female $Ca_v1.2$ -Nex CKO mice

Hyperactivity or novelty induced hyperlocomotion is considered as a rodent correlate of positive symptoms of SCZ or a “manic-like” behavior in response to novelty (P. J. Fitzgerald et al. 2010; Kulak, Cuenod, and Do 2012; Procaccini et al. 2013). The OFT is commonly used to investigate both exploratory behavior and anxiety in rodents. By allowing the mice to explore the open field apparatus for 30 minutes, I could target both the exploratory behavior during the duration of the experiment and anxiety levels in the first five minutes of the test. I observed a strong hyperlocomotion and slower habituation in female CKO animals in the OFT. The current results are in line with previous report of hyperactivity in  $Ca_v1.2$ -Nex male mice from our lab (Dedic et al. 2018). Notably, female  $Ca_v1.2$ -Nex CKO mice showed similar hyperlocomotion in the first

hour of being introduced to a novel home cage for the home cage activity monitoring. But upon habituation, their activity returned to the levels of their Ctrl littermates with both groups displaying higher activity during the dark phase compared to the light phase as is the case for nocturnal animals. The comparable activity levels in the home cage/ familiar environment suggests that the hyperlocomotion in CKO mice is likely induced by a novel or stressful environment which could be a manifestation of a manic-like behavior or hyperarousal in response to novelty or stress. To confirm this theory, a prolonged exposure to the open field apparatus might bring additional inputs to whether hyperactivity is indeed novelty-induced. Additionally, the animals were habituated to the novel home cage for three days before data was collected for home cage monitoring. Monitoring the activity and habituation levels during those three days would have been pertinent to understanding the difference in habituation levels of the two groups since CKO animals showed slower habituation in the open field test.

Another notable observation was the reduced immobility and enhanced swimming of CKO females in the FST. Reduced immobility in the FST suggests an enhanced active stress coping response to an acute stressor which probably is a consequence of the hyperactivity seen in these CKO mice in response to a novel or a stressful environment. In other behavioral tests, however,  $Ca_v1.2$ -Nex knockout mice do not show hyperactivity. Thus, it is currently unclear whether hyperactivity induced here is indeed due to a novel environment or a task-specific response. To ensure that hyperactivity was not an innate behavior of Nex-Cre mice as a result of the insertion of Cre recombinase into the *Nex/Neurod6* locus, I ran validation experiments with Ctrl and Nex-Cre positive mice. I did not observe any significant behavioral differences between the two groups suggesting that the hyperactivity was due to  $Ca_v1.2$  deficiency specifically in glutamatergic neurons of the forebrain. Further studies are required to truly dissect the neurobiological mechanisms that underlie the hyperactivity and active stress-coping behaviors seen in these CKO mice.

Other mouse models of SCZ and BD (including those with specific deletion of disease associated genes in glutamatergic neurons) are also known to exhibit a similar novelty induced hyperlocomotion (Karlsson et al. 2008; P. J. Fitzgerald et al. 2010; Beyer and Freund 2017; Kulak, Cuenod, and Do 2012; Zhu et al. 2017; Tatsukawa et al. 2019; Götze et al. 2021). Excitatory/ inhibitory imbalance is an often-suggested hypothesis in the development of psychiatric disorders

(Kehrer 2008; Culotta and Penzes 2020). A plausible explanation for hyperactivity is E/I imbalance because of lower activation of inhibitory circuits or higher activation of excitatory circuits (Zhu et al. 2017; Tatsukawa et al. 2019). In fact, deficiency of  $Ca_v1.2$  in glutamatergic neurons of mice resulted in higher E/I ratio while a pan-neuronal deletion of *Cacna1c* resulted in a significant shift in E/I balance (Z. D. Kabir et al. 2017; Temme and Murphy 2017). Interestingly, the gain of function TS2-neo mouse model of *Cacna1c* is reported to show hypoactivity in a novel environment while showing enhanced active stress coping behavior with an increased axonal innervation of the striatum (Bader et al. 2011; Ehlinger and Commons 2017). This might suggest that either gain or loss of function of  $Ca_v1.2$  causes an E/I imbalance leading to altered locomotor activity. Whether  $Ca_v1.2$ -Nex female CKO mice would also show an E/I imbalance and how this relates to hyperactivity remains to be investigated. In additional support of the E/I imbalance theory, dopaminergic circuits are also often implicated in hyperlocomotive phenotype along with hippocampal hyperactivity (Tomasella et al. 2018; Fujita et al. 2020; Wiedholz et al. 2008; Sotnikova, Efimova, and Gainetdinov 2020; Procaccini et al. 2013). Further studies targeting different circuits implicated in disinhibition due to loss of E/I balance in novelty-induced hyperlocomotion are required to understand the underlying mechanisms that bring about this manic-like behavior in response to novelty or stress.

### 5.2.2. Loss of $Ca_v1.2$ in excitatory neurons induces anxiety

Anxiety is considered one of the endophenotypes shared across psychiatric disorders. In addition, anxiety disorders often have high comorbidity with SCZ, BD and MD (Freeman, Freeman, and McElroy 2002; Braga, Reynolds, and Siris 2013; Hirschfeld 2001). Preclinical studies with  $Ca_v1.2$  rodent models have repeatedly revealed elevated anxiety-related behavior (A S Lee et al. 2012; Chantelle E. Terrillion et al. 2017; Dedic et al. 2018; Ehlinger and Commons 2019). In line with these studies,  $Ca_v1.2$ -Nex female CKO mice showed elevated anxiety in OFT and EPM but not in LDB. However, CKO mice did show a tendency toward increased latency to enter the lit zone which could possibly indicate a decreased risk-taking or a risk avoidance behavior. Similar to this study, some other studies in  $Ca_v1.2$  mouse models have also reported anxiety behavior in one test and not the other (EPM or LDB) (Dao et al. 2010; A. S. Lee et al. 2012; Dedic et al. 2018). For this reason, more than one anxiety test was used. Anxiety is a multidimensional construct and a multidimensional approach is often recommended while studying mouse behavior (Ramos and Mormède 1997; Crawley and Bailey 2008). Thus, it can be concluded that loss of  $Ca_v1.2$  in

glutamatergic neurons of the forebrain induces anxiogenic behavior in female mice. Interestingly,  $Ca_v1.2$  deficiency does not always induce anxiety in mice. While constitutive *Cacna1c* haploinsufficiency and cell type-specific deletion induced anxiogenic behavior in rodents, mice with pan-neuronal deletion and region-specific inactivation in the ACC had normal anxiety levels (Dao et al. 2010; De Jesús-Cortés, Rajadhyaksha, and Pieper 2016; A. S. Lee et al. 2012; Z. D. Kabir et al. 2017; Dedic et al. 2018; Bavley et al. 2020; Jeon et al. 2010; Temme and Murphy 2017). From these reports and the current study, it is clear that anxiety-related behavior is mediated by  $Ca_v1.2$  via specific brain circuitries. Further studies are required to truly dissect mechanisms via which  $Ca_v1.2$  mediate the anxiety-related behavior.

### **5.2.3. Altered cognition, structural morphology, and basal activity in $Ca_v1.2$ -Nex CKO mice**

Cognitive impairment is another shared endophenotype seen across psychiatric disorders such as SCZ, BD, and MD. In clinical studies, associations of *CACNA1C* with cognitive impairments and structural changes in the brain are most robustly replicated (Krug et al. 2010; Márcio Gerhardt Soeiro-de-Souza et al. 2012; M G Soeiro-de-Souza et al. 2017; Takeuchi et al. 2018). Similarly, in preclinical studies, cognitive impairments in  $Ca_v1.2$  rodent models are among the most robustly replicated findings (S. Moosmang 2005; White et al. 2008; Temme et al. 2016). Thus, in this study, I designed a behavioral test battery to include four cognitive tasks (Y maze, NOR, SOR and MWM for spatial learning) that target different aspects of cognitive learning. Working memory impairments are considered one of the key aspects of schizophrenia and *CACNA1C* has often been associated with such impairments in patients as well as healthy carriers (Frydecka et al. 2014; Eryilmaz et al. 2016; Z. Zhang et al. 2018).  $Ca_v1.2$  deficiency specifically in glutamatergic neurons of the forebrain introduced significant deficits in working memory (Y maze task) as observed in this study. Previous studies on other  $Ca_v1.2$  rodent models, however, did not yield similar working memory deficits, which is in contrast to the current study (Zanos et al. 2015; Braun et al. 2018). The contradictory effect on working memory originates perhaps from the use of different models for the task. While Zanos et.al., and Braun et.al., used constitutive heterozygous mice and rat models of *Cacna1c* respectively, in this study I used mice with *Cacna1c* deficiency specifically in glutamatergic neurons of the forebrain. Such a cell type-specific deletion perhaps induces stronger behavioral phenotypes compared to haploinsufficient models. Interestingly, female  $Ca_v1.2$ -Nex CKO mice exhibited similar object recognition and relocation memory compared to their control littermates, thus revealing a lack of effect of  $Ca_v1.2$  deficiency on these forms of memory. Even

with procedural differences, this is in agreement with other reports exploring the effects of  $Ca_v1.2$  on object recognition memory (Zanos et al. 2015; Braun et al. 2018; Jeon et al. 2010). Spatial memory impairments, though sometimes contradictory, are another consistently reported phenotypes in  $Ca_v1.2$  rodent models (White et al. 2008; Burgdorf et al. 2017; S. Moosmang 2005; Dedic et al. 2018). Similar to previous reports, the current study also revealed spatial memory impairments (especially remote spatial memory) in female CKO mice during the probe test of the water maze. Like the Y-maze and water maze tasks, object recognition and relocation tasks are also hippocampus dependent. Thus, stronger effects of cell type-specific  $Ca_v1.2$  deficiency on all cognitive functions could be expected since glutamatergic neurons are abundant in the hippocampus. However, it appears that the deficiency alters only specific cognitive functions while sparing the others. Why there is such a task-specific mediation of cognitive functions by  $Ca_v1.2$  remains to be explored.

In support of the cognitive deficits observed in female CKO mice, structural morphology of pyramidal neurons of the hippocampus were also altered in the CKO mice. Neuronal tracings revealed that  $Ca_v1.2$  deficiency during development introduces alterations in dendritic complexity and spine density in CA1 hippocampal pyramidal neurons. Although structural plasticity has not been explored in loss-of-function models of *Cacna1c*, neurons derived from the TS2-neo gain-of-function model revealed activity dependent dendritic retraction, providing a direct evidence for the involvement of  $Ca_v1.2$  in dendritic development (Krey et al. 2013).  $Ca_v1.2$  are localized on dendrites and spines, and they play a vital role in activity dependent signaling by modulating calcium entry. Calcium influx through  $Ca_v1.2$  triggers multiple pathways downstream that are involved in structural plasticity. More importantly,  $Ca_v1.2$  are highly expressed during development (embryonic stages) with a gradual decrease in expression levels postnatally and in adulthood which further supports the theory that  $Ca_v1.2$  are vital during development (Schlick, Flucher, and Obermair 2010). During development, expansion of pyramidal dendritic arbors is fundamental to development and maturation of neuronal circuits. After maturation, dendritic arbors are much more stable and less dynamic compared to spines (Forrest, Parnell, and Penzes 2018). Since Cre recombination in the female CKO mice begins during embryonic development in forebrain glutamatergic neurons, it results in the deletion of  $Ca_v1.2$  channels during early stages of development (Goebbels et al. 2006). This would in turn alter the signaling cascades, thereby

resulting in structural alterations which lead to the behavioral deficits observed in female CKO mice.

pCREB, a molecule downstream of  $Ca_v1.2$  signaling pathway, is also known to be involved in dendritic branching and spine density (Redmond, Kashani, and Ghosh 2002; Pignataro et al. 2015). In this study, however, basal expression levels of pCREB were not different in CKO mice compared to control littermates. Since differences in pCREB expression levels can be detected even at basal levels in  $Ca_v1.2$  models, a stimulation is not necessarily required to activate the CREB phosphorylation (S. Moosmang 2005). It is possible that alterations in pCREB expression levels in glutamatergic neurons are obscured by the pCREB expression in other types of neurons in the hippocampus and prefrontal cortex, even though hippocampal neurons are predominantly excitatory. Extraction of synaptosomes instead of total proteins could solve this issue and provide better insights into the effects of  $Ca_v1.2$  deficiency on pCREB expression and whether this mediates the alterations in structural morphology.

$Ca_v1.2$  channels, upon depolarization, activate several signaling cascades and thus play a vital role in excitation-transcription coupling and protein synthesis. To get a more global overview of how  $Ca_v1.2$  deficiency alters these signaling cascades and for further drug screening, a minPROFILER assay was performed. The minPROFILER assay on cortical primary cultures derived from Ctrl and CKO mice revealed interesting phenotypes. Unstimulated CKO cortical neurons showed higher basal activity levels compared to unstimulated Ctrl neurons while CKO neurons showed less stimulability compared to Ctrl neurons. It is currently unclear whether increased basal activity seen in CKO neurons is indeed a true phenotype or an artefact of the experiment. Thus, validation experiments are required to confirm the phenotype after which further analysis and drug screening experiments will be performed.

To summarize, I was able to replicate many of the behavioral phenotypes previously reported in male  $Ca_v1.2$  rodent models in  $Ca_v1.2$ -Nex female CKO mice, which were reminiscent of endophenotypes of psychiatric disorders. The genotype differences in these behavioral phenotypes were independent of the estrous cycle. *In vitro* studies have indicated a possible interaction of estrogen with  $Ca_v1.2$  channels, however direct effects of estrogen on  $Ca_v1.2$  and behavioral phenotypes have not been reported so far (Sarkar et al. 2008). In this study, I did not find any

evidence of behavioral phenotypes being influenced by estrous cycle stages in the two groups indicating a lack of interaction between those hormones and Ca<sub>v</sub>1.2 to shape the observed behavioral differences. Future studies will venture into the electrophysiological aspects to understand the basis of cognitive dysfunction and further delve into the E/I imbalance theory which might be responsible for certain behavioral aspects. Further exploration of the minPROFILER data is also needed to understand the global effects of Ca<sub>v</sub>1.2 deficiency and how it mediates the behavioral outcome.

### 5.3. Generation of a novel mouse model with Ca<sub>v</sub>1.2 deficiency in GABAergic neurons

Recently, there is a growing body of evidence implicating GABAergic neuron dysfunction in the pathogenesis of psychiatric disorders (Rossignol 2011; Marín 2012; van Bokhoven, Selten, and Nadif Kasri 2018; Yang and Tsai 2017; Fogaça and Duman 2019). Since Ca<sub>v</sub>1.2 are also expressed in GABAergic neurons, a novel mouse model with a pan-GABAergic neuron-specific deletion of *Cacna1c* was generated to investigate the involvement of GABAergic Ca<sub>v</sub>1.2 in behaviors related to psychiatric disorders (Dedic et al. 2018). Using the inducible GAD2-CreER<sup>T2</sup> driver line to achieve deletion at different timepoints, however, did not yield the expected patterns of *Cacna1c* deletion. Cre recombination was induced in adulthood with tamoxifen-containing chow or a single dose of tamoxifen injection, but neither approach yielded satisfactory results. In both cases, there was a lack of Cre-dependent HA-tagged reporter expression in regions where GABAergic interneurons are predominant. Other inducible Cre driver lines are known to produce sufficient recombination in mice with procedures similar to those used in the current study. Thus, the reason for an absence of Cre recombination in the tamoxifen-inducible Ca<sub>v</sub>1.2-GABA mouse line is currently unclear. Since pan-GABAergic neurons-specific deletion of *Cacna1c* could not be achieved, I decided to move forward with the generation of mouse line with specific deletion in parvalbumin expressing neurons during development. Parvalbumin interneuron dysfunction is also quite often implicated in psychiatric disorders where they result in a shift in the E/I balance (Rotaru, Lewis, and Gonzalez-Burgos 2012; Ferguson and Gao 2018; Ruden, Dugan, and Konradi 2020). Additionally, one *in vitro* study also suggested a role for LTCCs in maturation of PV<sup>+</sup> hippocampal neurons. Thus, after confirming the expression of the Cre-dependent HA-tagged reporter in Ca<sub>v</sub>1.2-PV mice, they were subjected to the previously used behavioral test battery that covered the spectrum of endophenotypes associated with psychiatric disorders. Ca<sub>v</sub>1.2-PV CKO

mice exhibited anxiogenic behavior along with a task-specific cognitive deficit and enhanced passive stress coping behavior.

### **5.3.1. $Ca_v1.2$ deficiency in PV<sup>+</sup> GABAergic neurons induces anxiety**

Anxiety-related behavior is one of the most replicated findings in rodent models of  $Ca_v1.2$  (refer Table 2). Not surprisingly,  $Ca_v1.2$  deficiency in PV<sup>+</sup> inhibitory neurons also induced increased anxiety-related behavior in a task-specific manner in OFT and LDB. This anxiety-related behavior was independent of locomotion since locomotion was unaltered in CKO-PV mice in the OFT. Although  $Ca_v1.2$ -PV mice were tested in EPM as well for anxiety-related behavior, CKO-PV mice showed anxiety levels similar to Ctrl mice in the EPM. Much like the current study, anxiogenic behavior was reported in one test and not the other in some other studies as well (EPM or LDB) (Dao et al. 2010; A. S. Lee et al. 2012; Dedic et al. 2018). Procedural differences and analysis of data might partly contribute to the disparity. Why such a disparity in anxiety exists, especially in the most commonly used EPM and LDB tests remain largely unexplored. Interestingly, cell type-specific or region-specific inactivation of  $Ca_v1.2$  seems to induce anxiety more robustly than pan-neuronal deletion (Jeon et al. 2010; Bavley et al. 2020; Temme and Murphy 2017; Dedic et al. 2018). Since anxiety-related behaviors are considered to be a multidimensional construct with involvement of several brain regions, cell type-specific inactivation of  $Ca_v1.2$  might provide insights into the brain circuitries involved in modulating anxiety-related behaviors (Ramos and Mormède 1997; Crawley and Bailey 2008; Jimenez 2018; Singewald 2007). Future studies should target specific regions/ circuits (e.g., ventral hippocampus) involved in anxiety to understand how  $Ca_v1.2$  regulates these circuits and affects anxiety-related behaviors.

### **5.3.2. $Ca_v1.2$ deficiency in PV<sup>+</sup> GABAergic neurons results in cognitive impairment**

Cognitive dysfunction remains a robust feature in the psychiatric disorder spectrum and thus is often explored in rodent models of psychiatric disorders. In this study, subjecting  $Ca_v1.2$ -PV mice to different cognitive tasks revealed an overall unaltered cognition with the exception of object recognition memory. CKO-PV mice were impaired in differentiating a novel object from a familiar object. Since the hippocampus plays a vital role in all the cognitive behavioral tasks used in the test battery (Y-maze, NOR, SOR and MWM), it is interesting that the effect of  $Ca_v1.2$  deficiency was task-specific in the case of short-term object recognition memory. Another reason why this task-specific effect is intriguing is because PV<sup>+</sup> interneurons, especially in the ventral

hippocampus (vHP), have been implied as discriminators in the social recognition task where inactivation of PV<sup>+</sup> interneurons results in social memory deficits (Deng et al. 2019). But in the current study, I found no alterations in social cognition and social novelty preference. CKO-PV mice were able to sufficiently discriminate between the novel and familiar social mice which also requires a similar exploration strategy. Since PV<sup>+</sup> neurons of the vHP have been implied as discriminators in social memory, it is possible that they play a similar role in object recognition task as well. Thus, exploring whether PV<sup>+</sup> interneurons of the vHP play a role in object discrimination in the NOR task and how Ca<sub>v</sub>1.2 deficiency alters the activity of PV<sup>+</sup> interneurons of the vHP resulting in object recognition deficits might provide some valuable insights into the mechanisms underlying short term object recognition memory.

### **5.3.3. Ca<sub>v</sub>1.2 deficiency in PV<sup>+</sup> GABAergic neurons induces passive stress coping behavior**

Stress coping strategies in the FST can be considered a behavioral response to an acute stressor which has a clinical relevance to certain psychiatric disorders such as ASD. In this study, CKO-PV mice showed a passive stress coping strategy in the FST represented by their enhanced immobility. Since CKO-PV mice showed no difference in locomotor activity in the OFT, the passive stress coping strategy observed in FST is independent of locomotor activity. Mice with Ca<sub>v</sub>1.2 deficiency in another type of inhibitory (serotonin-expressing) neurons also showed a similar enhanced passive stress coping behavior while deficiency in glutamatergic neurons results in more active coping (Ehlinger and Commons 2019; Dedic et al. 2018). Acute stressors are a risk factors for the pathogenesis of psychiatric disorders and maladaptive responses to an acute stressor could be indicative of disease progression or even contribute to the same (McEwen 2004; McLaughlin et al. 2010). Thus, a passive stress coping strategy could be considered a maladaptive response to acute stressors.

Altered cFos expression was observed in the IL, M1 and NAc regions in CKO-PV mice compared to their Ctrl littermates. Since PV<sup>+</sup> interneurons comprise only 1-2% of NAc, co-localization studies of cFos with parvalbumin marker is required to confirm that the differential cFos expression arises in PV<sup>+</sup> expressing neurons due to Ca<sub>v</sub>1.2 deficiency (Xiaoting Wang et al. 2018; Warren and Whitaker 2018). The nucleus accumbens (NAc) has previously been implicated in conferring susceptibility to stressors (with a specific role for Ca<sub>v</sub>1.2 in NAc) and depression and is part of a vital pathway within the reward circuitry (Chantelle E. Terrillion et al. 2017; Bagot

2015; C E Terrillion et al. 2017; Wendel et al. 2021). Similarly, PV<sup>+</sup> interneurons of the IL-PFC region are also often implicated in stress responses and coping strategies (Page et al. 2019; Nawreen et al. 2020; Perlman, Tanti, and Mechawar 2021). In fact, a recent study by Nawreen et.al., revealed that acute inhibition of prefrontal cortex PV<sup>+</sup> interneurons resulted in passive stress coping strategy (Nawreen et al. 2020). Since CKO-PV mice in this study also showed an enhanced passive stress coping, it is possible that Ca<sub>v</sub>1.2 deficiency specifically in the PV<sup>+</sup> interneurons result in hypofunction of the prefrontal cortex thereby mediating the passive coping response. However, this response to an acute stressor cannot be mediated by only one brain region as seen by the cFos expression study. Thus, further analysis is required to truly delve into the interplay of Ca<sub>v</sub>1.2 in PV<sup>+</sup> neurons and the different brain regions contributing to the responses to acute stressors.

#### 5.4. Differential expression of cFos in CKO-Nex and CKO-PV mice

One interesting observation in this study with two different mouse lines was the opposing stress coping response in the FST. While CKO-PV mice showed a passive coping strategy, CKO-Nex mice showed a more active coping strategy in the FST compared to their respective Ctrl mice. cFos quantification to understand the brain circuits involved in this opposing stress coping responses revealed differential cFos expression in the LS, PVT, CA1, DG and LA regions in CKO-Nex mice and IL, M1 and NAc regions in CKO-PV compared to their respective Ctrl. The difference in activation of brain regions during FST in the two lines suggests that different brain circuits may be activated/ inactivated in response to the acute stressor (FST) depending on the cell populations in which Ca<sub>v</sub>1.2 was inactivated. The distribution of excitatory and PV<sup>+</sup> inhibitory neurons in each of these regions is quite variable, which could further add to the complexity of the brain circuits involved. Since cFos expression would be activated in all types of neurons in response to a stimulus, it is imperative to first isolate cFos expression in the specific cell types (glutamatergic neurons in Ca<sub>v</sub>1.2-Nex mice and PV<sup>+</sup> interneurons in Ca<sub>v</sub>1.2-PV mice) in the two mouse lines and then study the effects of Ca<sub>v</sub>1.2 deficiency on the coping strategies in these respective mouse lines. One limitation of this study is that baseline expression of cFos was not quantified. Thus, in addition to colocalization studies baseline cFos quantification is required to verify the differences in expression levels seen above.

## 6. Conclusion and future directions

In conclusion, the LBN stress yielded only moderate effects on behavioral phenotypes of  $Ca_v1.2$ -Nex mice while inducing dendritic atrophy. It is possible that the mild effects of the LBN stress are lost during adulthood. Two-hit stress models are often reported to produce much stronger effects on behavioral phenotypes. Thus, a two-hit stress model combining the LBN stress with another stressor such as restraint stress during adulthood could be considered for future studies. In female  $Ca_v1.2$ -Nex mice,  $Ca_v1.2$  inactivation in a cell type-specific manner yielded alterations in behavioral phenotypes reminiscent of the endophenotypes of psychiatric disorders. However, the downstream mechanisms driving these behavioral phenotypes still remain elusive. Electrophysiological and molecular studies targeting known signaling pathways downstream of  $Ca_v1.2$  channels would allow to untangle mechanisms underlying some of the behavioral phenotypes. Furthermore, after completion of *in vitro* validation experiments, data from the minPROFILER assay and a subsequent *in vitro* drug screening assay could provide further insights into the global effects of  $Ca_v1.2$  deficiency. In addition, this approach might also identify target pathways for future therapeutic intervention which could be tested in these animal models. Characterization of  $Ca_v1.2$ -PV mice harboring specific deletion of *Cacna1c* in  $PV^+$  interneurons further revealed interesting behavioral phenotypes such as altered anxiety-related behavior, cognitive impairment specifically in the NOR and a more passive stress coping behavior. Since E/I imbalance is an often-suggested hypothesis in the pathogenesis of psychiatric disorders, future studies therefore will involve electrophysiological studies to characterize the E/I balance in the two mouse lines. To understand more about  $Ca_v1.2$  functions in  $PV^+$  GABAergic neurons, future studies will also further probe into effects of  $Ca_v1.2$  inactivation on  $PV^+$  neuron maturation and on adult neurogenesis. Investigating the role of vHP  $PV^+$  neurons as discriminators and why  $Ca_v1.2$  inactivation in  $PV^+$  neurons leads to a specific deficit in the NOR also represent research questions to be studied in the future.

## Bibliography

- Aleman, André, René S. Kahn, and Jean Paul Selten. 2003. "Sex Differences in the Risk of Schizophrenia: Evidence from Meta-Analysis." *Archives of General Psychiatry* 60 (6): 565–71. <https://doi.org/10.1001/archpsyc.60.6.565>.
- Altemus, Margaret, Nilofar Sarvaiya, and C. Neill Epperson. 2014. "Sex Differences in Anxiety and Depression Clinical Perspectives." *Frontiers in Neuroendocrinology*. NIH Public Access. <https://doi.org/10.1016/j.yfrne.2014.05.004>.
- Amare, Azmeraw T., Ahmad Vaez, Yi Hsiang Hsu, Nese Direk, Zoha Kamali, David M. Howard, Andrew M. McIntosh, et al. 2020. "Bivariate Genome-Wide Association Analyses of the Broad Depression Phenotype Combined with Major Depressive Disorder, Bipolar Disorder or Schizophrenia Reveal Eight Novel Genetic Loci for Depression." *Molecular Psychiatry* 25 (7): 1420–29. <https://doi.org/10.1038/s41380-018-0336-6>.
- Antunes, M., and G. Biala. 2012. "The Novel Object Recognition Memory: Neurobiology, Test Procedure, and Its Modifications." *Cognitive Processing*. Springer. <https://doi.org/10.1007/s10339-011-0430-z>.
- Arnegard, Matthew E., Lori A. Whitten, Chyren Hunter, and Janine Austin Clayton. 2020. "Sex as a Biological Variable: A 5-Year Progress Report and Call to Action." *Journal of Women's Health* 29 (6): 858–64. <https://doi.org/10.1089/jwh.2019.8247>.
- Arnett, Anne B, Bruce F Pennington, Erik G Willcutt, John C DeFries, and Richard K Olson. 2015. "Sex Differences in ADHD Symptom Severity." *Journal of Child Psychology and Psychiatry* 56 (6): 632–39. <https://doi.org/10.1111/jcpp.12337>.
- Atrooz, Fatin, Hesong Liu, and Samina Salim. 2019. "Stress, Psychiatric Disorders, Molecular Targets, and More." In *Progress in Molecular Biology and Translational Science*, 167:77–105. Elsevier B.V. <https://doi.org/10.1016/bs.pmbts.2019.06.006>.
- Bader, Patrick L, Mehrdad Faizi, Leo H Kim, Scott F Owen, Michael R Tadross, Ronald W Alfa, Glenna C L Bett, Richard W Tsien, Randall L Rasmusson, and Mehrdad Shamloo. 2011. "Mouse Model of Timothy Syndrome Recapitulates Triad of Autistic Traits." *Proceedings of the National Academy of Sciences* 108 (37): 15432–37. <https://doi.org/10.1073/pnas.1112667108>.
- Bagot, R C. 2015. "Ventral Hippocampal Afferents to the Nucleus Accumbens Regulate Susceptibility to Depression." *Nat. Commun.* 6. <https://doi.org/10.1038/ncomms8062>.
- Baram, Tallie Z., Elysia P. Davis, Andre Obenaus, Curt A. Sandman, Steven L. Small, Ana Solodkin, and Hal Stern. 2012. "Fragmentation and Unpredictability of Early-Life Experience in Mental Disorders." *American Journal of Psychiatry*. American Psychiatric Association Arlington, VA. <https://doi.org/10.1176/appi.ajp.2012.11091347>.
- Bauer, Elizabeth P, Glenn E Schafe, and Joseph E LeDoux. 2002. "NMDA Receptors and L-Type Voltage-Gated Calcium Channels Contribute to Long-Term Potentiation and Different Components of Fear

- Memory Formation in the Lateral Amygdala.” *The Journal of Neuroscience: The Official Journal of the Society for Neuroscience* 22 (12): 5239–49. <https://doi.org/22/12/5239> [pii].
- Bavley, Charlotte C., Delaney K. Fischer, Bryant K. Rizzo, and Anjali M. Rajadhyaksha. 2017. “Cav1.2 Channels Mediate Persistent Chronic Stress-Induced Behavioral Deficits That Are Associated with Prefrontal Cortex Activation of the P25/Cdk5-Glucocorticoid Receptor Pathway.” *Neurobiology of Stress* 7: 27–37. <https://doi.org/10.1016/j.ynstr.2017.02.004>.
- Bavley, Charlotte C, Zeeba D Kabir, Alexander P Walsh, Maria Kosovsky, Jonathan Hackett, Herie Sun, Edwin Vázquez-Rosa, et al. 2020. “Dopamine D1R-Neuron Cacna1c Deficiency: A New Model of Extinction Therapy-Resistant Post-Traumatic Stress.” *Molecular Psychiatry*. <https://doi.org/10.1038/s41380-020-0730-8>.
- Becker, Jill B., Brian J. Prendergast, and Jing W. Liang. 2016. “Female Rats Are Not More Variable than Male Rats: A Meta-Analysis of Neuroscience Studies.” *Biology of Sex Differences* 7 (1): 1–7. <https://doi.org/10.1186/s13293-016-0087-5>.
- Beery, Annaliese K. 2018. “Inclusion of Females Does Not Increase Variability in Rodent Research Studies.” *Current Opinion in Behavioral Sciences*. Elsevier. <https://doi.org/10.1016/j.cobeha.2018.06.016>.
- Belovicova, Kristina, Eszter Bogi, Kristina Csatosova, and Michal Dubovicky. 2017. “Animal Tests for Anxiety-like and Depression-like Behavior in Rats.” *Interdisciplinary Toxicology* 10 (1): 40–43. <https://doi.org/10.1515/intox-2017-0006>.
- Berger, Stefan M., and Dusan Bartsch. 2014. “The Role of L-Type Voltage-Gated Calcium Channels Cav1.2 and Cav1.3 in Normal and Pathological Brain Function.” *Cell and Tissue Research* 357 (2): 463–76. <https://doi.org/10.1007/s00441-014-1936-3>.
- Bett, Glenna Cl, Agnieszka Lis, Scott R Wersinger, Joan S Baizer, Michael E Duffey, and Randall L Rasmusson. 2012. “A Mouse Model of Timothy Syndrome: A Complex Autistic Disorder Resulting from a Point Mutation in Cav1.2.” *North American Journal of Medicine & Science* 5 (3): 135–40. <https://doi.org/10.7156/najms.2012.053135>.
- Beyer, Dominik K.E., and Nadja Freund. 2017. “Animal Models for Bipolar Disorder: From Bedside to the Cage.” *International Journal of Bipolar Disorders*. Springer. <https://doi.org/10.1186/s40345-017-0104-6>.
- Bhat, Shambhu, David T. Dao, Chantelle E. Terrillion, Michal Arad, Robert J. Smith, Nikolai M. Soldatov, and Todd D. Gould. 2012. “CACNA1C (Cav1.2) in the Pathophysiology of Psychiatric Disease.” *Progress in Neurobiology* 99 (1): 1–14. <https://doi.org/10.1016/j.pneurobio.2012.06.001>.
- Bigos, Kristin L., Venkata S. Mattay, Joseph H. Callicott, Richard E. Straub, Radhakrishna Vakkalanka, Bhaskar Kolachana, Thomas M. Hyde, Barbara K. Lipska, Joel E. Kleinman, and Daniel R. Weinberger. 2010. “Genetic Variation in CACNA1C Affects Brain Circuitries Related to Mental

- Illness.” *Archives of General Psychiatry* 67 (9): 939. <https://doi.org/10.1001/archgenpsychiatry.2010.96>.
- Bock, J., S. Breuer, G. Poeggel, and K. Braun. 2017. “Early Life Stress Induces Attention-Deficit Hyperactivity Disorder (ADHD)-like Behavioral and Brain Metabolic Dysfunctions: Functional Imaging of Methylphenidate Treatment in a Novel Rodent Model.” *Brain Structure and Function* 222 (2): 765–80. <https://doi.org/10.1007/s00429-016-1244-7>.
- Bokhoven, Hans van, Martijn Selten, and Nael Nadif Kasri. 2018. “Inhibitory Control of the Excitatory/Inhibitory Balance in Psychiatric Disorders.” *F1000Research*. Faculty of 1000 Ltd. <https://doi.org/10.12688/f1000research.12155.1>.
- Bolton, Jessica L., Jenny Molet, Limor Regev, Yuncai Chen, Neggy Rismanchi, Elizabeth Haddad, Derek Z. Yang, Andre Obenaus, and Tallie Z. Baram. 2018. “Anhedonia Following Early-Life Adversity Involves Aberrant Interaction of Reward and Anxiety Circuits and Is Reversed by Partial Silencing of Amygdala Corticotropin-Releasing Hormone Gene.” *Biological Psychiatry* 83 (2): 137–47. <https://doi.org/10.1016/j.biopsych.2017.08.023>.
- Bolton, Jessica L., Christina M. Ruiz, Neggy Rismanchi, Gissell A. Sanchez, Erik Castillo, Jeff Huang, Christopher Cross, Tallie Z. Baram, and Stephen V. Mahler. 2018. “Early-Life Adversity Facilitates Acquisition of Cocaine Self-Administration and Induces Persistent Anhedonia.” *Neurobiology of Stress* 8 (February): 57–67. <https://doi.org/10.1016/j.ynstr.2018.01.002>.
- Bolton, Jessica L., Jenny Molet, Autumn Ivy, and Tallie Z. Baram. 2017. “New Insights into Early-Life Stress and Behavioral Outcomes.” *Current Opinion in Behavioral Sciences* 14 (April): 133–39. <https://doi.org/10.1016/j.cobeha.2016.12.012>.
- Braga, Raphael J., Graham P. Reynolds, and Samuel G. Siris. 2013. “Anxiety Comorbidity in Schizophrenia.” *Psychiatry Research*. Elsevier. <https://doi.org/10.1016/j.psychres.2013.07.030>.
- Braun, Moria D., Theresa M. Kisko, Débora Dalla Vecchia, Roberto Andreatini, Rainer K.W. Schwarting, and Markus Wöhr. 2018. “Sex-Specific Effects of Cacna1c Haploinsufficiency on Object Recognition, Spatial Memory, and Reversal Learning Capabilities in Rats.” *Neurobiology of Learning and Memory*, no. March (May). <https://doi.org/10.1016/j.nlm.2018.05.012>.
- Bromet, Evelyn, Laura Helena Andrade, Irving Hwang, Nancy A Sampson, Jordi Alonso, Giovanni de Girolamo, Ron de Graaf, et al. 2011. “Cross-National Epidemiology of DSM-IV Major Depressive Episode.” *BMC Medicine* 9 (1): 1–16. <https://doi.org/10.1186/1741-7015-9-90>.
- Burgdorf, Caitlin E, Kathryn C Schierberl, Anni S Lee, Delaney K Fischer, Tracey A Van Kempen, Vladimir Mudragel, Richard L Haganir, Teresa A Milner, Michael J Glass, and Anjali M Rajadhyaksha. 2017. “Extinction of Contextual Cocaine Memories Requires Ca v 1.2 within D1R-Expressing Cells and Recruits Hippocampal Ca v 1.2-Dependent Signaling Mechanisms.” *The Journal of Neuroscience* 37 (49): 11894–911. <https://doi.org/10.1523/JNEUROSCI.2397-17.2017>.

- Cardno, Alastair G., E. Jane Marshall, Bina Coid, Alison M. Macdonald, Tracy R. Ribchester, Nadia J. Davies, Piero Venturi, et al. 1999. "Heritability Estimates for Psychotic Disorders: The Maudsley Twin Psychosis Series." *Archives of General Psychiatry* 56 (2): 162–68. <https://doi.org/10.1001/archpsyc.56.2.162>.
- Catterall, William A., Michael J. Seagar, Masami Takahashi, and Benson M. Curtis. 1988. "Molecular Properties of Voltage-Sensitive Calcium Channels." *Current Topics in Membranes and Transport* 33 (C): 369–91. [https://doi.org/10.1016/S0070-2161\(08\)60908-9](https://doi.org/10.1016/S0070-2161(08)60908-9).
- Chadman, Kathryn K., Mu Yang, and Jacqueline N. Crawley. 2009. "Criteria for Validating Mouse Models of Psychiatric Diseases." *American Journal of Medical Genetics, Part B: Neuropsychiatric Genetics* 150 (1): 1–11. <https://doi.org/10.1002/ajmg.b.30777>.
- Chameau, Pascal, Yongjun Qin, Sabine Spijker, Guus Smit, and Marian Joëls. 2007. "Glucocorticoids Specifically Enhance L-Type Calcium Current Amplitude and Affect Calcium Channel Subunit Expression in the Mouse Hippocampus." *Journal of Neurophysiology* 97 (1): 5–14. <https://doi.org/10.1152/jn.00821.2006>.
- Cheli, Veronica T., Diara A. Santiago González, Tenzing Namgyal Lama, Vilma Spreuer, Vance Handley, Geoffrey G. Murphy, and Pablo M. Paez. 2016. "Conditional Deletion of the L-Type Calcium Channel Cav1.2 in Oligodendrocyte Progenitor Cells Affects Postnatal Myelination in Mice." *Journal of Neuroscience* 36 (42): 10853–69. <https://doi.org/10.1523/JNEUROSCI.1770-16.2016>.
- Cheli, Veronica T., Diara A. Santiago González, Norma N. Zamora, Tenzing N. Lama, Vilma Spreuer, Randall L. Rasmusson, Glenna C. Bett, Georgia Panagiotakos, and Pablo M. Paez. 2018. "Enhanced Oligodendrocyte Maturation and Myelination in a Mouse Model of Timothy Syndrome." *GLIA* 66 (11): 2324–39. <https://doi.org/10.1002/glia.23468>.
- Chen, Yuncai, and Tallie Z Baram. 2016. "Toward Understanding How Early-Life Stress Reprograms Cognitive and Emotional Brain Networks." *Neuropsychopharmacology* 41 (1): 197–206. <https://doi.org/10.1038/npp.2015.181>.
- Cichon, Sven, Nick Craddock, Mark Daly, Stephen V. Faraone, Pablo V. Gejman, John Kelsoe, Thomas Lehner, et al. 2009. "Genomewide Association Studies: History, Rationale, and Prospects for Psychiatric Disorders." *American Journal of Psychiatry*. American Psychiatric Association. <https://doi.org/10.1176/appi.ajp.2008.08091354>.
- Cohen, C, GH Perrault, and D J Sanger. 1997. "Assessment of the Antidepressant-like Effects of L-Type Voltage-Dependent Channel Modulators." *Behavioural Pharmacology* 8 (6): 629–38. <https://doi.org/10.1097/00008877-199711000-00019>.
- Corfield, E. C., Y. Yang, N. G. Martin, and D. R. Nyholt. 2017. "A Continuum of Genetic Liability for Minor and Major Depression." *Translational Psychiatry* 7 (5): e1131–e1131. <https://doi.org/10.1038/tp.2017.99>.

- Cosgrove, Donna, Omar Mothersill, Kimberley Kendall, Bettina Konte, Denise Harold, Ina Giegling, Annette Hartmann, et al. 2017. "Cognitive Characterization of Schizophrenia Risk Variants Involved in Synaptic Transmission: Evidence of CACNA1C's Role in Working Memory." *Neuropsychopharmacology* 42 (13): 2612–22. <https://doi.org/10.1038/npp.2017.123>.
- Crawley, Jacqueline, and Kathleen Bailey. 2008. "Anxiety-Related Behaviors in Mice." In , 77–101. CRC Press/Taylor & Francis. <https://doi.org/10.1201/noe1420052343.ch5>.
- Cui, Minghu, Ya Yang, Jianli Yang, Jichuan Zhang, Huili Han, Wenpei Ma, Hongbin Li, et al. 2006. "Enriched Environment Experience Overcomes the Memory Deficits and Depressive-like Behavior Induced by Early Life Stress." *Neuroscience Letters* 404 (1–2): 208–12. <https://doi.org/10.1016/J.NEULET.2006.05.048>.
- Culotta, Lorenza, and Peter Penzes. 2020. "Exploring the Mechanisms Underlying Excitation/Inhibition Imbalance in Human iPSC-Derived Models of ASD." *Molecular Autism*. BioMed Central. <https://doi.org/10.1186/s13229-020-00339-0>.
- Dao, David T., Pamela Belmonte Mahon, Xiang Cai, Colleen E. Kovacsics, Robert A. Blackwell, Michal Arad, Jianxin Shi, et al. 2010. "Mood Disorder Susceptibility Gene CACNA1C Modifies Mood-Related Behaviors in Mice and Interacts with Sex to Influence Behavior in Mice and Diagnosis in Humans." *Biological Psychiatry* 68 (9): 801–10. <https://doi.org/10.1016/j.biopsych.2010.06.019>.
- Deal, Aaron, Nicholas Cooper, Haley Ann Kirse, Ayse Uneri, Kimberly Raab-Graham, Jeffrey L. Weiner, and Leah C. Solberg Woods. 2021. "Early Life Stress Induces Hyperactivity but Not Increased Anxiety-like Behavior or Ethanol Drinking in Outbred Heterogeneous Stock Rats." *Alcohol* 91 (March): 41–51. <https://doi.org/10.1016/j.alcohol.2020.11.007>.
- Dedic, N., M. L. Pöhlmann, J. S. Richter, D. Mehta, D. Czamara, M. W. Metzger, J. Dine, et al. 2018. "Cross-Disorder Risk Gene CACNA1C Differentially Modulates Susceptibility to Psychiatric Disorders during Development and Adulthood." *Molecular Psychiatry* 23 (3): 533–43. <https://doi.org/10.1038/mp.2017.133>.
- Deng, Xiaofei, Lijia Gu, Nan Sui, Jianyou Guo, and Jing Liang. 2019. "Parvalbumin Interneuron in the Ventral Hippocampus Functions as a Discriminator in Social Memory." *Proceedings of the National Academy of Sciences of the United States of America* 116 (33): 16583–92. <https://doi.org/10.1073/pnas.1819133116>.
- Dubovsky, Steven L. 2019. "Applications of Calcium Channel Blockers in Psychiatry: Pharmacokinetic and Pharmacodynamic Aspects of Treatment of Bipolar Disorder." *Expert Opinion on Drug Metabolism and Toxicology* 15 (1): 35–47. <https://doi.org/10.1080/17425255.2019.1558206>.
- Egervari, Gabor, Alexey Kozlenkov, Stella Dracheva, and Yasmin L. Hurd. 2019. "Molecular Windows into the Human Brain for Psychiatric Disorders." *Molecular Psychiatry*. Nature Publishing Group. <https://doi.org/10.1038/s41380-018-0125-2>.

- Ehlinger, Daniel G., and Kathryn G. Commons. 2017. "Altered Cav1.2 Function in the Timothy Syndrome Mouse Model Produces Ascending Serotonergic Abnormalities." *European Journal of Neuroscience* 46 (8): 2416–25. <https://doi.org/10.1111/ejn.13707>.
- Ehlinger, Daniel G., and Kathryn G. Commons. 2019. "Cav1.2 L-Type Calcium Channels Regulate Stress Coping Behavior via Serotonin Neurons." *Neuropharmacology* 144 (January): 282–90. <https://doi.org/10.1016/j.neuropharm.2018.08.033>.
- Eiland, Lisa, and Bruce S. McEwen. 2012. "Early Life Stress Followed by Subsequent Adult Chronic Stress Potentiates Anxiety and Blunts Hippocampal Structural Remodeling." *Hippocampus* 22 (1): 82–91. <https://doi.org/10.1002/hipo.20862>.
- Erk, Susanne, Andreas Meyer-Lindenberg, David E.J. Linden, Thomas Lancaster, Sebastian Mohnke, Oliver Grimm, Franziska Degenhardt, et al. 2014. "Replication of Brain Function Effects of a Genome-Wide Supported Psychiatric Risk Variant in the CACNA1C Gene and New Multi-Locus Effects." *NeuroImage* 94 (July): 147–54. <https://doi.org/10.1016/j.neuroimage.2014.03.007>.
- Erk, Susanne, Andreas Meyer-Lindenberg, Phöbe Schmierer, Sebastian Mohnke, Oliver Grimm, Maria Garbusow, Leila Haddad, et al. 2014. "Hippocampal and Frontolimbic Function as Intermediate Phenotype for Psychosis: Evidence from Healthy Relatives and a Common Risk Variant in CACNA1C." *Biological Psychiatry* 76 (6): 466–75. <https://doi.org/10.1016/j.biopsych.2013.11.025>.
- Erk, Susanne, Andreas Meyer-Lindenberg, Knut Schnell, Carola Opitz von Boberfeld, Christine Esslinger, Peter Kirsch, Oliver Grimm, et al. 2010. "Brain Function in Carriers of a Genome-Wide Supported Bipolar Disorder Variant." *Archives of General Psychiatry* 67 (8): 803. <https://doi.org/10.1001/archgenpsychiatry.2010.94>.
- Eryilmaz, Hamdi, Alexandra S. Tanner, New Fei Ho, Adam Z. Nitenson, Noah J. Silverstein, Liana J. Petruzzi, Donald C. Goff, Dara S. Manoach, and Joshua L. Roffman. 2016. "Disrupted Working Memory Circuitry in Schizophrenia: Disentangling fMRI Markers of Core Pathology vs Other Aspects of Impaired Performance." *Neuropsychopharmacology* 41 (9): 2411–20. <https://doi.org/10.1038/npp.2016.55>.
- Farrell, M. R., F. H. Holland, R. M. Shansky, and H. C. Brenhouse. 2016. "Sex-Specific Effects of Early Life Stress on Social Interaction and Prefrontal Cortex Dendritic Morphology in Young Rats." *Behavioural Brain Research* 310 (September): 119–25. <https://doi.org/10.1016/j.bbr.2016.05.009>.
- Ferguson, Brielle R., and Wen Jun Gao. 2018. "Pv Interneurons: Critical Regulators of E/I Balance for Prefrontal Cortex-Dependent Behavior and Psychiatric Disorders." *Frontiers in Neural Circuits*. Frontiers Media S.A. <https://doi.org/10.3389/fncir.2018.00037>.
- Finsterwald, Charles, Hubert Fiumelli, Jean René Cardinaux, and Jean Luc Martin. 2010. "Regulation of Dendritic Development by BDNF Requires Activation of CRTCL1 by Glutamate." *Journal of Biological Chemistry* 285 (37): 28587–95. <https://doi.org/10.1074/jbc.M110.125740>.

- Fitzgerald, Eamon, Matthew C. Sinton, Sara Wernig-Zorc, Nicholas M. Morton, Megan C. Holmes, James P. Boardman, and Amanda J. Drake. 2021. "Altered Hypothalamic DNA Methylation and Stress-Induced Hyperactivity Following Early Life Stress." *Epigenetics and Chromatin* 14 (1): 1–14. <https://doi.org/10.1186/s13072-021-00405-8>.
- Fitzgerald, Paul J., Chris Barkus, Michael Feyder, Lisa M. Wiedholz, Yi Chyan Chen, Rose Marie Karlsson, Rodrigo Machado-Vieira, et al. 2010. "Does Gene Deletion of AMPA GluA1 Phenocopy Features of Schizoaffective Disorder?" *Neurobiology of Disease* 40 (3): 608–21. <https://doi.org/10.1016/j.nbd.2010.08.005>.
- Fogaça, Manoela V., and Ronald S. Duman. 2019. "Cortical GABAergic Dysfunction in Stress and Depression: New Insights for Therapeutic Interventions." *Frontiers in Cellular Neuroscience*. Frontiers Media S.A. <https://doi.org/10.3389/fncel.2019.00087>.
- Forrest, Marc P., Euan Parnell, and Peter Penzes. 2018. "Dendritic Structural Plasticity and Neuropsychiatric Disease." *Nature Reviews Neuroscience*. Nature Publishing Group. <https://doi.org/10.1038/nrn.2018.16>.
- Franke, Barbara, Alejandro Arias Vasquez, Joris A. Veltman, Han G. Brunner, Mark Rijpkema, and Guillén Fernández. 2010. "Genetic Variation in CACNA1C, a Gene Associated with Bipolar Disorder, Influences Brainstem Rather than Gray Matter Volume in Healthy Individuals." *Biological Psychiatry* 68 (6): 586–88. <https://doi.org/10.1016/j.biopsych.2010.05.037>.
- Franklin, Keith B J, and George Paxinos. 1997. "The Mouse Brain in Stereotaxic Coordinates." In .
- Freeman, Marlene P., Scott A. Freeman, and Susan L. McElroy. 2002. "The Comorbidity of Bipolar and Anxiety Disorders: Prevalence, Psychobiology, and Treatment Issues." *Journal of Affective Disorders*. Elsevier. [https://doi.org/10.1016/S0165-0327\(00\)00299-8](https://doi.org/10.1016/S0165-0327(00)00299-8).
- Frydecka, Dorota, Abeer M. Eissa, Doaa H. Hewedi, Manal Ali, Jarosław Drapała, Błażej Misiak, Ewa Kłosińska, Joseph R. Phillips, and Ahmed A. Moustafa. 2014. "Impairments of Working Memory in Schizophrenia and Bipolar Disorder: The Effect of History of Psychotic Symptoms and Different Aspects of Cognitive Task Demands." *Frontiers in Behavioral Neuroscience* 8 (NOV): 416. <https://doi.org/10.3389/fnbeh.2014.00416>.
- Fujita, Masayo, Yukiko Ochiai, Taishi Clark Takeda, Yoko Hagino, Kazuto Kobayashi, and Kazutaka Ikeda. 2020. "Increase in Excitability of Hippocampal Neurons during Novelty-Induced Hyperlocomotion in Dopamine-Deficient Mice." *Molecular Brain* 13 (1): 1–4. <https://doi.org/10.1186/s13041-020-00664-8>.
- Gandal, Michael J., Jillian R. Haney, Neelroop N. Parikshak, Virpi Leppä, Gokul Ramaswami, Chris Hartl, Andrew J. Schork, et al. 2018. "Shared Molecular Neuropathology across Major Psychiatric Disorders Parallels Polygenic Overlap." *Science* 359 (6376): 693–97. <https://doi.org/10.1126/science.aad6469>.
- Gershon, E. S., K. Grennan, J. Busnello, J. A. Badner, F. Ovsiew, S. Memon, N. Alliey-Rodriguez, J.

- Cooper, B. Romanos, and C. Liu. 2014. "A Rare Mutation of CACNA1C in a Patient with Bipolar Disorder and Decreased Gene Expression Associated with a Bipolar-Associated Common SNP of CACNA1C in Brain." *Molecular Psychiatry* 19 (8): 890–94. <https://doi.org/10.1038/mp.2013.107>.
- Goebbels, Sandra, Ingo Bormuth, Ulli Bode, Ola Hermanson, Markus H. Schwab, and Klaus Armin Nave. 2006. "Genetic Targeting of Principal Neurons in Neocortex and Hippocampus of NEX-Cre Mice." *Genesis* 44 (12): 611–21. <https://doi.org/10.1002/DVG.20256>.
- Goldstein, Jill M., Lee S. Cohen, Nicholas J. Horton, Hang Lee, Scott Andersen, Mauricio Tohen, Ann Marie K. Crawford, and Gary Tollefson. 2002. "Sex Differences in Clinical Response to Olanzapine Compared with Haloperidol." *Psychiatry Research* 110 (1): 27–37. [https://doi.org/10.1016/S0165-1781\(02\)00028-8](https://doi.org/10.1016/S0165-1781(02)00028-8).
- Goodwill, Haley L., Gabriela Manzano-Nieves, Meghan Gallo, Hye-In Lee, Esther Oyerinde, Thomas Serre, and Kevin G. Bath. 2018. "Early Life Stress Leads to Sex Differences in Development of Depressive-like Outcomes in a Mouse Model." *Neuropsychopharmacology*, September, 1. <https://doi.org/10.1038/s41386-018-0195-5>.
- Götze, Tilmann, Maria Clara Soto-Bernardini, Mingyue Zhang, Hendrik Mießner, Lisa Linhoff, Magdalena M. Brzózka, Viktorija Velanac, et al. 2021. "Hyperactivity Is a Core Endophenotype of Elevated Neuregulin-1 Signaling in Embryonic Glutamatergic Networks." *Schizophrenia Bulletin* 47 (5): 1409–20. <https://doi.org/10.1093/schbul/sbab027>.
- Green, E K, D Grozeva, I Jones, L Jones, G Kirov, S Caesar, K Gordon-Smith, et al. 2010. "The Bipolar Disorder Risk Allele at CACNA1C Also Confers Risk of Recurrent Major Depression and of Schizophrenia." *Molecular Psychiatry* 15 (10): 1016–22. <https://doi.org/10.1038/mp.2009.49>.
- Hedges, Dawson W., and Fu Lye Woon. 2011. "Early-Life Stress and Cognitive Outcome." *Psychopharmacology*. Springer. <https://doi.org/10.1007/s00213-010-2090-6>.
- Heilbronner, Urs, Dörthe Malzahn, Jana Strohmaier, Sandra Maier, Josef Frank, Jens Treutlein, Thomas W Mühleisen, et al. 2015. "A Common Risk Variant in CACNA1C Supports a Sex-Dependent Effect on Longitudinal Functioning and Functional Recovery from Episodes of Schizophrenia-Spectrum but Not Bipolar Disorder." *European Neuropsychopharmacology* 25 (12): 2262–70. <https://doi.org/10.1016/j.euroneuro.2015.09.012>.
- Heim, Christine, and Charles B Nemeroff. 2001. "The Role of Childhood Trauma in the Neurobiology of Mood and Anxiety Disorders: Preclinical and Clinical Studies." *Biological Psychiatry*. Elsevier. [https://doi.org/10.1016/S0006-3223\(01\)01157-X](https://doi.org/10.1016/S0006-3223(01)01157-X).
- Herholt, Alexander, Ben Brankatschk, Nirmal Kannaiyan, Sergi Papiol, Sven P. Wichert, Michael C. Wehr, and Moritz J. Rossner. 2018. "Pathway Sensor-Based Functional Genomics Screening Identifies Modulators of Neuronal Activity." *Scientific Reports* 8 (1): 17597. <https://doi.org/10.1038/s41598-018-36008-9>.

- Hilker, Rikke, Dorte Helenius, Birgitte Fagerlund, Axel Skytthe, Kaare Christensen, Thomas M. Werge, Merete Nordentoft, and Birte Glenthøj. 2018. "Heritability of Schizophrenia and Schizophrenia Spectrum Based on the Nationwide Danish Twin Register." *Biological Psychiatry* 83 (6): 492–98. <https://doi.org/10.1016/j.biopsych.2017.08.017>.
- Hill, Rachel A., Maren Klug, Szerenke Kiss Von Soly, Michele D. Binder, Anthony J. Hannan, and Maarten van Den Buuse. 2014. "Sex-Specific Disruptions in Spatial Memory and Anhedonia in a 'Two Hit' Rat Model Correspond with Alterations in Hippocampal Brain-Derived Neurotrophic Factor Expression and Signaling." *Hippocampus* 24 (10): 1197–1211. <https://doi.org/10.1002/hipo.22302>.
- Hirschfeld, Robert M.A. 2001. "The Comorbidity of Major Depression and Anxiety Disorders: Recognition and Management in Primary Care." *Primary Care Companion to the Journal of Clinical Psychiatry* 3 (6): 244–54. <https://doi.org/10.4088/pcc.v03n0609>.
- Hoeijmakers, Lianne, Silvie R. Ruigrok, Anna Amelianchik, Daniela Ivan, Anne-Marie van Dam, Paul J. Lucassen, and Aniko Korosi. 2017. "Early-Life Stress Lastingly Alters the Neuroinflammatory Response to Amyloid Pathology in an Alzheimer's Disease Mouse Model." *Brain, Behavior, and Immunity* 63 (July): 160–75. <https://doi.org/10.1016/j.bbi.2016.12.023>.
- Hofmann, F., L. Lacinová, and N. Klugbauer. 1999. "Voltage-Dependent Calcium Channels: From Structure to Function." *Reviews of Physiology, Biochemistry and Pharmacology*. Springer, Berlin, Heidelberg. <https://doi.org/10.1007/bfb0033648>.
- Hopp, Sarah C. 2021. "Targeting Microglia L-Type Voltage-Dependent Calcium Channels for the Treatment of Central Nervous System Disorders." *Journal of Neuroscience Research*. <https://doi.org/10.1002/jnr.24585>.
- Itoh, Yuichiro, and Arthur P Arnold. 2015. "Are Females More Variable than Males in Gene Expression? Meta-Analysis of Microarray Datasets." *Biology of Sex Differences* 6 (1). <https://doi.org/10.1186/s13293-015-0036-8>.
- Ivy, Autumn S., Christopher S. Rex, Yuncai Chen, Céline Dubé, Pamela M. Maras, Dimitri E. Grigoriadis, Christine M. Gall, Gary Lynch, and Tallie Z. Baram. 2010. "Hippocampal Dysfunction and Cognitive Impairments Provoked by Chronic Early-Life Stress Involve Excessive Activation of CRH Receptors." *Journal of Neuroscience* 30 (39): 13005–15. <https://doi.org/10.1523/JNEUROSCI.1784-10.2010>.
- Jaric, Ivana, Devin Rocks, Heining Cham, Alice Herchek, and Marija Kundakovic. 2019. "Sex and Estrous Cycle Effects on Anxiety- and Depression-Related Phenotypes in a Two-Hit Developmental Stress Model." *Frontiers in Molecular Neuroscience* 12 (April): 74. <https://doi.org/10.3389/fnmol.2019.00074>.
- Jeon, Daejong, Sangwoo Kim, Mattu Chetana, Daewoong Jo, H Earl Ruley, Shih-Yao Lin, Dania Rabah, Jean-Pierre Kinet, and Hee-Sup Shin. 2010. "Observational Fear Learning Involves Affective Pain

- System and Cav1.2 Ca<sup>2+</sup> Channels in ACC.” *Nature Neuroscience* 13 (4): 482–88. <https://doi.org/10.1038/nn.2504>.
- Jesús-Cortés, Héctor De, Anjali M. Rajadhyaksha, and Andrew A. Pieper. 2016. “Cacna1c: Protecting Young Hippocampal Neurons in the Adult Brain.” *Neurogenesis* 3 (1): e1231160. <https://doi.org/10.1080/23262133.2016.1231160>.
- Jia, Xiao Can, Yong Li Yang, Yuan Cheng Chen, Zhi Wei Cheng, Yuhui Du, Zhenhua Xia, Weiping Zhang, et al. 2019. “Multivariate Analysis of Genome-Wide Data to Identify Potential Pleiotropic Genes for Five Major Psychiatric Disorders Using MetaCCA.” *Journal of Affective Disorders* 242 (January): 234–43. <https://doi.org/10.1016/j.jad.2018.07.046>.
- Jiang, M., and J. W. Swann. 2005. “A Role for L-Type Calcium Channels in the Maturation of Parvalbumin-Containing Hippocampal Interneurons.” *Neuroscience* 135 (3): 839–50. <https://doi.org/10.1016/j.neuroscience.2005.06.073>.
- Jimenez, J. C. 2018. “Anxiety Cells in a Hippocampal-Hypothalamic Circuit.” *Neuron* 97. <https://doi.org/10.1016/j.neuron.2018.01.016>.
- Joëls, Marian, and Henk Karst. 2012. “Corticosteroid Effects on Calcium Signaling in Limbic Neurons.” *Cell Calcium* 51 (3–4): 277–83. <https://doi.org/10.1016/j.ceca.2011.11.002>.
- Jogia, J, G Ruberto, G Lelli-Chiesa, E Vassos, M Maierú, R Tatarelli, P Girardi, D Collier, and S Frangou. 2011. “The Impact of the CACNA1C Gene Polymorphism on Frontolimbic Function in Bipolar Disorder.” *Molecular Psychiatry* 16 (11): 1070–71. <https://doi.org/10.1038/mp.2011.49>.
- Johansson, Viktoria, Ralf Kuja-Halkola, Tyrone D. Cannon, Christina M. Hultman, and Anna M. Hedman. 2019. “A Population-Based Heritability Estimate of Bipolar Disorder – In a Swedish Twin Sample.” *Psychiatry Research* 278 (August): 180–87. <https://doi.org/10.1016/j.psychres.2019.06.010>.
- Jones, Ca, Djg Watson, and Kcf Fone. 2011. “Animal Models of Schizophrenia.” *British Journal of Pharmacology* 164 (4): 1162–94. <https://doi.org/10.1111/j.1476-5381.2011.01386.x>.
- Kabir, Z. D., A. Che, D. K. Fischer, R. C. Rice, B. K. Rizzo, M. Byrne, M. J. Glass, N. V. De Marco Garcia, and A. M. Rajadhyaksha. 2017. “Rescue of Impaired Sociability and Anxiety-like Behavior in Adult Cacna1c-Deficient Mice by Pharmacologically Targeting EIF2 $\alpha$ .” *Molecular Psychiatry* 22 (8): 1096–1109. <https://doi.org/10.1038/mp.2017.124>.
- Kabir, Z. D., A. S. Lee, and A. M. Rajadhyaksha. 2016. “L-Type Ca<sup>2+</sup>channels in Mood, Cognition and Addiction: Integrating Human and Rodent Studies with a Focus on Behavioural Endophenotypes.” *Journal of Physiology* 594 (20): 5823–37. <https://doi.org/10.1113/JP270673>.
- Kabir, Zeeba D., Anni S. Lee, Caitlin E. Burgdorf, Delaney K. Fischer, Aditi M. Rajadhyaksha, Ethan Mok, Bryant Rizzo, et al. 2017. “Cacna1c in the Prefrontal Cortex Regulates Depression-Related Behaviors via REDDI.” *Neuropsychopharmacology* 42 (10): 2032–42. <https://doi.org/10.1038/npp.2016.271>.
- Kabir, Zeeba D., Arlene Martínez-Rivera, and Anjali M. Rajadhyaksha. 2017. “From Gene to Behavior: L-

- Type Calcium Channel Mechanisms Underlying Neuropsychiatric Symptoms.” *Neurotherapeutics* 14 (3): 588–613. <https://doi.org/10.1007/s13311-017-0532-0>.
- Kamijo, Satoshi, Yuichiro Ishii, Shin-Ichiro Horigane, Kanzo Suzuki, Masamichi Ohkura, Junichi Nakai, Hajime Fujii, Sayaka Takemoto-Kimura, and Haruhiko Bito. 2018. “A Critical Neurodevelopmental Role for L-Type Voltage-Gated Calcium Channels in Neurite Extension and Radial Migration.” *The Journal of Neuroscience* 38 (24): 2357–17. <https://doi.org/10.1523/JNEUROSCI.2357-17.2018>.
- Karlsson, Rose Marie, Kohichi Tanaka, Markus Heilig, and Andrew Holmes. 2008. “Loss of Glial Glutamate and Aspartate Transporter (Excitatory Amino Acid Transporter 1) Causes Locomotor Hyperactivity and Exaggerated Responses to Psychotomimetics: Rescue by Haloperidol and Metabotropic Glutamate 2/3 Agonist.” *Biological Psychiatry* 64 (9): 810–14. <https://doi.org/10.1016/j.biopsych.2008.05.001>.
- Karst, Henk, Suresh Nair, Els Velzing, Lisette Rumpff-van Essen, Eelco Slagter, Patricia Shinnick-Gallagher, and Marian Joels. 2002. “Glucocorticoids Alter Calcium Conductances and Calcium Channel Subunit Expression in Basolateral Amygdala Neurons.” *European Journal of Neuroscience* 16 (6): 1083–89. <https://doi.org/10.1046/j.1460-9568.2002.02172.x>.
- Kehrer, Colin. 2008. “Altered Excitatory-Inhibitory Balance in the NMDA-Hypofunction Model of Schizophrenia.” *Frontiers in Molecular Neuroscience* 1:6. <https://doi.org/10.3389/neuro.02.006.2008>
- Kempton, Matthew J., Gaia Ruberto, Evangelos Vassos, Roberto Tatarelli, Paolo Girardi, David Collier, and Sophia Frangou. 2009. “Effects of the CACNA1C Risk Allele for Bipolar Disorder on Cerebral Gray Matter Volume in Healthy Individuals.” *American Journal of Psychiatry*. *Am J Psychiatry*. <https://doi.org/10.1176/appi.ajp.2009.09050680>.
- Khan, Arif, Amy E. Brodhead, Kelly A. Schwartz, Russell L. Kolts, and Walter A. Brown. 2005. “Sex Differences in Antidepressant Response in Recent Antidepressant Clinical Trials.” *Journal of Clinical Psychopharmacology* 25 (4): 318–24. <https://doi.org/10.1097/01.jcp.0000168879.03169.ce>.
- Kisko, Theresa M., Moria D. Braun, Susanne Michels, Stephanie H. Witt, Marcella Rietschel, Carsten Culmsee, Rainer K.W. W. Schwarting, and Markus Wöhr. 2018. “Cacna1c Haploinsufficiency Leads to Pro-Social 50-KHz Ultrasonic Communication Deficits in Rats.” *Disease Models & Mechanisms* 11 (May): dmm.034116. <https://doi.org/10.1242/dmm.034116>.
- Kisko, Theresa M., Moria D. Braun, Susanne Michels, Stephanie H. Witt, Marcella Rietschel, Carsten Culmsee, Rainer K.W. Schwarting, and Markus Wöhr. 2020. “Sex-Dependent Effects of Cacna1c Haploinsufficiency on Juvenile Social Play Behavior and pro-Social 50-KHz Ultrasonic Communication in Rats.” *Genes, Brain and Behavior* 19 (2): e12552. <https://doi.org/10.1111/gbb.12552>.
- Klaus, K., K. Butler, H. Gutierrez, S.J. Durrant, and K. Pennington. 2018. “Interactive Effects of Early Life Stress and CACNA1C Genotype on Cortisol Awakening Response.” *Biological Psychology* 136

- (July): 22–28. <https://doi.org/10.1016/j.biopsycho.2018.05.002>.
- Koch, Katharina, Sophia Stegmaier, Lena Schwarz, Michael Erb, Mara Thomas, Klaus Scheffler, Dirk Wildgruber, Vanessa Nieratschker, and Thomas Ethofer. 2019. “CACNA1C Risk Variant Affects Microstructural Connectivity of the Amygdala.” *NeuroImage: Clinical* 22 (January): 101774. <https://doi.org/10.1016/j.nicl.2019.101774>.
- Kohl, Christine, Xiao Dong Wang, Jocelyn Grosse, Céline Fournier, Daniela Harbich, Sören Westerholz, Ji Tao Li, et al. 2015. “Hippocampal Neuroligin-2 Links Early-Life Stress with Impaired Social Recognition and Increased Aggression in Adult Mice.” *Psychoneuroendocrinology* 55 (May): 128–43. <https://doi.org/10.1016/j.psyneuen.2015.02.016>.
- Kramer, Audra A, Nicholas E Ingraham, Emily J Sharpe, and Michelle Mynlieff. 2012. “Levels of 1.2 L-Type Channels Peak in the First Two Weeks in Rat Hippocampus Whereas 1.3 Channels Steadily Increase through Development.” *Journal of Signal Transduction* 2012: 1–11. <https://doi.org/10.1155/2012/597214>.
- Krauthaim, Johannes T, Benjamin Straube, Udo Dannowski, Martin Pyka, Henriette Schneider-Hassloff, Rebecca Drexler, Axel Krug, et al. 2018. “Outgroup Emotion Processing in the VACC Is Modulated by Childhood Trauma and CACNA1C Risk Variant.” *Social Cognitive and Affective Neuroscience* 13 (3): 341–48. <https://doi.org/10.1093/scan/nsy004>.
- Krey, Jocelyn F., Sergiu P. Pașca, Aleksandr Shcheglovitov, Masayuki Yazawa, Rachel Schwemberger, Randall Rasmusson, and Ricardo E. Dolmetsch. 2013. “Timothy Syndrome Is Associated with Activity-Dependent Dendritic Retraction in Rodent and Human Neurons.” *Nature Neuroscience* 16 (2): 201–9. <https://doi.org/10.1038/nn.3307>.
- Krug, Axel, Vanessa Nieratschker, Valentin Markov, Sören Krach, Andreas Jansen, Klaus Zerres, Thomas Eggermann, et al. 2010. “Effect of CACNA1C Rs1006737 on Neural Correlates of Verbal Fluency in Healthy Individuals.” *NeuroImage* 49 (2): 1831–36. <https://doi.org/10.1016/j.neuroimage.2009.09.028>.
- Krug, Axel, Stephanie H. Witt, Heidelore Backes, Bruno Dietsche, Vanessa Nieratschker, N. Jon Shah, Markus M. Nöthen, Marcella Rietschel, and Tilo Kircher. 2014. “A Genome-Wide Supported Variant in CACNA1C Influences Hippocampal Activation during Episodic Memory Encoding and Retrieval.” *European Archives of Psychiatry and Clinical Neuroscience* 264 (2): 103–10. <https://doi.org/10.1007/s00406-013-0428-x>.
- Krugers, Harm J., J. Marit Arp, Hui Xiong, Sofia Kanatsou, Sylvie L. Lesuis, Aniko Korosi, Marian Joels, and Paul J. Lucassen. 2017. “Early Life Adversity: Lasting Consequences for Emotional Learning.” *Neurobiology of Stress*. Elsevier. <https://doi.org/10.1016/j.ynstr.2016.11.005>.
- Kulak, Anita, Michel Cuenod, and Kim Q. Do. 2012. “Behavioral Phenotyping of Glutathione-Deficient Mice: Relevance to Schizophrenia and Bipolar Disorder.” *Behavioural Brain Research* 226 (2): 563–

70. <https://doi.org/10.1016/j.bbr.2011.10.020>.
- Kundakovic, Marija, Sean Lim, Kathryn Gudsnuk, and Frances A. Champagne. 2013. "Sex-Specific and Strain-Dependent Effects of Early Life Adversity on Behavioral and Epigenetic Outcomes." *Frontiers in Psychiatry* 4 (AUG): 78. <https://doi.org/10.3389/fpsy.2013.00078>.
- Kunwar, Arun, Mantosh Dewan, and Stephen V. Faraone. 2007. "Treating Common Psychiatric Disorders Associated with Attention-Deficit/Hyperactivity Disorder." <https://doi.org/10.1517/14656566.8.5.555>.
- Lancaster, T. M., S. Foley, K. E. Tansey, D. E. J. Linden, and X. Caseras. 2016. "CACNA1C Risk Variant Is Associated with Increased Amygdala Volume." *European Archives of Psychiatry and Clinical Neuroscience* 266 (3): 269–75. <https://doi.org/10.1007/s00406-015-0609-x>.
- Lancaster, T M, E A Heerey, K Mantripragada, and D E J Linden. 2014. "CACNA1C Risk Variant Affects Reward Responsiveness in Healthy Individuals." *Translational Psychiatry* 4 (10): e461–e461. <https://doi.org/10.1038/tp.2014.100>.
- Langwieser, N., C. J. Christel, T. Kleppisch, F. Hofmann, C. T. Wotjak, and S. Moosmang. 2010. "Homeostatic Switch in Hebbian Plasticity and Fear Learning after Sustained Loss of Cav1.2 Calcium Channels." *Journal of Neuroscience* 30 (25): 8367–75. <https://doi.org/10.1523/JNEUROSCI.4164-08.2010>.
- Lee, A. S., S. Ra, Aditi M. Rajadhyaksha, J. K. Britt, H. De Jesus-Cortes, K. L. Gonzales, A. Lee, et al. 2012. "Forebrain Elimination of Cacna1c Mediates Anxiety-like Behavior in Mice." *Molecular Psychiatry* 17 (11): 1054–55. <https://doi.org/10.1038/mp.2012.71>.
- Lee, A S, K. L. Gonzales, A. Lee, S. Moosmang, F. Hofmann, A. A. Pieper, and A. M. Rajadhyaksha. 2012. "Selective Genetic Deletion of Cacna1c in the Mouse Prefrontal Cortex." *Molecular Psychiatry* 17 (11): 1051–1051. <https://doi.org/10.1038/mp.2012.149>.
- Lee, Anni S., Héctor De Jesús-Cortés, Zeeba D. Kabir, Whitney Knobbe, Madeline Orr, Caitlin Burgdorf, Paula Huntington, et al. 2016. "The Neuropsychiatric Disease-Associated Gene Cacna1c Mediates Survival of Young Hippocampal Neurons." *ENeuro* 3 (2): 3576–81. <https://doi.org/10.1523/ENEURO.0006-16.2016>.
- Lee, Phil H., Verner Anttila, Hyejung Won, Yen Chen A. Feng, Jacob Rosenthal, Zhaozhong Zhu, Elliot M. Tucker-Drob, et al. 2019. "Genomic Relationships, Novel Loci, and Pleiotropic Mechanisms across Eight Psychiatric Disorders." *Cell* 179 (7): 1469–1482.e11. <https://doi.org/10.1016/J.CELL.2019.11.020/ATTACHMENT/F121305A-BC31-46E9-BEBF-D97E8A0527B7/MMC11>. PDF.
- Lee, S. Hong, Stephan Ripke, Benjamin M. Neale, Stephen V. Faraone, Shaun M. Purcell, Roy H. Perlis, Bryan J. Mowry, et al. 2013. "Genetic Relationship between Five Psychiatric Disorders Estimated from Genome-Wide SNPs." *Nature Genetics* 2013 45:9 45 (9): 984–94.

- <https://doi.org/10.1038/ng.2711>.
- Leitch, B., A. Szostek, R. Lin, and O. Shevtsova. 2009. "Subcellular Distribution of L-Type Calcium Channel Subtypes in Rat Hippocampal Neurons." *Neuroscience* 164 (2): 641–57. <https://doi.org/10.1016/j.neuroscience.2009.08.006>.
- Li, Hui Juan, Chen Zhang, Li Hui, Dong Sheng Zhou, Yi Li, Chu Yi Zhang, Chuang Wang, et al. 2021. "Novel Risk Loci Associated with Genetic Risk for Bipolar Disorder among Han Chinese Individuals: A Genome-Wide Association Study and Meta-Analysis." *JAMA Psychiatry* 78 (3): 320–30. <https://doi.org/10.1001/jamapsychiatry.2020.3738>.
- Li, Jun, Linnan Zhao, Yang You, Tianlan Lu, Meixiang Jia, Hao Yu, Yanyan Ruan, et al. 2015. "Schizophrenia Related Variants in CACNA1C Also Confer Risk of Autism." Edited by Deyou Zheng. *PLOS ONE* 10 (7): e0133247. <https://doi.org/10.1371/journal.pone.0133247>.
- Li, Rena, Xin Ma, Gang Wang, Jian Yang, and Chuanyue Wang. 2016. "Why Sex Differences in Schizophrenia?" *Journal of Translational Neuroscience* 1 (1): 37–42. <http://www.ncbi.nlm.nih.gov/pubmed/29152382>.
- Lin, Kangguang, Guiyun Xu, Lingling Shi, Weicong Lu, Lijie Guan, Huiyi Ouyang, Kun Chen, Yamei Dang, Libing Zhou, and Kwok-Fai So. 2017. "CACNA1C Polymorphisms Impact Cognitive Recovery in Patients with Bipolar Disorder in a Six-Week Open-Label Trial." *Scientific Reports* 7 (1): 7022. <https://doi.org/10.1038/s41598-017-07368-5>.
- Liu, Na, Yulu Wang, Aerin Y. An, Christopher Banker, Yi Hua Qian, and James M. O'Donnell. 2020. "Single Housing-Induced Effects on Cognitive Impairment and Depression-like Behavior in Male and Female Mice Involve Neuroplasticity-Related Signaling." *European Journal of Neuroscience* 52 (1): 2694–2704. <https://doi.org/10.1111/ejn.14565>.
- Liu, Y, D H Blackwood, S Caesar, E J C de Geus, A Farmer, M A R Ferreira, I N Ferrier, et al. 2011. "Meta-Analysis of Genome-Wide Association Data of Bipolar Disorder and Major Depressive Disorder." *Molecular Psychiatry* 16 (1): 2–4. <https://doi.org/10.1038/mp.2009.107>.
- Lo, Shun Qiang, Judy C.G. Sng, and George J. Augustine. 2017. "Defining a Critical Period for Inhibitory Circuits within the Somatosensory Cortex." *Scientific Reports* 7 (1): 1–13. <https://doi.org/10.1038/s41598-017-07400-8>.
- Lueptow, Lindsay M. 2017. "Novel Object Recognition Test for the Investigation of Learning and Memory in Mice." *Journal of Visualized Experiments* 2017 (126): 55718. <https://doi.org/10.3791/55718>.
- Macharadze, Tamar, Eike Budinger, Michael Brosch, Henning Scheich, Frank W. Ohl, and Julia U. Henschke. 2019. "Early Sensory Loss Alters the Dendritic Branching and Spine Density of Supragranular Pyramidal Neurons in Rodent Primary Sensory Cortices." *Frontiers in Neural Circuits* 13 (September): 61. <https://doi.org/10.3389/fncir.2019.00061>.
- Mallas, E., F. Carletti, C. A. Chaddock, S. Shergill, J. Woolley, M. M. Picchioni, C. McDonald, et al. 2017.

- “The Impact of CACNA1C Gene, and Its Epistasis with ZNF804A, on White Matter Microstructure in Health, Schizophrenia and Bipolar Disorder 1.” *Genes, Brain and Behavior* 16 (4): 479–88. <https://doi.org/10.1111/gbb.12355>.
- Marcantoni, Andrea, Chiara Calorio, Enis Hidisoglu, Giuseppe Chiantia, and Emilio Carbone. 2020. “Cav1.2 Channelopathies Causing Autism: New Hallmarks on Timothy Syndrome.” *Pflugers Archiv European Journal of Physiology*. <https://doi.org/10.1007/s00424-020-02430-0>.
- Marín, Oscar. 2012. “Interneuron Dysfunction in Psychiatric Disorders.” *Nature Reviews Neuroscience*. Nature Publishing Group. <https://doi.org/10.1038/nrn3155>.
- McEwen, Bruce S. 2004. “Protection and Damage from Acute and Chronic Stress: Allostasis and Allostatic Overload and Relevance to the Pathophysiology of Psychiatric Disorders.” In *Annals of the New York Academy of Sciences*, 1032:1–7. John Wiley & Sons, Ltd. <https://doi.org/10.1196/annals.1314.001>.
- McGuffin, Peter, Fruhling Rijdsijk, Martin Andrew, Pak Sham, Randy Katz, and Alastair Cardno. 2003. “The Heritability of Bipolar Affective Disorder and the Genetic Relationship to Unipolar Depression.” *Archives of General Psychiatry* 60 (5): 497–502. <https://doi.org/10.1001/archpsyc.60.5.497>.
- McLaughlin, K. A., K. J. Conron, K. C. Koenen, and S. E. Gilman. 2010. “Childhood Adversity, Adult Stressful Life Events, and Risk of Past-Year Psychiatric Disorder: A Test of the Stress Sensitization Hypothesis in a Population-Based Sample of Adults.” *Psychological Medicine* 40 (10): 1647–58. <https://doi.org/10.1017/S0033291709992121>.
- McMahon, Francis J. 2018. “Population-Based Estimates of Heritability Shed New Light on Clinical Features of Major Depression.” *American Journal of Psychiatry*. American Psychiatric Association. <https://doi.org/10.1176/appi.ajp.2018.18070789>.
- Miró, Xavier, Sandra Meier, Marie Luise Dreisow, Josef Frank, Jana Strohmaier, René Breuer, Christine Schmä, et al. 2012. “Studies in Humans and Mice Implicate Neurocan in the Etiology of Mania.” *American Journal of Psychiatry* 169 (9): 982–90. <https://doi.org/10.1176/APPI.AJP.2012.11101585/ASSET/IMAGES/LARGE/982F3.JPEG>.
- Mogilnicka, Ewa, Anna Czyrak, and Jerzy Maj. 1988. “BAY K 8644 Enhances Immobility in the Mouse Behavioral Despair Test, an Effect Blocked by Nifedipine.” *European Journal of Pharmacology*. Vol. 151. [https://ac.els-cdn.com/0014299988908138/1-s2.0-0014299988908138-main.pdf?\\_tid=a684c700-ec0a-4ea6-967ba8a93b6eff8a&acdnat=1533134787\\_5d108dd5932ea0a2e4d9b1c164fe9aa0](https://ac.els-cdn.com/0014299988908138/1-s2.0-0014299988908138-main.pdf?_tid=a684c700-ec0a-4ea6-967ba8a93b6eff8a&acdnat=1533134787_5d108dd5932ea0a2e4d9b1c164fe9aa0).
- Molet, J., K. Heins, X. Zhuo, Y. T. Mei, L. Regev, T. Z. Baram, and H. Stern. 2016. “Fragmentation and High Entropy of Neonatal Experience Predict Adolescent Emotional Outcome.” *Translational Psychiatry* 6 (1): e702–e702. <https://doi.org/10.1038/tp.2015.200>.
- Molet, Jenny, Pamela M. Maras, Sarit Avishai-Eliner, and Tallie Z. Baram. 2014. “Naturalistic Rodent Models of Chronic Early-Life Stress.” *Developmental Psychobiology*. John Wiley & Sons, Ltd. <https://doi.org/10.1002/dev.21230>.

- Moon, Anna L, Niels Haan, Lawrence S Wilkinson, Kerrie L Thomas, and Jeremy Hall. 2018. "CACNA1C: Association with Psychiatric Disorders, Behavior and Neurogenesis." *Schizophrenia Bulletin*. <https://doi.org/10.1093/schbul/sby096>.
- Moosmang, S. 2005. "Role of Hippocampal Cav1.2 Ca<sup>2+</sup> Channels in NMDA Receptor-Independent Synaptic Plasticity and Spatial Memory." *Journal of Neuroscience* 25 (43): 9883–92. <https://doi.org/10.1523/JNEUROSCI.1531-05.2005>.
- Moosmang, Sven, Peter Lenhardt, Nicole Haider, Franz Hofmann, and Jörg W. Wegener. 2005. "Mouse Models to Study L-Type Calcium Channel Function." *Pharmacology and Therapeutics* 106 (3): 347–55. <https://doi.org/10.1016/j.pharmthera.2004.12.003>.
- Morton, R.A., M.S. Norlin, C.C. Vollmer, and C.F. Valenzuela. 2013. "Characterization of L-Type Voltage-Gated Ca<sup>2+</sup> Channel Expression and Function in Developing CA3 Pyramidal Neurons." *Neuroscience* 238 (May): 59–70. <https://doi.org/10.1016/j.neuroscience.2013.02.008>.
- Naninck, Eva F.G., Lianne Hoeijmakers, Nefeli Kakava-Georgiadou, Astrid Meesters, Stanley E. Lazic, Paul J. Lucassen, and Aniko Korosi. 2015. "Chronic Early Life Stress Alters Developmental and Adult Neurogenesis and Impairs Cognitive Function in Mice." *Hippocampus* 25 (3): 309–28. <https://doi.org/10.1002/hipo.22374>.
- Nanou, Evanthia, and William A. Catterall. 2018. "Calcium Channels, Synaptic Plasticity, and Neuropsychiatric Disease." *Neuron*. <https://doi.org/10.1016/j.neuron.2018.03.017>.
- Nawreen, Nawshaba, Evelin M. Cotella, Rachel Morano, Parinaz Mahbod, Khushali S. Dalal, Maureen Fitzgerald, Susan Martelle, et al. 2020. "Chemogenetic Inhibition of Infralimbic Prefrontal Cortex Gabaergic Parvalbumin Interneurons Attenuates the Impact of Chronic Stress in Male Mice." *ENeuro* 7 (5). <https://doi.org/10.1523/ENEURO.0423-19.2020>.
- Nestler, Eric J, and Steven E Hyman. 2010. "Animal Models of Neuropsychiatric Disorders." *Nature Neuroscience* 13 (10): 1161–69. <https://doi.org/10.1038/nn.2647>.
- Norris, Christopher M, Shelley Halpain, and Thomas C Foster. 1998. "Reversal of Age-Related Alterations in Synaptic Plasticity by Blockade of L-Type Ca<sup>2+</sup> Channels." *The Journal of Neuroscience* 18 (9): 3171–79. <https://doi.org/10.1523/JNEUROSCI.18-09-03171.1998>.
- Obermair, Gerald J, Zsolt Szabo, Emmanuel Bourinet, and Bernhard E Flucher. 2004. "Differential Targeting of the L-Type Ca<sup>2+</sup> Channel Alpha 1C (CaV1.2) to Synaptic and Extrasynaptic Compartments in Hippocampal Neurons." *The European Journal of Neuroscience* 19 (8): 2109–22. <https://doi.org/10.1111/j.0953-816X.2004.03272.x>.
- Owen, Michael J. 2014. "New Approaches to Psychiatric Diagnostic Classification." *Neuron*. Cell Press. <https://doi.org/10.1016/j.neuron.2014.10.028>.
- Page, Chloe E., Ryan Shepard, Kelsey Heslin, and Laurence Coutellier. 2019. "Prefrontal Parvalbumin Cells Are Sensitive to Stress and Mediate Anxiety-Related Behaviors in Female Mice." *Scientific*

- Reports* 9 (1): 1–9. <https://doi.org/10.1038/s41598-019-56424-9>.
- Pasparakis, E, E Koiliari, C Zouraraki, E-M Tsapakis, P Roussos, S.G. Giakoumaki, and P Bitsios. 2015. “The Effects of the CACNA1C Rs1006737 A/G on Affective Startle Modulation in Healthy Males.” *European Psychiatry* 30 (4): 492–98. <https://doi.org/10.1016/j.eurpsy.2015.03.004>.
- Paulus, Frieder M., Johannes Bedenbender, Sören Krach, Martin Pyka, Axel Krug, Jens Sommer, Miriam Mette, et al. 2014. “Association of Rs1006737 in CACNA1C with Alterations in Prefrontal Activation and Fronto-Hippocampal Connectivity.” *Human Brain Mapping* 35 (4): 1190–1200. <https://doi.org/10.1002/hbm.22244>.
- Perlman, George, Arnaud Tanti, and Naguib Mechawar. 2021. “Parvalbumin Interneuron Alterations in Stress-Related Mood Disorders: A Systematic Review.” *Neurobiology of Stress*. Elsevier. <https://doi.org/10.1016/j.ynstr.2021.100380>.
- Perrier, E, F Pompei, G Ruberto, E Vassos, D Collier, and S Frangou. 2011. “Initial Evidence for the Role of CACNA1C on Subcortical Brain Morphology in Patients with Bipolar Disorder.” *European Psychiatry* 26 (3): 135–37. <https://doi.org/10.1016/j.eurpsy.2010.10.004>.
- Pignataro, Annabella, Antonella Borreca, Martine Ammassari-Teule, and Silvia Middei. 2015. “CREB Regulates Experience-Dependent Spine Formation and Enlargement in Mouse Barrel Cortex.” *Neural Plasticity* 2015. <https://doi.org/10.1155/2015/651469>.
- Pinares-Garcia, Paulo, Marielle Stratikopoulos, Alice Zagato, Hannah Loke, and Joohyung Lee. 2018. “Sex: A Significant Risk Factor for Neurodevelopmental and Neurodegenerative Disorders.” *Brain Sciences*. Multidisciplinary Digital Publishing Institute. <https://doi.org/10.3390/brainsci8080154>.
- Pitman, Kimberley A., Raphael Ricci, Robert Gasperini, Shannon Beasley, Macarena Pavez, Jac Charlesworth, Lisa Foa, and Kaylene M. Young. 2020. “The Voltage-Gated Calcium Channel CaV1.2 Promotes Adult Oligodendrocyte Progenitor Cell Survival in the Mouse Corpus Callosum but Not Motor Cortex.” *GLIA* 68 (2): 376–92. <https://doi.org/10.1002/glia.23723>.
- Procaccini, C., M. Maksimovic, T. Aitta-aho, E. R. Korpi, and A. M. Linden. 2013. “Reversal of Novelty-Induced Hyperlocomotion and Hippocampal c-Fos Expression in GluA1 Knockout Male Mice by the mGluR2/3 Agonist LY354740.” *Neuroscience* 250 (October): 189–200. <https://doi.org/10.1016/j.neuroscience.2013.07.010>.
- Prusator, D. K., and B. Greenwood-Van Meerveld. 2015. “Gender Specific Effects of Neonatal Limited Nesting on Viscerosomatic Sensitivity and Anxiety-like Behavior in Adult Rats.” *Neurogastroenterology and Motility* 27 (1): 72–81. <https://doi.org/10.1111/nmo.12472>.
- Radua, J, S A Surguladze, N Marshall, M Walshe, E Bramon, D A Collier, D P Prata, R M Murray, and C McDonald. 2013. “The Impact of CACNA1C Allelic Variation on Effective Connectivity during Emotional Processing in Bipolar Disorder.” *Molecular Psychiatry* 18 (5): 526–27. <https://doi.org/10.1038/mp.2012.61>.

- Raineki, Charlis, Millie Rincón Cortés, Laure Belnoue, and Regina M. Sullivan. 2012. "Effects of Early-Life Abuse Differ across Development: Infant Social Behavior Deficits Are Followed by Adolescent Depressive-Like Behaviors Mediated by the Amygdala." *Journal of Neuroscience* 32 (22): 7758–65. <https://doi.org/10.1523/JNEUROSCI.5843-11.2012>.
- Rajadhyaksha, Anjali, Amy Barczak, Wendy Macías, Jean Christophe Leveque, Susan E. Lewis, and Christine Konradi. 1999. "L-Type Ca<sup>2+</sup> Channels Are Essential for Glutamate-Mediated CREB Phosphorylation and c-Fos Gene Expression in Striatal Neurons." *Journal of Neuroscience* 19 (15): 6348–59. <https://doi.org/10.1523/jneurosci.19-15-06348.1999>.
- Ramasamy, Adaikalavan, Daniah Trabzuni, Sebastian Guelfi, Vibin Varghese, Colin Smith, Robert Walker, Tisham De, et al. 2014. "Genetic Variability in the Regulation of Gene Expression in Ten Regions of the Human Brain." *Nature Neuroscience* 17 (10): 1418–28. <https://doi.org/10.1038/nn.3801>.
- Ramos, André, and Pierre Mormède. 1997. "Stress and Emotionality: A Multidimensional and Genetic Approach." *Neuroscience and Biobehavioral Reviews* 22 (1): 33–57. [https://doi.org/10.1016/S0149-7634\(97\)00001-8](https://doi.org/10.1016/S0149-7634(97)00001-8).
- Redmond, Lori, Amir H. Kashani, and Anirvan Ghosh. 2002. "Calcium Regulation of Dendritic Growth via CaM Kinase IV and CREB-Mediated Transcription." *Neuron* 34 (6): 999–1010. [https://doi.org/10.1016/S0896-6273\(02\)00737-7](https://doi.org/10.1016/S0896-6273(02)00737-7).
- Reinwald, Jonathan Rochus, Robert Becker, Anne Stephanie Mallien, Claudia Falfan-Melgoza, Markus Sack, Christian Clemm von Hohenberg, Urs Braun, et al. 2018. "Neural Mechanisms of Early-Life Social Stress as a Developmental Risk Factor for Severe Psychiatric Disorders." *Biological Psychiatry* 84 (2): 116–28. <https://doi.org/10.1016/j.biopsych.2017.12.010>.
- Rice, Courtney J, Curt A Sandman, Mohammed R Lenjavi, and Tallie Z Baram. 2008. "A Novel Mouse Model for Acute and Long-Lasting Consequences of Early Life Stress." *Endocrinology* 149 (10): 4892–4900. <https://doi.org/10.1210/en.2008-0633>.
- Rincón-Cortés, Millie, and Regina M. Sullivan. 2014. "Early Life Trauma and Attachment: Immediate and Enduring Effects on Neurobehavioral and Stress Axis Development." *Frontiers in Endocrinology*. Frontiers Media SA. <https://doi.org/10.3389/fendo.2014.00033>.
- Rossignol, E. 2011. "Genetics and Function of Neocortical GABAergic Interneurons in Neurodevelopmental Disorders." *Neural Plasticity*. Hindawi Publishing Corporation. <https://doi.org/10.1155/2011/649325>.
- Rotaru, Diana C., David A. Lewis, and Guillermo Gonzalez-Burgos. 2012. "The Role of Glutamatergic Inputs onto Parvalbumin-Positive Interneurons: Relevance for Schizophrenia." *Reviews in the Neurosciences*. Rev Neurosci. <https://doi.org/10.1515/revneuro-2011-0059>.
- Ruden, Jacob B., Laura L. Dugan, and Christine Konradi. 2020. "Parvalbumin Interneuron Vulnerability and Brain Disorders." *Neuropsychopharmacology*. Springer Nature. <https://doi.org/10.1038/s41386->

020-0778-9.

- Sánchez, M. Mar, Charlotte O. Ladd, and Paul M. Plotsky. 2001. "Early Adverse Experience as a Developmental Risk Factor for Later Psychopathology: Evidence from Rodent and Primate Models." *Development and Psychopathology* 13 (3): 419–49. <https://doi.org/10.1017/S0954579401003029>.
- Sarkar, Saumyendra N., Ren Qi Huang, Shaun M. Logan, Don Yi Kun, Glenn H. Dillon, and James W. Simpkins. 2008. "Estrogens Directly Potentiate Neuronal L-Type Ca<sup>2+</sup> Channels." *Proceedings of the National Academy of Sciences of the United States of America* 105 (39): 15148–53. <https://doi.org/10.1073/pnas.0802379105>.
- Schlick, B., B.E. Flucher, and G.J. Obermair. 2010. "Voltage-Activated Calcium Channel Expression Profiles in Mouse Brain and Cultured Hippocampal Neurons." *Neuroscience* 167 (3): 786–98. <https://doi.org/10.1016/j.neuroscience.2010.02.037>.
- Schmitt, Andrea, Berend Malchow, Alkomiet Hasan, and Peter Falkai. 2014. "The Impact of Environmental Factors in Severe Psychiatric Disorders." *Frontiers in Neuroscience*. Frontiers Media SA. <https://doi.org/10.3389/fnins.2014.00019>.
- Servili, Evrim, Michael Trus, Daphne Maayan, and Daphne Atlas. 2018. "β-Subunit of the Voltage-Gated Ca<sup>2+</sup> Channel Cav1.2 Drives Signaling to the Nucleus via H-Ras." *Proceedings of the National Academy of Sciences of the United States of America* 115 (37): E8624–33. <https://doi.org/10.1073/pnas.1805380115>.
- Servili, Evrim, Michael Trus, Julia Sajman, Eilon Sherman, and Daphne Atlas. 2020. "Elevated Basal Transcription Can Underlie Timothy Channel Association with Autism Related Disorders." *Progress in Neurobiology* 191 (August): 101820. <https://doi.org/10.1016/j.pneurobio.2020.101820>.
- Shansky, Rebecca M, and Catherine S. Woolley. 2016. "Considering Sex as a Biological Variable Will Be Valuable for Neuroscience Research." *Journal of Neuroscience* 36 (47): 11817–22. <https://doi.org/10.1523/JNEUROSCI.1390-16.2016>.
- Shi, Dong Dong, Ying Dan Zhang, Yan Yan Ren, Shi Yu Peng, Ti Fei Yuan, and Zhen Wang. 2021. "Predictable Maternal Separation Confers Adult Stress Resilience via the Medial Prefrontal Cortex Oxytocin Signaling Pathway in Rats." *Molecular Psychiatry*, September, 1–12. <https://doi.org/10.1038/s41380-021-01293-w>.
- Shibasaki, Masahiro, Kazuhiro Kurokawa, and Seitaro Ohkuma. 2010. "Upregulation of L-Type Cav1 Channels in the Development of Psychological Dependence." *Synapse* 64 (6): 440–44. <https://doi.org/10.1002/syn.20745>.
- Singewald, Nicolas. 2007. "Altered Brain Activity Processing in High-Anxiety Rodents Revealed by Challenge Paradigms and Functional Mapping." *Neuroscience and Biobehavioral Reviews*. <https://doi.org/10.1016/j.neubiorev.2006.02.003>.
- Sinnegger-Brauns, Martina J., Alfred Hetzenauer, Irene G. Huber, Erik Renström, Georg Wietzorrek,

- Stanislav Berjukov, Maurizio Cavalli, et al. 2004. "Isoform-Specific Regulation of Mood Behavior and Pancreatic  $\beta$  Cell and Cardiovascular Function by L-Type  $\text{Ca}^{2+}$  Channels." *Journal of Clinical Investigation* 113 (10): 1430–39. <https://doi.org/10.1172/JCI20208>.
- Smoller, Jordan W., Ole A. Andreassen, Howard J. Edenberg, Stephen V. Faraone, Stephen J. Glatt, and Kenneth S. Kendler. 2019. "Psychiatric Genetics and the Structure of Psychopathology." *Molecular Psychiatry*. Nature Publishing Group. <https://doi.org/10.1038/s41380-017-0010-4>.
- Smoller, Jordan W., Kenneth Kendler, Nicholas Craddock, Phil Hyoun Lee, Benjamin M. Neale, John N. Nurnberger, Stephan Ripke, et al. 2013. "Identification of Risk Loci with Shared Effects on Five Major Psychiatric Disorders: A Genome-Wide Analysis." *The Lancet* 381 (9875): 1371–79. [https://doi.org/10.1016/S0140-6736\(12\)62129-1](https://doi.org/10.1016/S0140-6736(12)62129-1).
- Sobanski, Esther. 2006. "Psychiatric Comorbidity in Adults with Attention-Deficit/Hyperactivity Disorder (ADHD)." *European Archives of Psychiatry and Clinical Neuroscience* 256:1 256 (1): i26–31. <https://doi.org/10.1007/S00406-006-1004-4>.
- Soeiro-de-Souza, M. G., D. S. Bio, V. V. Dias, E. Vieta, R. Machado-Vieira, and R. A. Moreno. 2013. "The CACNA1C Risk Allele Selectively Impacts on Executive Function in Bipolar Type I Disorder." *Acta Psychiatrica Scandinavica* 128 (5): 362–69. <https://doi.org/10.1111/acps.12073>.
- Soeiro-de-Souza, M G, B Lafer, R A Moreno, F G Nery, T Chile, K Chaim, C da Costa Leite, R Machado-Vieira, M C G Otaduy, and H Vallada. 2017. "The CACNA1C Risk Allele Rs1006737 Is Associated with Age-Related Prefrontal Cortical Thinning in Bipolar I Disorder." *Translational Psychiatry* 7 (4): e1086. <https://doi.org/10.1038/tp.2017.57>.
- Soeiro-de-Souza, Márcio Gerhardt, Maria Concepción Garcia Otaduy, Carolina Zadres Dias, Danielle S Bio, Rodrigo Machado-Vieira, and Ricardo Alberto Moreno. 2012. "The Impact of the CACNA1C Risk Allele on Limbic Structures and Facial Emotions Recognition in Bipolar Disorder Subjects and Healthy Controls." *Journal of Affective Disorders* 141 (1): 94–101. <https://doi.org/10.1016/j.jad.2012.03.014>.
- Sotnikova, Tatyana D., Evgeniya V. Efimova, and Raul R. Gainetdinov. 2020. "Enhanced Dopamine Transmission and Hyperactivity in the Dopamine Transporter Heterozygous Mice Lacking the D3 Dopamine Receptor." *International Journal of Molecular Sciences* 21 (21): 1–11. <https://doi.org/10.3390/ijms21218216>.
- Splawski, Igor, Katherine W Timothy, Niels Decher, Pradeep Kumar, Frank B Sachse, Alan H Beggs, Michael C Sanguinetti, and Mark T Keating. 2005. "Severe Arrhythmia Disorder Caused by Cardiac L-Type Calcium Channel Mutations." *Proceedings of the National Academy of Sciences* 102 (23): 8089–96. <https://doi.org/10.1073/pnas.0502506102>.
- Splawski, Igor, Katherine W Timothy, Leah M Sharpe, Niels Decher, Pradeep Kumar, Raffaella Bloise, Carlo Napolitano, et al. 2004. "CaV1.2 Calcium Channel Dysfunction Causes a Multisystem Disorder

- Including Arrhythmia and Autism.” *Cell* 119 (1): 19–31. <https://doi.org/10.1016/j.cell.2004.09.011>.
- Stahl, Eli A., Gerome Breen, Andreas J. Forstner, Andrew McQuillin, Stephan Ripke, Vassily Trubetsky, Manuel Mattheisen, et al. 2019. “Genome-Wide Association Study Identifies 30 Loci Associated with Bipolar Disorder.” *Nature Genetics* 51 (5): 793–803. <https://doi.org/10.1038/s41588-019-0397-8>.
- Sumner, Jennifer A., Margaret A. Sheridan, Stacy S. Drury, Kyle C. Esteves, Kate Walsh, Karestan C. Koenen, and Katie A. McLaughlin. 2015. “Variation in CACNA1C Is Associated with Amygdala Structure and Function in Adolescents.” *Journal of Child and Adolescent Psychopharmacology* 25 (9): 701–10. <https://doi.org/10.1089/cap.2015.0047>.
- Suwalska, Aleksandra, and Dorota Łojko. 2014. “Sex Dependence of Cognitive Functions in Bipolar Disorder.” *The Scientific World Journal* 2014. <https://doi.org/10.1155/2014/418432>.
- Sykes, Lucy, Josephine Haddon, Thomas M Lancaster, Arabella Sykes, Karima Azzouni, Niklas Ihssen, Anna L Moon, et al. 2018. “Genetic Variation in the Psychiatric Risk Gene CACNA1C Modulates Reversal Learning Across Species.” *Schizophrenia Bulletin*, October. <https://doi.org/10.1093/schbul/sby146>.
- Takahashi, Aki. 2021. “Toward Understanding the Sex Differences in the Biological Mechanism of Social Stress in Mouse Models.” *Frontiers in Psychiatry* 12 (February): 139. <https://doi.org/10.3389/fpsy.2021.644161>.
- Takeuchi, Hikaru, Hiroaki Tomita, Yasuyuki Taki, Yoshie Kikuchi, Chiaki Ono, Zhiqian Yu, Rui Nouchi, et al. 2018. “A Common CACNA1C Gene Risk Variant Has Sex-Dependent Effects on Behavioral Traits and Brain Functional Activity.” *Cerebral Cortex*, August. <https://doi.org/10.1093/cercor/bhy189>.
- Tannenbaum, Cara, and Patricia Boksa. 2019. “Sex: A Key Consideration in Understanding the Etiology of Psychiatric Disorders and Improving Treatment.” *Journal of Psychiatry and Neuroscience*. *Journal of Psychiatry and Neuroscience*. <https://doi.org/10.1503/jpn.190165>.
- Tatsukawa, Tetsuya, Matthieu Raveau, Ikuo Ogiwara, Satoko Hattori, Hiroyuki Miyamoto, Emi Mazaki, Shigeyoshi Itoharu, Tsuyoshi Miyakawa, Mauricio Montal, and Kazuhiro Yamakawa. 2019. “Scn2a Haploinsufficient Mice Display a Spectrum of Phenotypes Affecting Anxiety, Sociability, Memory Flexibility and Ampakine CX516 Rescues Their Hyperactivity.” *Molecular Autism* 10 (1): 1–15. <https://doi.org/10.1186/s13229-019-0265-5>.
- Teegarden, Sarah. 2012. “Behavioral Phenotyping in Rats and Mice.” *Materials and Methods* 2 (June). <https://doi.org/10.13070/mm.en.2.122>.
- Temme, Stephanie J., and Geoffrey G. Murphy. 2017. “The L-Type Voltage-Gated Calcium Channel Ca<sub>v</sub>1.2 Mediates Fear Extinction and Modulates Synaptic Tone in the Lateral Amygdala.” *Learning & Memory* 24 (11): 580–88. <https://doi.org/10.1101/lm.045773.117>.
- Temme, Stephanie J, Ryan Z Bell, Grace L Fisher, and Geoffrey G Murphy. 2016. “Deletion of the Mouse

- Homolog of CACNA1C Disrupts Discrete Forms of Hippocampal-Dependent Memory and Neurogenesis within the Dentate Gyrus.” *ENeuro* 3 (6). <https://doi.org/10.1523/ENEURO.0118-16.2016>.
- Terrillion, C E, D T Dao, R Cachope, M K Lobo, A C Puche, J F Cheer, and T D Gould. 2017. “Reduced Levels of Cacna1c Attenuate Mesolimbic Dopamine System Function.” *Genes, Brain and Behavior* 16 (5): 495–505. <https://doi.org/10.1111/gbb.12371>.
- Terrillion, Chantelle E., T. Chase Francis, Adam C. Puche, Mary Kay Lobo, and Todd D. Gould. 2017. “Decreased Nucleus Accumbens Expression of Psychiatric Disorder Risk Gene Cacna1c Promotes Susceptibility to Social Stress.” *International Journal of Neuropsychopharmacology* 20 (5): 428–33. <https://doi.org/10.1093/ijnp/pyw112>.
- Tesli, Martin, Kristina C. Skatun, Olga Therese Ousdal, Andrew Anand Brown, Christian Thoresen, Ingrid Agartz, Ingrid Melle, Srdjan Djurovic, Jimmy Jensen, and Ole A. Andreassen. 2013. “CACNA1C Risk Variant and Amygdala Activity in Bipolar Disorder, Schizophrenia and Healthy Controls.” Edited by Hossein Fatemi. *PLoS ONE* 8 (2): e56970. <https://doi.org/10.1371/journal.pone.0056970>.
- Thimm, M, T Kircher, T Kellermann, V Markov, S Krach, A Jansen, K Zerres, et al. 2011. “Effects of a CACNA1C Genotype on Attention Networks in Healthy Individuals.” *Psychological Medicine* 41 (07): 1551–61. <https://doi.org/10.1017/S0033291710002217>.
- Tomasella, Eugenia, Lucila Bechelli, Mora Belén Ogando, Camilo Mininni, Mariano N. Di Guilmi, Fernanda De Fino, Silvano Zanutto, Ana Belén Elgoyhen, Antonia Marin-Burgin, and Diego M. Gelman. 2018. “Deletion of Dopamine D2 Receptors from Parvalbumin Interneurons in Mouse Causes Schizophrenialike Phenotypes.” *Proceedings of the National Academy of Sciences of the United States of America* 115 (13): 3476–81. <https://doi.org/10.1073/pnas.1719897115>.
- Uhrig, Stefanie, David Vandael, Andrea Marcantoni, Nina Dedic, Ainhoa Bilbao, Miriam A Vogt, Natalie Hirth, et al. 2017. “Differential Roles for L-Type Calcium Channel Subtypes in Alcohol Dependence.” *Neuropsychopharmacology* 42 (5): 1058–69. <https://doi.org/10.1038/npp.2016.266>.
- Veng, Lone M., Michael H. Mesches, and Michael D. Browning. 2003. “Age-Related Working Memory Impairment Is Correlated with Increases in the L-Type Calcium Channel Protein A1D (Cav1.3) in Area CA1 of the Hippocampus and Both Are Ameliorated by Chronic Nimodipine Treatment.” *Molecular Brain Research* 110 (2): 193–202. [https://doi.org/10.1016/S0169-328X\(02\)00643-5](https://doi.org/10.1016/S0169-328X(02)00643-5).
- Viguera, A. C., L. Tondo, and R. J. Baldessarini. 2000. “Sex Differences in Response to Lithium Treatment.” *American Journal of Psychiatry* 157 (9): 1509–11. <https://doi.org/10.1176/appi.ajp.157.9.1509>.
- Völkening, Bianca, Kai Schönig, Golo Kronenberg, Dusan Bartsch, and Tillmann Weber. 2017. “Deletion of Psychiatric Risk Gene Cacna1c Impairs Hippocampal Neurogenesis in Cell-Autonomous Fashion.” *Glia* 65 (5): 817–27. <https://doi.org/10.1002/glia.23128>.

- Walker, Claire Dominique, Kevin G Bath, Marian Joels, Aniko Korosi, Muriel Larauche, Paul J Lucassen, Margaret J Morris, et al. 2017. "Chronic Early Life Stress Induced by Limited Bedding and Nesting (LBN) Material in Rodents: Critical Considerations of Methodology, Outcomes and Translational Potential." *Stress*. NIH Public Access. <https://doi.org/10.1080/10253890.2017.1343296>.
- Wang, Fei, Andrew M McIntosh, Yong He, Joel Gelernter, and Hilary P Blumberg. 2011. "The Association of Genetic Variation in CACNA1C with Structure and Function of a Frontotemporal System." *Bipolar Disorders* 13 (7–8): 696–700. <https://doi.org/10.1111/j.1399-5618.2011.00963.x>.
- Wang, Xiao-Dong, Christiana Labermaier, Florian Holsboer, Wolfgang Wurst, Jan M. Deussing, Marianne B. Müller, and Mathias V. Schmidt. 2012. "Early-Life Stress-Induced Anxiety-Related Behavior in Adult Mice Partially Requires Forebrain Corticotropin-Releasing Hormone Receptor 1." *European Journal of Neuroscience* 36 (3): 2360–67. <https://doi.org/10.1111/j.1460-9568.2012.08148.x>.
- Wang, Xiao Dong, Gerhard Rammes, Igor Kraev, Miriam Wolf, Claudia Liebl, Sebastian H. Scharf, Courtney J. Rice, et al. 2011. "Forebrain CRF1 Modulates Early-Life Stress-Programmed Cognitive Deficits." *Journal of Neuroscience* 31 (38): 13625–34. <https://doi.org/10.1523/JNEUROSCI.2259-11.2011>.
- Wang, Xiaoting, David A. Gallegos, Vladimir M. Pogorelov, Justin K. O'Hare, Nicole Calakos, William C. Wetsel, and Anne E. West. 2018. "Parvalbumin Interneurons of the Mouse Nucleus Accumbens Are Required for Amphetamine-Induced Locomotor Sensitization and Conditioned Place Preference." *Neuropsychopharmacology* 43 (5): 953–63. <https://doi.org/10.1038/npp.2017.178>.
- Wang, Xinshuang, Hironao Saegusa, Soontaraporn Huntula, and Tsutomu Tanabe. 2019. "Blockade of Microglial Cav1.2 Ca<sup>2+</sup> Channel Exacerbates the Symptoms in a Parkinson's Disease Model." *Scientific Reports* 9 (1). <https://doi.org/10.1038/s41598-019-45681-3>.
- Warren, Brandon L., and Leslie R. Whitaker. 2018. "Parvalbumin-Expressing Neurons in the Nucleus Accumbens: A New Player in Amphetamine Sensitization and Reward." *Neuropsychopharmacology*. Nature Publishing Group. <https://doi.org/10.1038/npp.2017.256>.
- Wendel, Kara M., Annabel K. Short, Brenda P. Noarbe, Elizabeth Haddad, Anton M. Palma, Michael A. Yassa, Tallie Z. Baram, and Andre Obenaus. 2021. "Early Life Adversity in Male Mice Sculpt Reward Circuits." *Neurobiology of Stress* 15 (November): 100409. <https://doi.org/10.1016/j.ynstr.2021.100409>.
- Werling, Donna M, and Daniel H Geschwind. 2013. "Sex Differences in Autism Spectrum Disorders." *Current Opinion in Neurology*. NIH Public Access. <https://doi.org/10.1097/WCO.0b013e32835ee548>.
- Wessa, M, J Linke, S H Witt, V Nieratschker, C Esslinger, P Kirsch, O Grimm, et al. 2010. "The CACNA1C Risk Variant for Bipolar Disorder Influences Limbic Activity." *Molecular Psychiatry* 15 (12): 1126–27. <https://doi.org/10.1038/mp.2009.103>.

- Wheeler, Damian G., Curtis F. Barrett, Rachel D. Groth, Parsa Safa, and Richard W. Tsien. 2008. "CaMKII Locally Encodes L-Type Channel Activity to Signal to Nuclear CREB in Excitation - Transcription Coupling." *Journal of Cell Biology* 183 (5): 849–63. <https://doi.org/10.1083/jcb.200805048>.
- White, J. A., B. C. McKinney, M. C. John, P. A. Powers, T. J. Kamp, and G. G. Murphy. 2008. "Conditional Forebrain Deletion of the L-Type Calcium Channel CaV1.2 Disrupts Remote Spatial Memories in Mice." *Learning & Memory* 15 (1): 1–5. <https://doi.org/10.1101/lm.773208>.
- Wiedholz, L. M., W. A. Owens, R. E. Horton, M. Feyder, R. M. Karlsson, K. Hefner, R. Sprengel, T. Celikel, L. C. Daws, and A. Holmes. 2008. "Mice Lacking the AMPA GluR1 Receptor Exhibit Striatal Hyperdopaminergia and 'schizophrenia-Related' Behaviors." *Molecular Psychiatry* 13 (6): 631–40. <https://doi.org/10.1038/sj.mp.4002056>.
- Wolf, Claudia, Holger Mohr, Thomas Schneider-Axmann, Andreas Reif, Thomas Wobrock, Harald Scherk, Susanne Kraft, Andrea Schmitt, Peter Falkai, and Oliver Gruber. 2014. "CACNA1C Genotype Explains Interindividual Differences in Amygdala Volume among Patients with Schizophrenia." *European Archives of Psychiatry and Clinical Neuroscience* 264 (2): 93–102. <https://doi.org/10.1007/s00406-013-0427-y>.
- Wong-Riley, Margaret T.T. 2021. "The Critical Period: Neurochemical and Synaptic Mechanisms Shared by the Visual Cortex and the Brain Stem Respiratory System." *Proceedings of the Royal Society B: Biological Sciences*. The Royal Society. <https://doi.org/10.1098/rspb.2021.1025>.
- Woon, Puay San, Min Yi Sum, Carissa Nadia Kuswanto, Guo Liang Yang, Yih Yian Sitoh, Tuck Wah Soong, Tih Shih Lee, Wieslaw Lucjan Nowinski, and Kang Sim. 2014. "CACNA1C Genomewide Supported Psychosis Genetic Variation Affects Cortical Brain White Matter Integrity in Chinese Patients With Schizophrenia." *The Journal of Clinical Psychiatry* 75 (11): e1284–90. <https://doi.org/10.4088/JCP.13m08777>.
- Xia, Lu, Kun Xia, Daniel Weinberger, and Fengyu Zhang. 2019. "Common Genetic Variants Shared among Five Major Psychiatric Disorders: A Large-Scale Genome-Wide Combined Analysis." *Global Clinical and Translational Research*, March, 21–30. <https://doi.org/10.36316/gcatr.01.0003>.
- Xu, Meng Yi, and Albert H.C. Wong. 2018. "GABAergic Inhibitory Neurons as Therapeutic Targets for Cognitive Impairment in Schizophrenia." *Acta Pharmacologica Sinica*. Nature Publishing Group. <https://doi.org/10.1038/aps.2017.172>.
- Yang, Albert C., and Shih Jen Tsai. 2017. "New Targets for Schizophrenia Treatment beyond the Dopamine Hypothesis." *International Journal of Molecular Sciences*. MDPI AG. <https://doi.org/10.3390/ijms18081689>.
- Yao, Xueming, Joseph T. Glessner, Junyi Li, Xiaohui Qi, Xiaoyuan Hou, Chonggui Zhu, Xiaoge Li, et al. 2021. "Integrative Analysis of Genome-Wide Association Studies Identifies Novel Loci Associated with Neuropsychiatric Disorders." *Translational Psychiatry* 11 (1): 1–12.

- <https://doi.org/10.1038/s41398-020-01195-5>.
- Yen, Yi Chun, Elmira Anderzhanova, Mirjam Bunck, Julia Schuller, Rainer Landgraf, and Carsten T. Wotjak. 2013. “Co-Segregation of Hyperactivity, Active Coping Styles, and Cognitive Dysfunction in Mice Selectively Bred for Low Levels of Anxiety.” *Frontiers in Behavioral Neuroscience* 0 (AUG): 103. <https://doi.org/10.3389/FNBEH.2013.00103/BIBTEX>.
- Yoshimizu, T., J. Q. Pan, A. E. Mungenast, J. M. Madison, S. Su, J. Ketterman, D. Ongur, et al. 2015. “Functional Implications of a Psychiatric Risk Variant within CACNA1C in Induced Human Neurons.” *Molecular Psychiatry* 20 (2): 162–69. <https://doi.org/10.1038/mp.2014.143>.
- Zamora, Norma N., Veronica T. Cheli, Diara A. Santiago González, Rensheng Wan, and Pablo M. Paez. 2020. “Deletion of Voltage-Gated Calcium Channels in Astrocytes during Demyelination Reduces Brain Inflammation and Promotes Myelin Regeneration in Mice.” *Journal of Neuroscience* 40 (17): 3332–47. <https://doi.org/10.1523/JNEUROSCI.1644-19.2020>.
- Zanos, Panos, Shambhu Bhat, Chantelle E. Terrillion, Robert J. Smith, Leonardo H. Tonelli, and Todd D. Gould. 2015. “Sex-Dependent Modulation of Age-Related Cognitive Decline by the L-Type Calcium Channel Gene *Cacna1c* (Ca v 1.2).” *European Journal of Neuroscience* 42 (8): 2499–2507. <https://doi.org/10.1111/ejn.12952>.
- Zhang, Sheng-Yu, Qiang Hu, Tao Tang, Chao Liu, Cheng-Chong Li, Xiao-Guang Yang, Yin-Yin Zang, and Wei-Xiong Cai. 2017. “Role of CACNA1C Gene Polymorphisms and Protein Expressions in the Pathogenesis of Schizophrenia: A Case-Control Study in a Chinese Population.” *Neurological Sciences* 38 (8): 1393–1403. <https://doi.org/10.1007/s10072-017-2963-0>.
- Zhang, Xu, Chen Zhang, Zhiguo Wu, Zuwei Wang, Daihui Peng, Jun Chen, Wu Hong, et al. 2013. “Association of Genetic Variation in CACNA1C with Bipolar Disorder in Han Chinese.” *Journal of Affective Disorders* 150 (2): 261–65. <https://doi.org/10.1016/j.jad.2013.04.004>.
- Zhang, Zhifang, Yanyan Wang, Qiumei Zhang, Wan Zhao, Xiongying Chen, Jinguo Zhai, Min Chen, et al. 2018. “The Effects of CACNA1C Gene Polymorphism on Prefrontal Cortex in Both Schizophrenia Patients and Healthy Controls.” *Schizophrenia Research* 0 (0). <https://doi.org/10.1016/j.schres.2018.09.007>.
- Zheng, Fanfan, Yue Cui, Hao Yan, Bing Liu, and Tianzi Jiang. 2016. “The Effects of a Genome-Wide Supported Variant in the CACNA1C Gene on Cortical Morphology in Schizophrenia Patients and Healthy Subjects.” *Scientific Reports* 6 (1): 34298. <https://doi.org/10.1038/srep34298>.
- Zheng, Fanfan, Yanling Zhang, Wuxiang Xie, Wenqiang Li, Chao Jin, Weifeng Mi, Fang Wang, et al. 2014. “Further Evidence for Genetic Association of CACNA1C and Schizophrenia: New Risk Loci in a Han Chinese Population and a Meta-Analysis.” *Schizophrenia Research* 152 (1): 105–10. <https://doi.org/10.1016/j.schres.2013.12.003>.
- Zhu, Shanshan, Zachary A. Cordner, Jiali Xiong, Chi Tso Chiu, Arabiye Artola, Yanning Zuo, Andrew D.

Nelson, et al. 2017. “Genetic Disruption of Ankyrin-G in Adult Mouse Forebrain Causes Cortical Synapse Alteration and Behavior Reminiscent of Bipolar Disorder.” *Proceedings of the National Academy of Sciences of the United States of America* 114 (39): 10479–84. <https://doi.org/10.1073/pnas.1700689114>.

## List of figures

Figure 1: Global prevalence of mental disorders.....	1
Figure 2: Shared symptomology across various psychiatric disorders.....	2
Figure 3: Structure of a voltage gated calcium channel.....	8
Figure 4: Expression of $Ca_v1.2$ calcium channels.....	9
Figure 5: Signaling cascades downstream of $Ca_v1.2$ channels.....	10
Figure 6: Gene $\times$ environment interaction contributes to etiology of psychiatric disorders.....	14
Figure 7: Different types of early life stress paradigms used in rodents.....	15
Figure 8: Mouse models used in this study.....	28
Figure 9: Tamoxifen administration via food or intraperitoneal injection.....	30
Figure 10: Limited bedding and nesting stress.....	30
Figure 11: Estrous cycle determination.....	31
Figure 12: Open field apparatus.....	33
Figure 13: Elevated plus maze apparatus.....	33
Figure 14: Light/ dark box apparatus.....	34
Figure 15: Three-chambered social interaction test.....	35
Figure 16: Novel object recognition task.....	36
Figure 17: Y maze apparatus.....	37
Figure 18: Novel (top) and spatial (bottom) object recognition in Y maze apparatus.....	38
Figure 19: Morris water maze.....	39
Figure 20: Sucrose preference test.....	40
Figure 21: Forced swim test.....	41
Figure 22: 20 selected brain regions for cFos positive cell quantification.....	46
Figure 23: Limited bedding and nesting paradigm (LBN).....	49
Figure 24: Assessment of locomotor activity and anxiety-related behavior after the LBN stress in male and female $Ca_v1.2$ -Nex animals.....	50
Figure 25: Assessment of anxiety-related behavior in $Ca_v1.2$ -Nex mice following the LBN stress in LDB test.....	52
Figure 26: Assessment of anxiety-related behavior in $Ca_v1.2$ -Nex mice after the LBN stress in the EPM test.....	53
Figure 27: Effect of LBN on social interaction in $Ca_v1.2$ -Nex mice.....	55
Figure 28: Effects of LBN stress on object recognition in $Ca_v1.2$ -Nex mice.....	57

---

Figure 29: Effects of LBN stress on depression-related behavior in Ca <sub>v</sub> 1.2-Nex mice .....	59
Figure 30: Characterization of anxiety-related behavior of Nex-Cre males.....	60
Figure 31: Characterization of anxiety-related behavior of Nex-Cre females.....	61
Figure 32: Characterization of cognitive performance of Nex-Cre males.....	62
Figure 33: Characterization of cognitive performance of Nex-Cre females.....	63
Figure 34: Characterization of social behavior of Nex-Cre male and female mice.....	64
Figure 35: Characterization of Nex-Cre mice in the forced swim test .....	65
Figure 36: Evaluation of dendritic complexity in unstressed and stressed female Ca <sub>v</sub> 1.2-Nex mice. .....	67
Figure 37: Western blot analysis of pCREB expression in hippocampal and PFC tissues in male and female mice. ....	68
Figure 38: Example of different stages of estrous cycle in Ctrl and CKO mice .....	69
Figure 39: Female Ca <sub>v</sub> 1.2-Nex CKO mice show hyperlocomotion and increased anxiety-related behavior in the OFT but normal basal activity .....	70
Figure 40: Female Ca <sub>v</sub> 1.2-Nex CKO mice show increased anxiety-related behavior in EPM but not LDB .....	71
Figure 41: Characterization of cognitive performance of female Ca <sub>v</sub> 1.2-Nex mice .....	74
Figure 42: Ca <sub>v</sub> 1.2-Nex CKO mice exhibit spatial memory deficits .....	75
Figure 43: Ca <sub>v</sub> 1.2-Nex female CKO mice showed enhanced active stress coping behavior .....	76
Figure 44: Dendritic branching complexity, spine density and pCREB expression in Ca <sub>v</sub> 1.2-Nex female mice.....	77
Figure 45: minPROFILER assay .....	78
Figure 46: Validation of Ca <sub>v</sub> 1.2-Gad2-CreER <sup>T2</sup> animals following tamoxifen administration ....	80
Figure 47: Validation of Ca <sub>v</sub> 1.2-PV mouse line .....	81
Figure 48: Ca <sub>v</sub> 1.2-PV CKO mice show normal exploratory but anxiogenic behavior.....	82
Figure 49: Assessment of social behavior in Ca <sub>v</sub> 1.2-PV mice .....	83
Figure 50: Assessment of cognitive performance of Ca <sub>v</sub> 1.2-PV mice .....	85
Figure 51: Ca <sub>v</sub> 1.2-PV CKO mice showed passive stress coping behavior.....	86
Figure 52: Stress coping strategies in Ca <sub>v</sub> 1.2-Nex and Ca <sub>v</sub> 1.2-PV mice.....	87
Figure 53: Representative images of cFos expression in different brain regions .....	87
Figure 54: Quantification of cFos positive cells in different brain regions .....	88

---

## List of tables

Table 1: Summary of reported single nucleotide polymorphisms (SNPs) of <i>CACNA1C</i> and the phenotypes (observed in healthy controls and patients) associated with them.....	5
Table 2: Summary of different animal models of Ca <sub>v</sub> 1.2.....	20
Table 3: Primers used for genotyping the different transgenic mouse lines.....	29
Table 4: Various stages of the estrous cycles and their characteristic features .....	32
Table 5: List of primary and secondary antibodies used for western blot and immunofluorescence experiments.....	44
Table 6: Genotypes of the animals that were used for behavioral testing following the LBN stress. .....	48

## Abbreviations

3CT	Three-chambered social interaction test
AAV	Adeno-associated viruses
A $\beta$	Amyloid beta
ADHD	Attention deficit hyperactivity disorder
AKAP	A-kinase anchoring protein
AMPA	$\alpha$ -amino-3-hydroxy-5-methyl-4-isoxazole propionic acid
Amyg	Amygdala
ANOVA	Analysis of variance
ASD	Autism spectrum disorders
BD	Bipolar disorder
BDNF	Brain-derived neurotrophic factor
BIC	Bicuculline
BLA	Basolateral amygdala
BNST	Bed nucleus of stria terminalis
BSA	Bovine serum albumin
CAMKII	Ca <sup>2+</sup> /calmodulin-dependent protein kinase II
cAMP	Cyclic adenosine monophosphate
CaN	Calcineurin
CeA	Central amygdala
Cg1	Cingulate cortex 1
CKO	Conditional knockout animals
CNS	Central nervous system
CPu	Caudate putamen
CREB	cAMP responsive element binding protein
Cre	cAMP responsive element
CRH	Corticotropin releasing hormone
CRHR1	Corticotropin releasing hormone receptor 1
Ctrl	Control animals
D	Diestrous
DAPI	4',6-diamidino-2-phenylindole
DG	Dentate gyrus

---

DHP	Dihydropyridine
DIV	Days in vitro
D1R	Dopamine receptor D1
DNA	Deoxy ribonucleic acid
DSM	Diagnostic and statistical manual of mental disorders
E	Estrous
E-T	Excitation-transcription
E/I	Excitatory/ inhibitory
ELS	Early life stress
EPM	Elevated plus maze
ERK	Extracellular signal-regulated kinase
GABA	Gamma-aminobutyric acid
Gad	Glutamic acid decarboxylase
GFAP	Glial fibrillary acidic protein
GluA1	Glutamate receptor 1
GP	Globus pallidus
GWAS	Genome wide association studies
HA	Hemagglutinin
HEK	Human embryonic kidney cells
HP	Hippocampus
HPA	Hypothalamus-pituitary-adrenal axis
HVA	High voltage activated
ICD	International classification of diseases
IL	Infralimbic cortex
ITI	Intertrial interval
LA	Lateral amygdala
LBN	Limited bedding and nesting stress paradigm
LDB	Light/dark box
LHbN	Lateral habenular nucleus
LS	Lateral septum
LTCC	L-type voltage gated calcium channels
LTD	Long term depression

---

LTP	Long term potentiation
LVA	Low voltage activated
M	Metestrous
M1	Primary motor cortex
M2	Secondary motor cortex
MAPK	Mitogen-activated protein kinase
MD	Major depression
mRNA	Messenger ribonucleic acid
MWM	Morris water maze
NAc	Nucleus accumbens
NE	Northeast
NFAT	Nuclear factor of activated T-cells
NGS	Normal goat serum
NIH	National institute of health
NMDA	N-methyl-D-aspartate
NMDAR	N-methyl-D-aspartate receptors
NOR	Novel object recognition
NW	Northwest
OFT	Open field test
OPC	Oligodendrocyte progenitor cells
P	Proestrous
PAGE	Polyacrylamide gel electrophoresis
PBS	Phosphate buffered saline
pCREB	Phosphorylated cAMP responsive element binding protein
PCR	Polymerase chain reaction
PFA	Paraformaldehyde
PFC	Prefrontal cortex
PMA	Phorbol 12-myristate 13-acetate
PrL	Prelimbic cortex
PV	Parvalbumin
PVDF	Polyvinylidene fluoride
PVH	Paraventricular hypothalamic nucleus

---

PVT	Paraventricular thalamic nucleus
Ras	Rat sarcoma related proteins
REDD1	Regulated in development and DNA damage responses 1
RIPA	Radioimmunoprecipitation buffer
Rpl22	Ribosomal protein L22
RTN	Reticular thalamic nucleus
S1	Primary somatosensory cortex
S2	Secondary somatosensory cortex
SCZ	Schizophrenia
SDS	Sodium dodecyl sulphate
SE	Southeast
S.E.M	Standard error mean
SNP	Single nucleotide polymorphisms
SOR	Spatial object recognition
SW	Southwest
US	Unstressed
UTR	Untranslated region
vACC	Ventral anterior cingulate cortex
VGCC	Voltage gated calcium channels
vHP	Ventral hippocampus
WHO	World health organization

## Acknowledgements

First of all, I would like to thank my supervisor, PD Dr. Jan M. Deussing for his guidance and support. He gave me the opportunity to pursue my interests, allowed me to work independently while also providing guidance throughout the years. I am grateful for everything that I have learnt from you.

I would like to thank Dr. Mathias Schmidt, Dr. Conny Koppscheinflug and Dr. Moritz Rossner for being part of my Thesis Advisory Committee. Thank you for your feedback and support. In addition, I want to thank our collaborators, Dr. Moritz Rossner and his team, for the minPROFILER data and their support with discussions and analysis of the data.

I would like to thank my colleagues Lidia Urbina, Clemens Ries, Ying Du, Simon Chang, Chen Zao, Iven-Alex von Muecke-Heim and my former colleagues Mira Jakovceski, Julia Richter, Paromita Sen and Laura Sotillos for all their support, scientific inputs, and the fun times. I would also like to thank Andrea Parl, Stefanie Unkmeir, Sabrina Bauer and Claudia Kuehne for their help and technical support.

Many thanks to Elena Brivio, Anthi Krontira, Fabian Stamp and Alessandro Ulivi for making my PhD years and stay in Germany fun and memorable. I am also grateful to have been a part of the IMPRS-TP graduate school at the Max Planck Institute of Psychiatry. These past years have been an exciting journey with many fun-filled memories.

I want to thank my friends, Dr. CH. Balavenkata Bharathi, Kiruthika Ganesan and Pavithra Suresh for always listening to me and cheering me in times of struggle. For those long conversations that covered any topic including science and working together virtually, I want to specially thank Kiruthika and Pavithra. Thank you for your support and encouragement.

Most importantly, I owe my deepest gratitude to my parents G. Loganathan and Radha Loganathan and my brother, Saravana Kumar L., for their loving support, and encouragement throughout my career plans. Thank you for all your love, for always believing in me and encouraging me to pursue my dreams, even if it meant moving away to another country. Without your love, support, and encouragement I would not be able to achieve my goals and I am deeply grateful for that.

